Towards the total synthesis of a potential M_1 muscarinic agonist and study on regioselective cyclisations for the synthesis of highly substituted piperazinones

by

Laura De Francesco

Submitted in accordance with the requirements
for the degree

of

Doctor of Philosophy

University of Cardiff
School of Chemistry

August 2006

ProQuest LLC
789 East Eisenhower Parkway
P.O. Box 1346
Ann Arbor, MI 48106-1346

ABSTRACT

The preparation of piperazinones, which are important pharmacophores, is reviewed in the introduction. This thesis provides an elucidation of the cyclisation mechanisms involving chiral secondary 1,2-diamines both with haloacetates and with 1,2-dicarbonyl compounds. The work on selective cyclisations consists of mainly three parts:

(i) Regioselective preparation of *N,N'*-disubstituted 5- and 6-piperazinones with elucidation of the cyclisation mechanism using D_2O and ^{13}C label;

(ii) Regioselective preparation of *N,N'*-dibenzyl 3,6- and 3,5-disubstituted piperazinones using methyl α-bromophenylacetate, methyl 2-bromopropionate, methylglyoxal, phenylglyoxal and benzil;

(iii) Selective preparation of *N*-acetates of 5-substituted piperazinones by hydrogenolysis and intramolecular cyclisation in the same reaction pot starting from substituted dibenzyl 1,2-diaminoacetates.

Additionally, the total synthesis of a potential M_1 muscarinic agonist for treatment of Alzheimer's disease was planned and almost completely carried out. The multistep sequence presented two challenging steps: regioselective preparation of a chiral piperazinone successfully achieved with the haloacetate cyclisation described above; Birch reduction of a lactam to an aminol, in presence of an amide, which acts as a nucleophile and cyclises to give a 1,1-aminoamide.

Acknowledgements

Many thanks to my supervisor Dr. David Kelly for the consistent support and advice, and to give me all the knowledge I needed to complete my work. I also would like to thank Dr. David King who has been an exemplar post-doc friend for me and helped me out when I was desperate in the lab. A special thank goes to Dr. Nick Tomkinson for being mentoring me during these three years.
I would also like to thank all the rest of the academic and support staff of the School of Chemistry, in particular Mr. Rob Jenkins for his help with NMR and Mr. Robin Hicks, a kind friend who was always available for any enquiry. I wish to thank Dr. Li-ling Ooi for providing the X-Ray Crystal data.

A big thank to my "collegue-friends", Elham Tahanpesar, Stewart Bissmire, Claire, Paula, Giovanna, Arturo Robertazzi, Antonio Lopez, Fabrizio Pertusati, for all the encouragement, advice and friendship shown during these three years.

I want to thank Betty to be part, once again, of such a big achievement in my life and to share with me every problem found on the way. Thanks to Marco for fathering me in times of hopelessness and to try to teach the real deep philosophy of science.

A special thank to my Mum, Dad, Mario and grandparents for their faith, endless patience and encouragement when it was most required.

Lastly a big thank you to the person that has shared life with me for these three years, giving me support, strength and love, encouraging me every single day.
Thank you Nico.

Table of Contents

List of Figures

Chapter 1

Chapter 2

Chapter 3

Chapter 4

Chapter 5

Chapter 7

Chapter 8

Chapter 9

List of Tables

Chapter 1

Chapter 3

Chapter 4

Chapter 5

Chapter 6

Chapter 7

Chapter 8

Chapter 9

List of abbreviations

Asp	Aspartic acid
APCI	Atmospheric pressure positive ion chemical ionization
Ac	Acetyl
Bn	Benzyl
Boc	*t*-Butyloxycarbonyl
Bz	Benzoyl
Cbz (Z)	Benzyloxycarbonyl
d	doublet
dd	double of doublet
δ	NMR chemical shift (ppm)
DCC	*N,N'*-Dicyclohexylcarbodiimide
DCU	*N,N'*-Dicyclohexylurea
DIEA	Diisopropylethylamine
DMF	*N,N'*-Dimethyl formamide
DMSO	Dimethyl sulfoxide
DMAP	4-Dimethylaminopyridine
EC_{50}	Effective concentration of a toxin that is required for 50% desired effect
EDC	1-[3-(Dimethylamino)propyl]-3-ethyl-carbodiimide hydrochloride
EEDQ	2-Ethoxy-1-ethoxycarbonyl-1,2-dihydroquinoline
Et	Ethyl
Et_3N	Triethylamine
EtOAc	Ethyl acetate
EtOH	Ethanol
GDP	Guanosine 5'-diphosphate
GTP	Guanosine 5'-triphosphate
Gly	Glycine
HATU	*O*-(7-Azabenzotriazole-1-yl)-1,1,3,3-tetramethyluronium hexafluorophosphate
His	Histidine
HRMS	High resolution mass spectrometry
HMBC	Heteronuclear multiple bond coherence
HMQC	Heteronuclear multiple quantum coherence
HMPA	Hexamethylphosphoramide
HPLC	High-performance liquid chromatography
Hz	Hertz
IPA (*i*-Pr)	Isopropyl alcohol
IR	Infra-red
Leu	Leucine
LRMS	Low resolution mass spectrometry
m	Multiplet
Me	Methyl
MeOH	Methanol
mg	Milligrams
MHz	MegaHertz
mol	Moles
mmol	millimoles
NMR	Nuclear Magnetic Resonance
p-TsOH	*para*-Toluenesulphonic acid
Ph	Phenyl
Phe	Phenylalanine

ppm	Parts per million
s	Singlet
Ser	Serine
S_N2	Nucleophilic substitution bimolecular
t	Triplet
t-Bu	*tert*-Butyl
THF	Tetrahydrofuran
TLC	Thin layer chromatography
TFA	Trifluoroacetic acid
Tyr	Tyrosine

CHAPTER 1 Introduction

1.1 Biological aspects of constrained peptidomimetics

1.1.1 Piperazinones: building blocks for peptidomimetics

Proteins have well defined three-dimensional conformations that are necessary to exhibit biological activity. Peptides play fundamental roles as ligands to protein receptors. However, peptides themselves are poor therapeutic agents due to low oral bioavailability as a consequence of degradation by proteolytic enzymes; and poor membrane permeability due to inefficient transport across cell membrane[1] and large molecular size[2]. Therefore, drug research is focused on the design and preparation of "peptidomimetics". This term describes a large family of compounds that show similar biological activity to native peptides. Peptidomimetics typically contain unnatural amino acids, conformational constraints and groups which mimic peptide bonds, but which are not susceptible to hydrolysis[3].

The design of a peptidomimetic is a complex operation that includes a clear understanding of structure-activity relationship and the conformational properties of the target peptide. Determination of peptide bioactive conformations can be achieved by studying multiple conformationally constrained non-peptide analogues[4], X-Ray crystallography analysis and a combination of computational and sophisticated spectroscopic methods. The introduction of constraints in peptide structures limits the number of conformational possibilities that they can adopt and consequently reduces the entropy cost upon folding into such a conformation. Ideally, small and constrained molecules able to "lock" the active conformation of a peptide should result in higher affinity with a receptor, increasing the stability of the binding and improving biological selectivity through elimination of bioactive conformers that give undesired biological responses. Model constrained peptides have been designed to study in detail the conformational preferences of natural and modified amino acid residues.

1.1.1.1 Types of modifications

Two basic types of conformational modifications have been used in analogues: non-covalent and covalent modifications. Non-covalent modifications include the incorporation of D-amino acids, *N*-methyl amino acids and α-methyl amino acids. Covalent modifications forming cyclic and polycyclic peptides include cyclic amino acids[5], disulphide bridges and cyclisation through amide bonds, all of which are known

to occur in nature. Covalent modifications can give two main groups of constraints, according to the degree of freedom shown by the peptides. One is known as "global" constraint that involves the modification of the peptide backbone, usually forcing the formation of secondary structures that provides higher conformational stability (Figure **1**). The second is the "local" constraint that is confined in a precise region of the peptide backbone and that involves modifications of only one or two residues of the peptide sequence (Figure **2**).

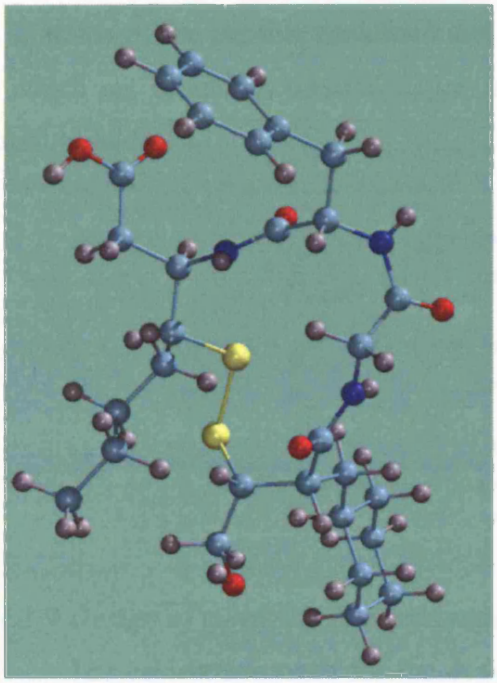

Figure 1. Global constraint

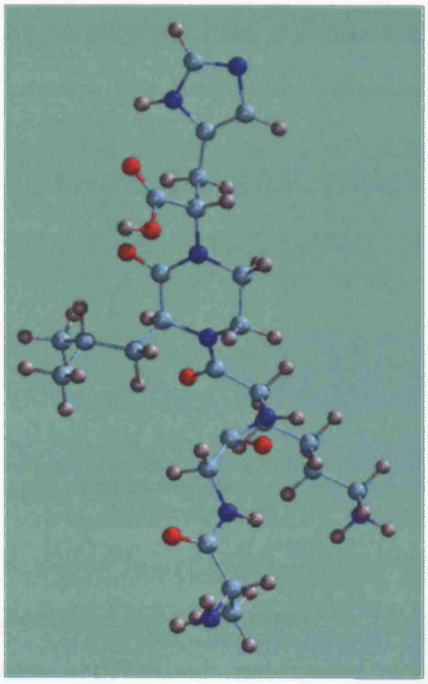

Figure 2. Local constraint

1.1.1.1.1 Global conformational constraint[6]

Formation of a covalent bond between two distant regions of a peptide creates macrocyclic structures that will adopt certain well defined stable conformations. Met-enkephalin **1** (Tyr-Gly^2-Gly-Phe-Met^5) is an endogenous ligand for δ-opioid receptors. Substitutions of Gly-2 and Met-5 with β,β-dimethyl penicillamine gave [D-Pen^2, D-Pen^5]-enkephalin (DPDPE) **2** (Scheme **1**), which was found to be a potent and selective δ-opioid receptor ligand, with strong analgesic activities[7].

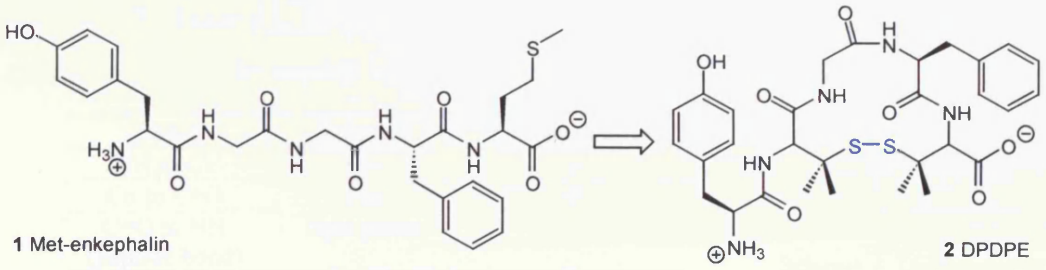

Scheme 1. Cyclisation side chain to side chain to constrain the global conformation

1.1.1.1.2 Local conformational constraint[6]

Piperazin-2-one (4-aza-δ-lactam) rings **3** are good examples of peptidomimetics that create a local constraint using a covalent modification, able to specifically stabilise some parts of a peptide side chain or backbone. Due to the relative rigidity of piperazinone rings and to the possibility of introducing different substituents on the ring, piperazinones have been introduced in peptide-like chain compounds as analogues of adjacent amino acids. 2-Piperazinones **3** are building blocks in which the N_i and the N_{i+1} atoms of the peptide backbone are linked by an ethylene bridge and consequently in which ω_i, φ_i and ψ_i torsion angles in compound **5** are restricted compared to the parent peptide **4**[8].

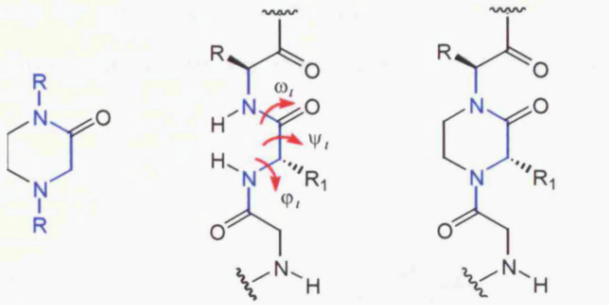

1.1.1.2 Design of constrained peptidomimetics based on piperazinones

The easiest approach for the design of new constrained analogues involves the identification of particular protons in the desired peptide conformation such as **6** that are spatially close together and replacing the protons with an appropriate bridge[9], such as an ethylene bridge in the case of piperazinone **7** (Scheme **2**).

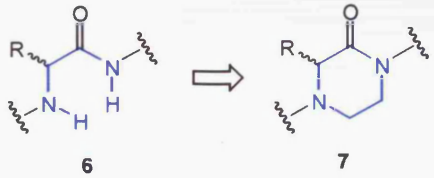

Scheme 2. Mimicking adjacent amino acids

The shape of a peptide bond is defined by the three consecutive torsional angles (Scheme **3**, Table **1**). The peptidic bond length is 1.33 Å, which indicated its double character, due to the second resonance form of the amide.

Bond	Rotation	Torsional angle
NH to Cα	free	ψ
Cα to C=O	free	Φ
C=O to NH (peptide bond)	rigid planar	ω

Table 1. Peptidic bond angles

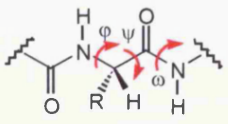

Scheme 3. Definitions of φ, ψ and ω torsional angles

Peptide bonds are almost invariably fixed at $\omega = 180°$ or *trans* based on the relative alignment of Cα atoms on either side of the peptide bond. The rigidity of the peptide bond limits the number of arrangements that Pauling's models[10] could fit, without distorting bonds or forcing atoms closer than van der Waals radii would allow. Without this constraint, the peptide would be free to adopt so many structures that no single consistent pattern would emerge. By reducing the degrees of freedom, a well defined set of states emerges. Pauling found two general patterns conformed to atomic geometry:

(i) A helical state in which the ψ and Φ were roughly 60°, twisting repeatedly in the same direction, known as an α-helix (Figure **3**);

(ii) An extended state for which $\psi = -135°$ and $\Phi = +135°$, where polypeptide chain alternates in a zig-zag structure, known as a β-sheet (Figure **4**);

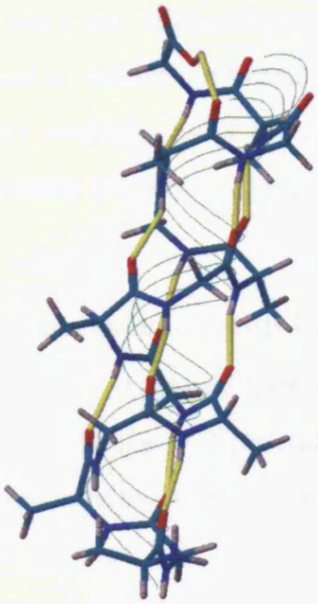

Figure 3. α-helix (PC Model 8)

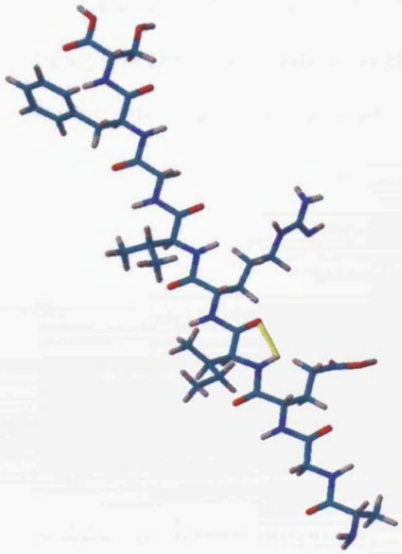

Figure 4. β-sheet (PC Model 8)

The Pauling model-building studies of the early 1950's were followed by an exhaustive calculation of ψ and Φ space, carried out by Ramachandran. The most informative local conformational constraints are those that constraint the backbone φ, ψ and ω torsional angles.

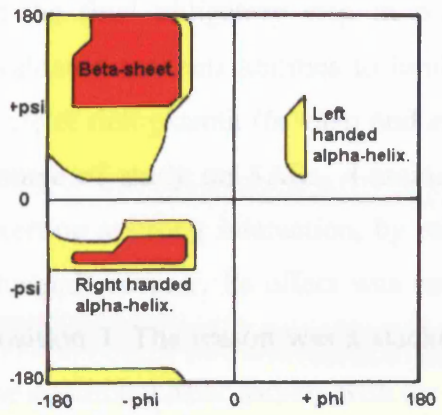

Figure 5. The Ramachandran Plot

Ramachandran and co-workers showed that serious steric interferences occurred between C=O groups and amino acid side chain centred at $\psi = 120°$ and serious interferences between peptide backbone CO and NH occurred at $\psi = \Phi = 0°$[11]. The Ramachandran plot described regions where these interactions were favourable or not possible (Figure **5**).

As amino acid mimics, piperazinones are designed to reduce the conformational flexibility and lead to a better binding with the receptor due to reduced entropy.

The substitution on piperazin-2-one rings is also an important aspect for the design of a peptidomimetic as it is possible to "predict" all the possible conformations that can exist. High substitution results in hindered structures that are more likely to be locked in precise conformations. Unsubstituted rings possess more freedom resulting in higher similarity with the endogenous compounds, i.e. acyclic amino acid sequences, increasing the possible number of conformations.

1.1.2 Therapeutic agents based on piperazinones

1.1.2.1 Potent dibasic GPIIb/IIIa Antagonists

A series of 2-piperazinone derivatives, possessing basic moieties at the 3- and the 4-positions, were synthesised and evaluated for their abilities to inhibit platelet aggregation and for their effect on bleeding times. Among these compounds, TAK-024 **8** showed the most potent inhibitory effect on platelet aggregation, making it a good candidate drug for treatment of thrombotic diseases.

8 TAK-024
Dibasic GPIIb/IIIa antagonist

The action of this drug involves the inhibition of the platelet membrane glycoprotein IIb/IIIa (GPIIb/IIIa), which cross-links with the plasma protein fibrinogen

in the final obligatory step in platelet aggregation. This class of compounds were evaluated for their abilities to inhibit ADP-induced platelet aggregation in guinea pig platelet rich plasma (*in vitro* and *ex vivo*) and for their effect on bleeding time. In the course of study on SARs, 4-amidinophenyl group was found to be indispensable for exerting a strong interaction, by reinforced ionic mode of binding with the negatively charged receptor. Its effect was enhanced by introduction of an extra basic moiety at position 3. The reason was π stacking and a lipophilic interaction of the phenyl ring in the additional basic moiety with the receptor, resulting also in higher potency[12].

1.1.2.2 Leu-Enkephalin analogues

Leu-enkephalin (Leu-Enk) **9** was the first endogenous opioid penta-peptide isolated (Tyr-Gly-Gly-Phe-Leu)[13,14]. Opioid ligands are produced by the hypophysis and hypothalamus in vertebrates and they exert their effect through three major types of opioid receptors (μ, δ, κ) as "natural pain killers". Leu-Enk is a potent agonist for δ-receptors. At the present it is thought that the morphine-like effect is due to the aromatic side chains (Tyr, Phe) present in the penta-peptide, that mimic a similar structure in morphine. It is also believed that the binding of the neuropeptide to the receptor occurs in a conformation containing a 5→2 β-turn[15].

Modifications on the structure of Leu-Enk, such as the introduction of a ring that bridges two consecutive amino acids created a constrained peptidomimetic **10**[16] that was used as a therapeutic agent.

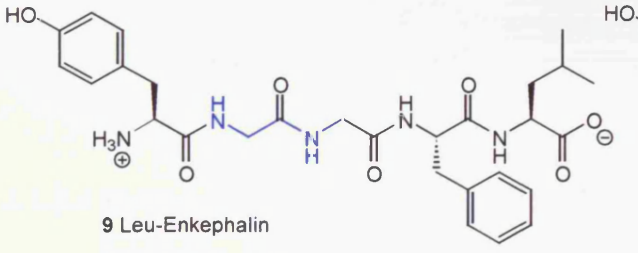

9 Leu-Enkephalin

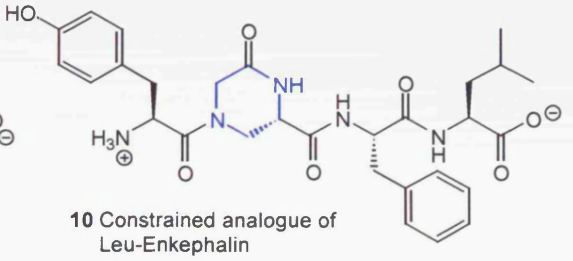

10 Constrained analogue of Leu-Enkephalin

A wide range of Leu-Enk analogues based on chiral piperazinone rings have been prepared[17]. Some analogues are based on piperazinones for the first and the second residues[18], and others for the second and third residues[17]. Introduction of constraints or *para*-substituents on Phe[4] in enkephalin derivatives, such as azide group or halogens have been reported to retain high δ receptor affinity. However, *p*-amino group and isothiocyanate derived substituents on Phe of DPDPE **10** resulted in large decrease of δ receptor affinity[4].

1.1.2.3 Growth Hormone mimetics

Growth hormone mimetics are used for the treatment of osteoporosis, wasting conditions, recovery and obesity[19] and their structure mimic the natural peptide. Among this class, growth hormone releasing peptide (GHRP) 1[20] **11** and NN703 **12** were prepared in the 1970s and shown to be potent therapeutics for the release of growth hormone (GH). The piperazinone functional group was introduced in this class of molecules, in order to synthesise constrained versions of a growth hormone mimetic, NN703[21]**12**. Evaluation with respect to GH-release on rat pituitary cells of NN703 **12** and its constrained analogues showed that compound **13** was either equipotent or even more potent than NN703 itself (EC_{50} 18 nM).

2-Piperazinone rings served as rigid units bridging two consecutive amino acids in a peptide and moreover, they lock the substituents in a conformation similar to the side chains of the parent peptide in its bioactive conformation[22].

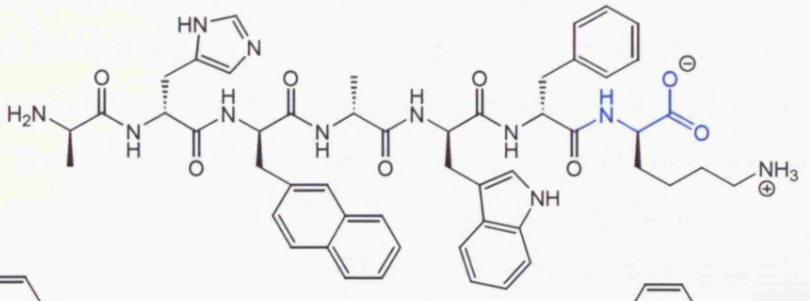

11 GHRP 1

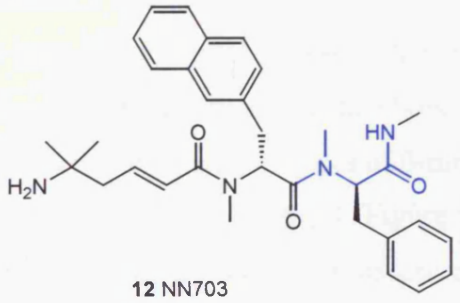

12 NN703

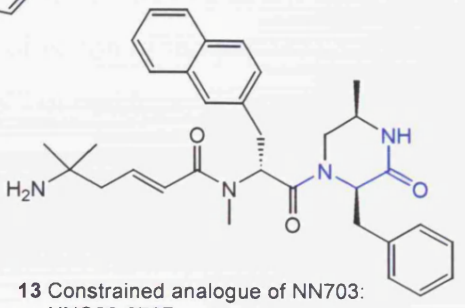

13 Constrained analogue of NN703: NNC26-0737

1.1.2.4 Substance P analogues

Substance P is a member of the mammalian tachykinin family of peptides and has been implicated in a number of disease states including arthritis, asthma, inflammatory bowel disease and depression. Substance P is an 11 amino acid peptide (Arg-Pro-Lys-Pro-Gln-Gln-Phe[7]-Phe[8]-Gly-Leu-Met[11]-NH_2). Two models of this peptide were proposed as potential conformations responsible for the interaction with the receptor NK_1. Two different agonists **15** and **17** were designed and prepared in order to mimic both conformations of Phe[7]-Phe[8] regions in **14** and 16 (Scheme **4**). All the analogues were examined for their ability to displace substance P from its NK_1 receptor. Bicyclic compounds such as **15** and **17** inhibited the binding only at high concentration

with IC_{50}values of ~32 μM. Under the same binding assay conditions Substance P itself exhibit an IC_{50} of 0.3 nM, indicating that the modification in the analogues reduced their affinity by approximately four orders of magnitudes[23].

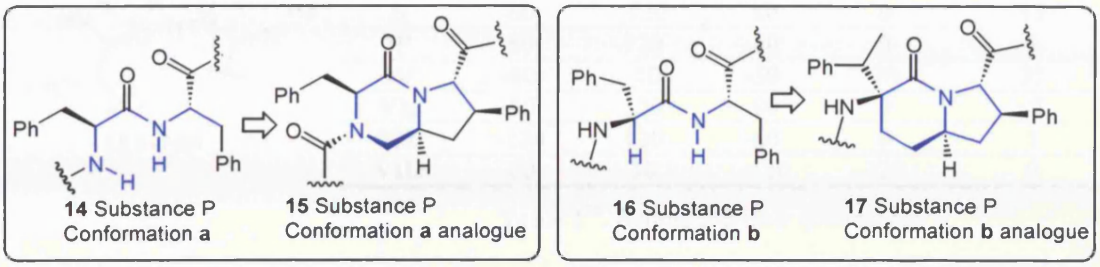

Scheme 4. Different spatial conformations of substance P

1.1.2.5 β-Turn peptidomimetics

1.1.2.5.1 Introduction

β-Turns are important motifs in biologically active peptides and they are responsible for their globularity. They are defined as any tetrapeptide sequence with 4-10 membered intramolecularly H-bonded ring, in which C_α^{i}—C_α^{i+3} distance varies from 4 to 7 Å[24,25]. These four consecutive residues are not present in α-helix and they fold back on themselves by nearly 180°[26]. Hydrogen bonding between the carbonyl of residue *i* and the amide hydrogen of residue *i* + 3 is often indicative of a β-turn, though it is not an essential feature[27]. A β-turn reverses the direction of the peptide chain and is classified by the Φ and Ψ backbone torsional angles[28] of residues *i* + 1 and *i* + 2 (Table **2**), there are at least 14 types of β-turn structure.

Type I (Figure **6**), II (Figure **7**), and IV β-turns are the most prevalent. Type VI[29] are the most rare secondary structures in that they bear a *cis*-amide bond between the *i* + 1 and *i* + 2 residues, and thus typically have a proline at the *i* + 3 residue[30].

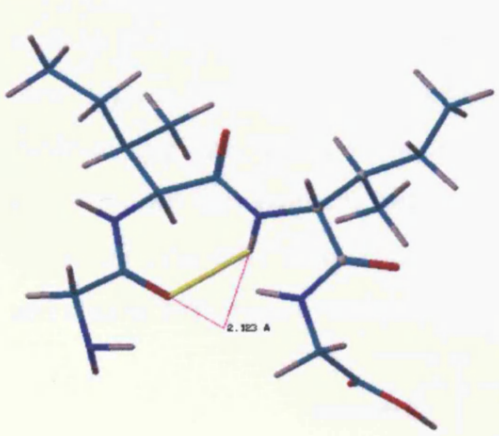

Figure 6. Type I β-turn (Gly-Ileu-Ileu-Gly)

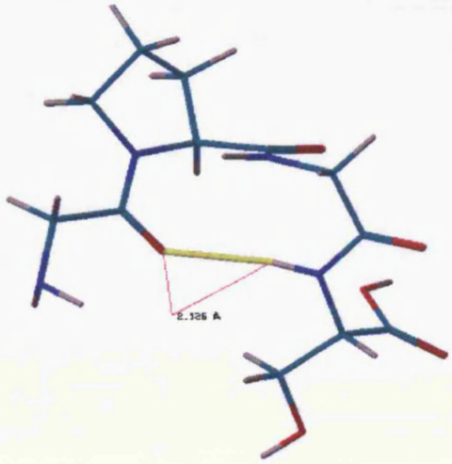

Figure 7. Type II glycine β-turn (Gly-Pro-Gly-Glu)

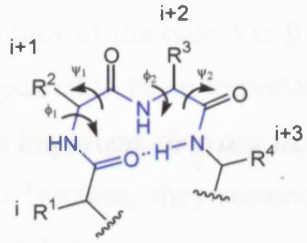

18 β–Turn

β-turn type	Position $i+1$: Φ_1	$i+1$: Ψ_1	$i+2$: Φ_2	$i+2$: Ψ_2	Abundances (%)
I	-60	-30	-90	0	34
I'	60	30	90	0	4
II	-60	120	80	0	13
II'	60	-120	-80	0	4
IV	-60	10	-50	20	35
VIa	-60	120	-90	0	<1
VIb	-120	120	-60	0	1
VIII	-60	30	-120	120	9

Table 2[28]. β-turns and their abundances

1.1.2.5.2 β-Turn mimics

β-Turns have been shown to be important for recognition, binding and for receptor affinity in biologically active peptides. Therefore, mimics of β-turns[31] are desirable tools for studying the structure-activity relationships responsible for protein and peptide biology[32].

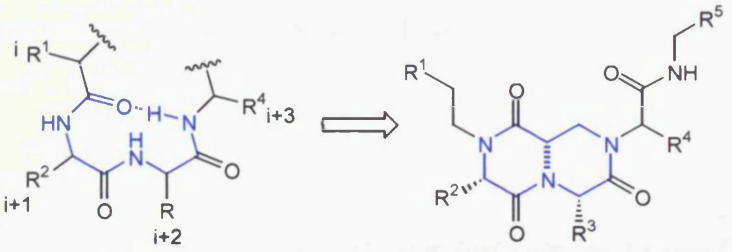

19 β–Turn 20 β–Turn mimetics

Strategies to design β-turn mimics have often constrained the peptide backbone dihedral angles[32,33]. Bicyclic fused systems such as diketopiperazines **20**[24], azabicyclo[X,Y,0]-alkanone amino acid **21**[32] have been used as rigid dipeptide surrogates that structurally constrain three consecutive dihedral angles, φ, ψ and ω, of a β-turn segment within the body of the heterocycle. Conformational analysis of **21** has shown that they mainly mimic type II and II′ β-turns. Macrocyclic dipeptide lactams such as **22** mimic better the natural diversity of a wide range of turn geometry, due to their higher flexibility. Unfortunately, due to the problems for the preparation of medium ring size, they have been less investigated. However, new strategies are arising to overcome the synthetic difficulties. A recent example, such as the ring closure metathesis, partially solved the problem and will lead to more efficient synthetic routes and clearer biological evaluation of these complex structures[32].

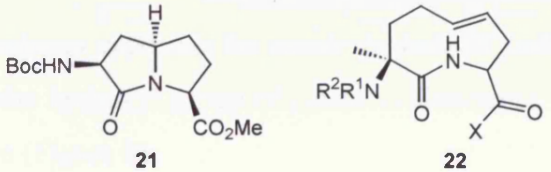

21 22

Substituted bicyclic lactams **24** have particularly been designed as peptide mimics of the type VIa β-turn **23**. Type VI turn has attracted a lot of attention since it appeared to be an important recognition feature for peptide bindings, besides possessing the important *cis-trans* isomerism, implicated in a large number of biological processes. For instance, they seemed to be indispensable for peptide binding to PPIases and for peptide hormones.

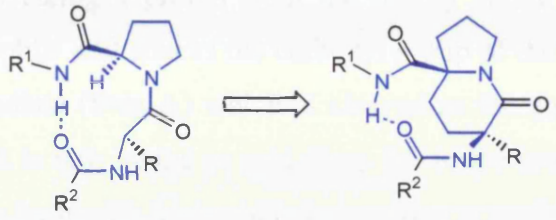

23 Type VIa β–turn

24 Bicyclic lactam β–turn mimetic

The mimic duplicates the conformation of the backbone and disposition of the side-chain atoms of the central two residues of the turn. In particular, bicyclic lactams **24** represented the two residues of a XaaPro dipeptide unit constrained to the type VI turn conformation[34].

1.1.2.6 Enzyme inhibition

Similarly, structures based on piperazinone rings are used as scaffolds to prepare enzyme inhibitors in particular as proteases inhibitors[35] and transition-state enzyme inhibitors.

1.1.2.6.1 Proteases inhibition

Proteases are enzymes that catalyse amide hydrolysis in proteins. Amides are hydrolytically stable under physiological conditions and their hydrolysis is slow. There are two classes of protease enzymes. One class catalyses direct amide hydrolysis using an enzyme-bound activated water molecule as the nucleophile.

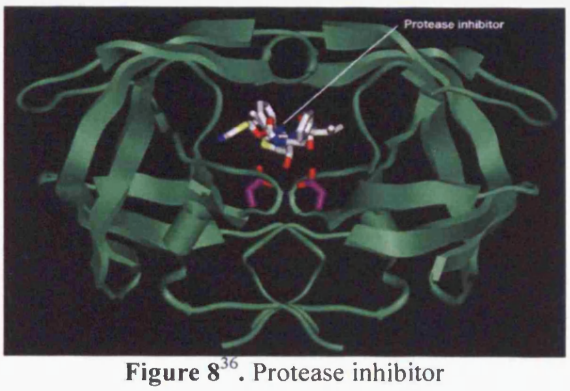

Figure 8[36]. Protease inhibitor

The second class of enzymes catalyses the amide hydrolysis indirectly by using amino acid residues, such as the hydroxyl group of serine or threonine, and the thiol group of cysteine as nucleophiles (Figure **8**).

1.1.2.6.2 Mechanism of peptidic bond cleavage

For the trypsin and chymotrypsin proteases, the three amino acids: histidine-57, aspartate-102 and serine-195 are crucial for the cleavage of the substrate. The mechanism is as follows (Scheme **5**). The carboxyl group of Asp-102 polarises the His-57 that then acts as base taking a proton from the nearby serine's hydroxyl group. Serine then acts as nucleophile and attacks the carbonyl group of the amide substrate to give a tetrahedral intermediate (Step A) which is cleaved as the amino group takes a hydrogen from His-57 that is now acting as acid (Step B). In the next step, His-57 acts as base again abstracting a hydrogen from water and making it nucleophilic ($^{-}$OH). The water nucleophile attacks the carbonyl of the serine ester (Step C). In the final step, the bond between serine oxygen and the tetrahedral intermediate is broken (Step D). The serine's oxygen regains its hydrogen from the nearby His-57 (Step E).

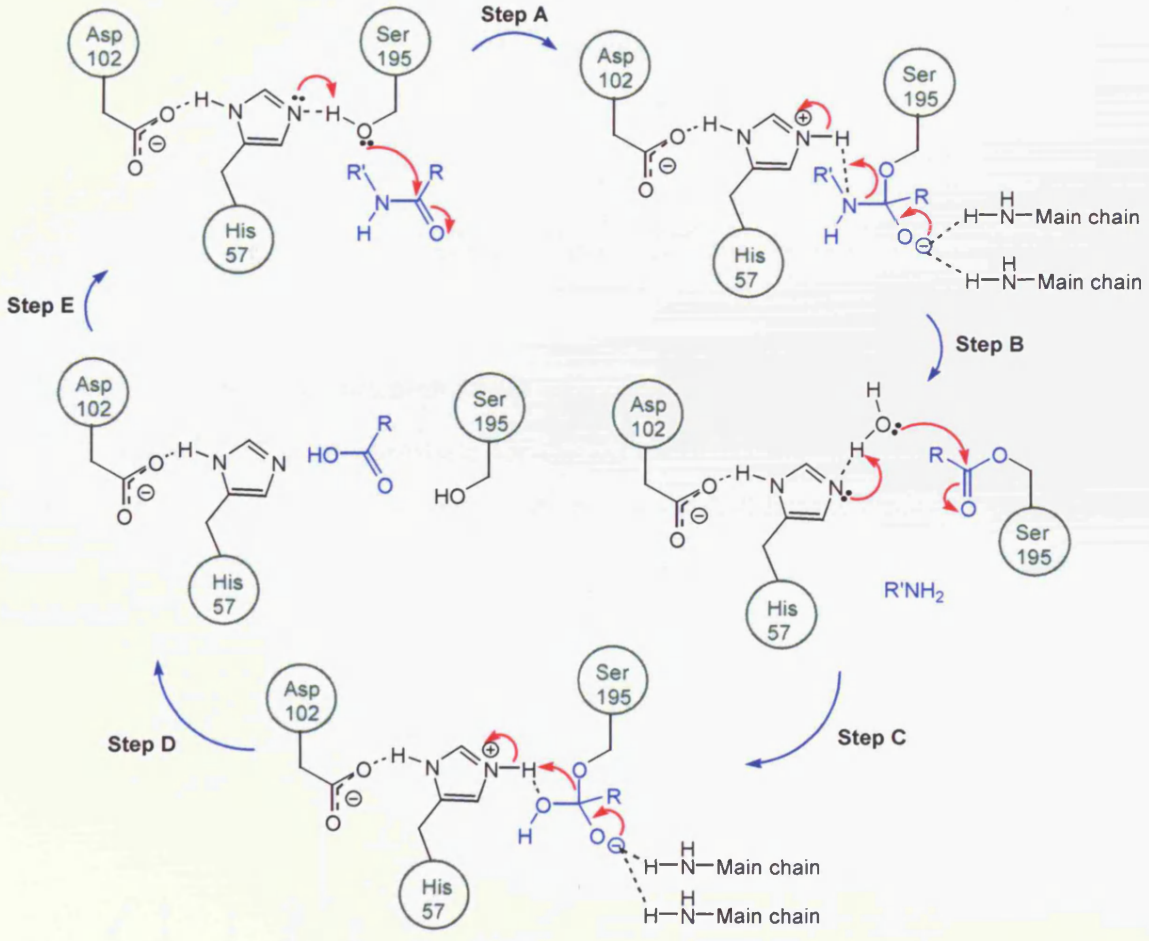

Scheme 5. Mechanism of peptide cleavage by trypsin and chymotrypsin (adapted from http://bmbiris.bmb.uga.edu/8010/moremen/weblinks/WebSerineProteases/ProteaseStep1.gif)

When the tetrahedral intermediates in the step **A** and step **C** are generated, the negative oxygen has accepted the electrons from the carbonyl double bond and fits perfectly into the oxyanion hole. Serine proteases preferentially bind the transition state and the overall structure is favored, lowering the activation energy of the reaction. This "preferential binding" is responsible for much of the catalytic efficiency of the enzyme.

Zinc metalloproteases such as angiotensin-converting enzyme, use zinc metallo protease to stabilise the transition state **25** (Step **A** and **C**, Scheme **5**). Inhibitors have been designed which resemble highly activated reaction intermediates[37]. Therefore, transition-state inhibitors such as **26** take full advantage of the ability of the enzyme to stabilise its transition state, blocking the enzymatic pathway and should not be hydrolysed by the enzyme, so often the amide bond is not present in the inhibitor. They bind transition-state better than substrate or products.

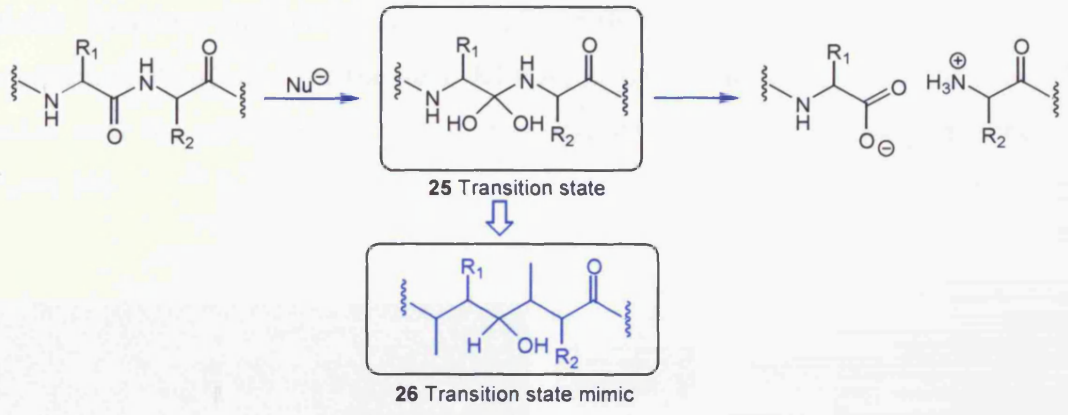

1.1.2.6.3 Transition-state inhibitors built on piperazinones

Factor X_a **27** is the substrate for the action of trypsin-like serine protease, that plays a central role in the blood coagulation cascade and homeostasis[38]. Piperazinone-based peptides **28** were designed and tested as potent transition-state factor X_a inhibitors[39,40].

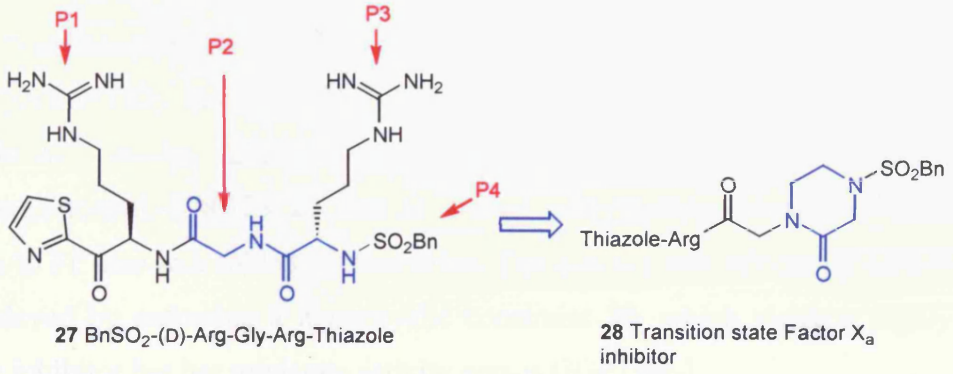

The sulphonamide nitrogen of the tripeptide **27** was cyclised on the glycine residue to give the unsubstituted piperazinone **28**, to introduce constraint into the peptide. In order to reduce the peptidic character and the high basicity of the endogenous agonist, a range of lactam ring systems was used as templates to mimic the P2-P3-P4 region of the tripeptide transition state inhibitor **28**. The novel inhibitor then displayed the desired inhibitory potency for factor X_a and also selectivity against thrombin, the final serine protease in the coagulation pathway.

1.1.2.7 Design of antineoplastic agents

Design of new antineoplastic agents is an area of a great interest nowadays. Important targets are Ras proteins, which are abnormally active in cancer. Ras proteins are small GTP-binding proteins (Figure **9**) that participate in the regulation of many cellular functions including cell growth, differentiation and intracellular signal transduction. Prenylation of the gene Ki-Ras, in particular farnesylation of a cysteine residue near the protein's C-terminus, was indispensable for its biological function[41] (Figure **10**).

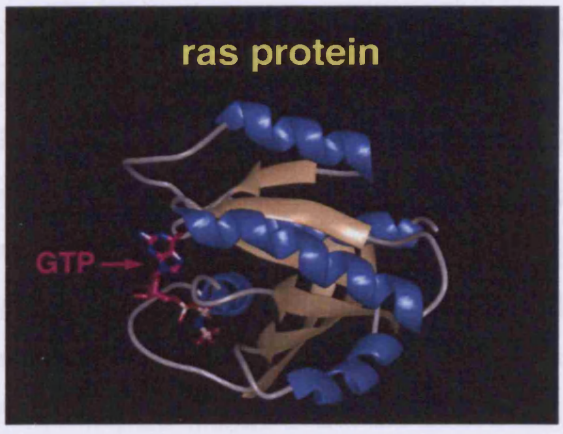

Figure 9[42]. GTP-bound Ras protein

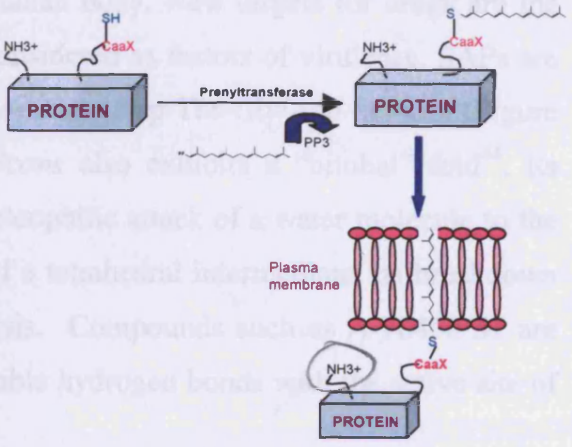

Figure 10. Mechanism of prenylation of Ras

Prenyltransferases catalyse the transfer of an isoprenoid (farnesyl FP or geranylgeranyl GG). Several FPTase inhibitors showed promising activity in preclinical and clinical studies, although they were incapable of inhibiting GGPT. *N*-arylpiperazinone L-178,123 **29** acts as a dual prenylprotein transferase inhibitor by binding to FPTase in a folded conformation. The potency and selectivity enhancements are achieved by enforcing a macrocyclic constraint **30**, which yields a highly potent FPTase inhibitor but has moderate activity versus GGPTase-I.

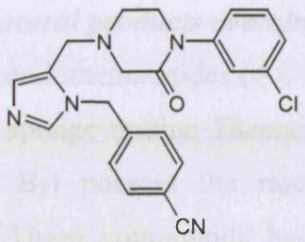

29 L-178,123

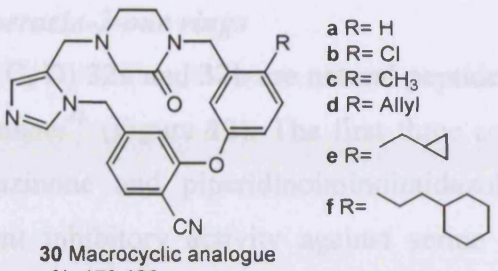

30 Macrocyclic analogue of L-178,123

The imidazole moiety is ligated to zinc, the cyanophenyl group is stacked against the isoprenoid chain of FPP, and the benzylpiperazinone portion is in contact with key hydrophobic residues. Notably, the cyclohexylethyl group of **30f** is angled toward a large cavity in the active site. Moreover **30f** potently inhibit both enzymes (FPTase, GGPTase-I) in cell cultures with relative activities that are almost optimally balanced for the inhibition of Ki-Ras prenylation[43].

1.1.2.8 Antifungal therapeutics

Deep mycosis (fungal infection) is difficult to treat without affecting the host organisms and nowadays a combination of azole derivatives is needed to treat them, due to resistance gained over the years by the human body. New targets for drugs are the SAPs (secreted aspartyl proteases) that are considered as factors of virulence. SAPs are mainly β-sheet structures organised in two domains: Asp-Thr-Gly/Asp-Ser-Gly (Figure **11**). In particular, SAP2X of *Candida albicans* also exhibits a "bilobal" fold[44]. Its mechanism of amide hydrolysis involves nucleophilic attack of a water molecule to the amide carbonyl with consequent formation of a tetrahedral intermediate; its breakdown generates the products of the amide hydrolysis. Compounds such as A-70450 **31** are shown to inhibit SAP2X by forming eight stable hydrogen bonds with the active site of the enzyme.

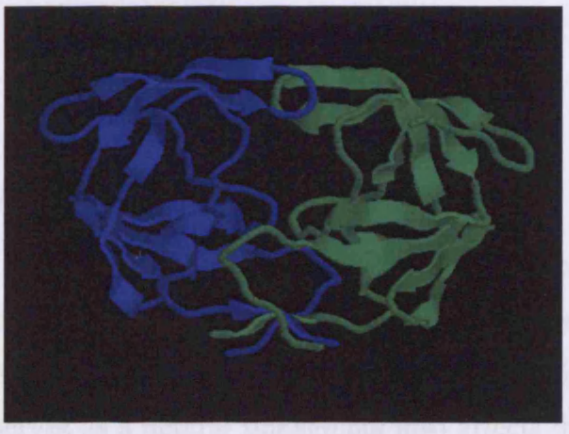

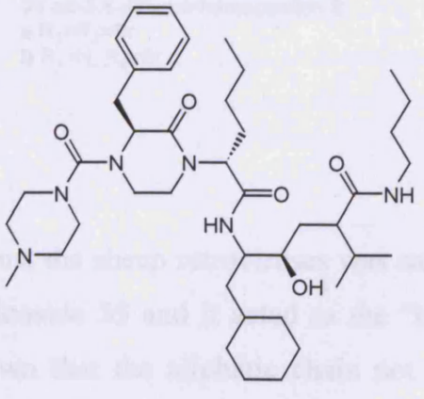

31 A-70450

Figure 11[45]. Secreted aspartyl protease

1.1.2.9 Natural products containing piperazin-2-one rings

Pseudotheonamides (A_1, A_2, B_2, C, D) **32a** and **32b** are natural peptides isolated from the sponge marine *Theonella swinhoei*[46] (Figure **12**). The first three compounds (A_1, A_2, B_2) possess the rare piperazinone and piperidinoiminoimidazolone ring systems. These compounds have potent inhibitory activity against serine proteases including thrombin, trypsin and plasmin[46].

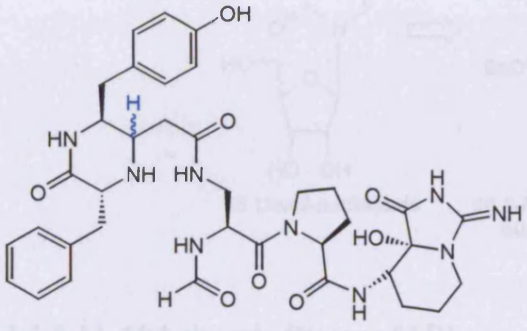

32 Pseudotheonamide
a *cis*-A_1
b *trans*-A_2

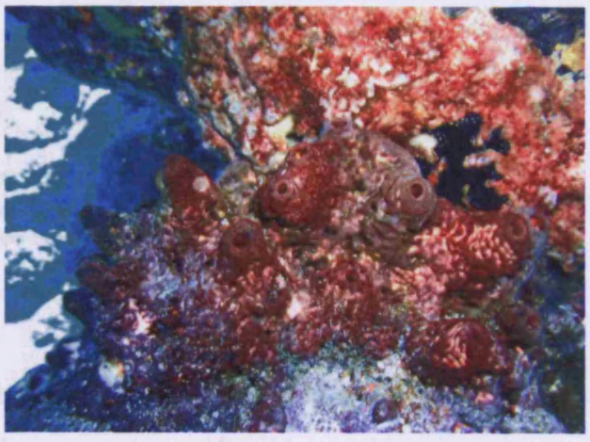

Figure 12[47]. Marine Sponge Theonella swinhoei

Substituted 2-piperazinones are present in other sponges, such as the Mediterranean sponge *Rhaphisia lacazei.* Bisindole alkaloid dihydrohamacanthins **33** and **34**[48] have been isolated and tested *in vitro* on NSCLC-N6 carcinoma cell line[49]. They show a myriad of biological responses including cytotoxicity and antitumor activities.

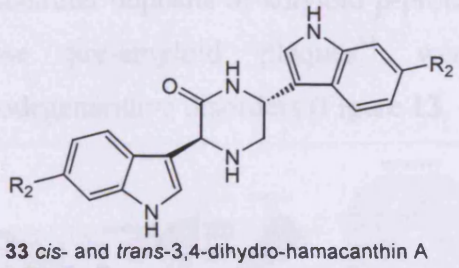

33 *cis*- and *trans*-3,4-dihydro-hamacanthin A
a R_1=R_2=Br
b R_1=H, R_2=Br

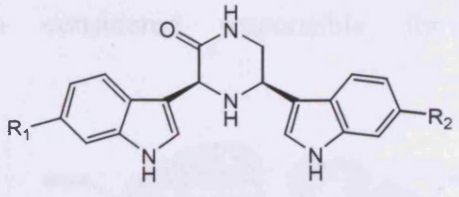

34 *cis*-3,4-dihydro-hamacanthin B
a R_1=R_2=Br
b R_1=H, R_2=Br

1.1.2.10 Anti-retroviruses

The synthesis of nucleoside analogues against the sheep retroviruses was carried out. Piperazinone ring was introduced in the nucleoside **35** and it acted as the "base" linked to a sugar by aliphatic chains[50]. It is known that the aliphatic chain not only serves as a neutral linkage but also affects the coiling of DNA. Increasing the length of

the spacer enhances bending of DNA, leading to base pair opening, consequently the bases then become susceptible to attack by reactive groups.

Nucleoside **36c** showed moderate antiviral activity against a mammalian retrovirus, the Visna virus, in sheep choroids plexus cells (SCP cells). It showed cytotoxicity though at concentration greater than 170 μM.

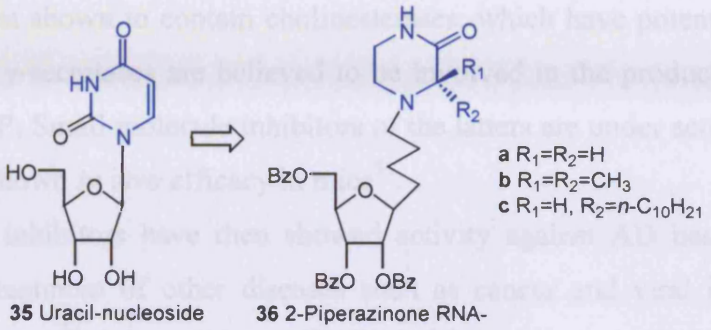

35 Uracil-nucleoside **36** 2-Piperazinone RNA-nucleoside analogue

1.1.2.11 Alzheimer's Disease (AD)

Among all the CNS diseases, AD has been long considered as one of the most obscure and intractable diseases. The syndrome starts with mild cognitive impairment with symptoms like occasional, minor lapses in recalling recent event of daily life that gradually deteriorate into a marked dementia, with full disorientation, profound memory loss and global cognitive deficits. In the early 70s it was believed that AD was caused by a disturbance of the acetylcholine functions in the brain, associated with decreased density of nicotinic acetylcholine receptors in the cerebral cortex. Lately, formation of extracellular deposits of amyloid β-protein (Aβ) fibrils, dystrophic axons, dendrites and diffuse pre-amyloid plaques[51] were also considered responsible for the neurodegenerative disorders (Figure **13**, **14**).

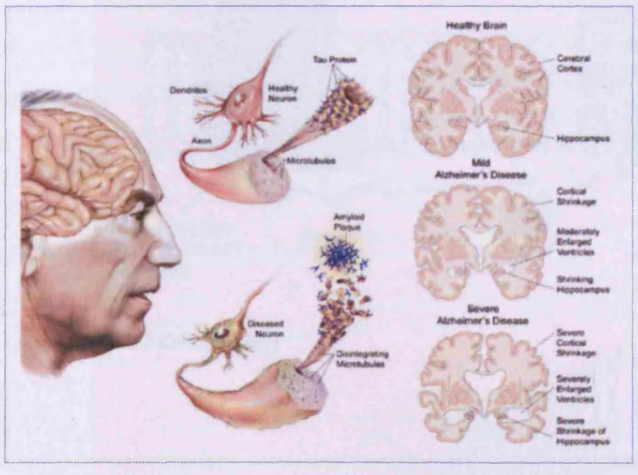

Figure 13[52]. How the brain and nerve cells change during Alzheimer's disease (Illustration by Bob Morreale, provided courtesy of the American Health Assistance Foundation)

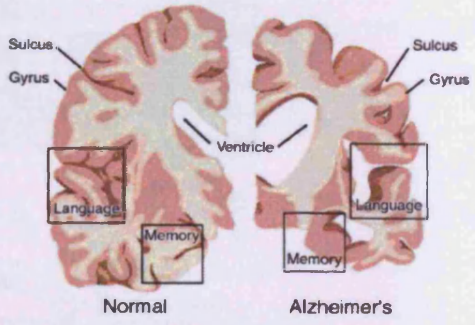

Figure 14[53]. Brain cross-sections

Amyloid deposits are aggregates of peptides of 40-43 amino acids. Aβs originate from the cleavage of glycoproteins called amyloid precursor protein (APP) and they are neurotoxic. Although no protease has yet been shown to produce Aβ proteins, a number of leads exist to help direct an empirical search for such protease. For instance, elastase, a serine protease is known to be bound to various amyloids. In addition, plaques and tangles have been shown to contain cholinesterases, which have potent serine protease activity. β- And γ-secretases are believed to be involved in the production of Aβ from its precursor APP. Small molecule inhibitors of the latters are under active development and some have shown *in vivo* efficacy in mice[51].

Serine protease inhibitors have then showed activity against AD besides being very useful for the treatment of other diseases such as cancer and viral infections (HIV, hepatitis and herpes) [54]. It is well know that muscarinic receptors play an important role in memory and the loss of their functions are strictly related with the symptoms of AD.

1.1.2.11.1 Muscarinic receptors

In the late 1980s, molecular cloning techniques identified five different subtypes of muscarinic receptors (m_1-m_5), which are the counterparts of the pharmacologically distinct muscarinic receptors (M_1-M_5). Each receptor shares common features including specificity of binding for the agonist acetylcholine, neurotransmitter of the para sympathetic autonomic nervous system, and the classical antagonist atropine. All muscarinic receptors belong to the family of G-protein-coupled receptors (GPCRs).

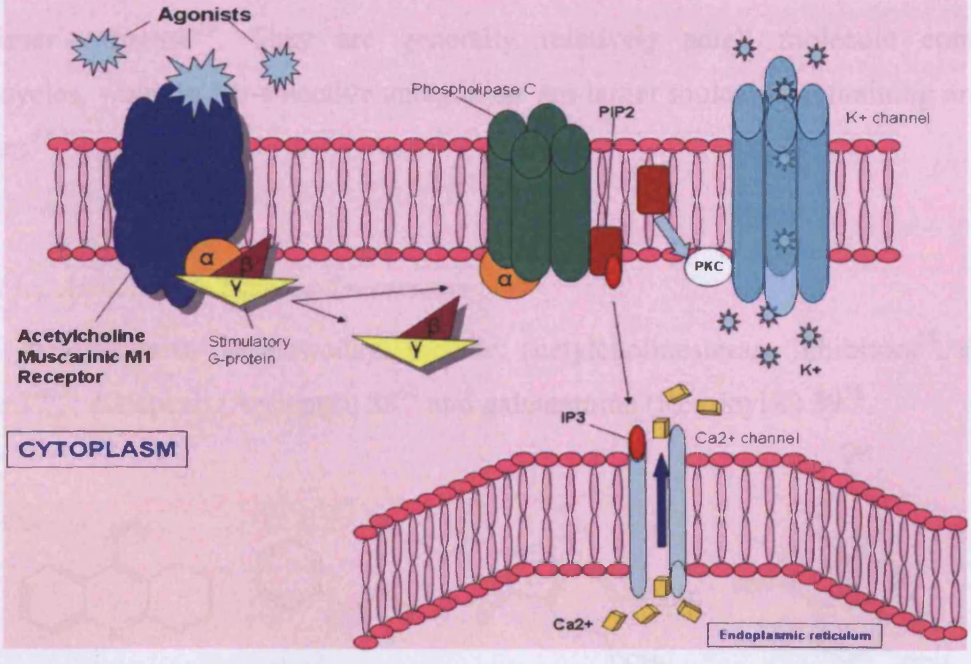

Figure 15. M_1 Muscarinic receptor-agonist interaction and effects

They are located in different areas of the brain and are likely to be involved in many different physiological processes. M_1 receptors are found in the forebrain, especially in the hippocampus and cerebral cortex. M_2 are found in the heart and brainstem whereas M_3 are found in smooth muscle, exocrine glands and cerebral cortex. M_4 receptors are found in the neostriatum and M_5 receptor mRNA is found in the substantia nigra[55].

The events associated with G protein-coupled receptor activation are as follows (Figure **15**). The agonists bind to the receptor that is consequently stabilised and can promote receptor/G protein coupling. GTP is exchanged to GDP on the G protein α subunit. The binding of GTP leads to the dissociation of the G protein from the receptor, thereby lowering agonist affinity whereas the agonist dissociates from the activated receptor. The G protein consists of three subunit (α, β and γ), which also are dissociated. The α subunit activates the second messenger, phospholipase C, and the β and γ subunits can exert independent actions. The α subunit is inactivated by the hydrolysis of GTP to form GDP by a GTPase intrinsic to the G protein and can then recombine with the β and γ subunits. At that stage, the receptor is then in a high affinity state and ready for binding another agonist.

The site of action of the M_1 receptor agonist appears to be an increase in the activity of a protease, α-secretase, through phosphoinositide turnover and stimulation of protein kinase C. α-Secretase cleaves the APP in the Aβ domain so that Aβ cannot be produced from APP; muscarinic agonists therefore reduce the levels of Aβ produced. M_1-Selective agonists may be useful to enhance cognitive function in the treatment of Alzheimer's disease[56]. They are generally relatively small molecule containing heterocycles, whereas M_1-selective antagonists are larger molecule containing aromatic moieties[57].

1.1.2.11.2 Alzheimer's Disease Treatments

Treatments in use nowadays include: acetylcholinesterase inhibitors[58], such as tacrine **37**[59], donepezil (Aricept®) **38**[60] and galantamine (Reminyl®) **39**[58].

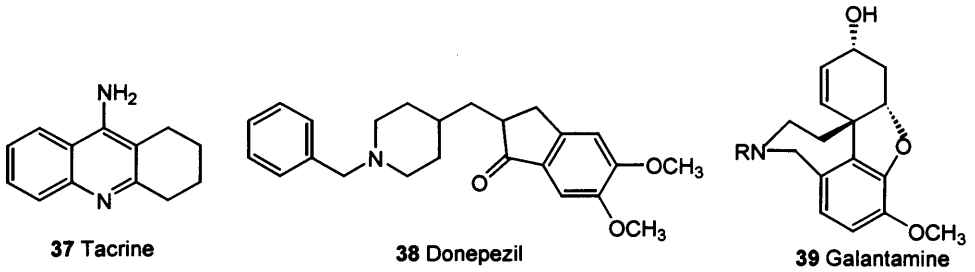

37 Tacrine **38** Donepezil **39** Galantamine

N-Methyl-D-aspartate (NMDA) antagonists, including memantine **40**, ketamine **41** and glutamate **42**; these drugs regulate the activity of glutamate, a chemical messenger involved in information processing and retrieval.

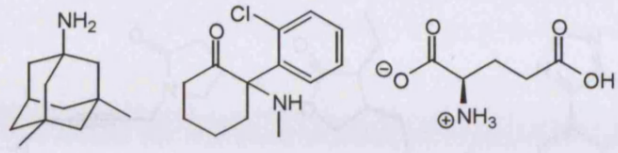

40 Memantine **41** Ketamine **42** Glutamate

Vaccines are a new approach for the prevention of AD. The principle is to make the immune system recognise and destroy the Aβ plaque formation, stopping the disease.

1.1.2.11.3 M_1 Muscarinic agonists design

M_1 receptors are found in the central nervous system, especially in the cerebral cortex and hippocampus, and in the stomach where they mediate gastric acid secretion. Based on their localisation in brain regions associated with learning and memory function, drug development efforts focused on the synthesis and biological characterisation of M_1 agonists. An ideal drug candidate would present several features including high CNS penetrance, high efficacy and selectivity for forebrain receptors and a low incidence of side effects[61].

Muscarine is the prototypical muscarinic agonist and it derives from the fly agaric mushroom *Amanita muscaria* (Figure **16**). Like acetylcholine, muscarine **43** contains a quaternary nitrogen, which is very important for the action at the receptor anionic site (an aspartate residue in transmembrane domain III).

Figure 16[62]. Amanita muscaria

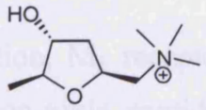

43 Muscarine

Classical muscarinic agonists such as arecoline **44**, oxotremorine **45** and pilocarpine **46** and the use of acetylcholinesterase inhibitors exhibited only modest

efficacy in the brain and produced a high incidence of side-effects, such as the progressive loss of cholinergic neurons and associated decrease in acetylcholine levels. Xanomeline **47** displayed higher activity at M_1 receptors than at M_2 or M_3 receptors[63].

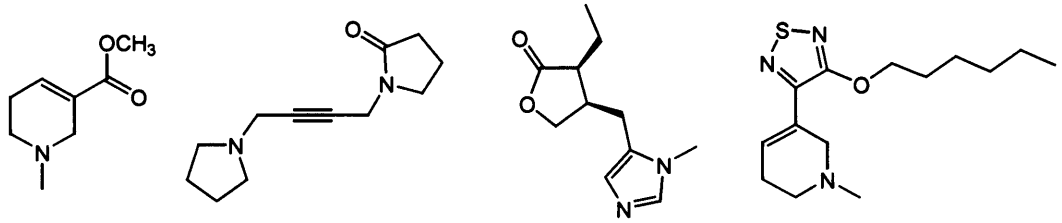

44 Arecoline **45** Oxotremorine **46** Pilocarpine **47** Xanomeline

Other compounds with improved selectivity for M_1 receptors include talsaclidine **48**, sabcomeline **49** and CDD-0102 **50**. In particular, the latter improved memory function in animal model and displayed a low side effect profile[63].

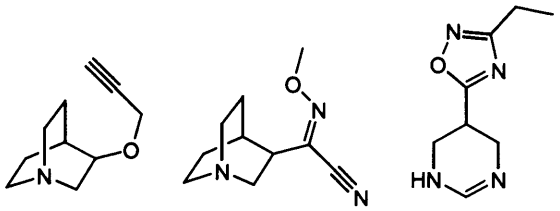

48 Talsaclidine **49** Sabcomeline **50** CDD-0102

The major problem of all the muscarinic agonists is the low selectivity towards the M_1 receptors. Medicinal chemists focused on developing larger molecules that could interact with accessory binding sites. By binding to sites outside of the primary agonist binding pocket, compounds could also interact with residues that are not highly conserved between receptor subtypes. Molecule such as CI-1017 **51** exhibited improved muscarinic receptor selectivity.

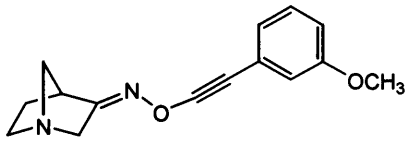

51 CI-1017

In addition to playing a role in cognitive function, M_1 receptors promote α-secretases activity, which results in the secretion of non-toxic peptide fragments of amyloid precursor protein, and hence decreased Aβ deposition.

Nowadays the design and development of muscarinic agonists is central in medicinal chemistry because they could become very useful therapeutics for preventing the amyloid plaques and neurofibrillary tangle formations, the two main hallmarks of Alzheimer's disease[63].

1.2 Chemistry of piperazinones

1.2.1 Strategies for preparation of piperazinones

Ketopiperazines, and their reduced derivatives piperazines, are valuable motifs that have found widespread use as conformationally constrained peptidomimetics, as well as synthetic intermediates for the construction of biologically active molecules, in total synthesis and in the pharmaceutical industry.

Analysis of the retrosynthesis of these structures leads to a large number of disconnections. Besides the six intramolecular cyclisations that create 12 possible electronic fragments, it is in principle possible to consider five [5+1] disconnections that lead to twenty possible electronic fragments, four [4+2] disconnections resulting in sixteen possible electronic fragments and three [3+3] with twelve possible electronic fragments. However, by screening all the possible approaches, and by following the natural reactivity of these compounds and the nature of the functional groups present, [4+2] disconnections could be considered the most accessible, also considering the easiness of starting materials preparation.

Three different approaches are shown below and will be illustrated in more details: one intramolecular cyclisation, one [4+2] and one [3+3] cyclisations (Scheme **6**).

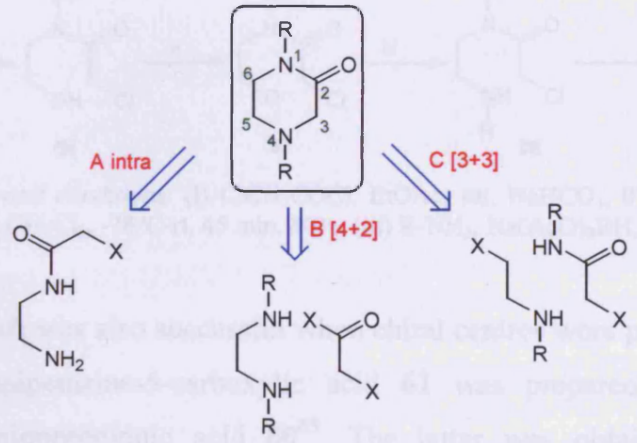

Scheme 6. Three possible disconnections for piperazinones

Moreover, since piperazinone rings are frequently included in the backbone of non-peptide structures, the presence of stereogenic centres is often found indispensable for the biological activity of these compounds.

One of the most facile approaches for the preparation of **52** is a [4+2] disconnection of N1-C2 and C3-N4, where R′ and R′′ are substituents on the 1,2-diamine derivatives **53** and R′′′ is substituent on the dielectrophile **54** (Scheme **7**).

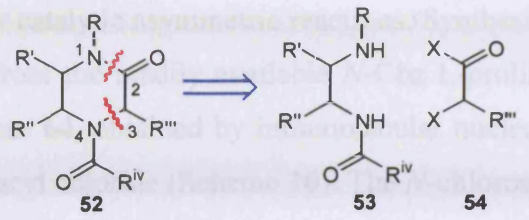

Scheme 7. Retrosynthetic approach for fully substituted piperazinones

In this case, the reactivity of the amino groups needs to be controlled to avoid formation of product mixtures, and this can be usually achieved by introducing different *N*-substituents on the 1,2-diamine. In addition, the nature of the leaving groups on the dielectrophile can direct formation of the desired products.

1.2.1.1 Intramolecular cyclisation: Route A

The cyclisation of compounds such as **58**, obtained from *N*-benzyl-2-chloro-*N*-(2-oxoethyl)acetamide **57** with primary amines by reductive amination, has been achieved starting from *N*-benzyl ethanolamine **55** (Scheme **8**).

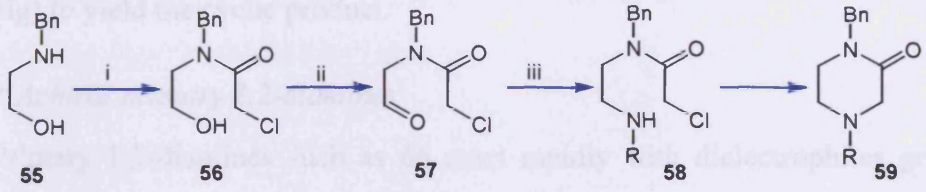

Scheme 8[64]. *Reagents and conditions*: (i) $ClCH_2COCl$, EtOAc, sat. $NaHCO_3$, 0°C, 20 min, 83%; (ii) DMSO, $(COCl)_2$, Et_3N, CH_2Cl_2, -78°C-rt, 45 min, 80%; (iii) R-NH_2, $Na(AcO)_3BH$, 0°C

This approach was also successful when chiral centres were present on the rings. In 1952, L-2-ketopiperazine-5-carboxylic acid **61** was prepared starting from β-chloroacetyl-L-diaminopropionic acid **60**[65]. The latter was obtained by enzymatic hydrolysis of α,β-dichloroacetyl-DL-diaminopropionic acid by hog kidney acylase I (Scheme **9**).

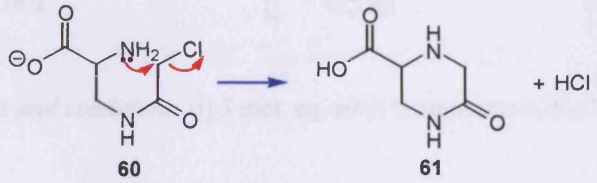

Scheme 9.

This procedure found excellent use for preparation of novel cholecystokinin receptor ligands[66], and especially for the synthesis of the bicyclic piperazine **65**, building block for the synthesis of analogues of HIV protease inhibitors[67] and auxiliaries used to study catalytic asymmetric reactions. Synthesis of the enantiopure **65** was achieved starting from the readily available *N*-Cbz L-proline **62** *via* formation of piperazinone intermediate **64**, obtained by intramolecular nucleophilic displacement of the cyclic amine to the acyl chloride (Scheme **10**). The *N*-chloroacetyl derivative **63** was obtained in four steps *via* formation of a α-azidoester that was consequently reduced to give the desired adduct **63**.

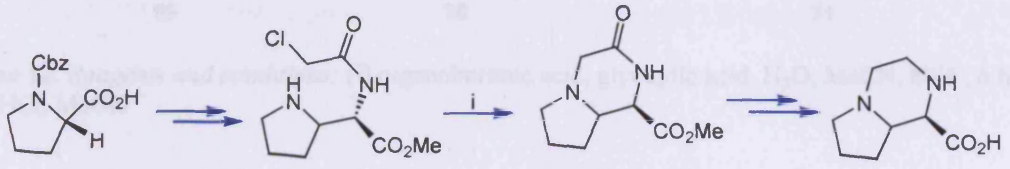

62 **63** **64** **65**

Scheme 10. *Reagents and conditions*: (i) Bu_4NI, Et_3N, DMAP, CH_2Cl_2, reflux, 70%

1.2.1.1 [4 + 2] disconnection: Route B

Condensation of 1,2-diamines with 1,2-dielectrophiles is a reliable method to prepare piperazin-2-ones. The mechanism involves two steps starting from a S_N2 of the amino group to the most reactive electrophilic centre followed by intramolecular $B_{Ac}2$ (6-*exo*-trig) to yield the cyclic product.

1.2.1.2.1 Achiral primary 1,2-diamines

Primary 1,2-diamines such as **66** react rapidly with dielectrophiles giving the fully substituted adducts. It is possible to obtain the piperazin-2-ones **68** only by controlling the moles equivalent of the reacting haloacetate[68,69]. The partially substituted secondary amine gives the intramolecular cyclisation with one aminoacetate arm of the adjacent nitrogen (Scheme **11**).

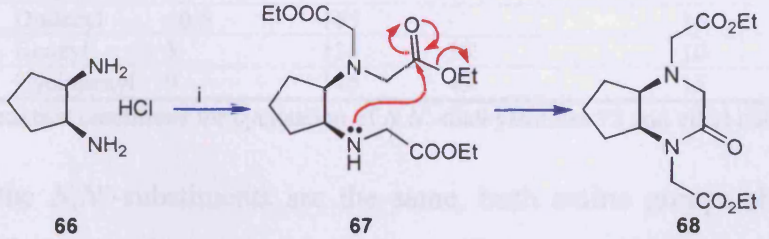

66 **67** **68**

Scheme 11[69]. *Reagents and conditions*: (i) 3 mol. eq. ethyl bromoacetate, K_2CO_3, KI, CH_3CN, 60° C

Primary aromatic 1,2-diamines react slower than the aliphatic ones with 1,2-dielectrophiles, due to the electron withdrawing effect of the phenyl ring. However, Boc monoprotection of the *o*-phenylendiamine **69** is required for the reaction with glyoxylic acid, to yield the piperazinone **71**[70], in order to avoid the formation of disubstituted products (Scheme **12**).

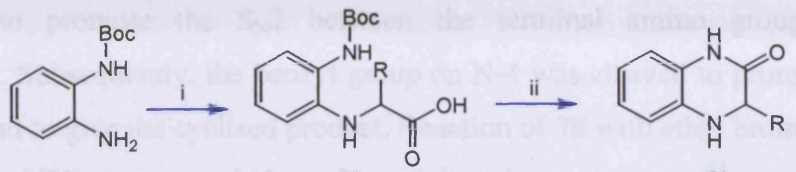

69 **70** **71**

Scheme 12. *Reagents and conditions:* (i) organoboronic acid, glyoxylic acid, H_2O, MeCN, 80°C, 6 h; (ii) conc. HCl, MeOH

1.2.1.2.2 Achiral secondary 1,2-diamines

One of the oldest example of the cyclisation between a *N,N′*-disubstituted-1,2-diamine **72** and ethyl chloroacetate **73** was described in 1899 by Bischoff *et al*[71]. They explored cyclisations using *N,N′*-diaryl derivatives with ethyl chloroacetate in presence of sodium acetate to prepare *N,N′*-diarylmonoketopiperazines. *N,N′*-dialkyl 1,2-diamine cyclisation with the same dielectrophile were reported in 1950. The procedure involved the slow addition of the dielectrophile to the boiling diamine[72], to prepare *N,N′*-dialkylmonoketopiperazines **76a-e** (Table **3**).

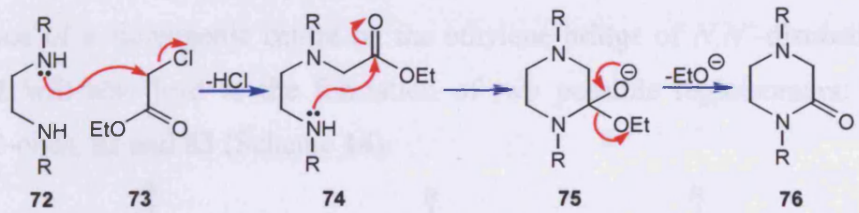

72 **73** **74** **75** **76**

	R	**Time** (h)	**T** (°C)	**72** recovered (%)	**76** (% yield)
a	Butyl	17	165	-	44
b	Octyl	5	145	-	6
c	Dodecyl	10.5	165	-	10
d	Benzyl	5	135	38	10
e	Cyclohexyl	9	145	43	15

Table 3. Reaction conditions for cyclisation of *N,N′*-dialkylamines **72** and ethyl chloroacetate

When the *N,N′*-substituents are the same, both amine groups show the same reactivity and the cyclisation reaction will give only one product. However, when the

substituents are different, the two amines will react differently and in theory, they could give mixture of products.

For instance, preparation of an agonist for h5-HT_{1D} receptor **80**, potential antimigraine agent, was achieved starting from 1,2-diamine and ethyl bromoacetate (Scheme **13**). Selective protection-deprotection sequences of the diamine was required to direct the exclusive formation of **80**. The Boc group was removed first, by treatment with TFA, to promote the S_N2 between the terminal amino group and ethyl bromoacetate. Subsequently, the benzyl group on N-4 was cleaved to promote the $B_{Ac}2$ to the ester and to give the cyclised product. Reaction of **78** with ethyl bromoacetate and then removal of Boc group would have formed the other regioisomer[73].

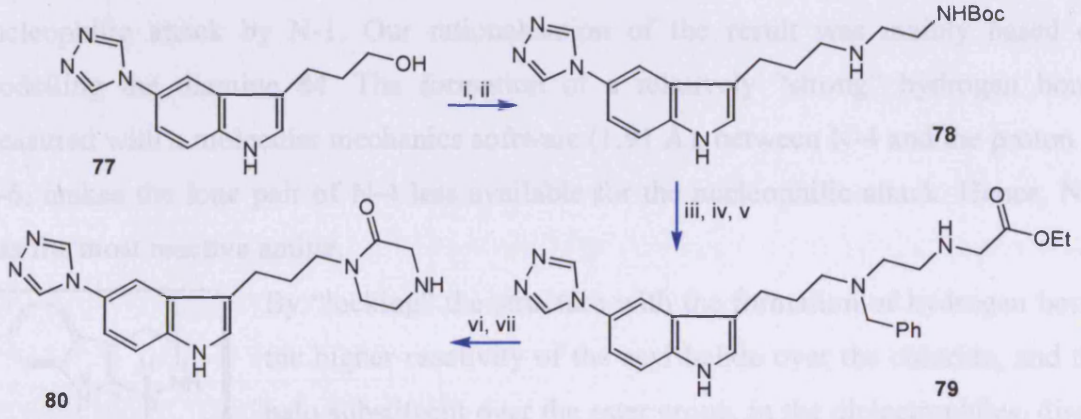

Scheme 13. *Reagents and conditions*: (i) $MeSO_2Cl$, Et_3N, CH_2Cl_2; (ii) 2-aminoethylcarbamic acid *tert*-butyl ester, K_2CO_3, NaI, reflux, IPA; (iii) PhCHO, $NaCNBH_3$, MeOH, AcOH; (iv) TFA, CH_2Cl_2; (v) ethyl bromoacetate, K_2CO_3, DMF; (vi) H_2, Pd on C, HCl (aq.), EtOH; (vii) EtOH, reflux

1.2.1.2.3 Secondary 1,2-diamines with one stereogenic centre

The presence of a stereogenic centre on the ethylene bridge of *N,N'*-disubstituted 1,2-diamine **81** will also lead to the formation of two possible regioisomers: 5- and 6-piperazin-2-ones, **82** and **83** (Scheme **14**).

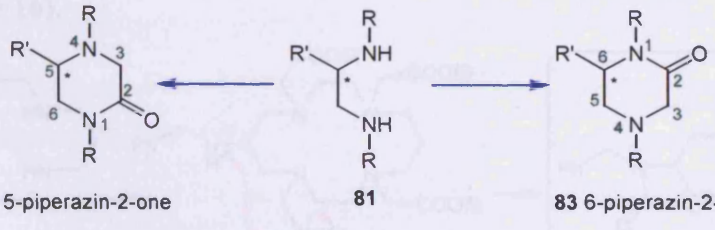

Scheme 14. Piperazinone regioisomers starting from a chiral secondary 1,2-diamine

The presence of a chiral centre could, in principle, modify the reactivity of the amino groups even if the *N,N'*-substituents are the same. Hence formation of one preferential product should be observed. For instance, regioisomers **85** and **86,**

intermediates for the synthesis of β-carbolines, have been prepared reacting the same chiral 1,2-diamine **84** with two different dielectrophiles[74] (Scheme **15**).

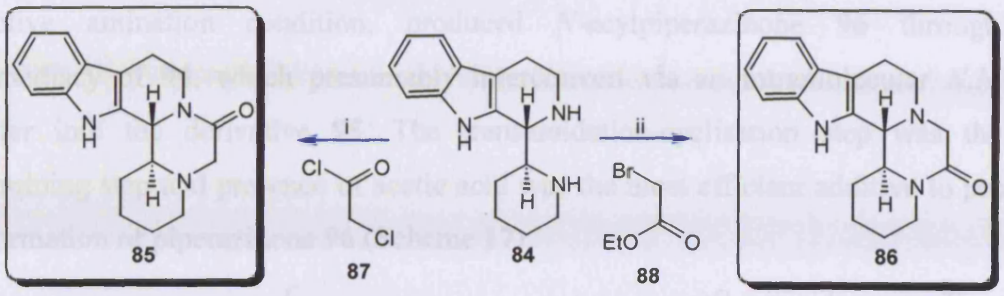

Scheme 15. Haloacetates cyclisations of a chiral 1,2-diamine

The mechanistic pathways for both cyclisations showed that there is preferential nucleophilic attack by N-1. Our rationalisation of the result was mainly based on modelling the diamine **84**. The formation of a relatively "strong" hydrogen bond, measured with a molecular mechanics software (1.91 Å), between N-4 and the proton of N-6, makes the lone pair of N-4 less available for the nucleophilic attack. Hence, N-1 was the most reactive amine.

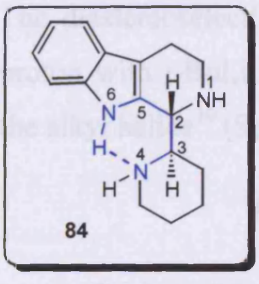

By "locking" the structure with the formation of hydrogen bond, the higher reactivity of the acyl halide over the chloride, and the halo substituent over the ester group, in the dielectrophiles, direct the regioselectivity of these cyclisations.

Preferential attack of one amino group over the other was also observed during the synthesis of macrocyclic compounds[75]. Piperazinone **91** was the exclusive regioisomer formed in the cyclisation step. The cyclic amine attacked the dielectrophile first, followed by intramolecular cyclisation of the acyclic amino group on the ester group. The presence of the chiral centre adjacent to N-1 promoted the higher reactivity of N-4 (Scheme **16**).

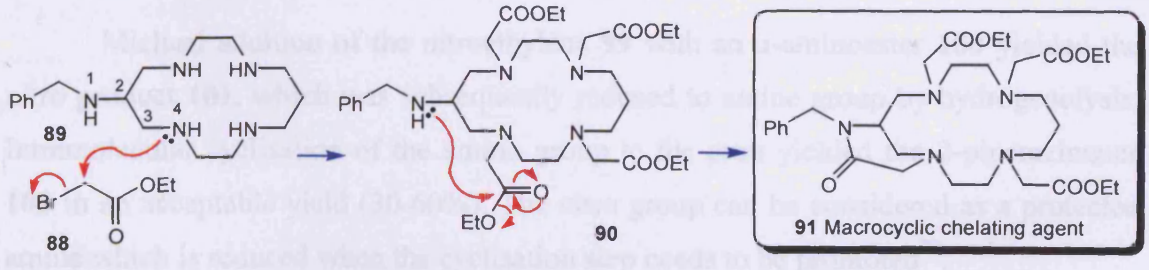

Scheme 16. Preferential attack of N-4 to the dielectrophile **88**

1.2.1.3 [3 + 3] disconnection: Route C

Compounds such as acetamide **92**, when treated with an α-aminoester **93** under reductive amination condition, produced *N*-acylpiperazinone **96** through the intermediacy of **94**, which presumably interconvert via an intramolecular *N,N'*-acyl transfer into the derivative **95**. The transamidation-cyclisation step was the rate determining step and presence of acetic acid was the most efficient additive to promote the formation of piperazinone **96** (Scheme **17**).

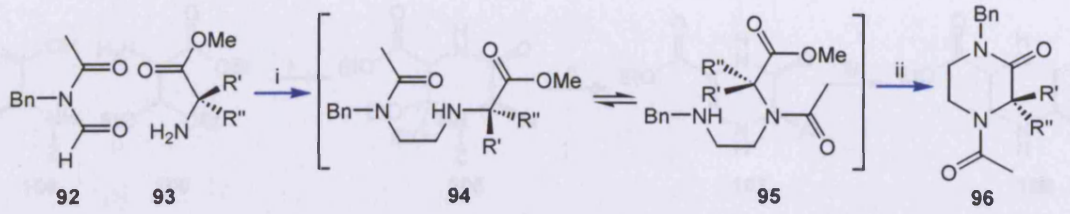

Scheme 17[76]. *Reagents and conditions*: (i) $Na(AcO)_3BH$, acetic acid, 0°C; (ii) Acetic acid, acetonitrile, 40°C, 24 hr

An attractive feature of this synthetic route is that the incorporation of C3-substitution is facilitated by the wide availability of natural and unnatural amino acids. The diastereoselective alkylation of C-3 was also achieved by extracting the α-amide proton with *t*-BuLi, which promoted formation of amide enolate, followed by S_N2 on the alkyl halide[10] (Scheme **18**).

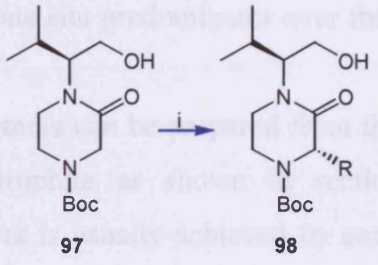

Scheme 18. *Reagents and conditions*: (i) *t*-BuLi, HMPA, RX, 30-90%

1.2.1.3.1 Alternative methods for preparation of 3-substituted piperazin-2-ones

Michael addition of the nitroethylene **99** with an α-aminoester **100** yielded the nitro product **101**, which was subsequently reduced to amine group by hydrogenolysis. Intramolecular cyclisation of the amino group to the ester yielded the 2-piperazinones **103** in an acceptable yield (30-60%). The nitro group can be considered as a protected amine which is reduced when the cyclisation step needs to be promoted[77].

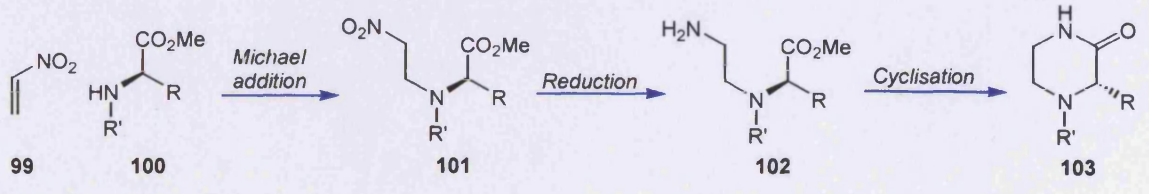

Piperazinone **108**, a peptidomimetic of the neurotransmitter Leu-enkephalin, was prepared in enantiomerically pure form starting from the protected tyrosine **104** with ethyl *N*-(2,2-dimethoxyethyl)glycinate **105** to give the corresponding dipeptide **106** in 80% yield. Further treatment of the acetate with TFA gives the enamine **107**, which is hydrogenated to the piperazinone **108** in 80% yield (Scheme 19)[18].

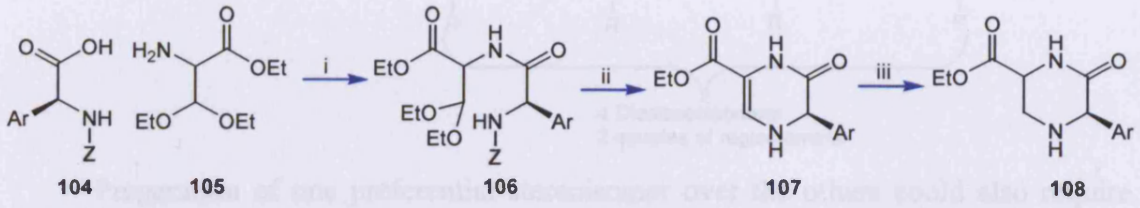

Scheme 19. *Reagents and conditions*: (i) EEDQ/MeOH; (ii) 70% aq. TFA, 2 h; (iii) $Pd(OH)_2$, H_2, HCl, EtOH

1.2.2 Regio- and stereoselectivity in the preparation of chiral piperazinones

A regioselective reaction is one in which one direction of bond making or breaking occurs preferentially over all the other possible directions. Reactions are termed completely (100%) regioselective if the discrimination is complete, or partially, if the product of reaction at one site predominates over the product of reaction at other sites.

Two possible regioisomers can be prepared from the cyclisation of a chiral 1,2-diamine and achiral dielectrophile as shown in section 1.2.1.2.3. Regioselective preparation of the two isomers is usually achieved by controlling the reactivity of the amino groups and by choosing the appropriate dielectrophile. When a chiral 1,2-diamine reacts with a chiral dielectrophile, the control of the stereoselectivity becomes more complex because of the possible formation of four diastereoisomers, as shown in the scheme below.

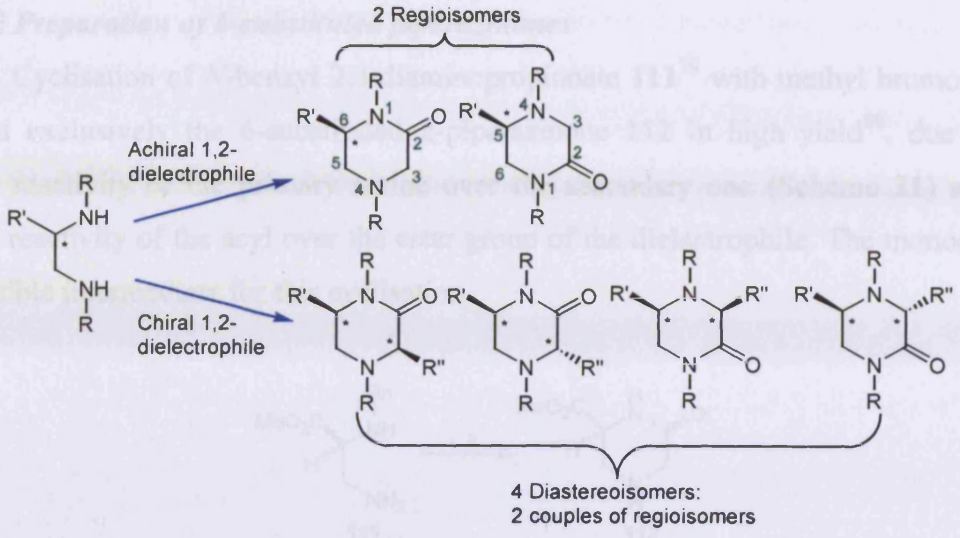

Preparation of one preferential stereoisomer over the others could also require tedious transformations of amines protection-cyclisation-deprotection. In order to summarise, for the asymmetric synthesis of piperazinones, regioselectivity can depend on two main factors:

- Reactivity of the amino groups (level of substitution of the starting material);
- Nature of the leaving groups in the dielectrophiles.

1.2.2.1 Preparation of 5-substituted piperazinones

The use of an amine protection-deprotection sequence is illustrated by the preparation of the 5-substituted piperazinone **110**. The Boc protecting group reduces the reactivity of the primary amine **109** allowing initial reaction of the secondary amine at the acyl bromide terminus of bromoacetyl bromide. Acidic deprotection revealed the primary amine which underwent base induced lactamisation to give exclusively 5-substituted piperazinone **110**; a modest antagonist of the substance P^{23} receptor (Scheme **20**) [78].

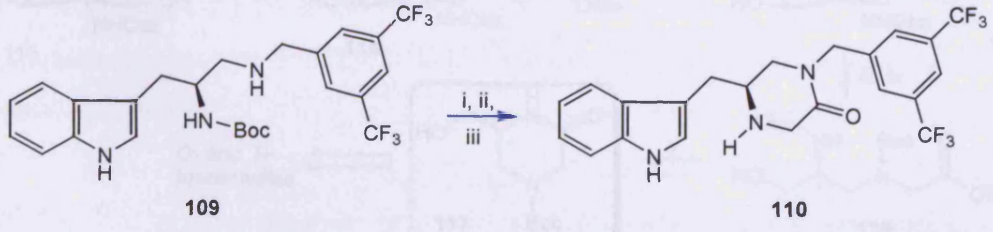

109 **110**

Scheme 20. *Reagents and conditions*: (i) $BrCH_2COBr$; (ii) MeOH, HCl; (iii) K_2CO_3

1.2.2.2 Preparation of 6-substituted piperazinones

Cyclisation of *N*-benzyl 2,3-diaminopropionate **111**[79] with methyl bromoacetate yielded exclusively the 6-substituted 2-piperazinone **112** in high yield[80], due to the higher reactivity of the primary amine over the secondary one (Scheme **21**) and the higher reactivity of the acyl over the ester group of the dielectrophile. The monoester is a plausible intermediate for this cyclisation.

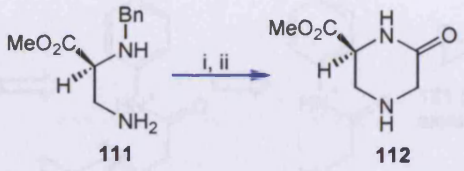

111 **112**

Scheme 21. *Reagents and conditions*: (i) $BrCH_2CO_2Me$, THF; (ii) H_2, Pd-C, MeOH

6-Hydroxymethyl piperazin-2-one **117** was obtained in 5 steps sequence starting from Cbz-D-glucosamine **113**. Protection of the newly generated secondary amine with Boc_2O is essential for the final cyclisation step in order to prevent attack of the reactive secondary amine to the ester. Selective removal of the protecting groups (Cbz and Boc) was indispensable for the preparation of only one product. Oxidative cleavage of the polyol **115** with sodium periodate and reduction of the aldehyde by sodium borohydride yielded the aminoalcohol **116** in high yield (87%). The piperazinone **117** was obtained through removal of Cbz group and spontaneous intramolecular cyclisation. The stereochemistry of the chiral centre at position 6, in the final product, is preserved during all the transformations (Scheme **22**). The piperazinone **117** could be further transformed in other target molecules, mimetics of the RGD (Arg-Gly-Asp) motif[22].

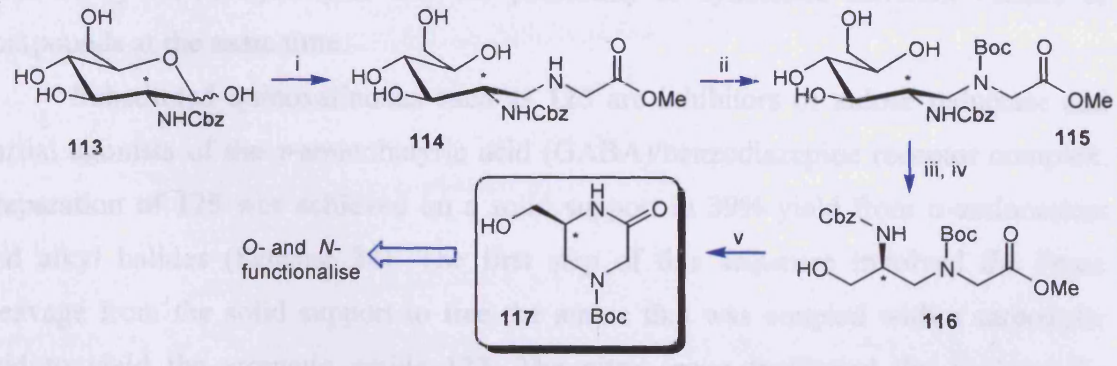

113 **114** **115** **116** **117**

Scheme 22. *Reagents and conditions*: (i) Gly-OMe-HCl, $NaCNBH_3$, MeOH, reflux; (ii) Boc_2O, MeOH; (iii) $NaIO_4$, H_2O; (iv) $NaBH_4$, EtOH; (v) H_2, Pd/C, MeOH

The synthesis of piperazinone **117** could also be acheived using an alternative retrosynthetic approach, involving the cleavage of N1-C6 bond and a further cleavage of N4-C5 bond. The main backbone was the α-aminoacetamide **120** and (*S*)-chloromethyloxirane **121** represented the source of the C6 chiral centre[81] (Scheme **23**). This method was successfully used for the synthesis of potent inhibitors of renin for treatment of hypertension[82,83].

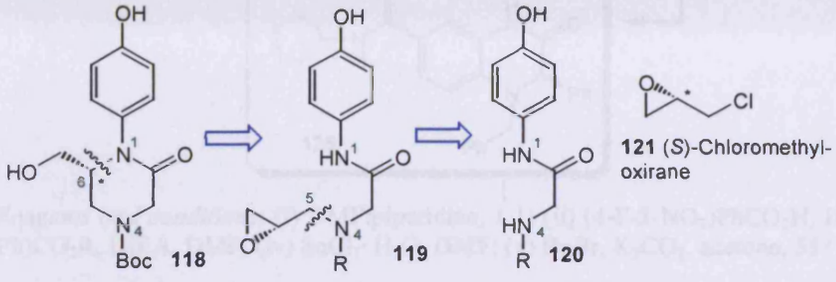

Scheme 23. Intramolecular 6-*exo* cyclisation of amide-epoxide

1.2.2.3 Solid-state synthesis of piperazinones

Solid phase synthesis has been used for the synthesis of β-turn analogues. Product purities achieved were in the range of 70-88%[84,85], starting from cheap starting materials. The use of solid phase synthetic methods has been enormously growing since these procedures allow the preparation of a large range of compounds, from simple peptide libraries to small heterocyclic libraries, usually using inexpensive and readily available starting materials. For instance, 2-oxopiperazines were obtained by the tandem S_N2/Michael addition of amines to unsaturated peptoids. The synthesis was based on the coupling between an FMOC-amino acid to an unsaturated peptoids anchored to the solid support[86]. The key feature of using solid support is the ease of solid support removal by acidic hydrolysis and the possibility to synthesise different classes of compounds at the same time.

Substituted quinoxalinones such as **125** are inhibitors of aldose reductase and partial agonists of the γ-aminobutyric acid (GABA)/benzodiazepine receptor complex. Preparation of **125** was achieved on a solid support in 39% yield from α-aminoesters and alkyl halides (Scheme **24**). The first step of this sequence involved the Fmoc cleavage from the solid support to free the amine that was coupled with a carboxylic acid to yield the aromatic amide **123**. The nitro group facilitated the nucleophilic aromatic substitution to replace the fluoride with an amino acidic residue and was then reduced to a primary amine, which then rapidly participated in intramolecular

cyclisation on the ester group to yield the piperazinone **125**. The secondary amine was then functionalised with a benzyl group[87].

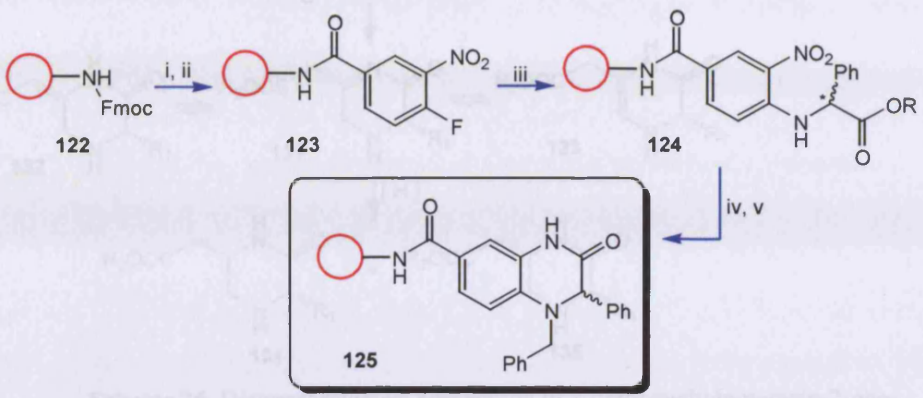

Scheme 24. *Reagents and conditions*: (i) DMF:piperidine, 1:1; (ii) (4-F-3-NO_2)$PhCO_2H$, HATU, DIEA; (iii) $H_2NCH(Ph)CO_2R$, DIEA, DMF; (iv) $SnCl_2 \cdot H_2O$, DMF; (v) BnBr, K_2CO_3, acetone, 55° C

It was also possible to obtain diastereochemically pure compounds, such as **128** and **129,** starting from the same substrate. The pseudopeptide **126** can be *N*-functionalised for example by acylation with chloroacetyl chloride. Deprotection, acid cleavage and a long reflux resulted in cyclisation to form piperazin-2-ones in reasonable yields. Moreover, if the protecting group is Boc, after treatment with trifluoroacetic acid, cyclisation to generate 3,4,6-trisubstituted piperazin-2-one **129** was achieved. Alternatively, if the protecting group is Fmoc, treatment with mild base formed 5-substituted piperazin-2-one **128** on-resin in 35% yield[88] (Scheme **25**).

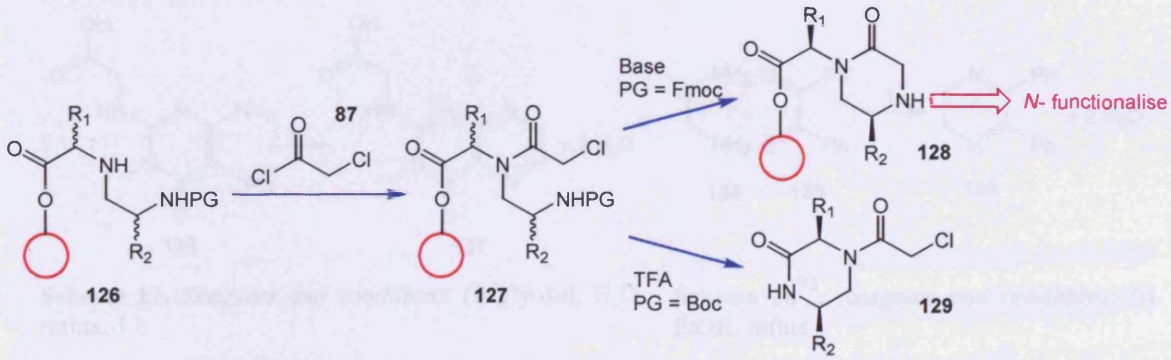

Scheme 25. Alternative cyclisation mechanistic pathways on solid support

Stereoselective reductive amination of β-ketoesters **130** by hydrogenation in presence of palladium on carbon as catalyst yielded 5-carbomethylpiperazin-2-ones **134** and **135**[89]. Removal of the terminal amine protecting group promoted intramolecular cyclisation to the carbonyl group at position 6 (Scheme **26**).

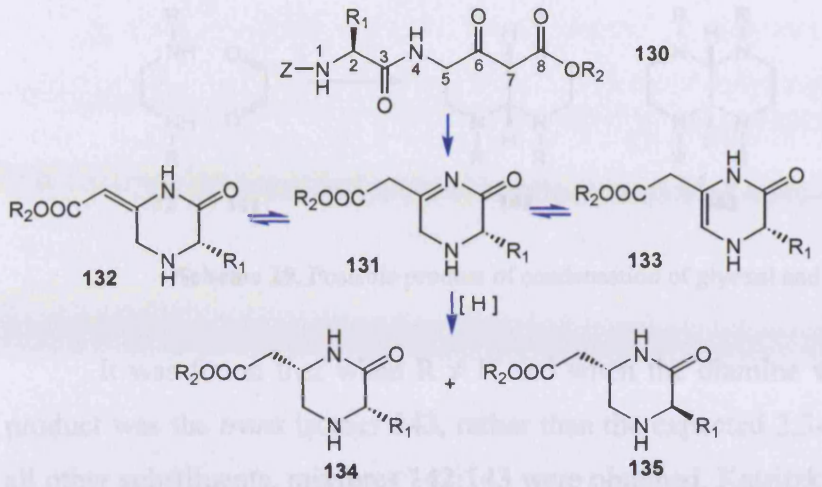

Scheme 26. Diastereoselective preparation of 5-carbomethylpiperazin-2-ones

1.2.3 1,2-Diamines with 1,2-dicarbonyl compounds: Condensation or Cyclisation?

Dielectrophiles such as 1,2-dicarbonyl compounds are used as cyclising agents and they show an interesting behaviour with 1,2-diamine[90]. For instance, aqueous glyoxal and its diphenyl derivative benzil have been largely used in condensation reaction with aromatic and primary aliphatic 1,2-diamines. The major products of these reactions are dehydrated adducts **137** and **140**[91]. The favourable formation of imines intermediates is due to the donation of the lone pair of the nitrogen and consequently loss of water molecules which is the driving force of the reaction (Scheme **27**, **28**).

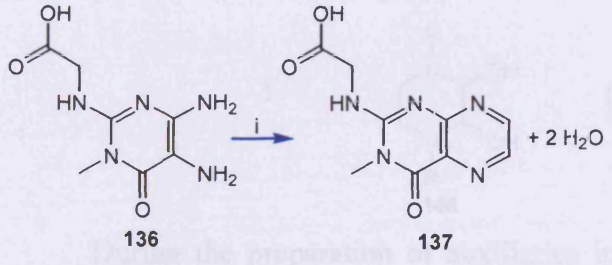

Scheme 27. *Reagents and conditions*: (i) glyoxal, H_2O, reflux, 1 h

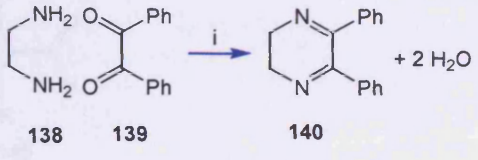

Scheme 28[92]. *Reagents and conditions*: (i) EtOH, reflux

1.2.3.1 Condensation of N,N′-disubstituted ethylenediamine with glyoxal

1,2-Dicarbonyl compounds react rapidly with secondary aliphatic and aromatic 1,2-diamines. Dehydration is not possible and different products can be prepared according to the reaction conditions. Reaction of *N,N′*-disubstituted ethylenediamine **72** with aqueous glyoxal can give three different products: mixture of cis- and trans-1,4,5,8-tetraazadecalins **142**, **143** and bisimidazolidine **144** (Scheme **29**).

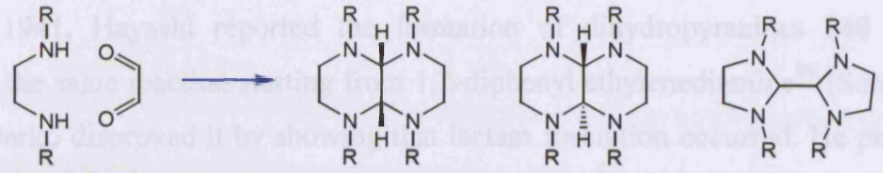

72 141 142 143 144

Scheme 29. Possible product of condensation of glyoxal and 1,2-diamines

It was found that when R ≠ H and when the diamine was in excess, the major product was the *trans* isomer **143**, rather than the expected 2,3-dihydropyrazine[92]. With all other substituents, mixtures **142**:**143** were obtained. Katritzky calculated the energies for the isomerisation of **142** and **143** and showed that the *trans* **143** was the most preferred thermodynamic conformation[93]. When R = Bn, the major product was bisimidazolidine **144** at 0° C. If the reaction was run in refluxing ethanol, a mixture **143**: **144** was formed. Subsequently, Willer and Moore postulated that the initial product of the cyclisation was the kinetic bisimidazolidine **144**[94].

A plausible explanation for the formation of bicyclic products involved the rates with which the intermediate 2,3-dihydroxypiperazines **145** either react with another mole of 1,2-diamine leading to the decalin product **142** and **143**, or undergo rearrangement to the carbaldehyde **146** leading to the bisimidazolidine derivative **144**. By increasing the reaction time or performing the reaction at higher temperature, the kinetic product **144** was slowly converted into the most stable adduct **143**.

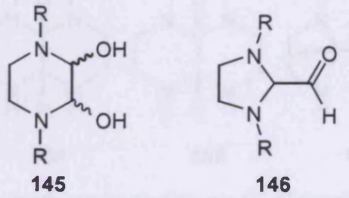

145 146

During the preparation of auxiliaries in asymmetric synthesis based on chiral diamines, reaction between aqueous glyoxal with *N,N'*-disubstituted-1,2-diamines **147**[95] gave preferentially aldehyde-aminals **148**, accompanied by a small amount of the piperazinone **149** (Scheme **30**).

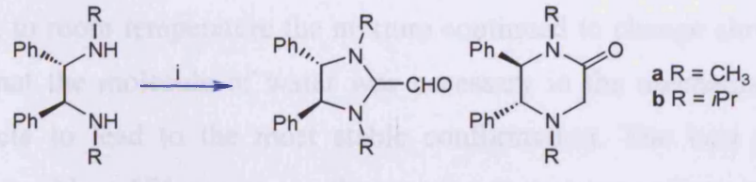

147 148 149

Scheme 30. *Reagents and conditions*: (i) glyoxal, H_2O, CH_2Cl_2

In 1941, Hayashi reported the formation of dihydropyrazines **140** as main product of the same reaction starting from 1,2-diphenyl ethylenediamine[96] (Scheme **31**). In 1971, Darko disproved it by showing that lactam formation occurred. He proposed a mechanism for this cyclisation, involving the formation of a polar intermediate diaminol **150** and an imino alcohol **151**, which by a protonation–deprotonation sequence form the tautomeric lactam **152**[97].

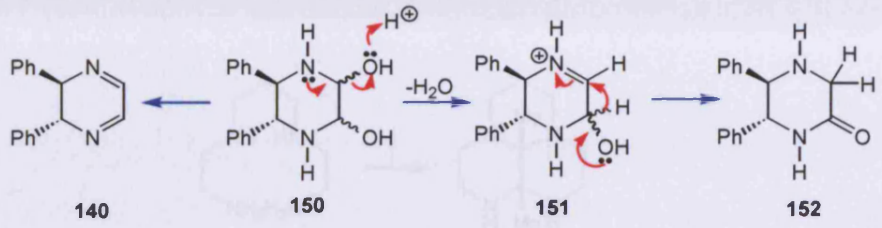

140 **150** **151** **152**

Scheme 31. Preferential elimination of one molecule of H_2O for the formation of piperazinone **152**

1.2.3.2 Condensation of glyoxal with triethylenetetraamine[98]

Theoretically, the condensation of aqueous glyoxal with tetraamine **153** could result in any of the 2,6,9-trimethyl-1,3,6,9-tetraaza-cycloundecane **154**, **155**, and the decahydro-diimidazo[1,2-*a*,2′,1′-*c*]pyrazine **156**, and **157**. Reaction in absolute ethanol at room temperature or in water or in acetonitrile[99] gave **154** and traces of **155**[100]. In water in the presence of calcium hydroxide at 5° C it gave a mixture of pyrazines **156**, **157** (Scheme **32**).

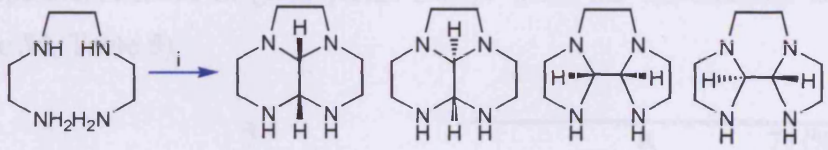

153 **154** **155** **156** **157**

Scheme 32. *Reagents and conditions*: (i) glyoxal, acetonitrile

When aqueous glyoxal was added slowly to a solution of tetraamine **153** at 0° C, formation of the mixture **154:155:156:157** was observed. When the temperature was increased, an irreversible isomerisation of species favouring the isomer **157** was observed. Back to room temperature the mixture continued to change slowly (Table **4**). It was found that the molecule of water was necessary in the mechanism, because it opened the cycle to lead to the most stable conformation. The best procedure for preparing the *cis*-adduct **154** was to run the reaction in presence of traces of water and with prolonged heating before the addition of the dielectrophile. Isomers **156**, **157** were considered to be the kinetic products of the condensation that slowly convert into the more stable thermodynamic geminal derivatives **154** and **155**.

Reaction condition	154	155	156	157
0° C	60	10	10	20
80° C H_2O traces	40	4	6	50
25° C	20	5	10	65

Table 4. Ratio of condensed compounds **154, 155, 156, 157** from ^{13}C-NMR.

Dimethylglyoxal was used in order to prepare C-functionalised tetraazamacrocycles **159** in a similar fashion (Scheme **33**)[101].

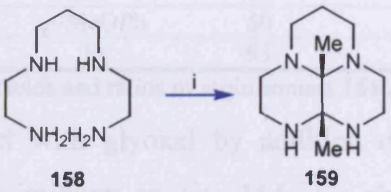

158 **159**

Scheme 33. *Reagents and conditions*: (i) Dimethylglyoxal, CH_3CN, 0° C, 2 h

1.2.3.3 Reaction of N,N′-disubstituted 1,2-diamines and glyoxal[102]

In the previous section, it was shown that the reaction of 1,2-diamines and glyoxal generally gives traces of piperazinones. However, changes and optimisation of the reaction conditions such as solvent, temperature and time, influence the formation of different products. A range of symmetric *N,N′*-disubstituted 1,2-diamines **72** were prepared and reacted with aqueous glyoxal in refluxing water for a maximum of 3 hours to give 2-piperazinones **76** in good yields except when the 1,2-diamine was aromatic **76f** (Scheme **34**, Table **5**).

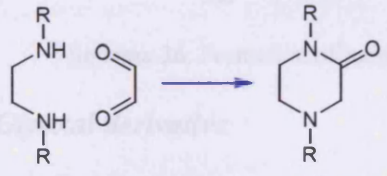

72 **141** **76**

Scheme 33. Cyclisation between *N,N′*-disubstituted 1,2-diamines and glyoxal

	R	76 (%) Yield
f	Me	96.4
g	Et	96.7
h	*i*-Pr	83.8
i	*t*-Bu	68.4
d	Bn	65
l	Ph	10

Table 5. *N,N′*-substituted piperazinones yields

When different substituents were present on the amino groups, reaction with aqueous glyoxal gave mixtures of products. The regioselectivity observed was probably directed by the higher nucleophilicity of aliphatic over aromatic amines. Consequently, 2-piperazinones **161** were major constituents of the **161**:**162** mixtures, which was determined by formation of the most stable iminium ion during cyclisation (Scheme **35**, Table **6**).

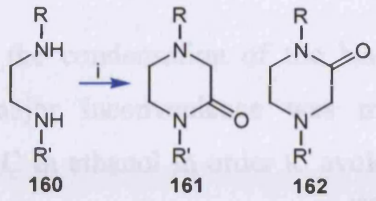

Scheme 35. *Reagents and conditions*: (i) glyoxal, H_2O, reflux, 1-24 h

	R	R´	% Yield	161:162 ratio
a	Me	Ph	90	92:8
b	Et	Ph	95	96:4
c	*n*-Pr	Ph	89	98:2
d	*n*-Bu	Ph	99	98:2
e	Me	*p*-MeOPh	60	75:25
f	Me	Et	93	25:75

Table 6. Yields and ratios of regioisomers **161** and **162**

β-Aminoalcohols react with glyoxal by addition of the amino group to the aldehyde function to give an iminium species **164** in a similar way to 1,2-diamines. However, oxazolidine **165** formation does not occur (cf. **148**) but rather hemiacetal **166** formation. The latter reacts with strong nucleophile (i.e. thiophenol) but otherwise undergo a head-to-tail dimerisation to give the tricyclic product **168**[103] (Scheme **36**).

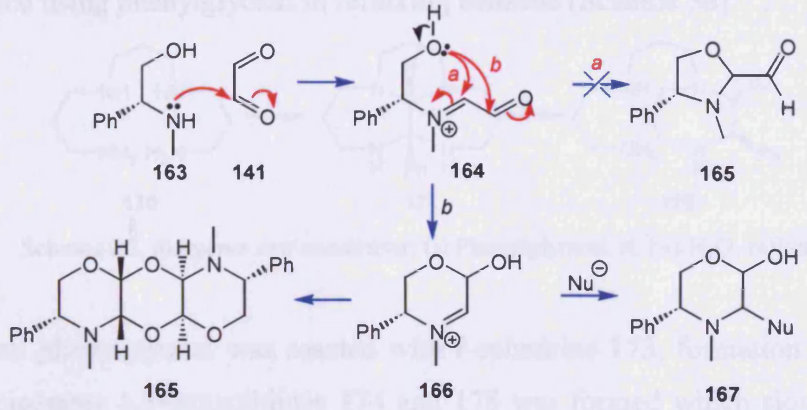

Scheme 36. Formation of iminium ion and different mechanistic pathways

1.2.3.4 Glyoxal derivative

1.2.3.4.1 Methylglyoxal cyclisation

Methylglyoxal has been used as a condensation agent with linear tetramines in order to prepare selectively functionalised tetraazacycloalkanes. The first step of the reaction is the formation of the bis-aminal derivative **159** (Scheme **37**).

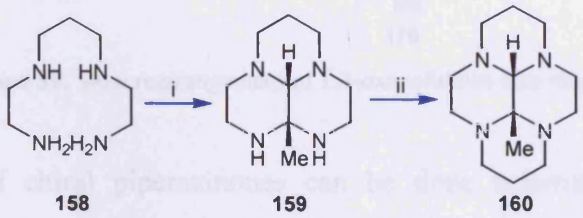

Scheme 37. *Reagents and conditions*: (i) Methylglyoxal; (ii) 1,3-Dibromopropane

The second step is the condensation of the bis-aminal compound with 1,3-dibromopropane[104]. The major inconvenience was methylglyoxal polymerisation. Reactions were run at -10° C in ethanol in order to avoid the polymers formation and also to reduce of any isomerisation of the products[105]. There are no examples of preparation of 3-methyl-2-piperazinone in literature starting from methylglyoxal.

1.2.3.4.2 Phenylglyoxal cyclisation

Reactions of phenylglyoxal with primary aliphatic amines give monoimines whereas reactions with aromatic amines give mixtures of imines, amino-hydroxy-ketones[106].

Phenylglyoxal also reacted with tetramines **170**, in order to prepare bis-aminals **171** at room temperature. In addition, piperazinones **172** can be yielded when the obtained bis-aminals are placed in refluxing water[107]. Bicyclic keto-aminals have also been prepared using phenylglyoxal in refluxing benzene (Scheme **38**)[108].

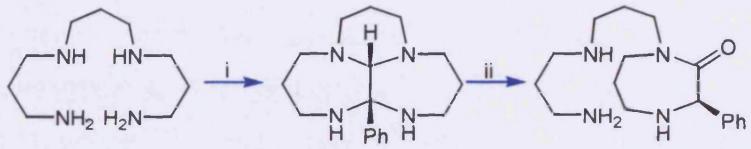

170 **171** **172**

Scheme 38. *Reagents and conditions*: (i) Phenylglyoxal, rt; (ii) H_2O, reflux

When phenylglyoxal was reacted with *l*-ephedrine **173**, formation of a mixture of diastereoisomers 1,3-oxazolidines **174** and **175** was formed which slowly rearrange to the morpholine derivative **176** (35% conversion)[109].

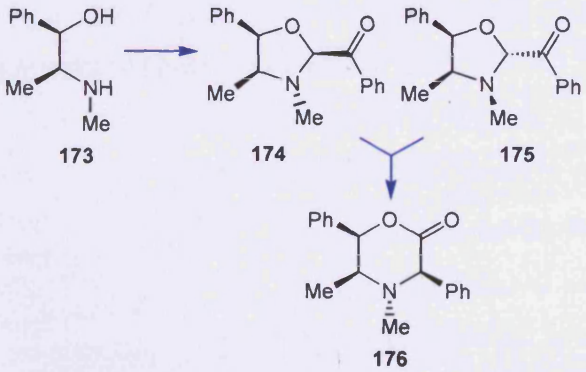

173 **174** **175**

176

Scheme 39. Slow rearrangement of 1,3-oxazolidines into morpholine

Synthesis of chiral piperazinones can be done referring to the morpholine synthesis starting from β-aminoalcohols and phenylglyoxal **177** as observed in Agami

work[103] (Scheme **39**). The higher nucleophilicity of the amino group over the hydroxyl group and the favourable formation of a lactone rather than a lactam lead to the formation of only one product (Scheme **40**)[110].

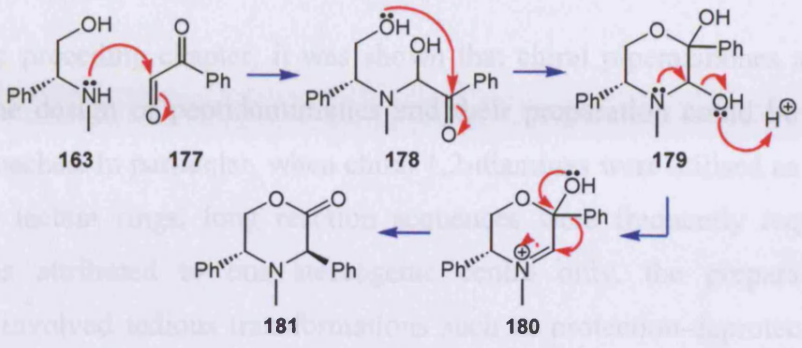

Scheme 40. Mechanistic pathway of phenylglyoxal cyclisation

CHAPTER 2 Synthesis of secondary chiral 1,2-diamines

2.1 Introduction

In the preceding chapter, it was shown that chiral piperazinones are important motifs for the design of peptidomimetics and their preparation could be achieved by several approaches. In particular, when chiral 1,2-diamines were utilised as scaffolds for building the lactam rings, long reaction sequences were frequently required. If the chirality was attributed to one stereogenic centre only, the preparation of one regioisomer involved tedious transformations such as protection-deprotection steps of the reacting diamine and the use of a particular dielectrophile in order to avoid formation of a mixture of products. Increasing the number of chiral centres on the piperazinone rings caused a large number of problems for planning of synthetic routes due to the possibility of formation of many stereoisomers.

For this reason, our attention was focused on the investigation of a novel and simpler way to prepare substituted piperazinones in a regioselective way when only one chiral centre was present, and stereoselectively in the presence of two or more. Moreover, this investigation was strongly related to the final part of my PhD studies, which consisted in the total synthesis of a potential drug for the treatment of Alzheimer's disease.

In particular, a range of (±) chiral *N,N'*-disubstituted 1,2-diamines **182a-e**, with only one stereogenic centre at position 2, was prepared. Subsequently, they were reacted with achiral 1,2-dielectrophiles. Different *N,N'*-substituents were placed on the diamines in order to observe changes of amino group reactivity towards the dielectrophile. The descriptor (±) will be omitted, as it will be assumed that the 1,2-diamines prepared were racemic, unless the stereochemistry is specified.

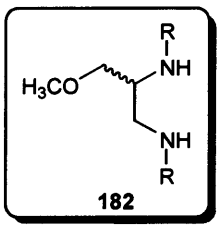

182

	R
a	Benzyl
b	Cyclohexyl
c	2-Methoxyethyl
d	Phenyl
e	*p*-Methoxyphenyl

The methoxymethyl group at position 2 was a fixed component on all the synthesised diamines. Besides being the main substituent of our M_1 muscarinic agonist target, it presented advantages such as easy detection by NMR and easy measurement of the starting material and product ratios.

2.1.1 Retrosynthetic approach for preparation of *N,N'*-disubstituted 1,2-diamines **182**

One of the most logical retrosynthetic approaches for the preparation of our 1,2-diamines **182a-e** involved the cleavage of N1-C2 and C3-N4 to give a dielectrophilic compound **183**. The addition of amines to the latter adduct **183** was well know and easy to achieve *via* formation of a three membered ring intermediate. The intermediate **184** can be prepared starting from the alkene **185** (Scheme **41**).

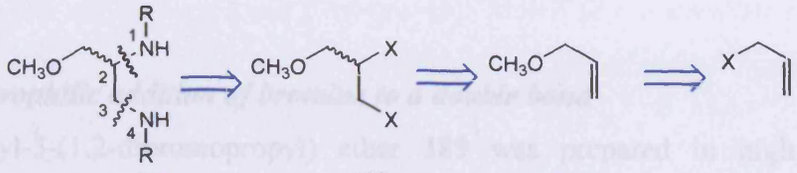

182 **183** **184** **185**

Scheme 41. Retrosynthesis for preparation of diamine **182** (X= Cl, Br)

According to our retrosynthetic approach, preparation of racemic 1,2-diamines was achieved in three steps, starting from the commercially available allyl bromide **186** (Scheme **41**). Initial results within the study on regioselective cyclisations starting from 1,2-diamines run previously in my group (Elsa Garcia Borrell[130], Paul Lewis[111]) showed that this route was successful for the preparation of dibenzyl diamines. The extension of this procedure for the preparation of different 1,2-diamines, with aliphatic or aromatic *N,N'*-substituents was then attempted.

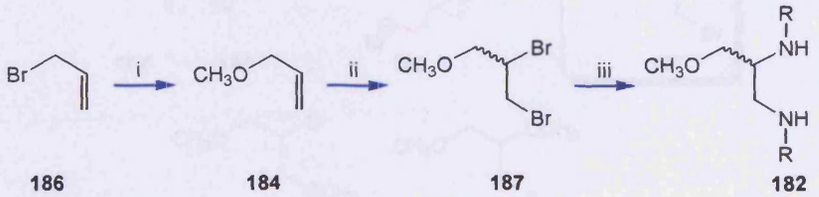

186 **184** **187** **182**

Scheme 42. *Reagents and conditions*: (i) MeONa, MeOH; (ii) Br_2, CH_2Cl_2; (iii) R-NH_2, xylene, *p*-TsOH

The first diamine prepared was the dibenzyl derivative **182a** and it was performed for the first time by EGB. At the beginning of my research project, the preparation of the dibenzyl diamine **182a** was repeated in order to confirm the procedure.

2.1.1.1 Displacement of the bromide by methoxide

Following a literature route[112], reaction of allyl bromide **186** with sodium methoxide in methanol afforded the allyl methyl ether **184** proceeding *via* S_N2 or S_N2' displacements. The desired ether **184** was very volatile with a boiling point of 42° C and

its purification from the reaction mixture, in particular from methanol, was arduous. At least three distillations were required, mainly due to the formation of hydrogen bonds between the ether **184** and methanol. However, traces of methanol were usually present in the final purified ether **184** (65% calculated yield).

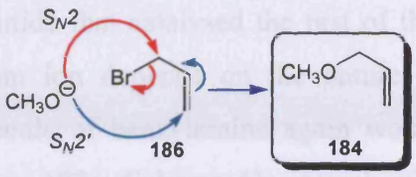

2.1.1.2 Electrophilic addition of bromine to a double bond

Methyl-3-(1,2-dibromopropyl) ether **189** was prepared in high purity and excellent yield (82 %). The mechanism of bromine addition to the alkene bond is well known[113]. It involves two steps starting with the attack of the alkene bond by the electrophile bromine **188**, to form a π-complex, followed by formation of cyclic bromonium ion **189** and finally the nucleophilic attack by bromide. The reaction is an *anti* addition and the rate increases as the degree of substitution of the alkene bond increases. The presence of methanol traces in the ether **184**, could result in formation of by-products such as **190** and **191** but they were not observed.

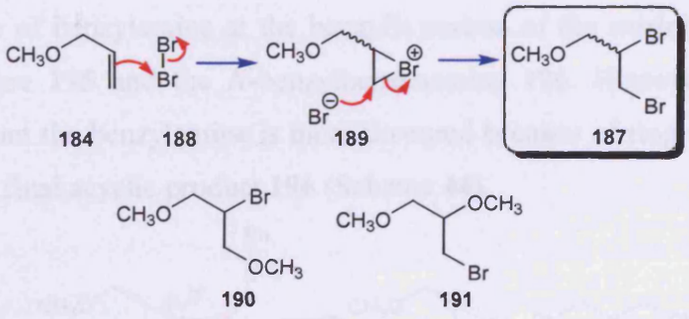

2.1.1.3 S_N2 displacement of the benzylamine to the dibromide 187

The diversity of the diamines **182a-e** is due to the range of amines used in this step. The mechanism is exemplified by the benzyl case. The predicted mechanism S_N2 displacement of the benzylamine **192** to the dibromide **187** involved the attack of benzylamine to displace the primary bromide followed by cyclisation to the intermediate aziridinium ion **194**[114]. The first displacement would occur on the less hindered centre. Both the initial rate of attack and the rate of formation of the aziridinium ion depend on the nucleophilicity of the nitrogen lone pair.

Traces of *p*-toluenesulphonic acid were added to the reaction mixture in order to keep the tertiary amine in the intermediate **194** protonated and ready to be attacked by the second benzylamine, therefore avoiding the formation of a stable aziridine adduct. Traces of the acid were enough to catalyse the first intermediates formed, until formation of hydrogen bromide that catalysed the rest of the reaction. The stability of the intermediate aziridinium ion depends on the nature of the substituents on the nitrogen. The second molecule of benzylamine again would attack the less hindered centre[115] to yield the diamine **182a** (Scheme **43**). Attack of the most hindered position occurs only when a benzylic position is present in the aziridine ring, due to the formation of the most stabilised carbocation[116,117].

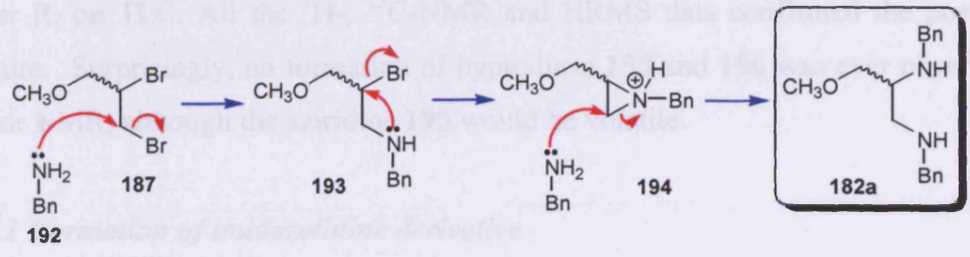

Scheme 43. S_N2 mechanism of the benzylamine to the dibromide

With benzylamine, a potential problem could occur by S_N2 substitution by a second molecule of benzylamine at the benzylic carbon of the aziridinium ion **194**, to form the aziridine **195** and the *N*-benzylbenzenamine **196**. However, attack on the aziridine ring from the benzylamine is more favoured because of ring strain release and formation of the final acyclic product **196** (Scheme **44**).

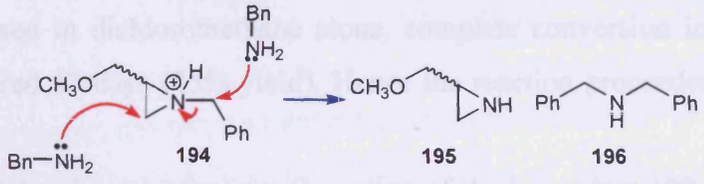

Scheme 44. Secondary S_N2 mechanism

2.2 Aliphatic 1,2-diamines

2.2.1 Synthesis of *N,N'*-dibenzyl-3-methoxy-propane-1,2-diamine 182a

Preparation of *N,N'*-dibenzyl-3-methoxy-propane-1,2-diamine **182a** was carried out using the standard procedure; the slow addition of methyl-3-(1,2-dibromopropyl) ether **187** to a refluxing solution of benzylamine (2.2 equivalents) in xylene, in presence of traces of *p*-toluenesulphonic acid for 24 hours.

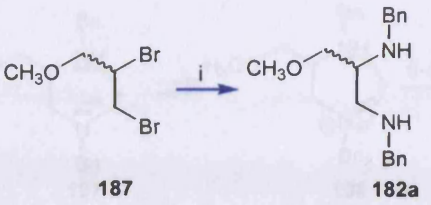

187 182a

Scheme 45. *Reagents and conditions*: (i) $BnNH_2$, xylene, *p*-TsOH

Purification of the 1,2-diamine **182a** from the crude mixture required filtration of benzylamine hydrobromide, extraction from sodium hydroxide solution with ethyl acetate and finally purification by flash chromatography (75%). The major problem consisted in the separation of the 1,2-diamine from the unreacted benzylamine. Flash chromatography was arduous, due to the high polarity of these compounds and to the similar R_f on TLC. All the ^1H-, ^{13}C-NMR and HRMS data confirmed the postulated structure. Surprisingly, no formation of byproducts **195** and **196** was ever observed by TLC or NMR, although the aziridine **195** would be volatile.

2.2.1.1 Formation of imidazolidine derivative

Unexpectedly, basic extraction of the diamine **182a** at pH > 11 from dichloromethane gave another adduct, the imidazolidine derivative **199** (58% yield), formed by nuclophilic substitution of dichloromethane by the diamine. NMR spectra of the crude mixture before the extraction showed the expected signals for the desired compound **182a**, by direct comparison with the standard diamine previously prepared. After extraction, new signals were found in the NMR spectra and TLC displayed a new apolar spot (R_f= 0.23 in petroleum ether: diethyl ether, 1:1). When the dibenzyl diamine **182a** was refluxed in dichloromethane alone, complete conversion into imidazolidine derivative required 13 days (85% yield). Hence the reaction proceeded very quickly at high pH.

The postulated mechanism for formation of the byproduct **199** involves the S_N2 from one amino group to the dichloromethane and intramolecular cyclisation, which could happen in two possible ways: either *via* formation of iminium chloride followed by a 5-*endo*-trig cyclisation, or *via* direct S_N2 of the *N*-chloro derivative in the 5-*exo*-tet mode.

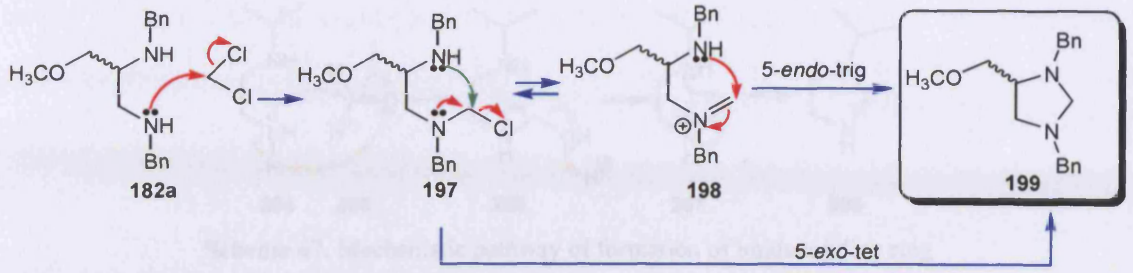

Scheme 46. S_N2 of 1,2-diamine to dichloromethane

Evidence of the formation of *N*-chloromethyl derivative **197** was found in the literature, when pyrrolidine was placed in dichloromethane at room temperature. However, the higher concentration of the iminium chloride **201** than the *N*-chloromethyl derivative **200** in solution was shown by NMR[118].

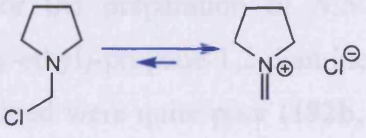

The strongly electrophilic iminium intermediate **202** could easily undergo a fast reaction in presence of a suitable nucleophile inter- or intramolecularly. Bicyclic systems such as pyrroloimidazolone **203** were isolated in high yield by intramolecular S_N2 from the amide amino group to the iminium chloride[119]. The formation of the iminium ion would also justify the 5-*endo*-trig cyclisation, which is not favoured according to Baldwin's rules[120].

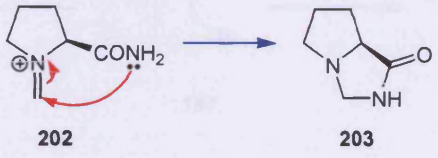

To the best of my knowledge, there is only one example closely related to our case, which reported the formation of imidazolidine rings by direct S_N2 of a 1,2-diamine to dichloromethane[121] by a 1,2-diamine, in presence of potassium carbonate. The procedure required three days in refluxing dichloromethane in order to have complete conversion into the desired product. However, more common procedures are the reactions of 1,2-diamines with formaldehyde. Reaction of *N-iso*-propylethylenediamine **204** with formaldehyde **205**, in presence of magnesium sulphate and potassium carbonate gave the imidazolidine ring **208** in high yield[122] (Scheme **47**). Also in this case, formation of the iminium intermediate allowed the 5-*endo*-trig cyclisation.

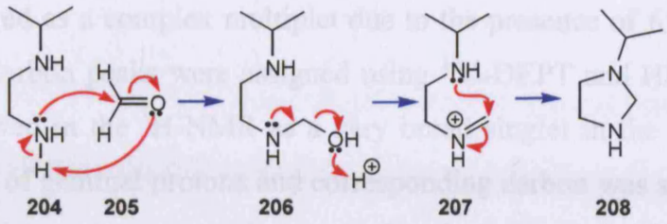

Scheme 47. Mechanistic pathway of formation of imidazolidine ring

2.2.2 Preparation of *N,N′*-dicyclohexyl-pentane-1,2-diamine 182b and 3-methoxy-*N,N′*-bis-(2-methoxy-ethyl)-propane-1,2-diamine 182c

Similarly to the preparation of the benzylamine derivative **182a**, cyclohexylamine **209** and 2-methoxyethylamine **210** were reacted with methyl-3-(1,2-dibromopropyl) ether **187** for the preparation of *N,N′*-dicyclohexyl- **182b** and 3-methoxy-*N,N′*-bis-(2-methoxy-ethyl)-propane-1,2-diamine **182c**, following the standard procedure but the yields obtained were quite poor (**182b**, 25%; **182c** 32%). In the case of the cyclohexylamine displacement, solvent concentration was decreased until the reaction was run in neat cyclohexylamine, but no improvement was achieved. ^{1}H-NMR spectra of the crude mixtures showed a mixture of compounds, which was purified by flash chromatography resulting in pure diamine **182b**.

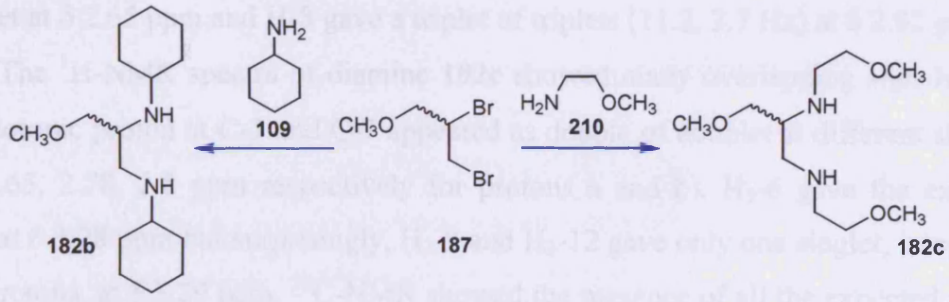

In case of the 2-methoxyethylamine, purification was not required because the ^{1}H-NMR spectra and TLC of the crude mixture after 24 hours in refluxing toluene only showed one compound. Extraction of the adduct **182c** after basic washes was arduous, due to the high water solubility of this diamine. Dichloromethane, chloroform and ethyl acetate were all used as extracting solvent but the highest yield obtained was 32%.

2.2.3 Proof of the structures for chiral 1,2-diamines

Each diastereotopic proton, H_2-3 and H_2-5 appeared as a double of doublet (dd) at different chemical shifts (mostly between 3-4 ppm) in the ^{1}H-NMR. H_3-6 was a singlet (s) at around 3.3 ppm and it was our guide signal for measurement of protons

ratios. H-2 appeared as a complex multiplet due to the presence of four non-equivalent vicinal protons. Carbon peaks were assigned using ^{13}C-DEPT and HMBC spectra. NH peaks were observed in the ^{1}H-NMR as a very broad singlet in the downfield region. Direct correlation of geminal protons and corresponding carbon was seen in the HMQC ($^{1}J_{H,C}$) spectra and unambiguous assignment of each proton and carbon was achieved using the long-range coupling observed in the HMBC ($^{3}J_{H,C}$) spectra. IR spectra displayed a broad peak at 3400 cm^{-1} which was attributed to NH stretching. The accurate mass peak measurements confirmed the expected molecular ions.

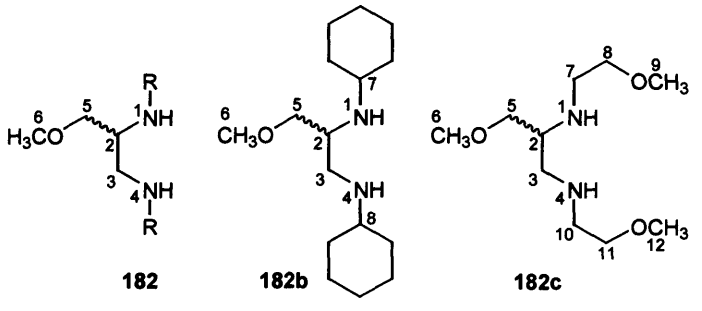

^{1}H-NMR spectra of diamine **182b** showed H_3-6 as a singlet at δ 3.3 ppm and all the other protons of the backbone gave the expected splittings. In particular, H-7 gave a multiplet at δ 2.65 ppm and H-8 gave a triplet of triplets (11.2, 3.7 Hz) at δ 2.92 ppm.

The ^{1}H-NMR spectra of diamine **182c** showed many overlapping signals. Each diastereotopic proton at C-3 and C-7 appeared as double of doublet at different shifts (δ 2.53, 2.65, 2.78, 2.8 ppm respectively for protons a and b). H_3-6 gave the expected singlet at δ 3.28 ppm but surprisingly, H_3-9 and H_3-12 gave only one singlet, integrating to six protons, at δ 3.29 ppm. ^{13}C-NMR showed the presence of all the expected signals and unambiguous assignment was done by HMBC.

2.3 Aromatic 1,2-diamines

2.3.1 Synthesis of aniline- and *p*-methoxyaniline derivatives

Methyl 3-(1,2-dibromopropyl) ether **187** was reacted with aniline **211** and *p*-anisidine **212** under similar conditions used for the benzylamine reaction.

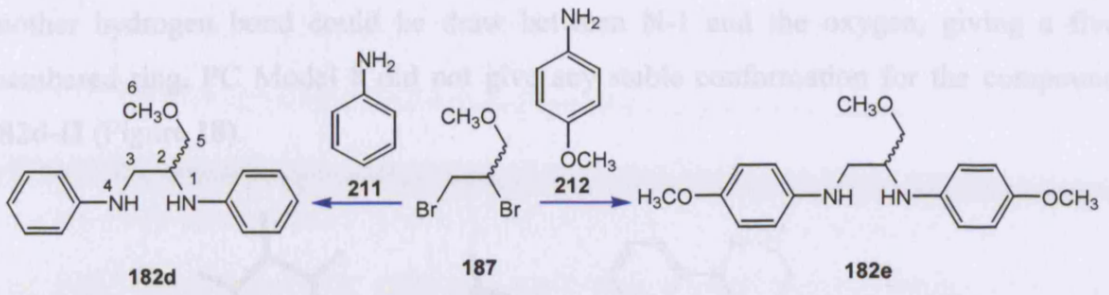

The reaction required 50 hrs in refluxing xylene, compared to the 20 hrs for the benzylamine displacement, due to the expected lesser nucleophilicity of aromatic amines. Longer reaction times and slower addition of the electrophile gave excellent yield of the desired adducts. The reaction progress was easily monitored by TLC, run in ethyl acetate:ethanol, 90:10. The diamines were purified by flash chromatography using a final gradient of ethyl acetate, ethanol for elution (85% yield for both diamines **182d-e**).

2.3.1.1 Methyl N,N'-diphenyl-2,3-diaminopropyl ether 182d

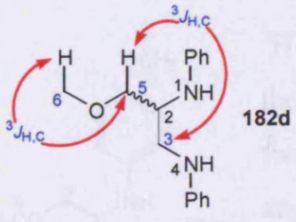

Figure 17. ^{3}J correlations

The singlet for the methoxy group (δ 3.4 ppm) was correlated by ^{3}J to C-5 and H_2-5 were correlated to C-3. Long-range couplings (HMBC) in conjunction with COSY spectra allowed unambiguous assignments for all protons and carbons. Moreover, it allowed avoiding the deep analysis of the complicated multiplet of H-2 (Figure **17**). Many overlapped signals were displayed in the aromatic region and consequently it was not possible to assign them. It was also possible to observe $^{2}J_{H,C}$ correlations between H_2-5 and H_2-3 with C-2.

2.3.1.2 Conformational analysis of methyl N,N'-diphenyl-2,3-diaminopropyl ether 182d

The molecular mechanics calculations for our compounds were done using PC Model 8. The software found the stable conformations according to the lowest energy possible for the structure. The forcefield is called MMX and derived directly from MM3. The most likely conformation for methyl *N,N'*-diphenyl-2,3-diaminopropyl ether **182d** possesses an hydrogen bond between the amino group far from the chiral centre and the oxygen of the methoxy group (PC Model 8) to form a six-membered ring. The hydrogen length was 1.535 Å and the MMX energy found was 18.882 kcal. In principle,

another hydrogen bond could be draw between N-1 and the oxygen, giving a five membered ring. PC Model 8 did not give any stable conformation for the compound **182d-II** (Figure **18**).

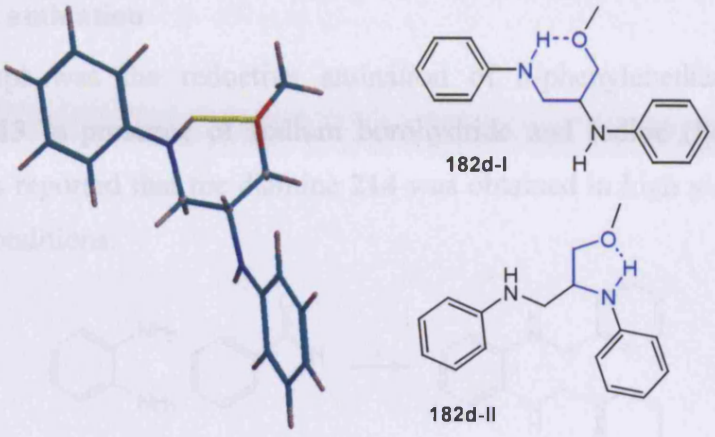

Figure 18. PC Model 8 representation of diamine **182d**

2.3.1.3 Methyl N,N'-di-(p-methoxy)phenyl-2,3-diaminopropyl ether 182e

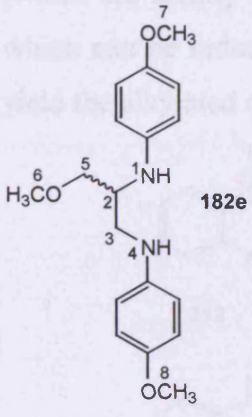

182e

^{1}H- and ^{13}C-NMR data for diamine **182e** were almost the same as those for **182d**, except for the appearance of extra signals for the two methoxy groups on the phenyl rings (δ 3.49, 3.52 ppm, H_3-7 and H_3-8 respectively). The molecular mechanics software (PC Model 8) showed that this compound possessed very low energy state (17.151 kcal) when a hydrogen bond (1.914 Å) was present between the amino group at position 4 and oxygen of methoxy at 5, as seen for the dianilino derivative **182d-I**.

The presence of *p*-methoxyphenyl groups created the same steric effects as the unsubstituted phenyl groups in 173e but the nitrogens could result in slightly higher nucleophilicity, due to the presence of a π-donor.

2.4 Synthesis of achiral secondary 1,2-diamine: N,N'-dibenzylbenzene-1,2-diamine 214

One achiral aromatic 1,2-diamine was also prepared in order to have a substrate that would not give chiral products when cyclisations were attempted. *N,N'*-

dibenzylbenzene-1,2-diamine was chosen for this purpose and two preparative methods were investigated.

2.4.1 Reductive amination

Our first attempt was the reductive amination of *o*-phenylenediamine **212** with benzaldehyde **213** in presence of sodium borohydride and iodine (Scheme **50**)[123] in methanol. It was reported that the diamine **214** was obtained in high yield (78%) under those reaction conditions.

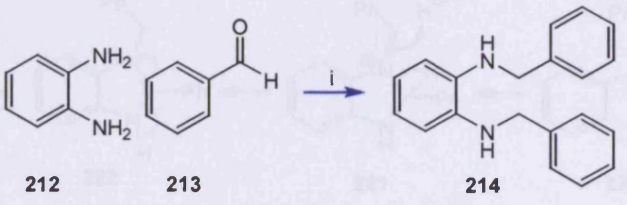

Scheme 50. *Reagents and conditions:* (i) $NaBH_4$, I_2, MeOH

The intended mechanism of the reductive amination involved initial formation of the aminol **215** which should dehydrate to form an imine. Under the reaction conditions, (which are usually weakly acidic to neutral) imines are protonated to form iminium ions which can be reduced with sodium borohydride or sodium triacetoxyborohydride[124] to yield the alkylated amine product **214** (Scheme **49**).

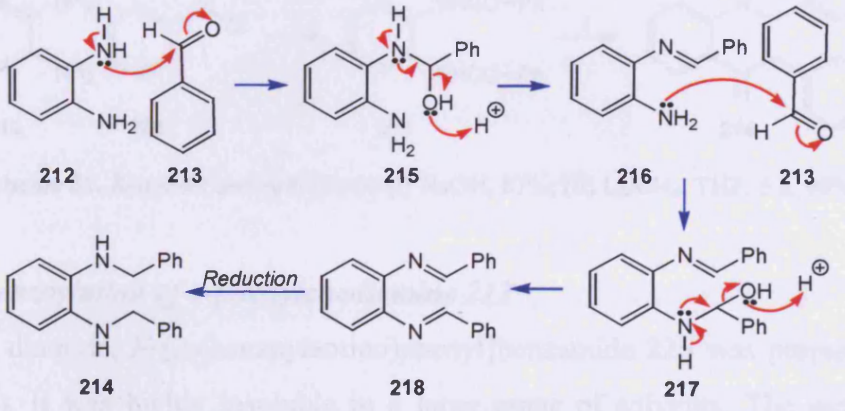

Scheme 49. Mechanism of reductive amination

In our case, reductive amination reaction did not proceed as expected since only traces of the desired diamine **214** were shown by ^{1}H-NMR spectra. TLC showed many spots and purification by flash chromatography gave the byproduct 1-benzyl-2-phenylbenzimidazole derivative **223** (30%) as the main reaction adduct. NMR data were compared with the literature[125] values and they were consistent with the postulated structure, which is derived from a secondary mechanism involving intramolecular

nucleophilic substitution from the primary amine to the carbon bonded to the iminium ion to form a five membered ring intermediate **219**. Further reactions led to formation of the stable adduct **223** (Scheme **50**).

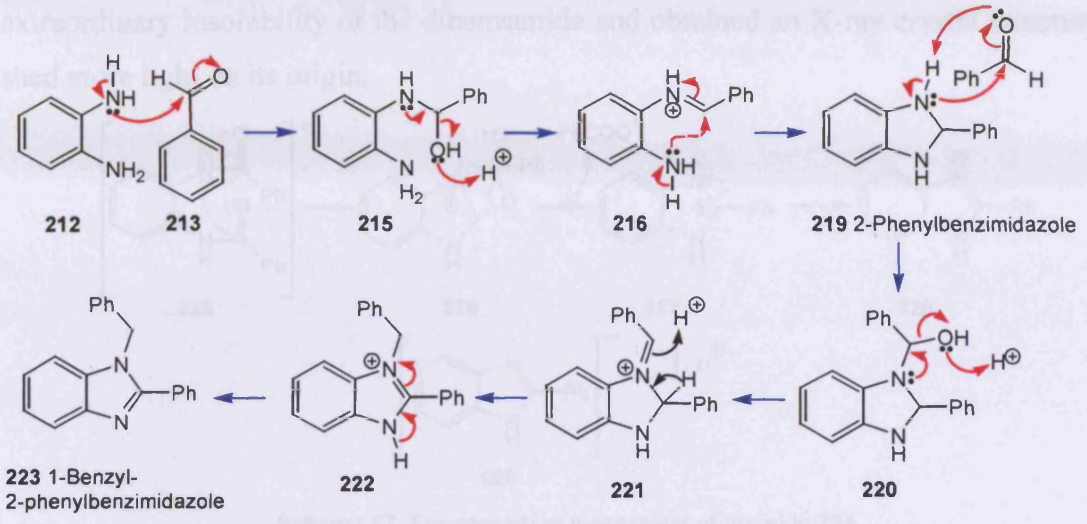

Scheme 48. Mechanism of formation of bicyclic products **219** and **223**

2.4.2 Dibenzoylation-Reduction

The successful procedure was a two-step sequence involving the dibenzoylation of *o*-phenylendiamine **212** followed by reduction with lithium aluminium hydride. *N,N'*-dibenzylbenzene-1,2-diamine **213** was obtained in 85% overall yield[126] (Scheme **51**).

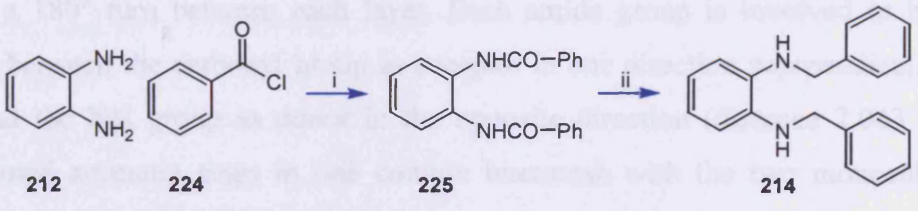

Scheme 51. *Reagents and conditions:* (i) NaOH, 87%; (ii) $LiAlH_4$, THF, 5 h, 98%.

2.4.2.1 Dibenzoylation of o-phenylenediamine 212

The diamide, *N*-[2-(benzoylamino)phenyl]benzamide **225** was prepared in high yield (87%). It was highly insoluble in a large range of solvents. The melting point found was 310° C, which suggested the formation of hydrogen bonds with a rigid structure. When the white solid **225** was crystallised from refluxing DMF, yellow needle crystals were obtained after the solution cooled down. ^{1}H-NMR spectra of the crystals in DMSO showed the presence of 14 aromatic protons and the NH groups at δ 10.5 ppm. ^{13}C-NMR showed the C=O at δ 165.9 ppm and many overlapped signals in the aromatic regions. NMR did not give us much information about this compound but fragmentation found in the mass spectrum (AP+) was quite indicative for this diamide. The main peaks observed were at 317 (48%, M+1), 195 (35%, M- PhCOO·) and 122

(100%, PhCOO·). This data matched the values found in literature[127]. The postulated mechanism of fragmentation is shown below. The loss of the benzoate is favoured and is the driving force of the fragmentation cascade. We were intrigued by the extraordinary insolubility of the dibenzamide and obtained an X-ray crystal structure to shed more light on its origin.

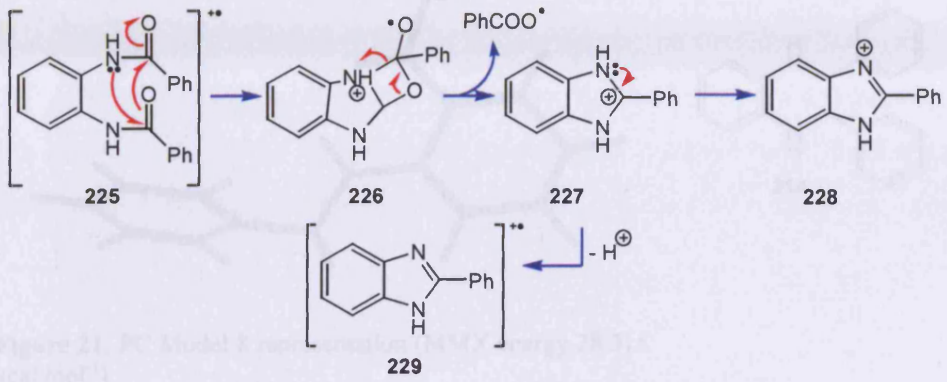

Scheme 52. Fragmentation mechanism of diamide **225**

2.4.2.1.1 X-Ray of crystals of N-[2-(benzoylamino)phenyl]benzamide diamide 225

In the X-ray crystal structure the two monosubstituted aromatic rings and the amide groups lie almost perpendicular to the disubstituted aromatic rings. The dibenzamides are arranged in columns with alternate layers in the same orientation and there is a 180° turn between each layer. Each amide group is involved in hydrogen bonding between the carbonyl group as acceptor in one direction peprpendicular to the plane and the NH group as donor in the opposite direction (distance 2.063 Å). The disubstituted aromatic rings in one column intermesh with the two monosubstituted rings of the adjacent column. The crystal overall consists of alternate layers with the same arrangement of bonding but orientated at 180° to each other (Figure **19**, **20**).

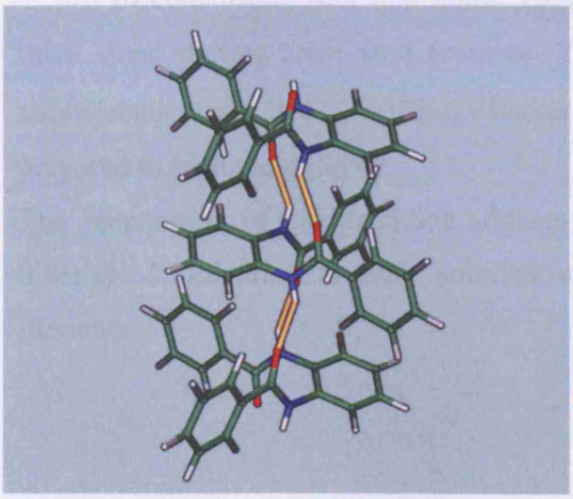

Figure 19. Off angle dibenzoate trimer **225**

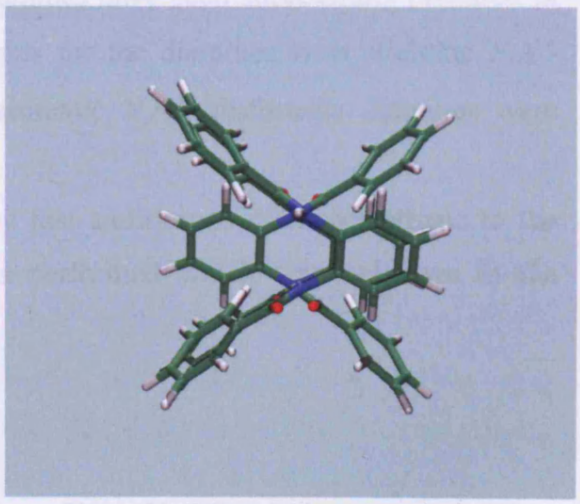

Figure 20. Eclipsed dibenzoate trimer **225**

2.4.2.2 Reduction of the diamide 225 to give N,N'-dibenzylbenzene-1,2-diamine 214

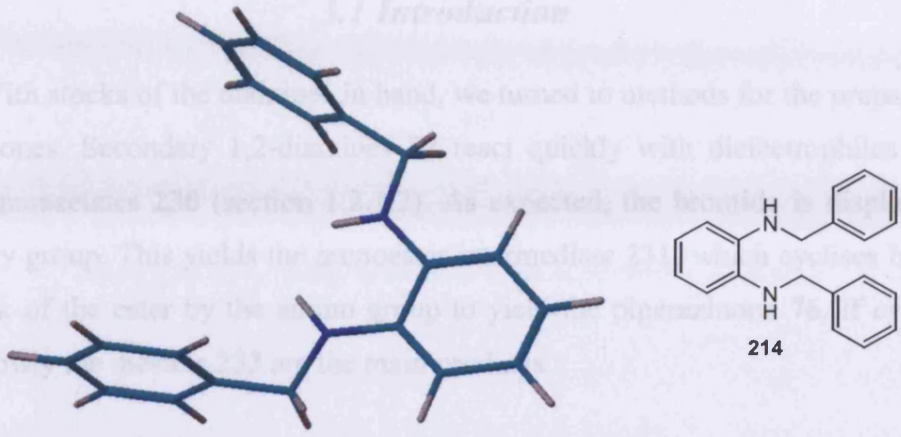

214

Figure 21. PC Model 8 representation (MMX energy 28.315 kcal mol^{-1})

The diamide **225** was successfully reduced using lithium aluminium hydride (4 equivalents) according to a known procedure[128]. The diamine **214** was obtained as an amber clear oil in high yield (98 %). ^{1}H-NMR spectra of the diamine **214** showed only two distinct signals, a doublet (5.8 Hz at δ 4.24 ppm) for the methylene groups and a triplet (5.4 Hz at δ 3.58 ppm) for the amino groups. ^{13}C-NMR showed only one CH_2 at δ 48.84 ppm and many overlapped signals in the aromatic region (111.98- 139.45 ppm). The structure was confirmed by high resolution mass spectrum and by comparison to literature values[129].

2.5 Conclusions

In conclusion, four new chiral 1,2-diamines have been successfully prepared in three steps starting from allyl bromide. Yields for the diamines with aliphatic *N,N'*-substituents were low (25-32%) whereas aromatic *N,N'*-substituents diamines were prepared in high yield (85%).

The preparation of imidazolidine adducts by fast addition of dichloromethane to the dibenzyl 1,2-diamine in basic solution was performed which was unknown in the literature.

Chapter 3 Cyclisation of 1,2-diamines and haloacetates

3.1 Introduction

With stocks of the diamines in hand, we turned to methods for the preparation of piperazinones. Secondary 1,2-diamines **72** react quickly with dielectrophiles such as alkyl bromoacetates **230** (section 1.2.1.2). As expected, the bromide is displaced first the alkoxy group. This yields the monoester intermediate **231**, which cyclises by 6-*exo*-trig attack of the ester by the amino group to yield the piperazinone **76**. If cyclisation occurs slowly the diesters **233** are the main products.

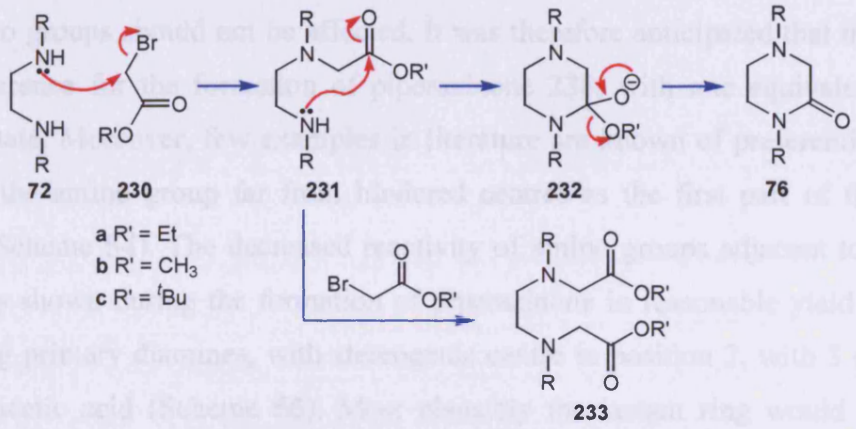

Scheme 53. Mechanism of cyclisation of secondary 1,2-diamine and ethyl bromoacetate

The structure of the alkoxy leaving groups on the ester is crucial for controlling selectivity. With methoxy leaving groups cyclisation to the piperazinone **76** virtually always occurs. Whereas with ethoxy leaving groups, the outcome depends on the temperature and the ratio of diamine to haloacetate. At high temperatures and a 1:1 ratio of diamine to bromoacetate, cyclisation gives the piperazinone **76**, but at 0°C and a high ratio of bromoacetate to diamine (e.g. 5:1) the diesters **233c** are formed. With *t*-butoxy leaving groups, cyclisation seldom if ever occurs and the main products are the diesters **233c**. No significant difference was observed in the reactions of bromo- and chloro-acetates with diamines[130].

3.1.1 Basis of work

When a stereogenic centre is present on the ethylene bridge of the 1,2-diamine **76**, the behaviour of the two amino groups towards the electrophile is different.

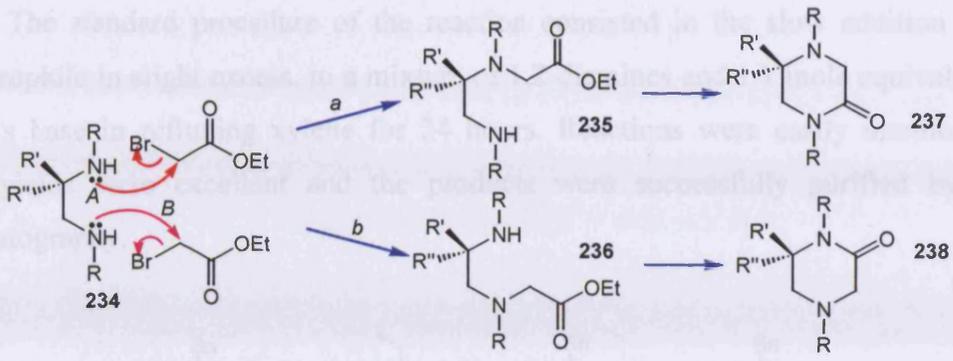

Scheme 54. Possible attacks of the diamines to the ethyl bromoacetate

It was believed that the presence of the chiral centre at position 2 could create a greater steric hindrance effect for N-1 than for N-4 but the nucleophilic character of both amino groups should not be affected. It was therefore anticipated that there should be a preference for the formation of piperazinone **238,** with one equivalent of ethyl bromoacetate. Moreover, few examples in literature are known of preferential or faster attack of the amino group far from hindered centres as the first part of the reaction (route *b*, Scheme **54**). The decreased reactivity of amino groups adjacent to the chiral centre was shown during the formation of piperazinone in reasonable yield (17- 57%) by reacting primary diamines, with stereogenic centre in position 2, with 3 equivalents of bromoacetic acid (Scheme **55**). Most plausibly the lactam ring would form from incomplete carboxymethylation of the nitrogen closest to the phenyl substituent with subsequent ring closure, due to the lower reactivity of N-1[131].

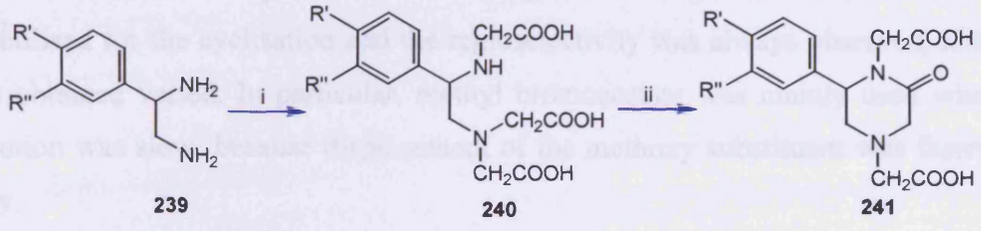

Scheme 55. Carboxymethylation of primary diamines. *Reagents and conditions*: (i) 6 eq. bromoacetic acid, H_2O, $NaHCO_3$, 45°C; (ii) HCl pH= 1

3.1.2 Previous work on cyclisation of *N,N'*-dibenzyl-3-methoxy-propane-1,2-diamine 182a

The cyclisation between *N,N'*-dibenzyl-3-methoxy-propane-1,2-diamine **182a** and ethyl bromoacetate **88** was deeply explored in the past few years in my group by EGB. Surprisingly, regioselective formation of one piperazinone over the other was always observed in all the attempts. Ratios found were ~ 90:10 for **243**:**244** (Table **7**).

The standard procedure of the reaction consisted in the slow addition of the dielectrophile in slight excess, to a mixture of 1,2-diamines and 1.1 mole equivalents of Hunig's base in refluxing xylene for 24 hours. Reactions were easily monitored by TLC, yields were excellent and the products were successfully purified by flash chromatography.

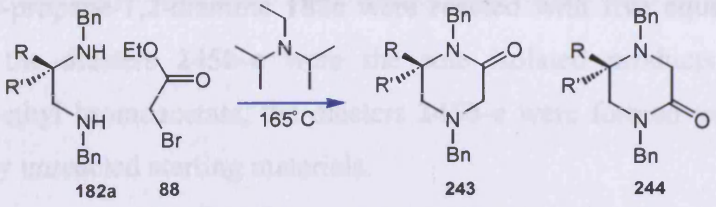

	R	R´	243	244
a	H	CH_2OCH_3	90	10
b	H	CH_3	89	11
c	H	Ph	95	5
d	CH_3	CH_3	80	20

Table 7. Cyclisation results of Elsa G. Borrell *N,N´*-dibenzyl-1,2 diamines with ethyl bromoacetate[130]

Since the two piperazinones **243** and **244** were regioisomers, they showed very similar R_f on TLC, hence the best method to guarantee their separation was to elute the column with a solvent gradient, usually starting from neat petroleum ether and slowly adding diethyl ether. This experiment was the starting point of my project and it was repeated under different conditions until the ratio 96:4 of products **243a**:**244a** was obtained when the reaction was performed at room temperature.

Different dielectrophiles such as methyl bromoacetate and ethyl chloroacetate were utilised for the cyclisation and the regioselectivity was always observed, although yields obtained varied. In particular, methyl bromoacetate was mainly used when the cyclisation was slow, because displacement of the methoxy substituent was faster than ethoxy.

3.2 Aliphatic and aromatic 1,2-diamines

In all the previous examples, benzylamines gave piperazinones regioselectively and in high yield. My investigation was focused on the extension of this procedure to new diamines with aliphatic and aromatic *N,N´*-substituents. Our expectation was to observe preferential formation of one regioisomer over the other, also when the reactivity of the amino groups was modified by the presence of different substituents. It

appeared possible that steric hindrance would have a larger effect with more weakly nucleophilic aromatic amines and hence enhance the regioselectivity.

3.2.1 Cyclisation of aliphatic diamines with ethyl bromoacetate

When *N,N'*-dicyclohexyl-pentane-1,2-diamine **182b** and 3-methoxy-*N,N'*-bis-(2-methoxy-ethyl)-propane-1,2-diamine **182c** were reacted with five equivalents of ethyl bromoacetate, the diesters **245b-c** were the sole isolated products. But with 1.5 equivalents of ethyl bromoacetate, the diesters **245b-c** were formed as main products, accompanied by unreacted starting materials.

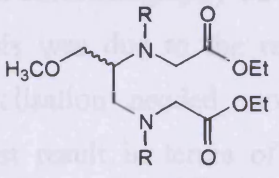

245

b R = C_6H_{11} 65 % yield
c R = $CH_2CH_2OCH_3$ 76% yield

However, when an equimolar amount of methyl bromoacetate was added very slowly to the diamines **182** at reflux, formation of piperazinones **246**, **247** was observed by TLC monitoring. As expected, the piperazinones appeared as close running spots which ran faster than the highly polar starting materials. When the amount of methyl bromoacetate was adjusted and the reaction conditions optimised, a 90:10 ratio of piperazinones **246**, **247** was observed by ^{1}H-NMR spectra of the crude mixtures.

Measurement of ratio was done on the integrations found for the methoxy groups. Upon basic work up and flash chromatography, analytical pure samples were obtained (Table **8**). The aliphatic derivatives **182b** and **182c** showed lower propensity to cyclise than the benzyl analogue **182a** although their reactivity was expected to be similar. This is probably a consequence of their greater flexibility (compared to the benzyl analogues) and hence a lower propensity to adopt conformations suitable for cyclisation.

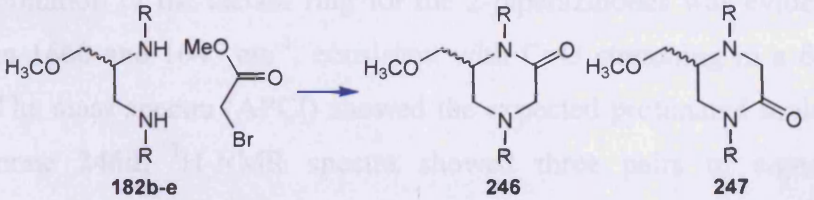

182b-e **246** **247**

	R	Ratio **246**:**247**	Yield **246**, %	Reaction time, hours
b	C_6H_{11}	90:10	75	20
c	$CH_3OCH_2CH_2$	90:10	50	138
d	Ph	90:10	35	140
e	*p*-CH_3OPh	95:5	30 (both)	140

Table 8. Ratio and yields for cyclisations of aliphatic and aromatic diamines **182b-e**

3.2.2 Cyclisation of *N,N'*-diphenyl-3-methoxy-propane-1,2-diamine 182b

The aim of these cyclisations was to determine if the regioselectivity achieved with benzyl and aliphatic diamines was maintained with aromatic diamines which are less nucleophilic. *N,N'*-Diphenyl-3-methoxy-propane-1,2-diamine **182d** was reacted with ethyl bromoacetate **88** according to our standard procedure. The ratio of regioisomers **246d:247d** found in the ^{1}H-NMR spectra of the crude mixture was 90:10.

The reaction was not complete after the standard 24 hours of reflux and the degree of conversion into products was ~30%. At that stage, the ratio of **246d**: **247d** became 92:8. After basic washes and extraction with ethyl acetate, the crude material was purified by flash chromatography but the yields of the two regioisomers were low (30%). Probably, this was due to the reduced nucleophilic character of the aniline derivative. This cyclisation needed more arduous conditions in order to go to completion. The best result in terms of ratio and yields was obtained running the reaction for 140 hours at reflux. The ratio for piperazinones **246d**:**247d** was 90:10. Upon work up and flash chromatography, analytically pure samples were obtained (Table **8**).

When the *p*-methoxyphenyldiamine **182e** was reacted with ethyl bromoacetate, the ratio of **246e**:**247e** found after 24 hours was 95:5. Once again, the crude was purified by flash chromatography but a mixture of regioisomers **246e:247e** was isolated (Table **8**). This represented the most selective cyclisation with ethyl bromoacetate performed at reflux temperature.

3.3 Proof of structure for 2-piperazinones

3.3.1 NMR of *N,N'*-1,4-diaryl-6-methoxymethyl-piperazin-2-one 246d-e

The formation of the lactam ring for the 2-piperazinones was evidenced by IR peaks between 1660 and 1645 cm^{-1}, consistent with C=O stretching in a 6-membered lactam ring. The mass spectra (APCI) showed the expected protonated molecular ions. For piperazinone **246d**, ^{1}H-NMR spectra showed three pairs of signals for the methylene groups: H_2-3 gave two doublets with large coupling constants (17 Hz) at δ 3.8 and 4.1 ppm; H_2-5 gave two double of doublet at δ 3.35 and 4.05 ppm; H_2-7 gave one apparent triplet and one double of doublet at δ 3.3 and 3.55 ppm. H-6 gave a

doublet of quartets and was useful to assign the axial and equatorial positions of each proton in the ring.

The methoxy group gave a sharp singlet at δ 3.21 ppm, which was used for calculation of the aromatic:aliphatic ratio of protons. The ^{13}C-NMR spectra in conjunction with the DEPT data showed three methylene carbons, one CH, one methyl group and one carbonyl group. The highest frequency signal was for C-2 at δ 168.3 ppm. The assignment was based on observation of long-range coupling HMBC, which also resulted to be the only technique useful to distinguish **246d** from its regioisomer. An interesting effect was observed for H_{eq}-5 and H_{eq}-3 which were engaged in a "W" coupling (1.3 Hz).

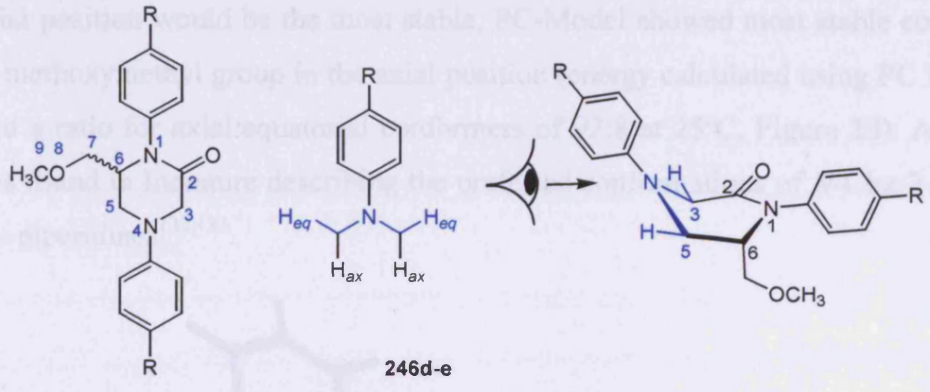

246d-e

Figure 22. "W" coupling constant

Similarly, the ^{1}H-NMR spectra of piperazinone **246e** showed three pairs of signals for the methylene groups at position 3, 5 and 7 and three singlets for methoxy groups at position 9, and those at *para* positions (δ 3.0, 3.39 and 3.43 ppm respectively). H_{eq}-3 showed A "W" coupling with H_{eq}-5 of 1.4 Hz as reported above (cf. **246d**).

3.3.1.1 Conformational analysis of N,N'-1,4-diphenyl-6-methoxymethyl-piperazin-2-one 246d

Piperazinones generally exist as a twisted half chair or sofa conformer. Atoms C-6, N-1 and C2 and the carbonyl oxygen define a plane, which is the "seat of the chair". C3- and C-5 lie just above and below this plane and N-4 is above the plane and constitutes the "back". In principle the substituent at C-6 can be in the axial or the equatorial position, but coupling constant data between H-6 and H_2-5 suggest it is in the axial position. The coupling constants between the signals for H-6 and H-5a or H-5b are 3.3, 2.6 Hz. These low values indicate that H-6 must be in the equatorial position, because in the axial position it would have a large coupling constant with H_{ax}-5. This

was confirmed by molecular modelling and estimation of the coupling constants using PC-Model (Table **9**).

	Coupling constants		
	Observed	Calculated	
	"H-6_{eq}"	H-6_{eq}	H-6_{ax}
H_{ax}-5	3.3	3.48	11.29
H_{eq}-5	2.6	2.09	3.29

Table 9. Coupling constants of vicinal protons observed and estimated by PC-Model 8

Although it might be expected that the conformer with the 6-substituent in the equatorial position would be the most stable, PC-Model showed most stable conformer had the methoxymethyl group in the axial position (energy calculated using PC Model 8 indicated a ratio for axial:equatorial conformers of 92:8 at 25°C, Figure **23**). A similar case was found in literature describing the preferred conformations of *N*-Cbz-2-alkyl-4-hydroxy-piperidines[132,133].

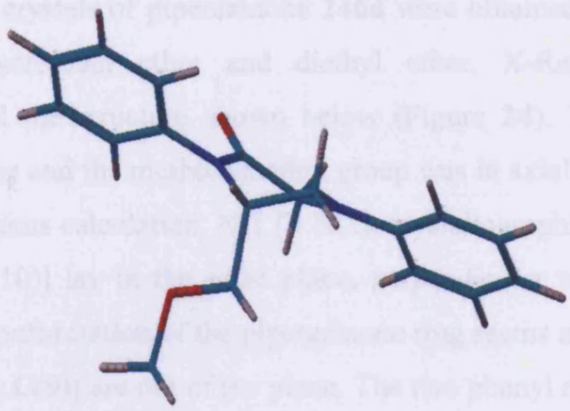

Figure 23. Methoxymethyl group present in the axial position for piperazinone **246d** (MMX Energy 27.559 kcal mol^{-1})

The 6-substituted piperazinone should show a ^3J correlation between the carbonyl group C-2 and H-6. If H-6 was axial, the bond angle between dihedral angle H-6, C-6, N-1, C-2 should have been ~150° (from molecular modelling) which enables a quite strong signal for that correlation. No correlation signal was observed, however this is not definitive because the signal for the H-6 is a broad signal hence it could have not appeared in the $^3J_{H,C}$ because of its low intensity and hence difficult to observe.

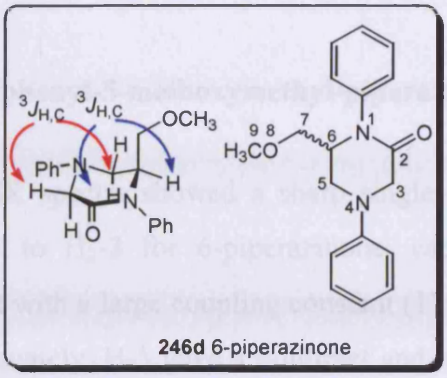

By modelling the piperazinone **246d** with PC Model 8, we found that the energy calculated for methoxymethyl group in the axial:equatorial conformers gave a ratio of 94:6, axial:equatorial at 25°C. This is essentially the same result as in the aniline derivative **246d**.

3.3.1.2 X-Ray Crystallographic data for N,N'-1,4-diphenyl-6-methoxymethyl-piperazin-2-one 246d

Single needle crystals of piperazinone **246d** were obtained by slow evaporation of a mixture of petroleum ether and diethyl ether. X-Ray diffraction crystal determination yielded the structure shown below (Figure **24**). The heterocyclic ring appeared almost planar and the methoxymethyl group was in axial position, as predicted by the coupling constants calculation. N-1 [= N(2), crystallographic numbering], C-2 [= C(8)] and C-6 [= C(10)] lay in the same plane, perpendicular to the adjacent phenyl ring. Therefore, the conformation of the piperazinone ring seems a "sofa" where only C-3 [= C(7)] and C-5 [= C(9)] are out of the plane. The two phenyl rings lay in two planes which are nearly perpendicular to each other.

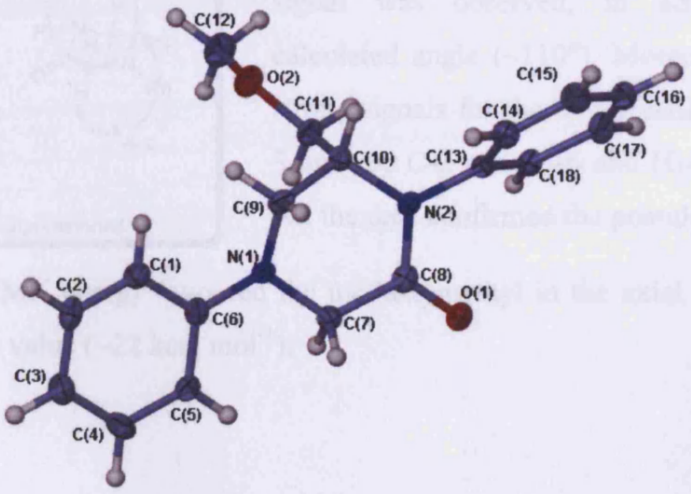

Figure 24. X-Ray Crystal structure of *N,N'*-1,4-diphenyl-6-methoxymethyl-piperazin-2-one **246d**

3.3.2 NMR of *N,N'*-1,4-diphenyl-5-methoxymethyl-piperazin-2-one 247d

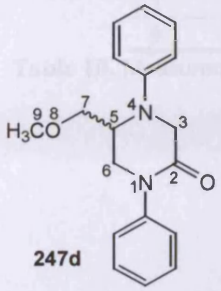

247d

^{1}H-NMR spectra showed a sharp singlet for H_3-9 at δ 3.28 ppm. Similar to H_2-3 for 6-piperazinone, each proton appeared as a doublet with a large coupling constant (17 Hz) at δ 3.9 and 4.1 ppm. Unfortunately, H-5 gave a multiplet and it was overlapped with the doublet of one proton at position 3.

By measuring the coupling constants for H_2-6 and H_2-7, it was postulated that H-5 was equatorial and subsequently the methoxymethyl group was again in the axial position. The coupling constants found for H_2-6 and H_2-7 were small (3.6, 2.4 Hz for H_2-6 to H-5 and (9.5 Hz and 4.5 Hz for H_2-7 to H-5). The large and small coupling constant to H_2-7 indicate that the side chain was fully staggered relative to H-5. The ^{13}C-NMR spectra in conjunction with the DEPT data showed three methylene carbons, one aliphatic CH, one methyl group and one carbonyl group, beside the aromatic CH.

3.3.2.1 Modelling of N,N'-1,4-diphenyl-5-methoxymethyl-piperazin-2-one 247d

According to the angles calculated with PC Model 8, we would have expected one strong signal (172°) and one weak signal (73°) for H_2-6 and C=O. What it was actually seen in the HMBC spectra were two strong signals, probably due to an overlapping of signals of ^{2}J correlation between H_2-3 and C-2.

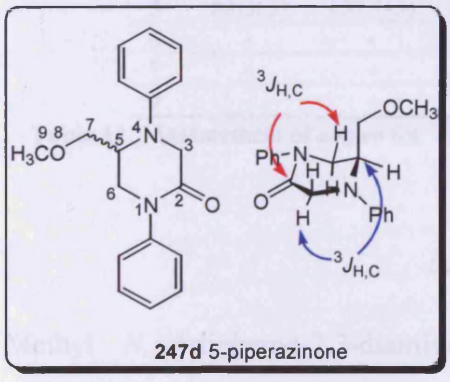

247d 5-piperazinone

Important information was provided by the ^{3}J correlation between H_2-5 and C-3. A very weak signal was observed, in accord with the calculated angle (~110°). Moreover, there were strong signals for the ^{2}J correlation between H_2-3 and the C-2 and H_2-6 and H_2-7 with the C-5. All the data confirmed the postulated structure.

Moreover, the MMX energy favoured the methoxymethyl in the axial position, giving the lowest energy value (~22 kcal mol^{-1}).

C	3-*ax*	3-*eq*	5	6-*ax*	6-*eq*	7a	7b
2	109.8(2)	109.8(2)	-	74.8(3)	167.1(3)	-	-
3	-	-	147.4(3)	-	-	-	-
5	106.5(3)	133.9(3)	-	111.3(2)	111.7(2)	112.6(2)	112.6(2)
6	-	-	110.7(2)	-	-	64.0(3)	177.5(3)
7	-	-	108.1(2)	178.9(3)	61.6(3)	-	-
9	-	-	-	-	-	52.7(3)	61.5(3)

Table 10. Measurement of angles for $^{3}J_{H,C}$ for the methoxymethylene group in the axial position for **247d** (Figure **25**)

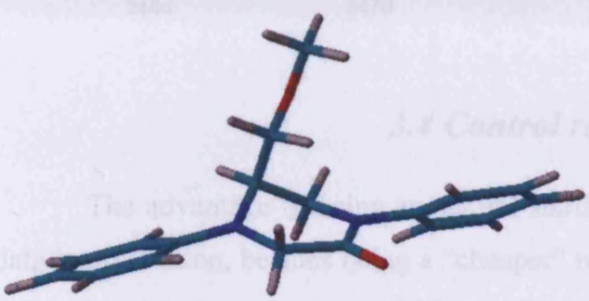

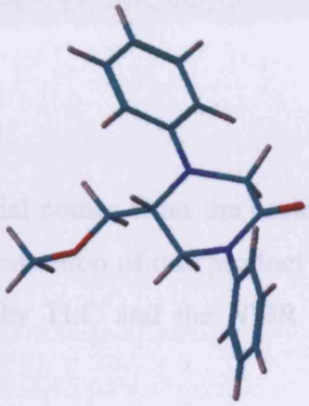

N,N'-1,4-diphenyl-5-methoxymethyl-piperazin-2-one **247d**

Figure 25. Methoxymethyl group in axial position (MMX energy 29.468 kcal mol^{-1})

Figure 26. Methoxymethyl group in equatorial position (MMX Energy 29.541 kcal mol^{-1})

The same angles were also measured for the conformer with methoxymethyl group in equatorial positions in order to have the other possible set of data to compare against the NMR signals.

C	3-*ax*	3-*eq*	5	6-*ax*	6-*eq*	7a	7b
2	108.9(2)	107.3(2)	-	73.3(3)	172.6(3)	-	-
3	-	-	110.7(3)	-	-	-	-
5	83.3(3)	157.1(3)	-	111.3(2)	111.3(2)	112.5(2)	110.0(2)
6	-	-	111.4(2)	-	-	177.8(3)	63.8(3)
7	-	-	109.6(2)	52.6(3)	64.2(3)	-	-
9	-	-	-	-	-	57.6(3)	56.5(3)

Table 11. Measurement of angles for $^{3}J_{H,C}$ for the methoxymethyl group in the equatorial position for **247d** (Figure **26**)

3.3.3 Conclusions

Methyl *N,N'*-diphenyl-2,3-diaminopropyl ether **182d** reacted poorly with ethyl bromoacetate, and the yields of purified compound were low (~30%).

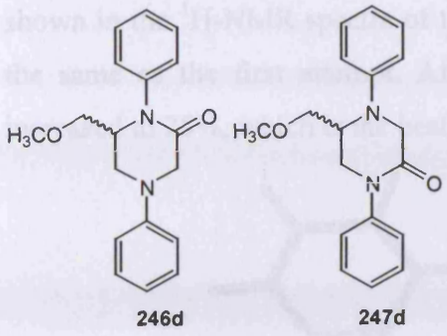

246d 247d

However the ratio of regioisomers observed was 90:10 for **246d**:**247d** hence the reaction was highly regioselective. In order to optimise the standard procedure for aniline derivatives, 1,2-dianilinoethane **72l** was chosen to attempt the cyclisation reactions.

3.4 Control reactions

The advantage of using an achiral starting material comes from the easiness for data interpretation, besides being a "cheaper" reagent. Formation of one product only in the region of piperazinone could be easily monitored by TLC and the NMR spectra would present simpler signals to interpret.

3.4.1 Cyclisation of 1,2-dianilinoethane 72l with methyl bromoacetate 230a

The first attempt for this cyclisation was done placing the diamine **72l** with ethyl bromoacetate for 24 hours in refluxing xylene, according to the standard procedure. After the standard reaction time, TLC and NMR of the crude mixture showed a mixture of products. Upon purification by flash chromatography, 1,4-diphenylpiperazin-2-one **76l** (10%), the diester **248** (33%) and the monoester **249** (31%) derivatives were isolated (Scheme **56**).

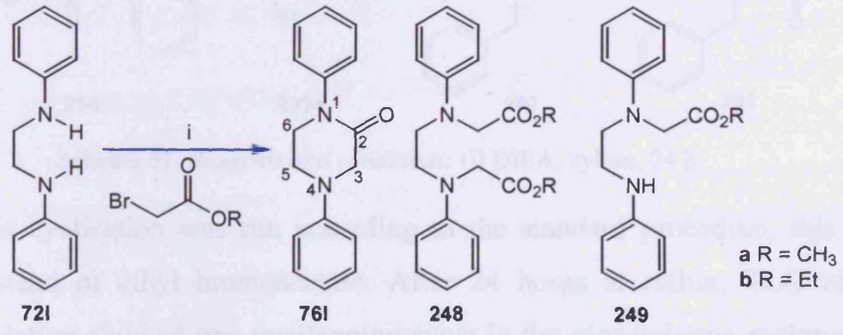

72l 76l 248 249

Scheme 56. *Reagents and conditions:* (i) Methyl or ethyl bromoacetate, DIEA, xylene, 24 h

In order to increase the yield and reduce the formation of the diester **248**, the cyclisation was repeated using methyl instead of ethyl bromoacetate which was added dropwise over 24 hours into the reaction mixture. After 24 hours at reflux, TLC did not show the presence of starting material and formation of the mixture was once again

shown in the ^{1}H-NMR spectra of the crude reaction mixture. The ratio of products was the same as the first attempt. After purification, the yield of piperazinone **76l** was increased to 25%, which is the best result obtained for this cyclisation.

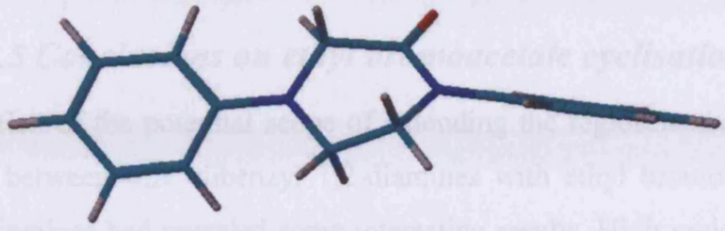

Figure 27. PC Model 8 representation of diphenyl piperazinone **76l**

IR showed a peak at 1690 cm^{-1}, which was slightly higher than the expected value for C=O stretching for a lactam ring. ^{1}H-NMR spectra only showed three kinds of alicyclic signals: H_2-3 appeared as a singlet at δ 4.0 ppm; H_2-5 gave a double of doublet (*J* 5.3, 5.3) at δ 3.8 ppm and H_2-6 gave another double of doublet (*J* 5.5, 5.0) at δ 3.52 ppm.

3.4.2 Cyclisation of *N,N'*-dibenzylbenzene-1,2-diamine with methyl bromoacetate

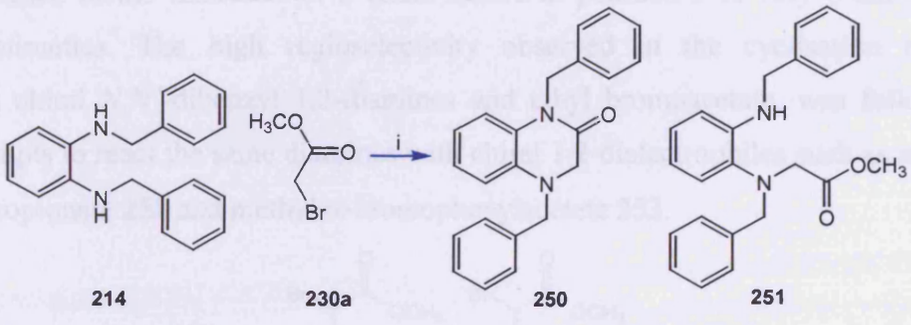

Scheme 57. *Reagents and conditions:* (i) DIEA, xylene, 24 h.

This cyclisation was run according to the standard procedure, this time using methyl instead of ethyl bromoacetate. After 24 hours at reflux, TLC of the crude reaction mixture showed two overlapping spots in the piperazinone region and the ^{1}H-NMR also confirmed a mixture of two components in the ratio 67:33. After flash chromatography, the fastest spot was collected and assigned the structure of the monoester derivative **251** (10% yield) and the slowest spot was the expected piperazinone **250** (70% yield). Absorptions in the infra-red spectrum at 1690 and 1743

cm^{-1} for **251** and **250** were indicative of lactam and ester carbonyl groups respectively. The secondary amine **251**, also gave a broad peak at 3349 cm^{-1} due to NH stretching.

3.5 Conclusions on ethyl bromoacetate cyclisation

Exploration of the potential scope of extending the regioselectivity observed in the cyclisation between *N,N'*-dibenzyl 1,2-diamines with ethyl bromoacetate, to new "non-benzyl" diamines had revealed some interesting results. High regioselectivity was found in all our attempts; therefore its dependency on the presence of the chiral centre was clearly demonstrated. However, the poor conversion of aromatic diamines into products represented a limit for the use of this procedure. In addition, a deep investigation on the stereochemistry and the conformational analysis of these important heterocycles has been completed using a large range of techniques, amongst which the HMBC NMR was the most useful one. Our decision was then to consider again the dibenzyl amines with the prospect of adding a second chiral centre in the piperazinone ring and to observe diastereoselectivity during the formation of products.

3.6 1,2-Diamines and chiral 1,2-dielectrophiles

As described in the introduction a chiral centre at position 3 is very often found in peptidomimetics. The high regioselectivity observed in the cyclisation reactions between chiral *N,N'*-dibenzyl 1,2-diamines and ethyl bromoacetate, was followed by our attempts to react the same diamines with chiral 1,2-dielectrophiles such as methyl 2-bromopropionate **252** and methyl α-bromophenylacetate **253**.

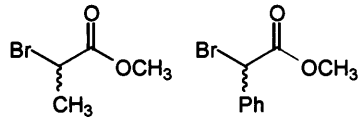

252 **253**

We had reason to think that the addition of an enantiomerically pure dielectrophile to the diamines could afford one diastereoisomer. The experimental method used was the same as the ethyl bromoacetate cyclisation reactions and we postulated the same mechanistic pathway, involving initial S_N2 from the most reactive amine to the most reactive electrophilic centre and intramolecular cyclisation from the second amine to displace the ethoxy group.

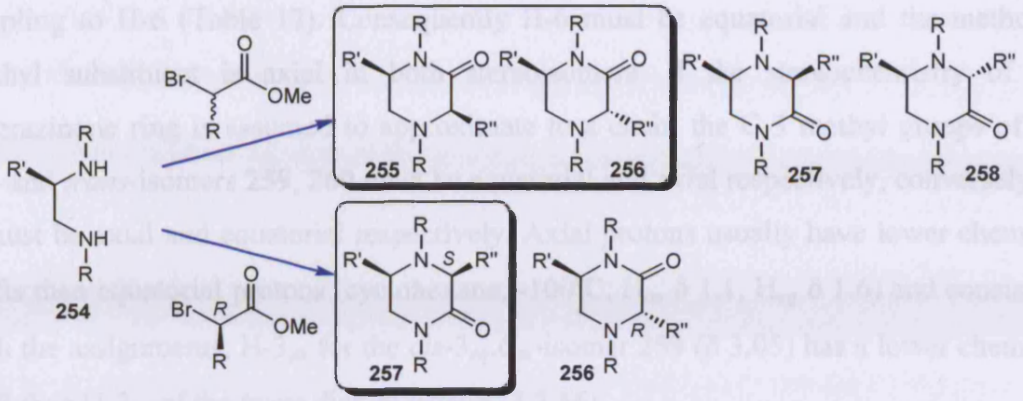

If the dielectrophile were enantiomerically pure and displacement of bromide followed a "pure" S_N2 mechanism a single stereoisomer would result e.g **255** or **257**. The dielectrophiles used in our work were racemic mixtures, consequently at best a mixture of epimers must be formed. However the newly formed chiral centre is adjacent to a carbonyl and hence could be equilibrated to a single thermodynamic product if the energies were favourable.

3.6.1 Methyl 2-bromopropionate cyclisation

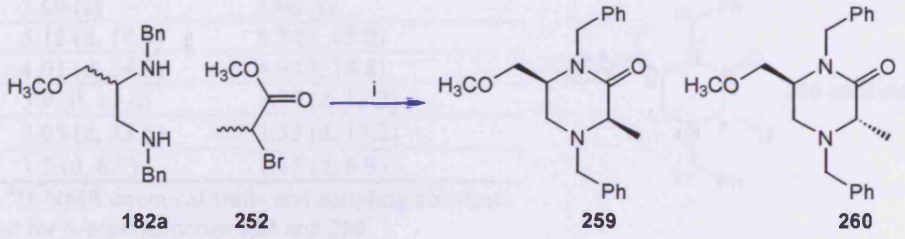

Scheme 58. *Reagents and conditions:* (i) DIEA, xylene, reflux, N_2 atm.

^{1}H-NMR spectra of the crude showed a mixture of compounds with a ratio 50:50, calculated using integration of methoxy groups. Upon basic work up, the ratio of the two adducts became 58:42 and purification by flash chromatography yielded pure sample of the two 6-piperazinone epimers **259**, **260** (30%, 25% respectively). 6-Piperazinone **259** had R_f = 0.51 and 6-piperazinone **260** had R_f = 0.39 in a mixture of petroleum ether:ethyl acetate, 3:1.

3.6.1.1 ^{1}H-NMR data analysis of epimers 259 and 260

The structures of the *cis*- and *trans*-adducts **259**, **260** were assigned on the basis of NMR data which was similar to that reported previously (Table **12**). In each case the splittings for the H-5 protons showed a large geminal coupling and a small vicinal

coupling to H-6 (Table 12). Consequently H-6 must be equatorial and the methoxymethyl substituent is axial in both stereoisomers. If the stereochemistry of the piperazinone ring is assumed to approximate to a chair, the C-3 methyl groups of the *cis*- and *trans*-isomers **259**, **260** must be equatorial and axial respectively, conversely H-3 must be axial and equatorial respectively. Axial protons usually have lower chemical shifts than equatorial protons (cyclohexane, -100°C, H_{ax} δ 1.1, H_{eq} δ 1.6) and consistent with the assignments, H-3_{ax} for the *cis*-3_{eq},6_{ax}-isomer **259** (δ 3.05) has a lower chemical shift than H-3_{eq} of the *trans*-diaxial isomer (δ 3.56).

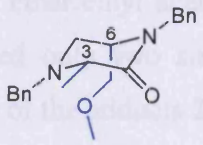

259 *cis*-3_{eq}, 6_{ax}-piperazinone

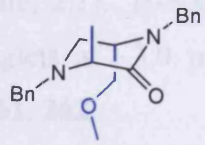

260 *trans-diaxial* piperazinone

Signal	6-*cis*- Piperazinone **259**	6-*trans*-Piperazinone **260**
H-3	3.055 (d, 6.6)	3.56 (obscured)
H-5a	2.7 (dd, 11.9, 2.3)	2.65 (dd, 12.0, 2.1)
H-5b	2.15 (dd, 11.9, 3.3)	2.55 (dd, 12.2, 2.5)
H-6	3.15 (m)	3.15 (m)
H-7a	3.5 (dd, 8.9, 7.6)	3.5 (dd, 8.9, 1.0)
H-7b	3.43 (dd, 9.0, 4.8)	3.4 (dd, 9.0, 3.8)
H_3-9	3.09 (s)	3.06 (s)
H-10a	5.12 (d, 14.9)	5.2 (d, 15.0)
H-10b	4.01 (d, 14.9)	4.0 (d, 14.8)
H-11a	3.9 (d, 13.6)	3.54 (d, 13.2)
H-11b	3.05 (d, 13.5)	3.55 (d, 13.2)
H_3-12	1.5 (d, 6.7)	1.35 (d, 6.9)

Table 12. ^{1}H-NMR chemical shifts and coupling constants comparison for 6-piperazinones **259** and **260**

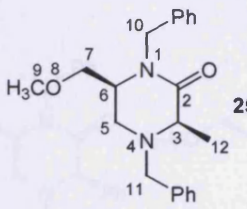

259 *cis*-3_{eq},6_{ax} adduct

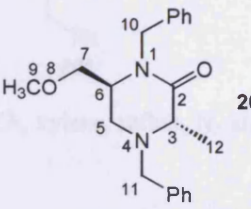

260 *trans-diaxial* adduct

3.6.1.2 Equilibration of 1,4-dibenzyl-6-methoxymethyl-3-methyl-piperazin-2-ones 259 and 260

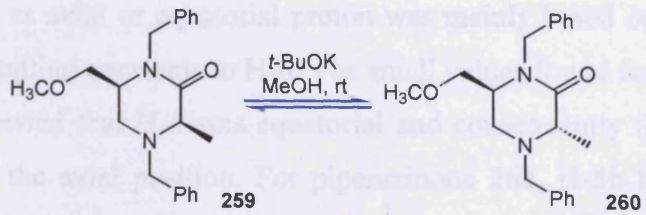

It was anticipated that the thermodynamically more stable 3-epimer could be formed by equilibration with potassium *t*-butoxide in methanol. After 7 days at room temperature the initial 50:50 mixture of piperazinones **259** and **260** was transformed to

69:31 (^{1}H-NMR spectrum). The *cis*-$3_{eq},6_{ax}$- adduct **259** predominated over the *trans*-diaxial adduct **260**, as was found in the phenyl series (section 3.6.2.1).

3.6.2 Methyl α-bromophenylacetate cyclisation

Cyclisation using methyl α-bromophenylacetate was run according to our standard procedure. After 3 hours of reflux, TLC showed the disappearance of the starting diamine and appearance of two running spots with very similar R_f (0.35 for **261** and 0.24 for **262** in petroleum ether:ethyl acetate, 2:1). ^{1}H-NMR spectra of the crude were very complex but showed only two singlets at ~3.0 ppm, in the ratio 50:50 assigned to the methoxy groups of the adducts **261**, **262**.

Only 6-piperazinone diastereoisomers **261**, **262** were isolated by flash chromatography using a slow gradient of petroleum ether to ethyl acetate (25%, 35% respectively). No 5-piperazinone diastereoisomer was observed or isolated in this reaction.

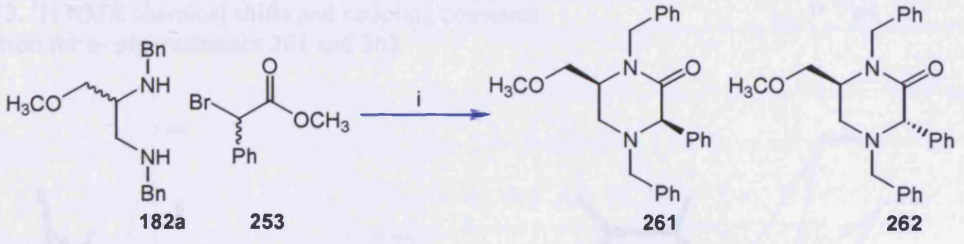

Scheme 59. *Reagents and conditions:* (i) DIEA, xylene, reflux, N_2 atm.

3.6.2.1 ^{1}H-NMR analysis for epimers 261, 262

Similar to the methyl diastereoisomers **259**, **260** described above, the assignment of the stereochemistry for the phenyl derivatives **261**, **262** was complex. Following the same considerations made for the previous piperazinones, analysis of coupling constants and chemical shift values was fundamental for determining the stereochemistry. The assignment of H-6 as axial or equatorial proton was mainly based on the values found for H_2-5 vicinal coupling constants to H-6. The small values found for piperazinone **261** (3.1, 3.5 Hz) suggested that H-6 was equatorial and consequently the methoxymethyl substituent was in the axial position. For piperazinone **262,** H-5b had a large vicinal coupling constant (7.2 Hz) which indicates that H-6 could be axial in this epimer. In this case the complex signal for H-6 was interpretable and confirmed the values assigned for the vicinal coupling constants for H_2-5. In previous assignments, the orientation of H-3 was based on chemical shift, assuming that axial protons are upfield relative to equatorial protons. If this method is used with these stereoisomers, the configurations

are $3_{eq},6_{ax}$ **261** and $3_{ax},6_{eq}$ **262** which are both *cis*, which is clearly impossible! If we accept the arguments for the orientation of the 6-methoxymethyl group, the phenyl groups at C-3 must both be axial or both be equatorial.

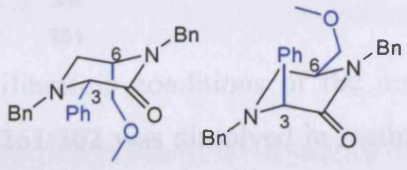

261 $3_{eq},6_{ax}$-piperazinone **261** $3_{ax},6_{eq}$-piperazinone

Signal	6-*cis*-piperazinone **261**	6-*trans*-piperazinone **262**
H-3	4.0 (s)	4.23 (s)
H-5a	3.0 (dd, 11.8, 3.5)	2.85 (dd, 12.2, 4.1)
H-5b	2.03 (dd, 12.1, 3.1)	2.44 (dd, 12.2, 7.2)
H-6	3.3 (m)	3.5 (dddd, 7.2, 5.6, 4.1, 3.6)
H-7a	3.61 (dd, 8.8, 4.5)	3.4 (dd, 9.6, 5.6)
H-7b	3.71 (t, 8.0)	3.25 (dd, 9.7, 3.6)
H_3-9	3.18 (s)	3.09 (s)
H-10a	3.95 (d, 14.8)	4.05 (d, 14.9)
H-10b	5.01 (d, 14.8)	5.25 (d, 14.9)
H-11a	3.71 (d, 13.4)	3.4 (d, 13.6)
H-11b	3.0 (d, 13.4)	3.18 (d, 13.5)

Table 13. ^{1}H NMR chemical shifts and coupling constants comparison for 6- piperazinones **261** and **262**

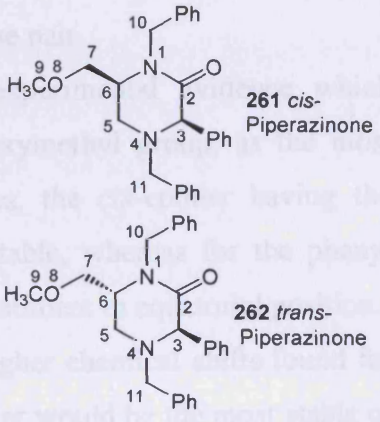

261 *cis*-Piperazinone

262 *trans*-Piperazinone

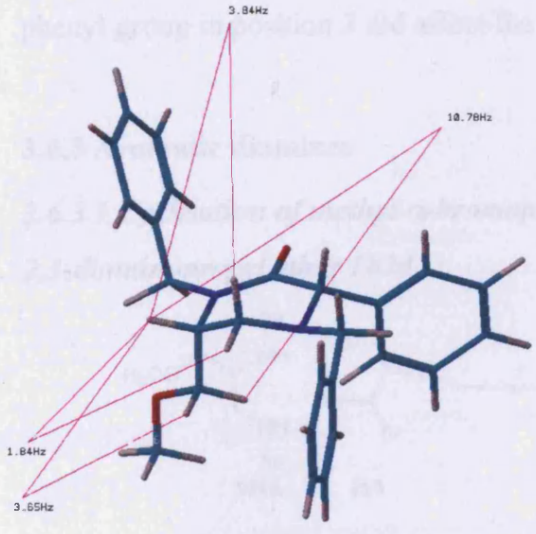

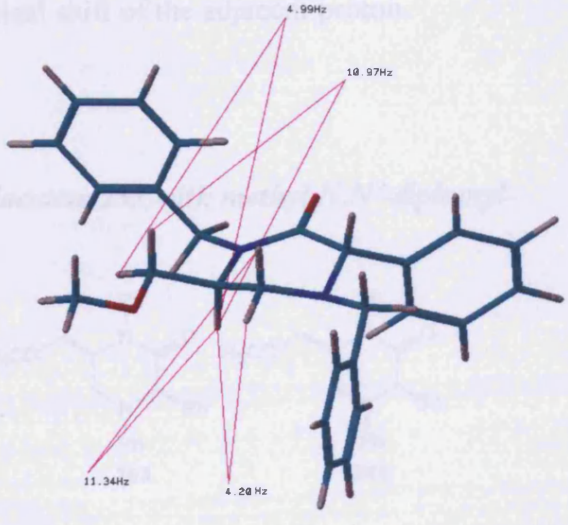

N,N'-dibenzyl-6-methoxymethyl-3-phenyl-piperazin-2-one **261**, **262**

Figure 28. Vicinal coupling constant prediction for H-6 in equatorial position (PC Model 8)

Figure 29. Vicinal coupling constant prediction for H-6 in axial position (PC Model 8)

Prediction of coupling constants values for H-6 with H_2-5 and H_2-7 was done using PC Model 8 (Figure **28**, **29**). We performed equilibration reaction of the pair of epimers in order to establish which conformation was the most stable, trying to find similarities with the previous methyl series (section 3.6.1.2)

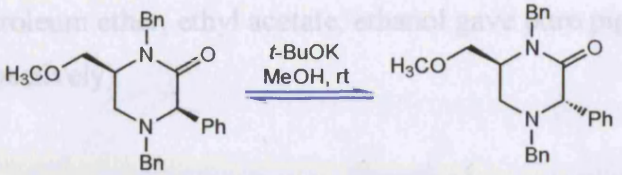

261 **262**

Similar to the equilibration conditions of the methyl derivatives **259**, **260**, a 50:50 mixture of epimers **261**:**262** was dissolved in methanol in presence of potassium *t*-butoxide. After 48 hours at room temperature, the ratio became 16:84 for **261**:**262**. In previous example, the *cis*-3_{eq},6_{ax}-isomer was the most stable, which indicated that in the phenyl series, the epimer **261** should be the preferred of the pair.

Unfortunately this was in contrast with the experimental evidence which indicated the piperazinone **262**, which has a 6_{eq}-methoxymethyl group, as the most stable of the pair. In conclusion, for the methyl series, the *cis*-epimer having the methoxymethyl group in axial position was the most stable, whereas for the phenyl series, the most stable epimer had the methoxymethyl substituent in equatorial position.

If we assume that H-6 is equatorial, due to the higher chemical shifts found for both phenyl epimers **261** and **262**, then *trans-diaxal* epimer would be the most stable of the pair. However, the assignment for H-6 remains unresolved, considering that the phenyl group in position 3 did affect the chemical shift of the adjacent proton.

3.6.3 Aromatic diamines

3.6.3.1 Cyclisation of methyl α-bromophenylacetate 253 with methyl N,N′-diphenyl-2,3-diaminopropyl ether 182d

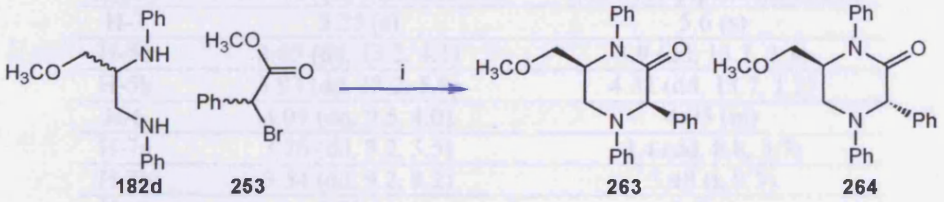

182d **253** **263** **264**

Scheme 60. *Reagents and conditions:* (i) DIEA, xylene, reflux, N_2 atm.

Cyclisation of methyl *N,N′*-diphenyl-2,3-diaminopropyl ether **182d** with methyl α-bromophenylacetate **253** was attempted. From the previous cyclisations performed with the aniline derivative **182d**, it was clearly established that longer reaction times were required to promote the cyclisation step, due to the lesser nucleophilicity of the aromatic amines. After 48 hours of reflux, a 50:50 mixture of two components was observed in the ^{1}H-NMR spectrum. Purification by column chromatography using a

slow gradient of petroleum ether, ethyl acetate, ethanol gave pure piperazinones **263** and **264** (34%, 29% respectively).

3.6.3.1.1 NMR data analysis for epimers 263 and 264

Coupling constants for H-6 and chemical shifts analysis for H-3, based on the same considerations made for the previous diastereoisomers, was made and the outcome was disappointing.

The isomer **263** should possess H-3 in axial position (δ 5.25) and H-6 also in axial position, according to the large coupling constant found for H-5b to H-6 (5.9 Hz). On the same basis, the isomer **264** should have H-3 in equatorial position (δ 5.6) and H-6 in equatorial, too. Once again, the two conformers **263**, **264** appeared to be *trans-diequatorial* and *trans-diaxial* respectively, which clearly cannot be possible.

However, the two epimers were recrystallised from a mixture of petroleum ether, diethyl ether and the X-ray crystallographic data were crucial for elucidating this matter.

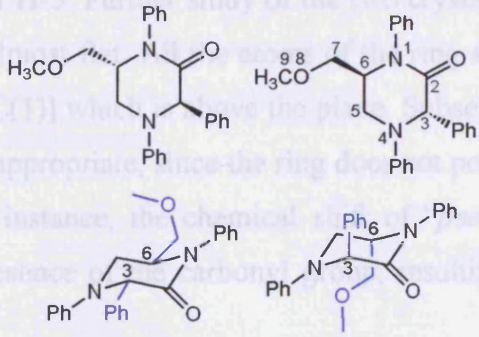

263 *trans-diequatorial*-piperazinone

264 *trans-diaxial*-piperazinone

Signal	*Trans*-3,6-piperazinone **263**	*Trans* 3,6-piperazinone **264**
H-3	5.25 (s)	5.6 (s)
H-5a	3.65 (dd, 13.2, 4.1)	3.9 (dd, 13.7, 3.1)
H-5b	3.93 (dd, 13.2, 5.9)	4.32 (dd, 13.7, 1.2)
H-6	4.09 (dq, 9.5, 4.0)	4.05 (m)
H-7a	3.26 (dd, 9.2, 3.5)	3.4 (dd, 8.8, 3.7)
H-7b	3.54 (dd, 9.2, 8.2)	3.48 (t, 9.3)
H_3-9	3.22 (s)	3.28 (s)

Table 14. NMR data comparison of piperazinones **263** and **264**

3.6.3.1.2 X-Ray Crystallographic data of piperazinones 263 and 264

Yellow needle crystals of epimers **263** and **264** were obtained by slow evaporation of a mixture of petroleum ether and diethyl ether. X-Ray crystallographic data of piperazinones **263** and **264** showed that H-3 was axial in both diastereoisomers.

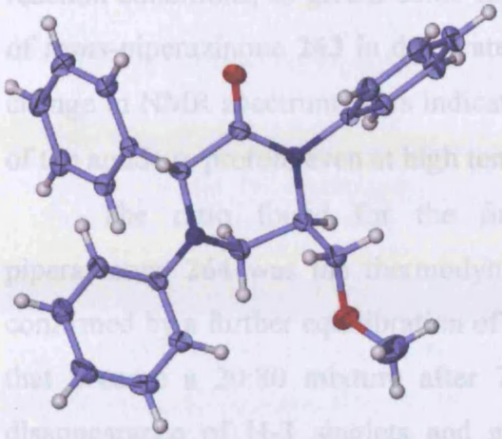

Figure 30. *trans-Diequatorial* piperazinone **263**

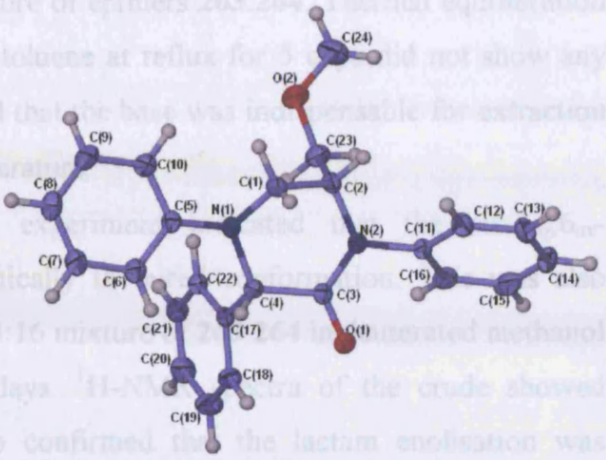

Figure 31. *cis*-3_{eq},6_{ax} Piperazinone **264**

This was in disagreement with our assignment, made on the basis of H-3 chemical shifts. H-6 appeared to be in equatorial position for the epimer **263**, giving the final conformation as *trans-diequatorial*. H-6 for epimer **264** was in equatorial position giving the final conformation as *cis*-3_{eq},6_{ax}. As anticipated above, this was controversial with our data analysis for H-3. Further study of the two crystal structures indicated that the heterocyclic ring is almost flat. All the atoms of the ring seemed to lay in the same plane except for C-5 [= C(1)] which is above the plane. Subsequently, the terms "axial" and "equatorial" are not appropriate, since the ring does not possess the conformation of a cyclohexyl chair. For instance, the chemical shift of "*pseudo*-axial" H-3 could be affected by the close presence of the carbonyl group, resulting in a shift of ^{1}H-NMR signal downfield.

3.6.3.2 Equilibration reaction for piperazinones 263 and 264

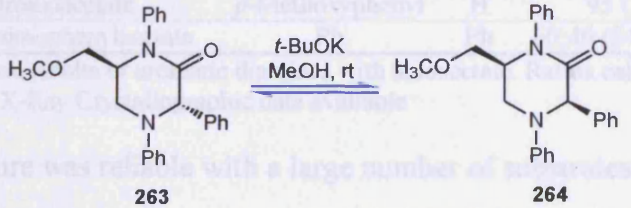

263 **264**

Similar to the equilibration reactions of the previous piperazinone epimers (sections 3.6.1.2, 3.6.2.1), pure crystals of *trans*-piperazinone **263** were dissolved in methanol in presence of potassium *t*-butoxide. After 48 hours at room temperature a 40:60 mixture of epimers **263**:**264** was observed in ^{1}H-NMR spectrum. Parallel to this experiment, also crystals of *cis*-piperazinone **264** was equilibrated under the same

reaction conditions, to give a 20:80 mixture of epimers **263**:**264**. Thermal equilibration of *trans*-piperazinone **263** in deuterated toluene at reflux for 5 days did not show any change in NMR spectrum. This indicated that the base was indispensable for extraction of the amide α-proton, even at high temperature.

The ratio found for the first experiment indicated that the *cis*-$3_{eq},6_{ax}$-piperazinone **264** was the thermodynamically favoured conformation. This was also confirmed by a further equilibration of 84:16 mixture of **263**:**264** in deuterated methanol that became a 20:80 mixture after 7 days. ^{1}H-NMR spectra of the crude showed disappearance of H-3 singlets and also confirmed that the lactam enolisation was complete by using 2 equivalents of base. The conversion of *cis*- into *trans*- isomers (80:20 ratio) described above was misleading since the rest of experiments suggested that *cis*-$3_{eq},6_{ax}$-piperazinone **264** had the most stable conformation.

3.7 Conclusions

In conclusion, 6-substituted piperazinones were successfully prepared regioselectively with simple addition of ethyl bromoacetate to the refluxing diamine. Yields were low with aromatic amines, due to their expected reduced nucleophilicity.

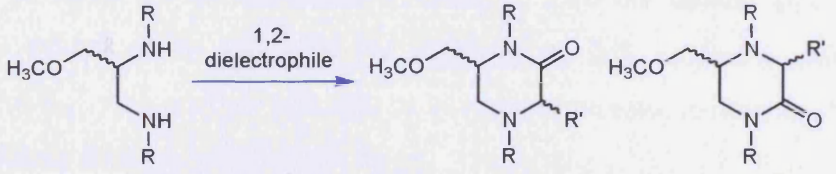

182 **265** **266**

	1,2-Dielectrophile	R	R´	265	266
b	ethyl bromoacetate	2-Methoxyethyl	H	90 (50%)	10
c	ethyl bromoacetate	Cyclohexyl	H	90 (75%)	10
d	ethyl bromoacetate	Ph	H	90 (35%)[1]	10
e	ethyl bromoacetate	*p*-Methoxyphenyl	H	95 (30%)	5
f	Methyl α-bromophenylacetate	Ph	Ph	60:40 (34%, 29%)[1]	-

Table 15. Cyclisation results of aromatic diamines with haloacetate. Ratios calculated in the crude ^{1}H-NMR (yields). [1] X-Ray Crystallographic data available

This procedure was reliable with a large number of substrates. Earlier experience showed that changing the substituent at position 2 did not significantly affect the regioselectivity.

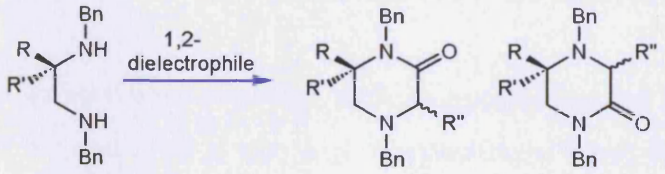

242 **267** **268**

	1,2-Dielectrophile	R	R′	R′′	267	268
a	Methyl bromoacetate	H	CH_2OCH_3	H	90	10
b	Methyl bromoacetate	H	CH_3	H	89	11
c	Methyl bromoacetate	CH_3	CH_3	H	80	20
d	Methyl bromoacetate	H	Ph	H	95	5
g	Methyl α-bromophenylacetate	H	CH_2OCH_3	Ph	40:60 (25%, 35%)	-
h	Methyl bromopropionate	H	CH_2OCH_3	CH_3	50:50 (30%, 25%)	-

Table 16. Cyclisation results of benzylamine derivative with haloacetates. All the reactions run for 24 hours at reflux. Ratios calculated in the crude ^{1}H-NMR (yields).

When a chiral dielectrophile was used, even better than expectation, only the two epimers of 6-piperazinones were formed. No trace of the other regioisomer was seen. This suggests that in the future, it would be worthwhile to attempt cyclisations with the pure enantiomeric form of the dielectrophile in order to control better the diastereoselectivity.

CHAPTER 4 A new regioselective way to prepare chiral piperazinones

4.1 Introduction

As introduced in chapter 3, chiral 1,2-diamines were reacted with ethyl bromoacetate for the preparation of chiral piperazinones **243a** and **244a** and the preferential formation of one regioisomer **243a** over the other **244a** was observed in all the cyclisations performed.

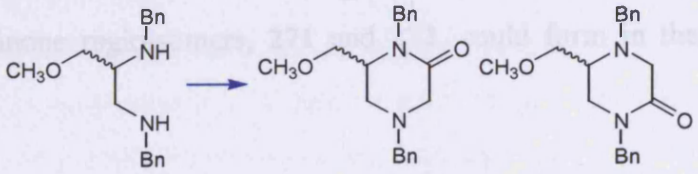

The mechanism of this reaction can be explained as a two steps sequence. The first step is a S_N2 of secondary amine to the dielectrophile **230** to displace the halo substituent first and to form the monoester derivative **236**. The second step could be competitive between the intramolecular cyclisation from the second amino group to displace the ethoxy group and give the piperazinone **246** (route ***a***) and a second intermolecular S_N2 with another molecule of ethyl bromoacetate to displace the bromide to give the diester derivative **245** (route ***b***).

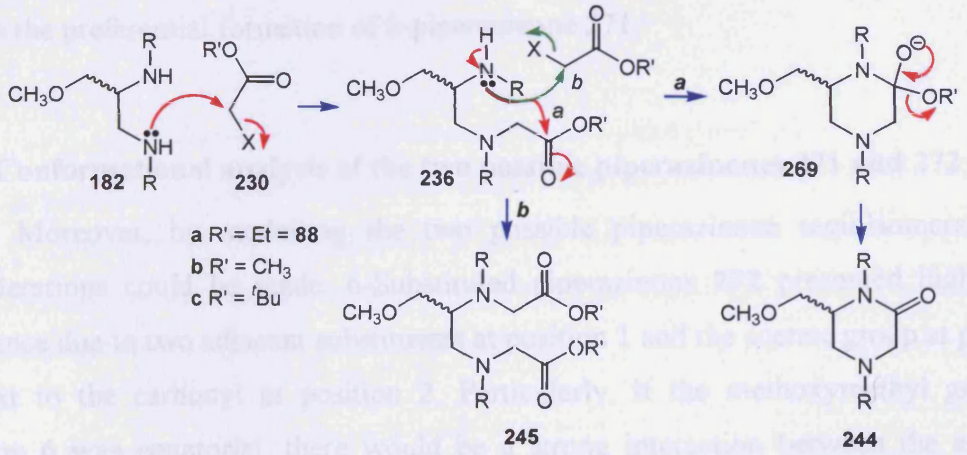

Scheme 61. Competitive mechanisms for diester and piperazinone formation

When the R groups were aliphatic, such as cyclohexyl and 2-methoxyethane, diesters were easily isolated even at very high temperatures. When the R groups were aromatic, their formation was rarely observed. Our experience showed that directing the

formation of one of the products **245** and **244a** was possible by changing the reaction conditions. In particular, low temperature, high concentration of the reagents and large excess of ethyl bromoacetate gave quantitatively the diester derivative **245**, whereas high temperature and equimolar concentrations of reagents gave preferentially the cyclised product **246**.

These diesters represented important intermediates for the preparation of a new range of chiral *N,N'*-diacetate 1,2-diamines. Benzyl groups acted as protecting groups and were easily cleaved by hydrogenolysis, catalysed by palladium catalysts. Our expectation was to promote the intramolecular cyclisation of this new class of 1,2-diamines in acidic conditions, after cleavage of the benzyl groups. Theoretically, two possible piperazinone regioisomers, **271** and **272**, could form in the cyclisation step (Scheme **62**).

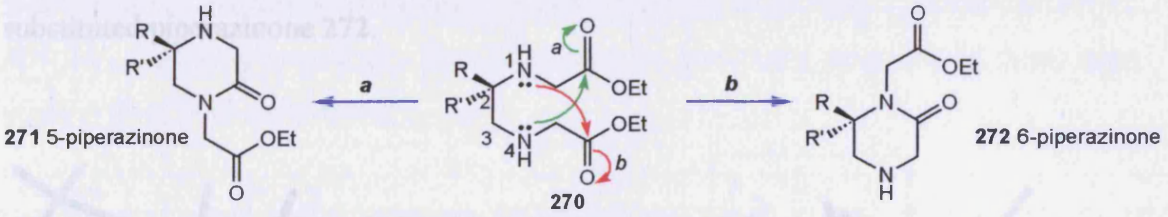

Scheme 62. Possible cyclisations of the 1,2-diamine **270**

It was established by previous experiments that the two amino groups possess different reactivity. Considering that N-4 is more reactive than N-1, confirmed by all our previous cyclisations, attack of the amino group remote from the chiral centre could lead to the preferential formation of 5-piperazinone **271**.

4.1.2 Conformational analysis of the two possible piperazinones 271 and 272

Moreover, by modelling the two possible piperazinone regioisomers, other considerations could be made. 6-Substituted piperazinone **272** presented high steric hindrance due to two adjacent substituents at position 1 and the acetate group at position 6, next to the carbonyl at position 2. Particularly, if the methoxymethyl group at position 6 was equatorial, there would be a strong interaction between the adjacent groups, which would increase the energy of these compounds.

5-Substituted piperazinone **271** only presented one group next to the carbonyl at position 2. Our hypothesis was that only the 5-substituted piperazinone **271** could easily be formed in the cyclisation step.

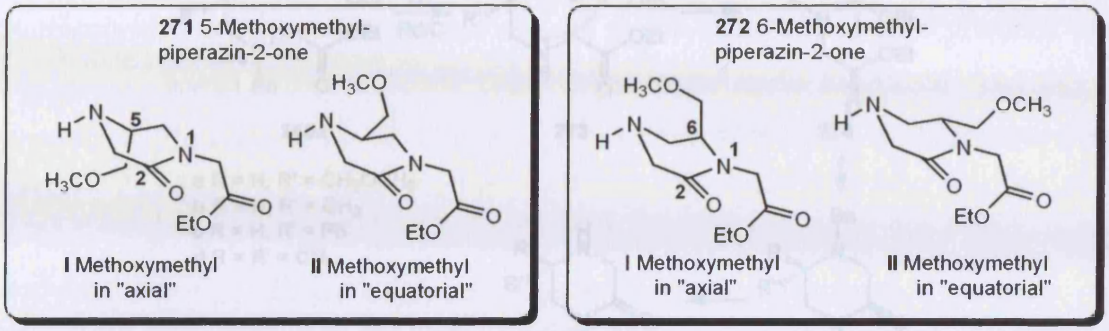

Scheme 63. Steric hindrance for the formation of 5- and 6-piperazinones **271**, **272**

Conformational analysis showed an energy value of -3.123 kcal mol^{-1} for 5-methoxymethyl-(2-oxo-piperazin-1-yl)-acetic acid ethyl ester **271**, showing the methoxymethyl group could be equatorial position, against 6.575 kcal mol^{-1} for the 6-substituted piperazinone **272**.

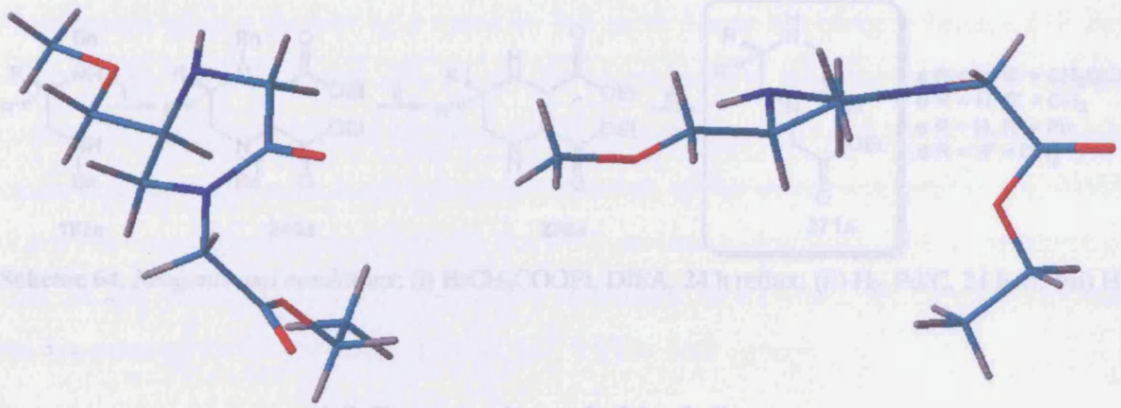

Figure 32. PC Model representation of 5-piperazinone **272**

In addition to the mechanistic proposal just made, it was also possible to postulate that the hydrogenolysis could have occurred regioselectively by cleaving the N-4 benzyl group first and promoting the cyclisation by N-4 alone.

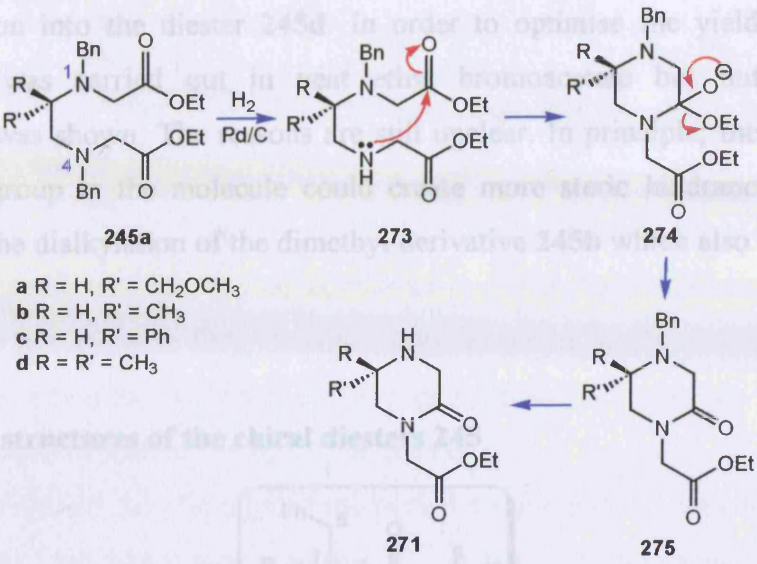

4.1.3 Planned synthesis

The overall planned synthesis involved three steps starting from *N,N'*-dibenzyl-2-substituted 1,2-diamine **182a**, previously prepared by EGB. One 1,2-diamine (R= H, R'= Ph) was enantiomerically pure (*R*) and was previously prepared in three steps starting from D-phenylalanine[130].

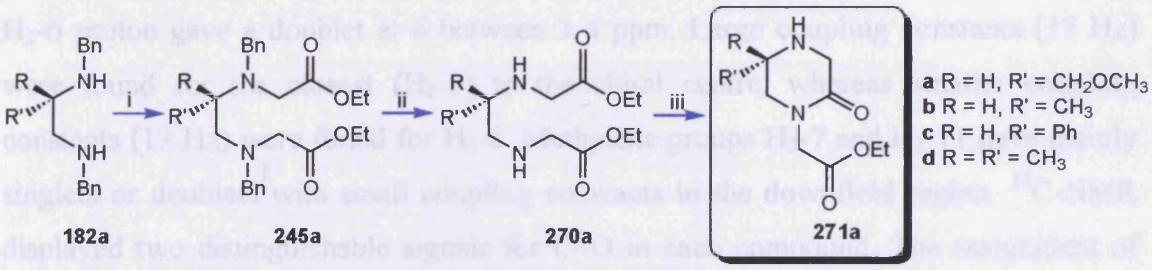

Scheme 64. *Reagents and conditions*: (i) $BrCH_2COOEt$, DIEA, 24 h reflux; (ii) H_2, Pd/C, 24 h, rt; (iii) H^+

4.2 Preparation of chiral diesters

Preparation of diesters **245a-d** was carried out by placing our 1,2-diamines **182a-d** with a large excess of ethyl bromoacetate (6-10 equivalents) in dichloromethane and keeping the reaction at 0° C, in order to avoid the competitive intramolecular cyclisation pathway.

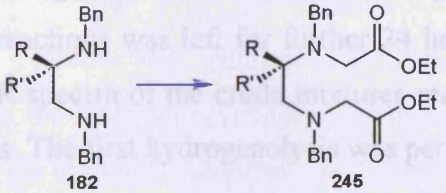

	R	R'	Rx time	% 245
a	CH_2OCH_3	H	2 hrs	85
b	CH_3	CH_3	48 hrs	43
c	CH_3	H	24 hrs	65
d	Ph	H	48 hrs	35

Table 17. Yields for diesters **245** formation

All the displacements were carried out at high concentration (60% v/v diamine/solvent). Yields were satisfactory (43-85%), except for the phenyl derivative **182d** that only gave

35% conversion into the diester **245d**. In order to optimise the yield of **245d**, the displacement was carried out in neat ethyl bromoacetate but unfortunately no improvement was shown. The reasons are still unclear. In principle, the presence of a third phenyl group in the molecule could create more steric hindrance and this is supported by the dialkylation of the dimethyl derivative **245b** which also had poor yield (43%).

4.2.1 Proof of structures of the chiral diesters 245

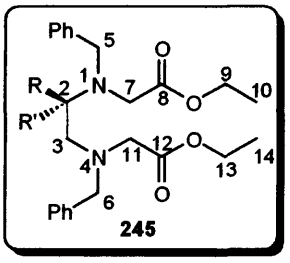

245

^{1}H-NMR spectra of **245a-c** displayed two distinguishable triplets in the upfield region and two quartets for the methylene of the ester groups. Each benzylic H_2-5 and H_2-6 proton gave a doublet at δ between 3-4 ppm. Large coupling constants (17 Hz) were found for the closest (H_2-5) to the chiral centre, whereas smaller coupling constants (13 Hz) were found for H_2-6. Methylene groups H_2-7 and H_2-11 gave mainly singlets or doublets with small coupling constants in the downfield region. ^{13}C-NMR displayed two distinguishable signals for C=O in each compound. The assignment of each proton was achieved unambiguously by HMBC correlation. IR spectra indicated the presence of C=O stretching at 1730 cm^{-1} for the ester groups.

4.3 Hydrogenolysis for N-benzyl groups cleavage

Cleavage of the benzyl groups was achieved by hydrogenolysis in presence of palladium (10%) on carbon in methanol or THF using an atmospheric pressure hydrogenator. Usually reaction times were 24 hours, although we experienced catalyst poisonings, when the conversion into products was ~50%. New catalyst was placed and the reactions was left for further 24 hours and left to go to completion. TLC and ^{1}H-NMR spectra of the crude mixtures mainly showed formation of one product in all the cases. The first hydrogenolysis was performed with the diester **245a**.

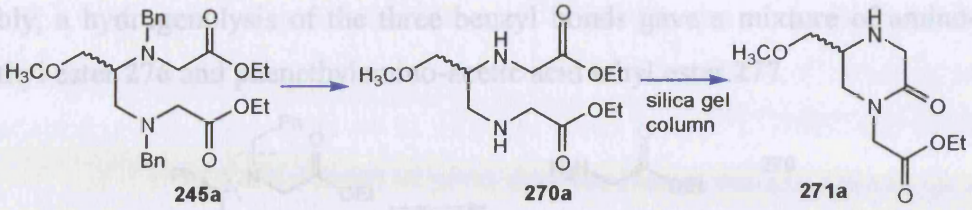

Only for this reaction, the crude mixture required flash chromatography due to the presence of two spots on TLC, one of which was on the baseline. NMR of the crude mixture displayed two triplets in the upfield region, attributed to the two ester functions **270a** and no aromatic peak in the downfield region.

This confirmed the cleavage of the benzyl groups and we decided to purify the diester **270a** by flash chromatography but to our surprise, piperazinone **271a** eluted from the column. Probably, the acidic groups of the silica gel catalysed the cyclisation of the reactive diester. No signals of the major compound found in the crude mixture were observed and the structure was unambiguously assigned. In all other hydrogenolysis carried out, 5-piperazin-2-ones **271** were directly formed by spontaneous cyclisation.

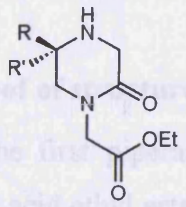

271

	R	R′	240*
a	CH_2OCH_3	H	72%
b	CH_3	CH_3	85%
c	CH_3	H	60%
d	Ph	H	-

Table 18. Yields of piperazinone after hydrogenation-cyclisation of diesters. * Yield of purified products

The crude mixtures, after hydrogenolysis, were mainly composed directly of piperazinones formed by spontaneous intramolecular cyclisation of the diesters and this theory could not be proved. However, when methoxymethyl diamine **242a** was reacted, we did observe formation of the diester intermediate **270a**, which indicates that the regioselective benzyl cleavage did not occur.

4.3.1 Cleavage of *N,N′*-dibenzyl-1,2-diaminoethylenebenzene 245d

When *N,N′*-dibenzyl-1,2-diaminoethylenebenzene **182d** was hydrogenolysed under the standard conditions, the benzyl groups were not cleaved by hydrogenolysis to give the expected "unprotected" diamine **245d**. No traces of the expected piperazinone were observed either, but TLC and NMR showed formation of mixture of products.

Probably, a hydrogenolysis of the three benzyl bonds gave a mixture of amino-acetic acid ethyl ester **276** and phenethylamino-acetic acid ethyl ester **277**.

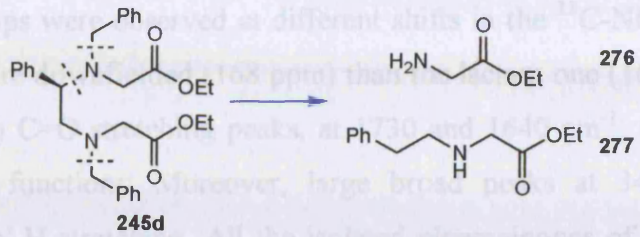

Scheme 65. Possible products of hydrogenolysis for phenyl derivative **245d**

^{1}H-NMR after 4 hours of hydrogenolysis showed signals of unreacted **245d** and a large number of complex, non-interpretable signals.

A new procedure was followed for the benzyl group cleavage for **245d.** *N*-Iodosuccinimide was used according to a new method reported by Grayson et al.[134] as successful reagent for *N*-benzyl cleavage. Unfortunately, a mixture of products were shown by TLC and ^{1}H-NMR. IR did not show any signal at ~1645 cm^{-1}; a common frequency for lactam carbonyl groups, but rather a sharp peak at 1744 which is indicative of esters and a broad peak at 3455 cm^{-1} due to the NH stretching.

4.3.2 Proof of structures of 5-substituted piperazinones 271

The first piperazinone isolated was the 5-methoxymethyl-(2-oxo-piperazin-1-yl)-acetic acid ethyl ester **271a**. The most indicative signals were the methoxy singlet at δ 3.3 ppm, H_2-3 that gave two doublets of 17.5 Hz at 3.5 and 3.6 ppm and the ethoxy signals consisting of one triplet for H_3-14 and one quartet for H_2-13. HMBC spectra confirmed the postulated structure and exclude the possibility of the other regioisomer formation. ^3J correlations seen were H_2-6 and C-2, and H_2-3 and C-5 and *vice versa*.

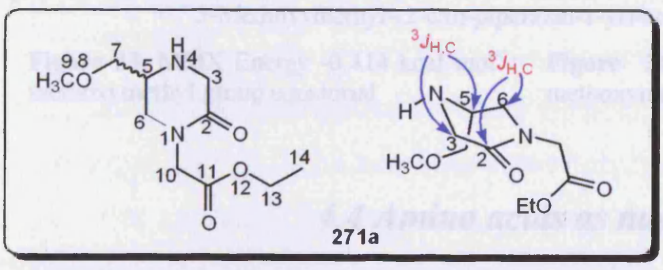

Signal	δ (coupling constant)
H-3a	3.5 (d, 17.5)
H-3b	3.59 (d, 17.5)
H-5	3.25 (dddd, 9.8, 5.2, 4.4, 3.3)
H-6a	3.19 (dd, 10.7, 3.3)
H-6b	3.29 (m)
H_2-7	3.37 (t, 4.9)
H_3-9	3.3 (s)
H_2-10	4.05 (d, 10.6)
H_2-13	4.2 (q, 7.1)
H_3-14	1.22 (t, 7.1)

Table 19. 1H-NMR signals for **271a**

The methoxy signals in the ^{1}H- and ^{13}C-NMR spectra were unequivocally assigned and were utilised as the starting point for the assignment of the other protons. The carbonyl groups were observed at different shifts in the ^{13}C-NMR and usually the ester C=O was more downfielded (168 ppm) than the lactam one (167 ppm). IR spectra also displayed two C=O stretching peaks, at 1730 and 1640 cm^{-1}, respectively for the ester and lactam functions. Moreover, large broad peaks at 3400 cm^{-1} indicated secondary amine N-H stretching. All the isolated piperazinones of this sequence gave comparable spectra.

Regarding the conformational analysis of these structures, it was predicted that substituents at position 2 prefer to be in equatorial position, despite the axial position was preferred in the previous series of piperazinones. The lone pair would prefer to be in equatorial position as observed in previous works[135] although our model prediction displayed them in axial position. In conclusion, no assignment was possible since we had insufficient data.

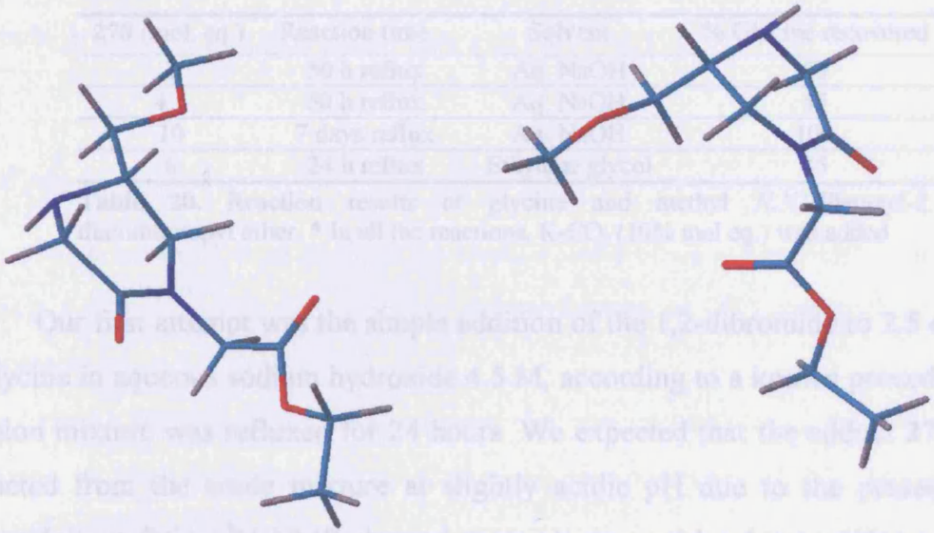

5-Methoxymethyl-(2-oxo-piperazin-1-yl)-acetic acid ethyl ester **271a**

Figure 33. MMX Energy -0.414 kcal mol^{-1}: methoxymethyl group equatorial

Figure 34. MMX Energy 0.268 kcal mol^{-1}: methoxymethyl group in axial position

4.4 Amino acids as nucleophiles

Subsequent to the discovery of regioselectivity for these novel cyclisations, there was the need to optimise the preparation of the "unprotected" diesters. Amino acids possess the potential to react as nucleophiles with a dielectrophile when they are placed in basic solution and could afford the desired diesters by direct reaction with the

dibromide **187**. In an overview, the nucleophilic displacement was efficient and reliable with compounds such as benzylamine, aniline, *p*-methoxyaniline, cyclohexylamine and methoxyethylamine.

According to the literature, attempts to prepare diglycylethylenediamine using glycine chloride or glycine were unsuccessful and the yields reported were usually very poor[136,141,137]. However, reaction of 1,2-dibromoethane with primary amine gave *N,N'*-disubstituted ethylenediamines and homologous polyamines at room temperature in good yield[138]. The most successful result was given by Allevi[139], which reported that a derivative of proline reacted with 1,2-dibromoethane to give the expected diamine in 60% yield.

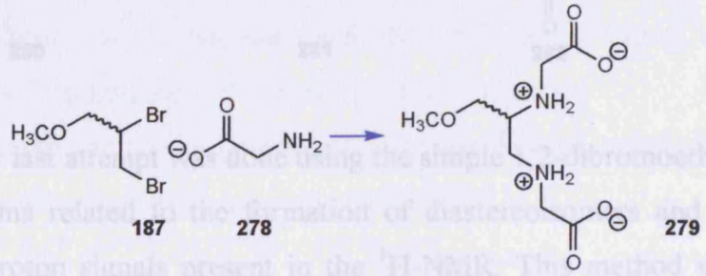

187 **278** **279**

278 (mol. eq.)	Reaction time	Solvent	% Glycine recovered
2	50 h reflux	Aq. NaOH	63
4.5	50 h reflux	Aq. NaOH	55
10	7 days reflux	Aq. NaOH	100
6	24 h reflux	Ethylene glycol	85

Table 20. Reaction results of glycine and methyl *N,N'*-dibenzyl-2,3-diaminopropyl ether. * In all the reactions, K_2CO_3 (10% mol eq.) was added

Our first attempt was the simple addition of the 1,2-dibromide to 2.5 equivalents of glycine in aqueous sodium hydroxide 4.5 M, according to a known procedure[139]. The reaction mixture was refluxed for 24 hours. We expected that the adduct **279** could be extracted from the crude mixture at slightly acidic pH due to the presence of two carboxylate moieties. ^{1}H-NMR showed some glycine residue (up to 65%) as the major part of the mixture and the rest of the signals were very complex. Unfortunately, TLC monitoring was not efficient to follow the progress of the reaction due to the extremely high polarity of these compounds. Higher temperature was reached in refluxing ethylene glycol (up to 210°C) for 24 hours but 85% of glycine was recovered.

The unreacted glycine was removed by several precipitations in ethanol. Different work up methods were attempted in order to extract the product: dissolution in alkali filtration and precipitation at pH 1[140]; neutralisation to pH 5[141] and pH 6.5-7.0 followed by extraction with organic solvents. Also recrystallisation in boiling water[142], butanol[143] and isopropanol: water mixtures[139] were unsuccessful to extract the product.

^{1}H-NMR spectra was very complex and the appearance of many overlapped signals indicated the presence of mixtures at least of four products. According to the presence of the glycine recovered it was postulated that other possible mechanisms could lead to the formation of other byproducts as **280** and **281.** Another plausible reason for the presence of many compounds could be the presence of different protonated forms of the same product as **282** and **283**.

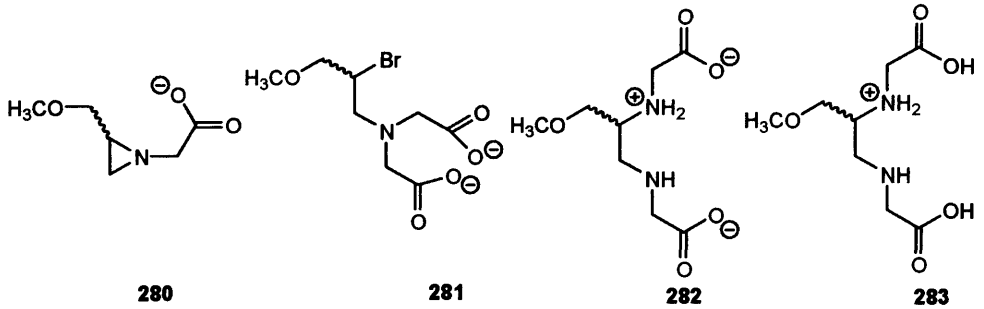

280 **281** **282** **283**

Our last attempt was done using the simple 1,2-dibromoethane with glycine to avoid problems related to the formation of diastereoisomers and the presence of diastereotopic proton signals present in the ^{1}H-NMR. This method was unsuccessful and 90% of glycine was recovered at the end of the reaction.

4.5 Conclusions

Ethyl bromoacetate addition to chiral 1,2-diamines gives preferentially diesters as main products, when the reactions are performed at 0°C and with an excess of dielectrophile.

High regioselectivity was achieved for the cyclisation of *N,N'*-diacetate 1,2-diamines to give exclusively 5-substituted piperazinones (60-85%). The cyclisations occurred spontaneously in presence of traces of acid. 6-Substituted piperazinone did not form due to high steric hindrance problem (three groups next one another).

Attempts of preparation of *N,N'*-diacetate 1,2-diamines starting from amino acids resulted in formation of mixture of products, impossible to separate by column chromatography.

CHAPTER 5 Chiral 1,2-diamines with glyoxal

5.1 Introduction

From the preceding chapters, it was established that the presence of a chiral centre on the ethylene bridge of a 1,2-diamine differentiated the reactivity of the two amino groups. Hence preparation of 6-piperazinones could be simply achieved with high regioselectivity and in good yield starting from aliphatic 1,2-diamines when ethyl bromoacetate was used as cyclising agent. Moreover, variation of the *N,N'*-substituents did not affect the regioselectivity, but did affect the yield.

Parallel to the ethyl bromoacetate cyclisations with *N,N'*-dibenzyl 2-substituted 1,2-diamines **242a-d**, carried out previously by EGB in my group, new attempts on cyclisations of the 1,2-diamines were performed with glyoxal.

The addition of glyoxal to the secondary diamines **242a-d** resulted in the selective formation of a 10:90 mixture of piperazinones **267**:**268**.

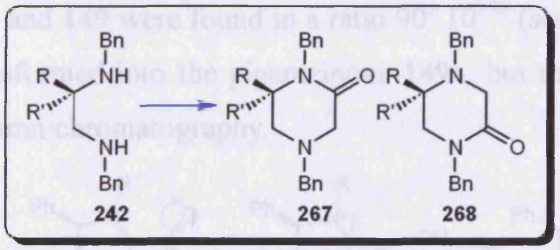

	R	R'	267	268
a	H	CH_2OCH_3	18	82
b	H	CH_3	14	86
c	H	Ph	23	77
d	CH_3	CH_3	14	86

Table 21. All the reactions run for 24 hours at reflux temperature

That result was completely unexpected and the cyclisation showed to be reliable with the whole range of dibenzyl diamines with different R substituents at position 2[130].

Described in this chapter is the investigation into glyoxal cyclisation mechanism. Similar to the ethyl bromoacetate cyclisations, our intention was to extend the procedure to 1,2-chiral diamines with different *N,N'*-substituents, and to clarify the reasons for the regioselectivity.

5.1.2 Glyoxal reactivity

Glyoxal is the simplest 1,2-dicarbonyl compound. It is an attractive synthon with great synthetic potential. Glyoxal is commercially available in different form, such as 40% *wt/wt* aqueous solution, dehydrated trimer or hydrated sodium bisulphite adduct. The two aldehyde functionalities are in equilibrium with the hydrate forms in water and they can be differentiated[144]. Glyoxal is very unstable and it reacts with alcohols to give

a range of products[145]. For instance, reaction with alcohols yields tetralkoxyethanes **284**, tetralkoxydioxanes **285** and tetralkoxynaphtodioxanes **286**.

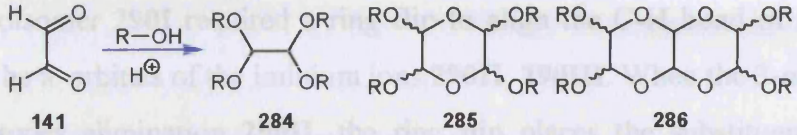

141 **284** **285** **286**

Reaction with methanol gives bisdioxolane derivatives **287** and **288**[145].

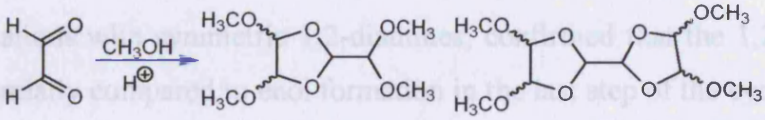

141 **287** **288**

5.1.2.1 Glyoxal and amines

It is well known that aqueous glyoxal reacts with *N,N'*-disubstituted 1,2-diamines to afford a range of products with the C_2-symmetric diamines. The products **148** and **149** were found in a ratio 90: 10[146] (section 1.2.3.1). Aldehyde **148a** was easily transformed into the piperazinone **149a**, but the *i*-propyl analogue **148b** was stable to column chromatography.

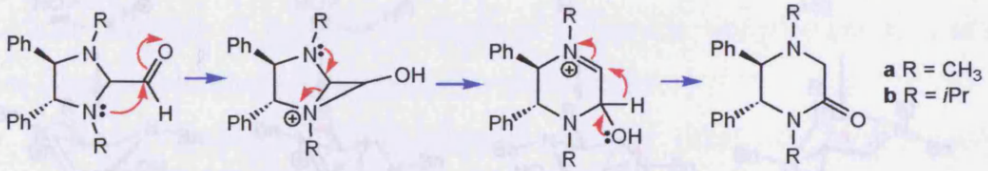

148 **289** **149**

All the known procedures described the formation of piperazinones as secondary products, coming from dehydration of a postulated intermediate diaminol derivative. When an equimolar concentration of glyoxal was used, condensation products were mainly observed[147].

5.1.3 Postulated mechanism of glyoxal cyclisation with secondary 1,2-diamines

The postulated mechanism for the glyoxal cyclisation is shown below (Scheme **66**). The initial hypothesis for the origin of the regioselectivity was based on the following scheme: there are four possible stereoisomers of the intermediate diaminols in which the R substituent is equatorial, but only those in which at least one of the hydroxyl groups is axial **290I-IV** benefit from assisted departure of the hydroxyl groups by the lone pairs on the nitrogens. Moreover the anomeric effect is stabilising for the ground state, and in the few cases in which diaminols have been isolated, the *trans*-

diaxial stereoisomers have been assigned as the major products. For the axial, equatorial-stereoisomers **290II**, **290III** *anti*-elimination of water is followed by a 1,2-hydride shift in competition with amide enol formation. Elimination from the *trans-diaxial* stereoisomer **290I** required a ring flip to align the C-H bond of the departing proton with the π-orbitals of the iminium ions **290II**, **290III**. When the 3-*axial* hydroxyl group, undergoes elimination **290II**, the ring flip places the substituent in the less favourable axial position **291II**, whereas elimination of the 2-*axial* hydroxyl group **290I**, only resulted in the flip of a methylene group **291I**. Previous investigations on glyoxal cyclisations with symmetric 1,2-diamines, confirmed that the 1,2-hydride shift occurs preferentially compared to enol formation in the last step of the cyclisation[102].

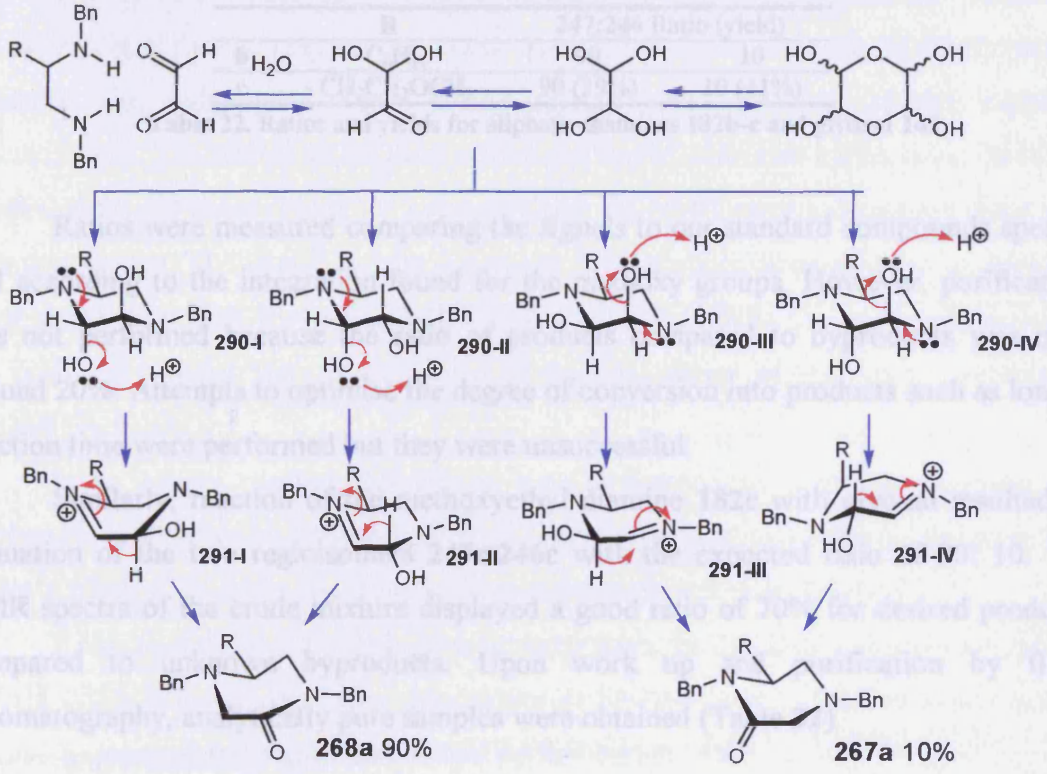

Scheme 66. Cyclisation mechanism of 1,2-diamine and glyoxal[148] (R= OMe)

5.2 Results and discussion

The original procedure used for the glyoxal cyclisations by EGB consisted in the slow addition of the dielectrophile to a refluxing mixture of diamine in ethanol: water/ 1:1. The standard reaction time was 24 hours and the reaction progress was easily monitored by TLC by workup of aliquots. The glyoxal used was a 40% aqueous solution which is commercially available.

5.2.1 Cyclisation of aliphatic *N,N'*-disubstituted 1,2-diamines and glyoxal

Reaction of cyclohexyl diamines **182b** with the aqueous glyoxal was carried out in mixture of water and ethanol (1:1) at reflux for 24 hours. TLC showed two new spots identified as regioisomers **246** and **247**, by direct comparison to our standard compounds, previously prepared in the ethyl bromoacetate cyclisations. ^{1}H-NMR spectra of the crude confirmed the presence of the expected products with a ratio of 90:10 for **247**: **246**.

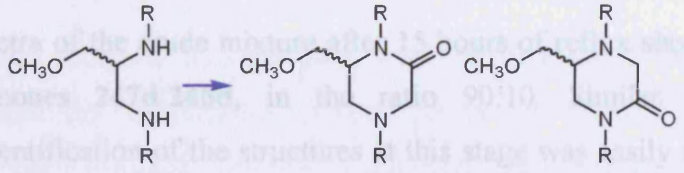

	R	247:246 Ratio (yield)	
b	- C_6H_{11}	90	10
c	- $CH_2CH_2OCH_3$	90 (39%)	10 (11%)

Table 22. Ratios and yields for aliphatic diamines **182b-c** and glyoxal **141**

Ratios were measured comparing the signals to our standard compounds spectra and according to the integration found for the methoxy groups. However, purification was not performed because the ratio of products compared to byproducts was only around 20%. Attempts to optimise the degree of conversion into products such as longer reaction time were performed but they were unsuccessful.

Similarly, reaction of the methoxyethyl diamine **182c** with glyoxal resulted in formation of the two regioisomers **247c**:**246c** with the expected ratio of 90: 10. ^{1}H-NMR spectra of the crude mixture displayed a good ratio of 70% for desired products compared to unknown byproducts. Upon work up and purification by flash chromatography, analytically pure samples were obtained (Table **22**).

5.2.2 Cyclisation of aromatic *N,N'*-disubstituted 1,2-diamines and glyoxal

Glyoxal cyclisations were also attempted using *N,N'*-diphenyl-3-methoxy-propane-1,2-diamine **182d**. From previous cyclisations of these diamines with ethyl bromoacetate, it was shown that the aromatic diamines needed stronger reaction conditions to react with the dielectrophiles, due to the lower nucleophilicity of the amino groups.

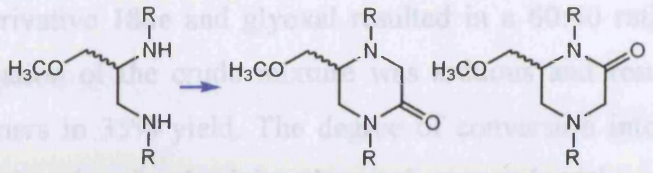

	R	247:246 Ratio (yield)	
d	- C_6H_5	90 (17%)	10 (15%)
e	*p*-CH_3O-C_6H_4 -	60	40

Table 23. Ratios (yields) in crude ^{1}H-NMR for aromatic diamines **182d-e** and glyoxal **141**

NMR spectra of the crude mixture after 15 hours of reflux showed the presence of the piperazinones **247d**:**246d**, in the ratio 90:10. Similar to the aliphatic piperazinones, identification of the structures at this stage was easily achieved by TLC and NMR spectra, using the standard compounds previously prepared. However, measurement of the ratio between aromatic and aliphatic protons in the ^{1}H-NMR spectra indicated that only 30% of the crude mixture was composed of the expected piperazinones. The rest of the mixture was composed of unknown byproducts. ^{1}H-NMR spectra displayed three extra CH_3O- singlets and ^{13}C-NMR spectra displayed three new carbonyl groups. TLC showed three overlapped apolar spots, impossible to separate by flash chromatography. Extraction of the desired products from the crude mixtures and the purification steps were difficult due to the consistency of the crude mixtures as gummy black oils.

More severe reaction conditions were attempted in order to optimise the conversion into products. When the diphenyl derivative **182d** was refluxed for up to 200 hours in place of 24 hours, no increase of conversion degree was observed.

It was postulated that elimination of water from the diaminol intermediate, might be rate limiting due to the lower availability of the lone pairs of the aromatic amine relative to those of the benzyl derivatives studied earlier. Addition of a catalytic amount of acid might protonate the aminol hydroxyl groups and facilitate loss of a water molecule. Indeed addition of 0.15 equivalents of *p*-toluenesulphonic acid, resulted in 70% conversion and the same regioselectivity observed previously (90:10, **247d**:**246d**) but the yields were still not satisfactory (10% yield for 5-piperazinone **247d** and 5% for 6-piperazinone **246d**).

The following attempt at this cyclisation with aromatic amines was performed using the *p*-methoxyaniline derivative **182e**. Our hypothesis was based on the presence of the electron-donating group on the phenyl ring that would increase the availability of the amine lone pair for the reaction with glyoxal. Unfortunately, cyclisation of *p*-

methoxyaniline derivative **182e** and glyoxal resulted in a 60:40 ratio of piperazinone **247e**:**246e**. Purification of the crude mixture was arduous and resulted in a mixture 90:10 of regioisomers in 35% yield. The degree of conversion into products did not improve and the reduced regioselectivity observed was unclear due to the similarity of reactivity between **182d** and **182e**.

5.3 Achiral aromatic diamines: procedure optimisation

Two achiral aromatic 1,2-diamines were utilised for investigating glyoxal cyclisations, without the complication of regioisomer formation. 1,2-Dianilinoethane **72l** was commercially available whereas *N,N'*-dibenzylbenzene-1,2-diamine **214** was chosen for its rigidity, which has the potential to facilitate cyclisation.

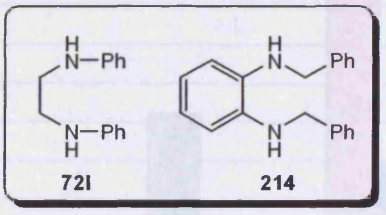

5.3.1 Cyclisation of 1,2-dianilinoethane with glyoxal

When the reaction was run in ethanol alone instead of the standard water: ethanol mixture, formation of a complex mixture was confirmed by ^{1}H-NMR, which displayed many overlapped signals.

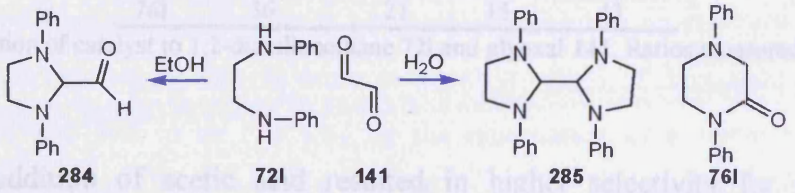

No piperazinone was detected by TLC or by ^{1}H-NMR spectra. The only product that could be isolated from this mixture was the fastest spot on TLC (R_f = 0.49 in petroleum ether:diethyl ether, 1:1) which was 1,3-diphenylimidazolidine-2-carbaldehyde **284** (5% yield). Reaction of the diamine **72l** with dilute aqueous glyoxal gave bis-imidazoline **285** (23%) and piperazinone **76l** (8%) plus unreacted starting material **72l** (31%). By comparing the results of the reaction in ethanol and water, it was clear that water was needed for the cyclisation step, probably for the formation of the diaminol.

5.3.1.1 Addition of catalyst

In order to enhance the selectivity towards the piperazinone ring formation and to optimise its yield, several catalysts were added to the water. Acetic acid, silica gel, sodium chloride and sodium iodide were added to the reaction mixture in catalytic amounts (0.1 equivalents). For all the reactions, it was possible to observe the formation of the aldehyde derivative **284**, the bis-imidazoline **285** and the piperazinone **76l**, in different ratios (Table **24**).

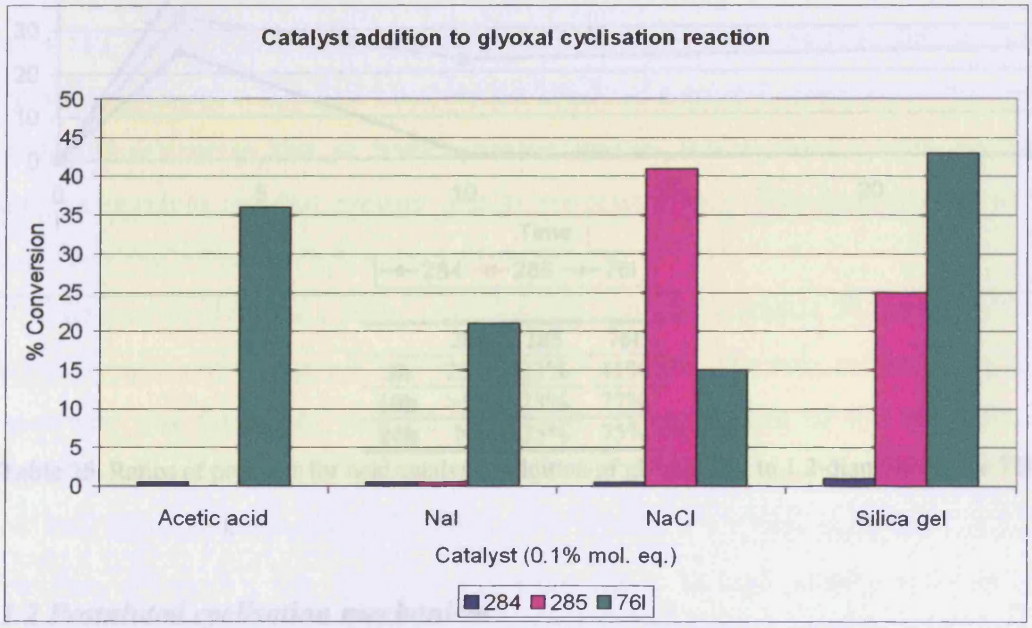

	Acetic acid	NaI	NaCl	Silica gel
284	0.5	traces	traces	1
285	-	traces	41	25
76l	36	21	15	43

Table 24. Addition of catalyst to 1,2-dianilinoethane **72l** and glyoxal **141**. Ratios measured relative to aromatics

The addition of acetic acid resulted in higher selectivity for piperazinone formation. The acid catalysed reaction was repeated and the ratio of products was monitor at different reaction times to observe the formation of piperazinone rings. The best ratio of products was obtained when the reaction mixture was refluxed for 24 hours (Table **25**).

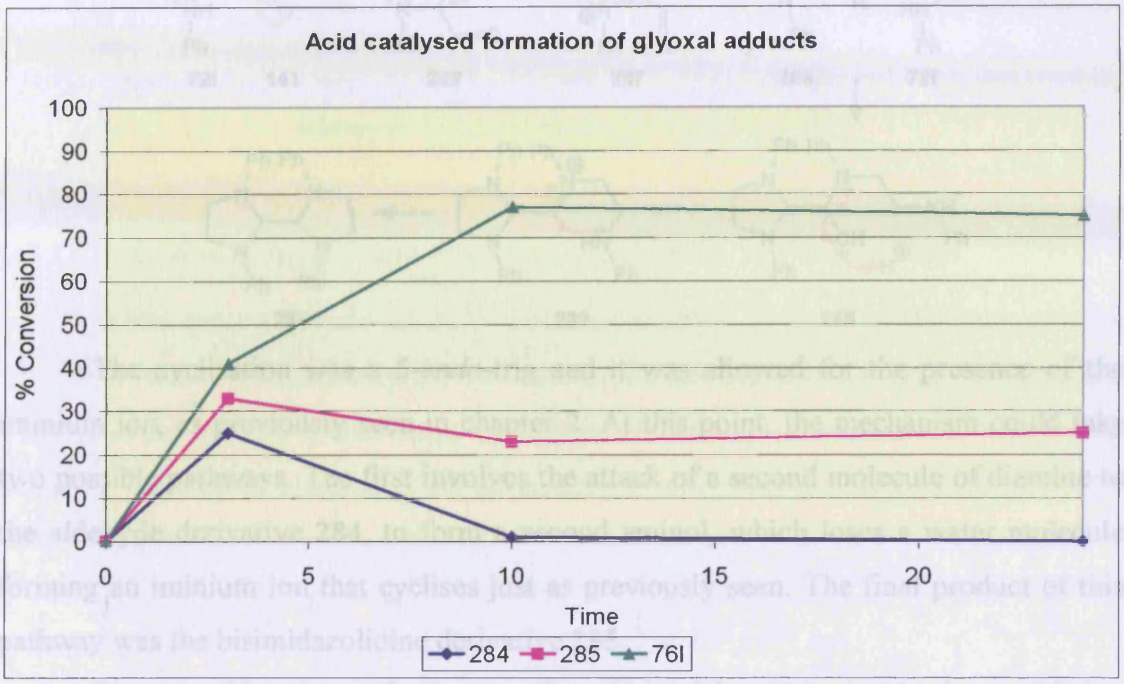

	284	285	76l
3h	25%	33%	41%
10h	>1%	23%	77%
24h	No	25%	75%

Table 25. Ratios of products for acid catalysed addition of glyoxal **141** to 1,2-dianilinoethane **72l**

5.3.1.2 Postulated cyclisation mechanism

The regular formation of the aldehyde derivative **284** at the first stage of the reaction suggested a new mechanism for the addition of glyoxal to the diamine. The first nucleophilic attack occurred from one amino group to one aldehydic function of glyoxal to form the aminol **286**. In order to have formation of the aldehyde derivative **284**, this first step had to be followed by the elimination of a water molecule and consequent formation of the iminium ion **287** rather than diaminol formation. The second amino group preferentially attacked intramolecularly the most electrophilic centre, next to the iminium ion rather than the second aldehydic function to form a second aminol.

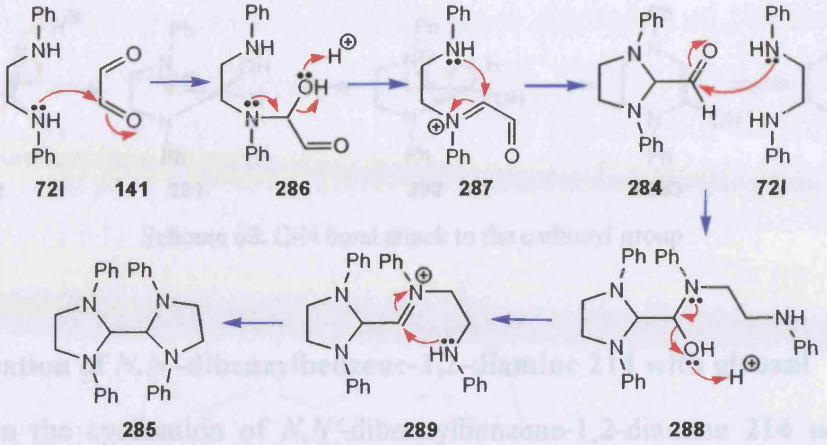

The cyclisation was a 5-*endo*-trig and it was allowed for the presence of the iminium ion, as previously seen in chapter 2. At this point, the mechanism could take two possible pathways. The first involves the attack of a second molecule of diamine to the aldehyde derivative **284**, to form a second aminol, which loses a water molecule forming an iminium ion that cyclises just as previously seen. The final product of this pathway was the bisimidazolidine derivative **285**.

The second involves a further transformation of the aldehyde **284** that could give an intramolecular rearrangement to yield the piperazinone. The only evidence found for this pathway was the linear correlation between disappearance of the aldehyde and appearance of piperazinone in the crude mixture ^{1}H-NMR spectra.

The diaminol formation, as postulated in section 5.1.3, was not observed during the reaction, although it was not easy to monitor due to its high polarity and reactivity. The piperazinone formation should then proceed only *via* rearrangement of the aldehyde derivative **284**. A reasonable hypothesis for the mechanism was the attack from the amino lone pair to the aldehyde intramolecularly and subsequent formation of ammonium ion **290**. The following step could involve the formation of ketone and breakage of the C-N bond to yield the piperazinone **76l** (Scheme **67**).

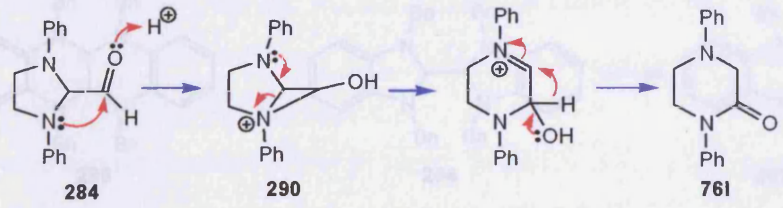

Scheme 67. Lone pair attack to the carbonyl group

Previous considerations of this rearrangement, made by EGB, postulated a bond migration to form the carbocation **291**, stabilised by amino lone pair (Scheme **68**).

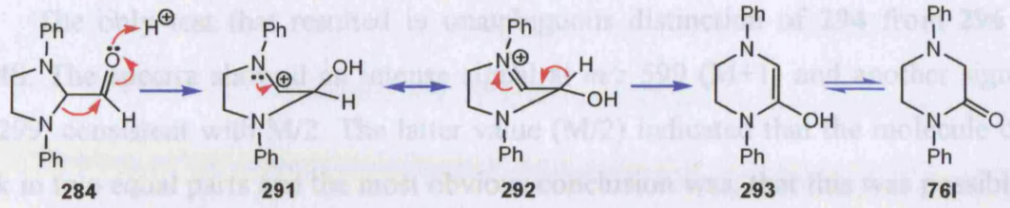

Scheme 68. C-N bond attack to the carbonyl group

5.3.2 Cyclisation of *N,N'*-dibenzylbenzene-1,2-diamine 214 with glyoxal

When the cyclisation of *N,N'*-dibenzylbenzene-1,2-diamine **214** with glyoxal was performed in ethanol, only the bis-imidazoline derivative **294** (42%) was obtained. The rest of the mixture was composed of unreacted starting material **214** (20%). For our surprise, no signals indicating the formation of the aldehyde derivative **295** were observed in the NMR spectra and on TLC.

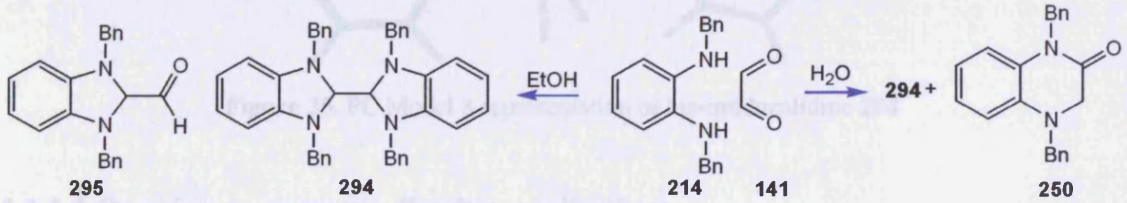

When water was used as solvent, adduct **294** (65%) and 1,4-dibenzyl-3,4-dihydroquinoxalin-2-(1*H*)-one **250** (3%) were obtained besides unreacted starting material (10%). Similarly to the 1,2-dianilinoethane reaction, no piperazinone was yielded from the reaction in ethanol. This evidence confirmed that the ethanol really interacted somehow stopping the cyclisation step, perhaps reacting with glyoxal itself or being too apolar for the formation of the intermediates. Moreover, for this kind of reactions with glyoxal, it was known that the major products are tetra-azadecalins **296** and not bis-imidazoline **294** as shown in our case.

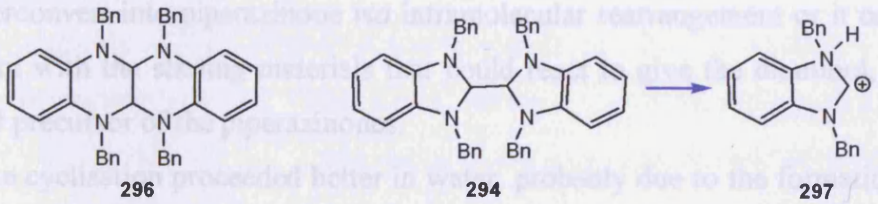

The distinction between structure **294** and **296** was complex due to the same numbers of atoms and indistinguishable NMR signals. Our data were compared to similar compounds[149] but the presence of different substituents created shifts for the NMR signals therefore they could not be compared.

The only test that resulted in unambiguous distinction of **294** from **296** was LRMS. The spectra showed an intense signal at *m/z* 599 (M+1) and another signal at *m/z* 299, consistent with M/2. The latter value (M/2) indicated that the molecule could break in two equal parts and the most obvious conclusion was, that this was possible for bis-imidazolidine **294** and not for the fused compound **296**.

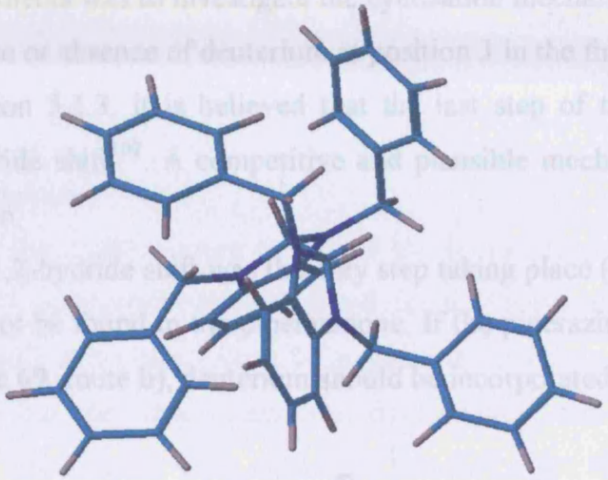

Figure 35. PC Model 8 representation of bis-imidazolidine **294**

5.3.1.3 Overview on aromatic diamines cyclisations

From the preceding paragraphs, it was shown that glyoxal reacted with chiral diamines in several ways affording different products. With aromatic diamines, the preferred products under standard conditions were aldehyde and bis-imidazolidine derivatives and in order to afford the piperazinone rings the reaction needed more energetic conditions, such as acid catalysis and longer reaction times.

In an overview for the diphenyl diamine, the imidazolidine derivative was considered the first kinetic adduct and its formation could be monitored due to the lower reactivity of the aromatic amines towards the electrophiles. The aldehyde then could either interconvert into piperazinone *via* intramolecular rearrangement or it could be in equilibrium with the starting materials that could react to give the diaminol, the other postulated precursor of the piperazinones.

The cyclisation proceeded better in water, probably due to the formation of very polar intermediates. The best ratio of piperazinone over the other possible products was achieved with addition of catalytic amount of *p*-toluenesulphonic acid. Either the diaminol or the imidazolidine derivatives could be protonated and converted into the thermodynamic piperazinones according to our postulated mechanism.

5.4 Understanding the glyoxal cyclisation mechanism: enol formation or hydride shift?

Parallel to the glyoxal cyclisation with aromatic diamines, further reactions between dibenzyl diamine **182a** and glyoxal were performed in deuterated water. The aim of these experiments was to investigate the cyclisation mechanistic pathway, on the basis of the presence or absence of deuterium at position 3 in the final piperazinones. As anticipated in section 5.1.3, it is believed that the last step of the lactam formation occurs *via* 1,2-hydride shift[102]. A competitive and plausible mechanism is represented by amide enolisation.

In case the 1,2-hydride shift was the only step taking place (Scheme **69**, route **a**), deuterium should not be found in the piperazinone. If the piperazinone was formed *via* amide enol (Scheme **69**, route **b**), deuterium should be incorporated in the final adducts.

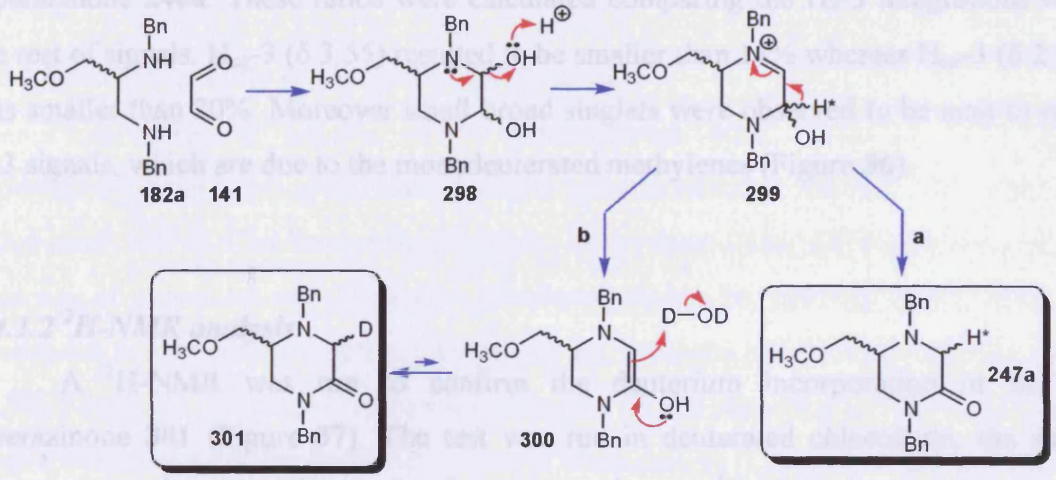

Scheme 69. Amide enol formation and 1,2-hydride shifts pathways

5.4.1 Deuteration experiments

The aqueous solution of glyoxal was concentrated with a high vacuum pump and diluted with deuterated water three times. Methyl *N,N'*-dibenzyl-2,3-diaminopropyl ether **182a** was placed with an 1:1 mixture of deuterated methanol and deuterated water. The reaction was refluxed for 24 hours and upon basic work up a 90:10 mixture of piperazinone **301**:**302** and **246a**:**247a** was formed. Analytically pure samples were obtained by flash chromatography (74%, mixture of **247a** and **301**; 26%, **246a** and **302**).

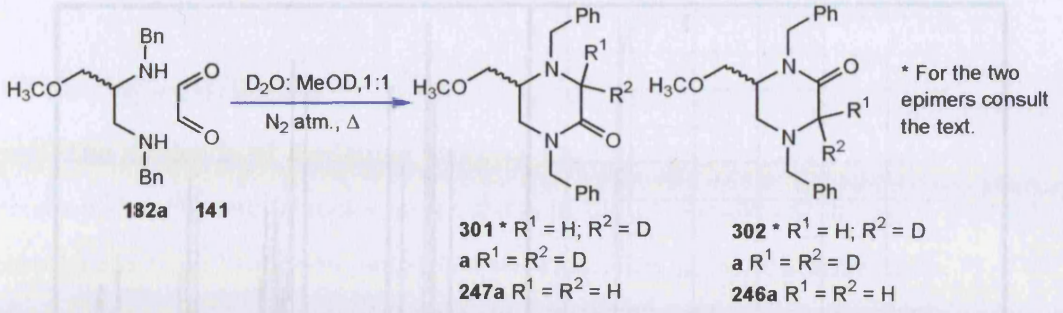

5.4.1.1 ^{1}H-NMR analysis

^{1}H-NMR of the crude mixture contained all the signals for both regioisomers. Integrations for H_2-3 were smaller than expected due to the incorporation of deuterium. The deuterium content of 5-piperazinone **247a** was not detectable by integration in the ^{1}H-NMR spectrum but the ratio proteo:monodeutero:dideutero was 64:28:8 for 6-piperazinone **246a**. These ratios were calculated comparing the H_2-3 integrations with the rest of signals. H_{eq}-3 (δ 3.55) resulted to be smaller than 14% whereas H_{ax}-3 (δ 2.98) was smaller than 20%. Moreover small broad singlets were observed to be next to each H-3 signals, which are due to the monodeuterated methylenes (Figure **36**).

5.4.1.2 ^{2}H-NMR analysis

A ^{2}H-NMR was run to confirm the deuterium incorporation in the 6-piperazinone **301** (Figure **37**). The test was run in deuterated chloroform, the same solvent as previous experiment, for direct comparison to ^{1}H-NMR spectra. Two broad singlets were observed at 2.98 ppm and 3.55 ppm. According to the proton assignment in the ^{1}H-NMR for the 6-piperazinone **302**, the downfield singlet (at 3.55 ppm) represented the deuterium in the equatorial position and the upfield represented the axial one. The deuterated chloroform peak was used as internal standard to adjust and assign the precise chemical shift to the singlets. The Hz difference measured between the two shifts was the same as the one measured for the corresponding signals in the ^{1}H-NMR spectra. Moreover, it was possible, using the integrations in ^{2}H-NMR spectrum, to calculate the ratio of the two peaks which was D_{ax}:D_{eq}, 61:39. It was plausible to suppose that also dideutero-isomer was present but the absence of coupled signals did not give us any way to confirm it.

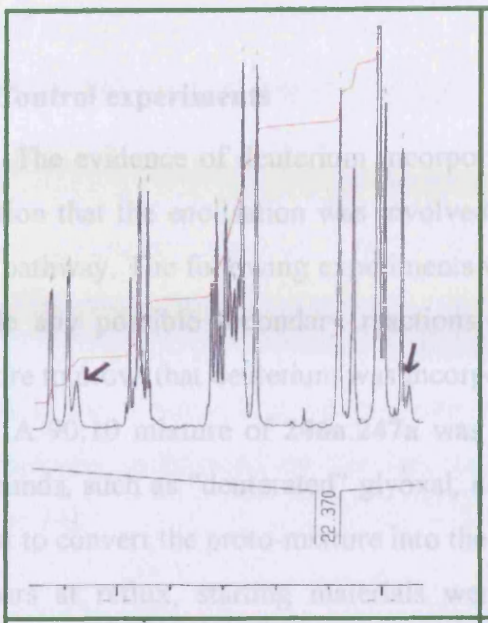

Figure 36. ^{1}H-NMR of 6-piperazinone **302**

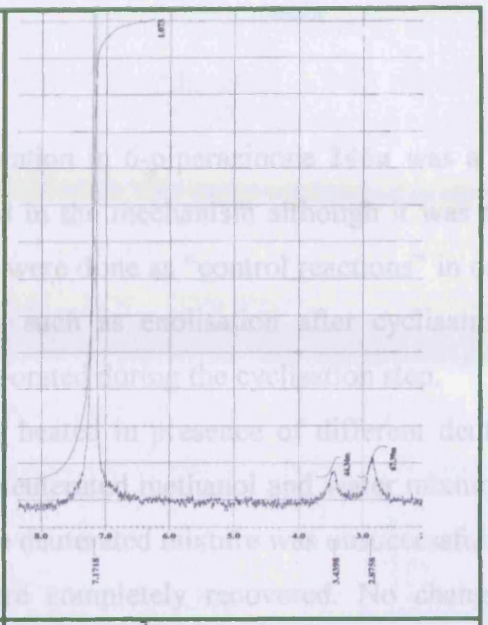

Figure 37. ^{2}H-NMR of 6-piperazinone **302**

5.4.1.3 Low Resolution Mass Spectrometry analysis

The molecular weights of the piperazinones **246a**, **247a** are 324. Upon protonation in the mass spectrometer (CI) a pseudomolecular ion *m/z* 325 is formed (abundance 100%). The unseparated mixture of products **246a**, **247a** also showed the presence of a peak at *m/z* 326 (36% abundance, Table **26**, column 2), whereas, the abundance of this peak due predominantly to the presence of ^{13}C was predicted to be 23.5% (Table **26**, column 5). Mass spectrometry of the separated products showed a large difference in the degree of incorporation of deuterium (Table **26**, columns 3,4).

		Found abundances		Theoretical abundances
Mass Peak	90:10 mixture of **301** and **302**	5-piperazinone **301**	6-piperazinone **302**	**246a**, **247a**
326 (M+D)	36	31	**58**	23.5
327 (M+D_2)	8	5	**21**	3.1
328	1	<1	**1**	-

Table 26. LRMS for the mixture 90:10 of **301** and **302** and isolated piperazinones
*The abundance for the mass peak at *m/z* 325 is 100%.

The abundances of the peaks at *m/z* 325-327 were modelled by permutating the proportions of the three components in 0.5 % increments

Ratio calculated for 5-piperazinone **301** was 93.5: 6.5, H: D.

Ratio calculated for 6-piperazinone **302** was 63: 26: 11, H: D: D_2.

It was then established by ^{1}H-NMR and MS tests that more deuterium was incorporated in the 6-piperazinone **302** than in the isomer **301**.

5.4.2 Control experiments

The evidence of deuterium incorporation in 6-piperazinone **246a** was a strong indication that the enolisation was involved in the mechanism although it was not the major pathway. The following experiments were done as "control reactions" in order to exclude any possible secondary reactions, such as enolisation after cyclisation and therefore to prove that deuterium was incorporated during the cyclisation step.

A 90:10 mixture of **246a**:**247a** was heated in presence of different deuterated compounds, such as "deuterated" glyoxal, deuterated methanol and water mixture. The attempt to convert the proto-mixture into the deuterated mixture was unsuccessful. After 24 hours at reflux, starting materials were completely recovered. No change into deuterated piperazinones was observed monitoring by ^{1}H-NMR and LRMS measurements (Table **27**).

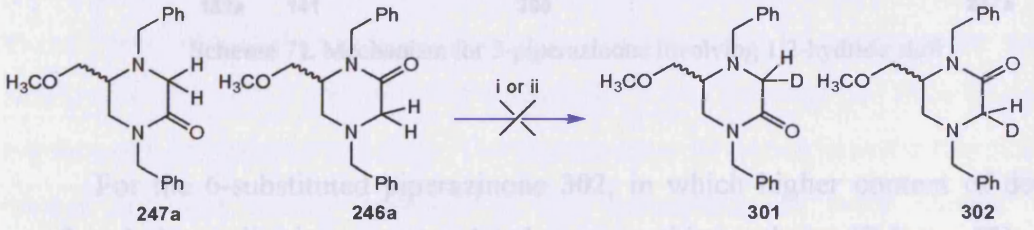

Scheme 70. *Reagents and conditions*: (i) D_2O:MeOD, 1:1, 24 h reflux; (ii) glyoxal, D_2O, 24 h reflux

Mass Peak	Found		Theoretical
	Piperazinone **301**	Piperazinone **302**	
326 (M+1)	24	18	23.6
327 (M+2)	4	2	3.1

Table 27. Abundances of M+2 in LRMS

It was clearly established that no deuterium was incorporated in any of the isomers and that enolisation did not take place with the standard reaction conditions. These results for both control experiments confirmed that piperazinones are stable and they cannot exchange protons in α to the carbonyl group unless a strong base (*t*-BuOK, MeOH) was present in the reaction mixture, i.e. equilibration of stereoisomers (cf. 3.6.1.2).

5.4.3 Postulated mechanism of glyoxal cyclisation in D_2O

Our initial hypothesis to explain the regioselectivity observed in the cyclisation between chiral 1,2-diamines and glyoxal was mainly based on the formation of only one

diaminol stereoisomer capable to lose a water molecule from position 5, in which the lone pair of the amino group were aligned with the antibonding orbital of the leaving group (section 5.1.3). Moreover, it was considerable that despite the higher nucleophilicity of N-4, observed in all previous work, the water molecule departed from the position adjacent to N-1 by donation of N-1 lone pair.

The deuteration experiment opened new considerations regarding the mechanism of formation of the two regioisomers. In particular, the mechanistic pathway that led to the 5-substituted piperazinone must have involved a 1,2- hydride shift as main pathway, confirmed by the low amount of deuterium present at position 3 (Scheme **71**).

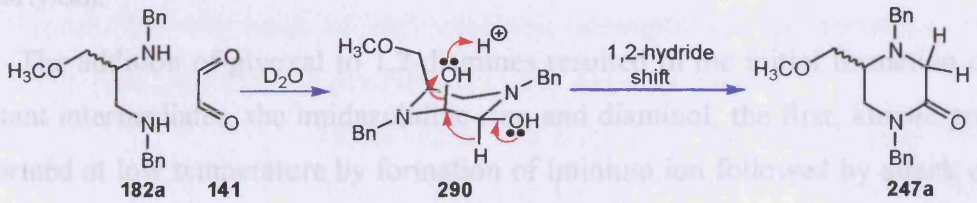

Scheme 71. Mechanism for 5-piperazinone involving 1,2-hydride shift

For the 6-substituted piperazinone **302**, in which higher content of deuterium was found, the enolisation was postulated as competitive pathway (Scheme **72**).

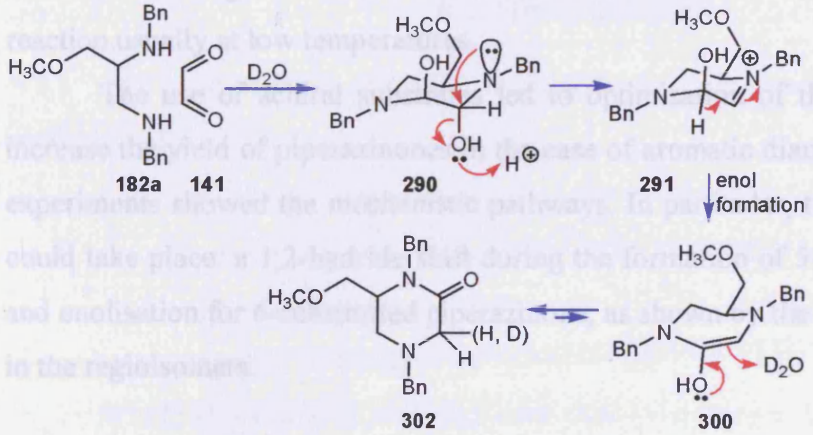

Scheme 72. Mechanism for 6-piperazinone involving amide enolisation

5.5 Conclusions

In conclusion, high regioselectivity for the preferential formation of 5-substituted piperazinones was shown in all glyoxal cyclisations.

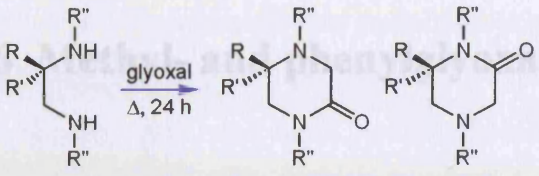

303 304 305

R	R′	R′′	304	305
H	CH_2OCH_3	2-methoxyethyl	90	10
H	CH_2OCH_3	2-methoxyethyl	90 (39)	10 (11)
H	CH_3	Bn	86	14
CH_3	CH_3	Bn	86	14
H	Ph	Bn	77	23
H	CH_2OCH_3	Ph	82 (10)	18 (1)
H	CH_2OCH_3	*p*-methoxyaniline	60	40

Table 28. Cyclisation results of chiral diamines with glyoxal. Ratios calculated in the crude ^{1}H-NMR spectrum (yield).

The addition of glyoxal to 1,2-diamines resulted in the initial formation of two important intermediates, the imidazolidine ring and diaminol; the first, kinetic product, was formed at low temperature by formation of iminium ion followed by attack of N-1 to the "new" electrophilic centre. The latter was generated by simultaneous and direct addition of both amino groups to the dialdehyde. It was believed that both intermediates rearranged into piperazinone rings. The piperazinone formation is under thermodynamic control and was usually obtained at high temperature in polar solvent whereas imidazolidine ring was formed under kinetic control and formed at the first stage of the reaction usually at low temperatures.

The use of achiral substrates led to optimisation of the procedure in order to increase the yield of piperazinones in the case of aromatic diamines and the deuteration experiments showed the mechanistic pathways. In particular, two possible mechanisms could take place: a 1,2-hydride shift during the formation of 5-substituted piperazinone and enolisation for 6-substituted piperazinone, as shown by the deuterium amount found in the regioisomers.

CHAPTER 6 Methyl- and phenylglyoxal cyclisations

6.1 Introduction

Parallel to the study on the diastereoselective preparation of 3,6-disubstituted piperazinones, starting from 2-substituted *N,N'*-dibenzyl 1,2-diamines and chiral haloacetates, further investigations on the cyclisations of the same chiral diamines with asymmetric 1,2-dicarbonyl compounds were performed.

From the preceding chapter, it was established that the addition of glyoxal to the 1,2-diamines occurred regioselectively with the preferential formation of 5-substituted piperazinones. On the basis of that evidence, attempts for the extension of this procedure to preparation of 3,5-disubstituted rings were carried out.

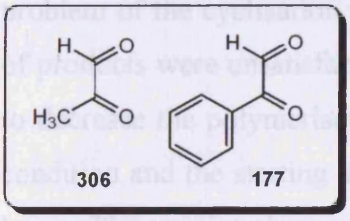

306 177

Described in this chapter are the cyclisations of methyl- **306** and phenylglyoxal **177** with the dibenzyl diamine as a potential stereoselective way to prepare 3,5-disubstituted piperazinones.

6.2 Methylglyoxal

6.2.1 Cyclisation of methyl *N,N'*-dibenzyl-2,3-diaminopropyl ether and methylglyoxal

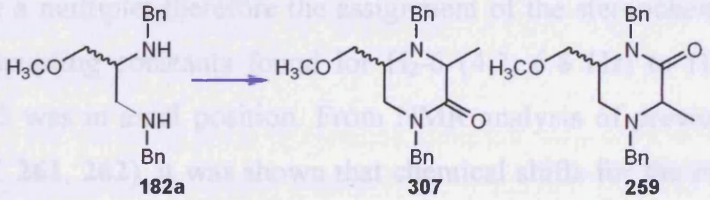

182a **307** **259**

When an excess of methylglyoxal **306** (5 mol/equivalents) was added to the refluxing mixture of dibenzyl diamine **182a** in water:ethanol, 1:1, the colour of the crude mixture went from clear yellow to dark red in a few seconds. The reaction progress was monitored by TLC and after 4 hours, the diamine was still present. This suggested that there was no reaction taking place. A possible explanation for this unsuccessful attempt was that the polymerisation of methylglyoxal occurred, also confirmed by colour changes of the crude mixture, and that consequently the diamine could not react with the dielectrophile. At the end of the experiment, after 24 hours, the diamine starting material was completely recovered.

The second attempt at the cyclisation was performed using a smaller amount of methylglyoxal (1.1 mole equivalents) and performing its addition dropwise over 6 hours. After 110 hours of reflux, TLC and NMR spectra showed the formation of two products. Their ratio based on the methoxy groups integrations was 90:10 in the ^{1}H-NMR spectra. The two adducts were purified by flash chromatography and identified as 3,5-disubstituted piperazinone **307** (15%) and 3,6-disubstituted piperazinone **259** (3%). The latter was previously prepared by addition of the dibenzyl diamine **182a** and methyl 2-bromopropionate **252.** The structure was confirmed by direct comparison of NMR data to the standard piperazinone **259**.

The other regioisomer **307** was a new compound and its structure was confirmed by full NMR data analysis. The formation of only one diastereoisomer for each pair of regioisomers showed that the cyclisation was somewhat stereoselective. The major problem of the cyclisation was the polymerisation of the methylglyoxal therefore yield of products were unsatisfactory. In order to optimise the yield of piperazinone **307**, and to decrease the polymerisation of methylglyoxal, the reaction was run in high dilution condition and the starting diamine and methylglyoxal were both added dropwise over 8 hours. The reaction time was prolonged until 210 hours. Several conditions did not give any improvement and the yield of 5-piperazinone obtained was always disappointing.

6.2.2 ^{1}H-NMR data analysis for 1,4-dibenzyl-5-methoxymethyl-3-methyl-piperazin-2-one 307

H-5 gave a multiplet therefore the assignment of the stereochemistry was based on the vicinal coupling constants found for H_2-6 (4.2, 6.8 Hz) to H-5, which could indicate that H-5 was in axial position. From NMR analysis of previous 3-substituted piperazinone (cf. **261**, **262**), it was shown that chemical shifts for the proton at position 3 were not useful in order to assign the stereochemistry at that centre. In this case, H-3 displays a doublet at δ 3.35 ppm, which is an intermediate value between the expected axial (δ 3.05, cf. **259**) and equatorial (δ 3.56, cf. **260**) protons. The two possibility for the conformation of the regioisomer **307** were *trans*-3_{ax},5_{eq} and *cis*-3_{eq},5_{eq}.

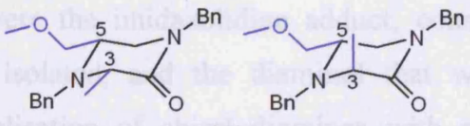

307

cis-3_{eq}, 5_{eq}-piperazinone

trans-3_{ax}, 5_{eq}-piperazinone

Unfortunately, the precise conformation of the adduct **307** could not be assigned for the reasons explained above. However, according to the energies calculated with PC Model 8, the most stable conformation possesses the methoxymethyl substituent and the methyl at position 3 both in axial position.

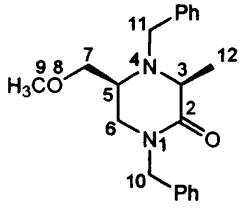

5-Piperazinone 307

	5-Piperazinone 307
H-3	3.35 (d, 6.9)
H-5	2.95 (m)
H-6a	3.3 (dd, 12.6, 4.2)
H-6b	3.2 (dd, 12.6, 6.8)
H-7a	3.25 (dd, 9.3, 4.2)
H-7b	3.05 (m)
H_3-9	3.03 (s)
H-10a	3.78 (dd, 17.4, 14.6)
H-10b	3.78 (dd, 17.4, 14.6)
H-11a	4.55 (d, 14.5)
H-11b	4.58 (d, 14.5)
H_3-12	1.37 (d, 9.6)

Table 29. ^{1}H-NMR chemical shifts and coupling constant for piperazinone **307**

6.3 Phenylglyoxal

6.3.1 Introduction

The cyclisation of methyl α-bromophenylacetate with dibenzyl diamine, described in chapter 3, showed to be 100% regioselective, due to the only formation of the pair of epimers of 3,6-disubstituted piperazinones. However, the ratio of these diastereoisomers found was 50:50 therefore the cyclisation did not show any diastereoselectivity. Our prediction for the phenylglyoxal cyclisation was mainly based, as for the methylglyoxal case, on the higher reactivity of the aldehyde function over the ketone ones present that could lead to formation of only one pair of epimers, 3,5-disubstituted piperazinones.

Moreover, the methylglyoxal cyclisation outcome was very encouraging for the ratio of products found and it would probably be a reliable procedure in absence of polymerisation reaction of the methylglyoxal.

6.3.2 Phenylglyoxal cyclisation: predicted mechanism

As seen in the glyoxal work, the key intermediates for the formation of the 5-piperazinone regioisomers were the imidazolidine adduct, considered as the kinetic intermediate, observed and isolated, and the diaminol that was not isolable. Our prediction regarding the cyclisation of chiral diamines with phenylglyoxal was as follow. Phenylglyoxal is a ketoaldehyde and consequently the most electrophilic centre

to be attacked by N-4 was the aldehyde part to form the keto-aminol **308**. At that stage, as already observed in previous cyclisations, two pathways (**a** and **b**) could take place.

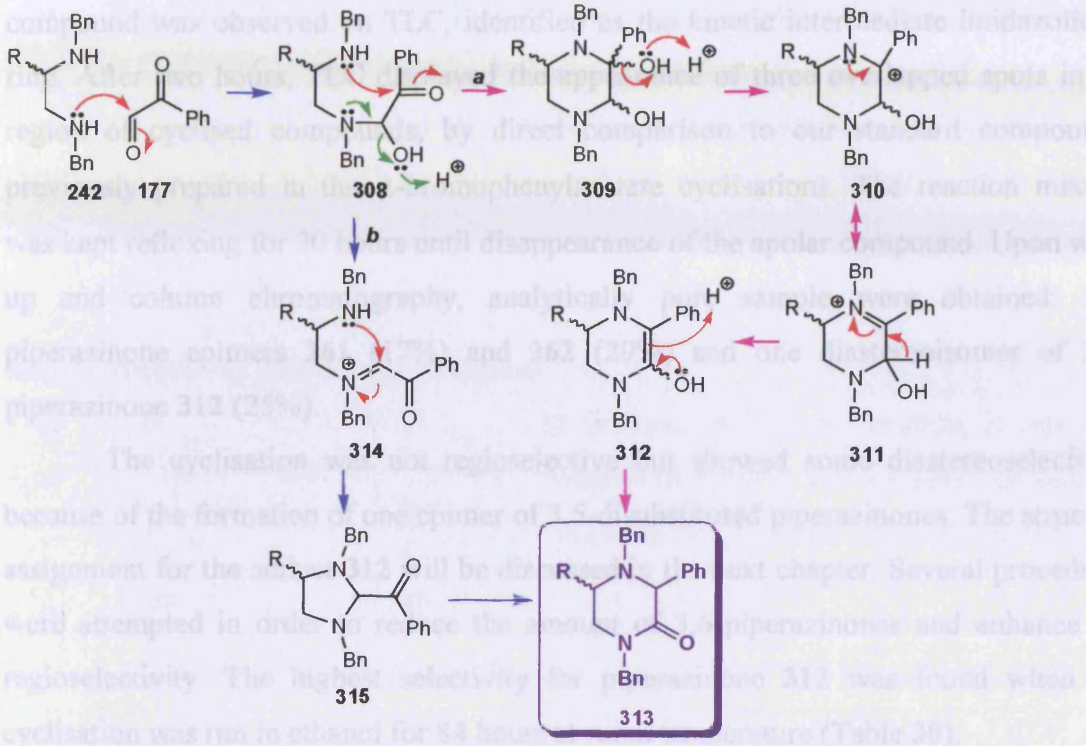

Scheme 73. Mechanistic pathways for phenylglyoxal addition to secondary diamines

The postulated path **a** involved attack of N-1 to the ketone and formation of the diaminol **309**[150]. The path **b** involved attack from N-1 to the electrophilic carbon of the iminium ion. We chose the pathway **a** as the most feasible leading to the formation of diaminol and consequent elimination of a water molecule at C-2 to generate a carbocation, highly stabilised by resonance from the lone pair of the nitrogen and from the phenyl group. The formation of a stable carbocation would have lead to the formation of the 3,5-disubstituted piperazinone **313**.

6.3.3 Cyclisation of methyl *N,N'*-dibenzyl-2,3-diaminopropyl ether 182a and phenylglyoxal 177

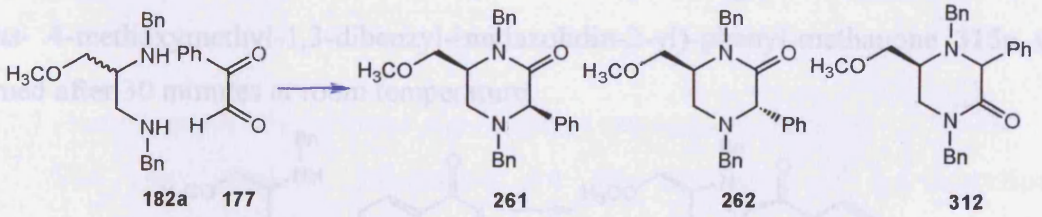

The cyclisation of diamine **182a** with phenylglyoxal **177** was performed in a mixture of ethanol and water, 9:1. As expected, after 30 minutes, formation of an apolar compound was observed on TLC, identified as the kinetic intermediate imidazolidine ring. After two hours, TLC displayed the appearance of three overlapped spots in the region of cyclised compounds, by direct comparison to our standard compounds, previously prepared in the α-bromophenylacetate cyclisations. The reaction mixture was kept refluxing for 20 hours until disappearance of the apolar compound. Upon work up and column chromatography, analytically pure sample were obtained: 3,6-piperazinone epimers **261** (17%) and **262** (29%) and one diastereoisomer of 3,5-piperazinone **312** (25%).

The cyclisation was not regioselective but showed some diastereoselectivity because of the formation of one epimer of 3,5-disubstituted piperazinones. The structure assignment for the adduct **312** will be discussed in the next chapter. Several procedures were attempted in order to reduce the amount of 3,6-piperazinones and enhance the regioselectivity. The highest selectivity for piperazinone **312** was found when the cyclisation was run in ethanol for 84 hours at room temperature (Table **30**).

Solvent	Reaction time	261	262	312
EtOH:H_2O/ 9:1	20 h reflux	17	29	25
EtOH:H_2O/ 9:1	**84 h rt**	**11**	**21**	**68**
EtOH/p-TsOH	24 h rt	14	28	56
EtOH	120 h rt	17	29	53
EtOH/silica gel	24 h rt	28	43	28
EtOH/silica gel	24 h reflux	38	31	30
H_2O/ NaI	24 h rt	18	42	40
H_2O/ NaI	24 h reflux	21	38	41
DMF	5h rt	42	17	40

Table 30. The ratios have been calculated in the crude ^{1}H-NMR over the aromatics

6.3.3.1 Isolation of five membered ring intermediate

At the beginning of the reaction of dibenzyl diamine **182a** and phenylglyoxal **177**, TLC showed the presence of two spots in the apolar region. A mixture of *cis*- and *trans*- 4-methoxymethyl-1,3-dibenzyl-imidazolidin-2-yl)-phenyl-methanone **315a** was formed after 30 minutes at room temperature.

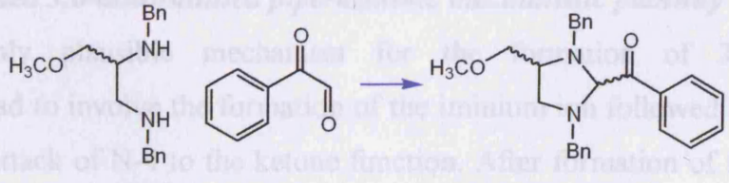

182a **177** **315a**

After one hour at room temperature, the adducts **315a** was isolated and purified (20% yield). After 48 hours their amount in the crude mixture decreased to 8%. They were the kinetic intermediates that could rearrange into the piperazinones[151].
Full NMR analysis showed that the mixture was composed of *cis* (65%) and *trans* (35%) isomers. Previous work also showed that the most favourable isomer was the *cis*-imidazolidine.

6.3.3.2 Isolation of diaminol intermediate

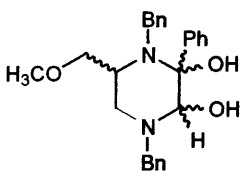

309

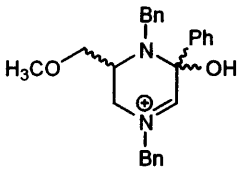

316

In the first part of the reaction, it was also possible to observe the formation of another important intermediate, the diaminol **309**.

After stirring for 2 hours at room temperature, the reaction mixture was composed of imidazolidine **315a** (20%), a mixture of piperazinones (32%) and diaminol **309** (30%).

The diaminol **309** was the slowest spot on TLC and its purification was impossible due to the continuous and spontaneous conversion into the piperazinones. The ^{1}H-NMR spectra showed the presence of two sharp singlets at 3.65 and 4.5 ppm that were assigned to the proton of the secondary and tertiary alcohol groups of both conformers, and the presence of piperazinones **261** and **262**, which initial ratio was 50:50. IR spectra displayed a weak broad band around 3000 cm^{-1} and signals due to the C-O stretching of the secondary alcohol.

By monitoring the isolated diaminol for one week, a change in its composition was observed by TLC and ^{1}H-NMR spectra. After 7 days in a vial, the ratio of **261**:**262** had changed to 27:73 and the diaminols signals had disappeared completely. It was expected that the diaminols would be converted into 3,5-piperazinone **312** but this was not seen.

6.3.3.3 Postulated 3,6-disubstituted piperazinone mechanistic pathway

The only plausible mechanism for the formation of 3,6-disubstituted piperazinone had to involve the formation of the iminium ion followed by formation of an aminol by attack of N-4 to the ketone function. After formation of the aminol **316**, the 1,2-phenyl group shift should be postulated as the main pathway. The preference of

N-4 to attack the ketone rather than the electrophilic carbon of the iminium ion could be unexpected, as previously seen in the glyoxal work where the same position was preferred in presence of another aldehydic function. The alternative and perhaps more reasonable mechanism would lead to the formation of the imidazolidine derivative, as seen in glyoxal cyclisations.

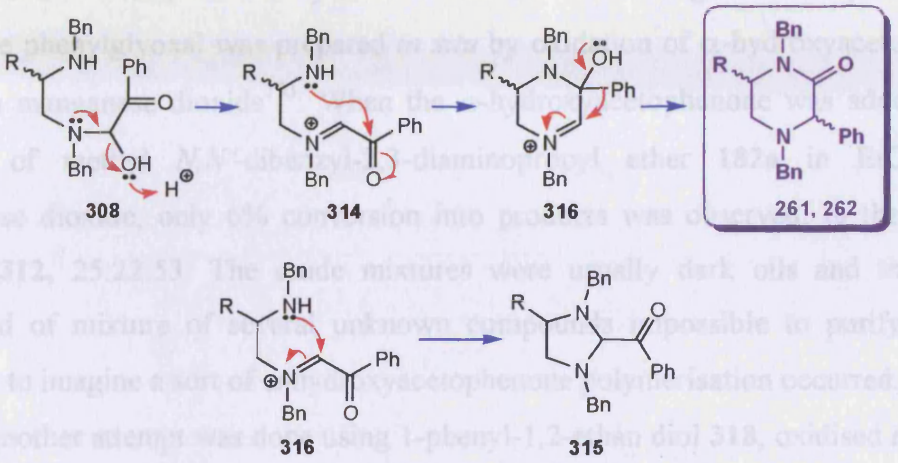

However, previous work by Agami showed that 1,2-phenyl shifts to iminium ions occurred during the synthesis of morpholine derivatives although after formation of the diol **179**. The higher nucleophilicity of the amino group over the hydroxyl group and the favourable formation of a lactone rather than a lactam lead to the formation of only one product[152].

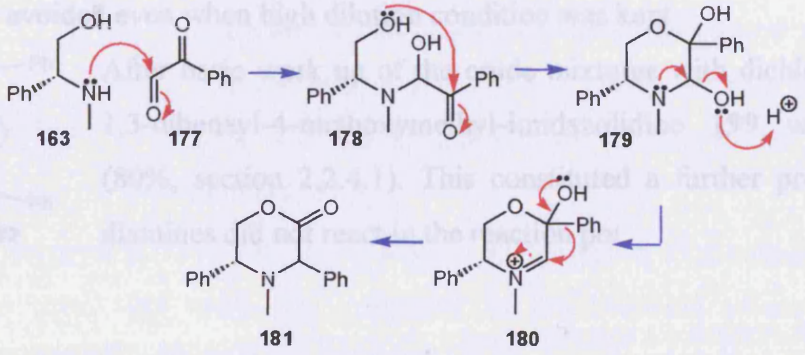

The partial loss of diastereoselectivity, observed in the phenylglyoxal cyclisations, was perhaps due to the higher rate of the iminium ion formation followed by the favourable 1,2-phenyl group shift. It was probable that the temperature was involved in the competition of these mechanisms, since it was observed that high temperatures promoted loss of diastereoselectivity, with consequent major formation of 6-piperazinone.

6.3.4 Oxidation *in situ* to prepare phenylglyoxal

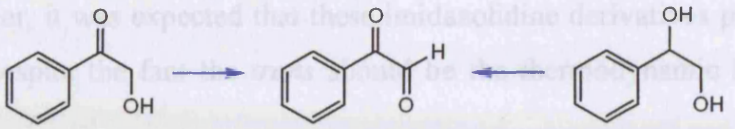

317 177 318

Another attempt at this cyclisation was done following a known procedure in which the phenylglyoxal was prepared *in situ* by oxidation of α-hydroxyacetophenone **317** with manganese dioxide[153]. When the α-hydroxyacetophenone was added to the mixture of methyl *N,N'*-dibenzyl-2,3-diaminopropyl ether **182a** in EtOH with manganese dioxide, only 6% conversion into products was observed, in the ratio of **261**:**262**:**312,** 25:22:53. The crude mixtures were usually dark oils and they were composed of mixture of several unknown compounds impossible to purify. It was plausible to imagine a sort of α-hydroxyacetophenone polymerisation occurred.

Another attempt was done using 1-phenyl-1,2-ethan diol **318**, oxidised *in situ* by manganese dioxide, to keep the concentration of phenylglyoxal low during the cyclisation step, to promote an higher regioselectivity and to avoid the starting material polymerisation. Unfortunately, the crude ^{1}H-NMR spectra showed, also in this case, mixtures of products. However, signals of the desired piperazinone were very weak (<3% conversion). Colour change of the crude mixture occurred hence polymerisation could not be avoided even when high dilution condition was kept.

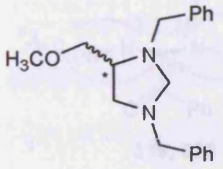

199

After basic work up of the crude mixtures with dichloromethane, 1,3-dibenzyl-4-methoxymethyl-imidazolidine **199** was isolated (80%, section 2.2.4.1). This constituted a further proof that the diamines did not react in the reaction pot.

6.3.5 Cyclisation of methyl *N,N'*-diphenyl-2,3-diaminopropyl ether 182d and phenylglyoxal 177

Phenylglyoxal was also reacted with the less reactive diphenyl diamine **182d**. After 24 hours at reflux in ethanol:water mixture, the products isolated were the *cis* and *trans* isomers of the imidazolidine derivatives **319** and **320**. The mixture seemed to be the final products of the reaction, also confirmed by running the reaction for longer times (72 hours, 40% yield).

^{1}H-NMR spectra of the crude after only 5 hours already showed the complete conversion of the diamine into two adducts in the ratio of *cis*: *trans*, 70:30. Purification

by column chromatography gave only one fraction containing both compounds. As mentioned earlier, it was expected that these imidazolidine derivatives preferred the *cis* conformation despite the fact the *trans* should be the thermodynamic isomer and the most stable.

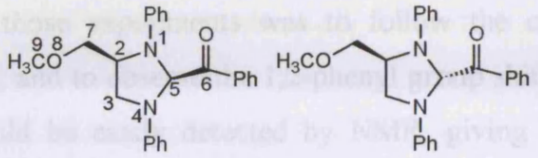

319 **320**

H	319	320
H-2	4.42 (pd, 4.6, 1.7)	4.13 (ddd, 12.3, 8.7, 4.3)
H-3a	3.6 (m)	3.6 (m)
H-3b	3.7 (dd, 9.6, 1.5)	3.76 (dd, 9.0, 7.8)
H-5	5.9 (s)	5.72 (s)
H-7a	2.92 (t, 7.1)	3.08 (t, 7.1)
H-7a	3.6 (m)	3.41 (dd, 9.3, 4.6)
H_3-9	3.23 (s)	3.2 (s)

Table 31. NMR data comparison of *cis*- **319** and *trans*-isomers **320**

Due to the similarity of these imidazolidine derivatives with piperazinones, most signals in the ^{1}H-NMR spectra were almost the same but the ^3J spectra showed correlations that were not present in the piperazinones spectra.

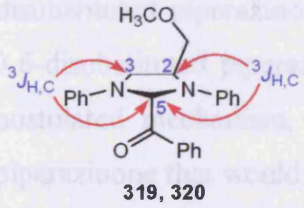

319, 320

In particular, the crucial correlation was found between for H-2 and H-3 to C-5 and *vice versa* for both compounds. This correlation clearly links all the atoms in a five-membered ring.

IR absorption at 1597 cm^{-1} could suggest the presence of a conjugated ketone, although the value was quite low compared to the literature values for similar imidazolidine rings[154], which were 1690 and 1675 cm^{-1} for that conjugated ketone. Finally, the LRMS showed one peak at 373 (M+1) and one peak at 265 due to the loss of the stable acylium ion. These data were confirmed by HRMS for both peaks.

6.4 Further investigations on 3,6-disubstituted piperazinone formation

Phenylglyoxal reacted with the dibenzyl diamine giving a mixture of three piperazinones. Even in our best attempt to enhance the selectivity towards our desired product, the ratios were disappointing. The high incidence of unexpected 3,6-piperazinone epimers formation suggested that there was a competitive mechanism

taking place that afforded these two piperazinone, besides the main pathways for 3,5-piperazinones.

By evaluating this alternative mechanism, which had to involve a 1,2-phenyl group shift we decided to follow further investigations. ^{13}C-labelled phenylglyoxal was prepared and reacted with the dibenzyl diamine and benzil was used as "new" cyclising agent. The scope of those experiments was to follow the cyclisation mechanistic pathway with the label, and to observe the 1,2-phenyl group shift. The label position in the piperazinones would be easily detected by NMR, giving important information regarding the cyclisation mechanism.

The experiment involving the ^{13}C labelled phenylglyoxal is described in following section whereas the benzil cyclisations are described in the next chapter.

6.4.1 ^{13}C-labelled phenylglyoxal

6.4.1.1 Postulated mechanism

The insertion of ^{13}C-label at the aldehydic function of phenylglyoxal represented a useful tool to understand the mechanism of its addition to the diamine. The position of the label in the final products could be easily monitored by NMR and could give important information regarding the preferential pathways that lead to 3,5- and 3,6-disubstituted piperazinones. In particular, our hypothesis concerning the formation of 3,6-disubstituted piperazinones was about a 1,2-phenyl group shift. According to our postulated mechanism, our expectation was to find the label at position 3 in the piperazinone that would agree with our hypothesis.

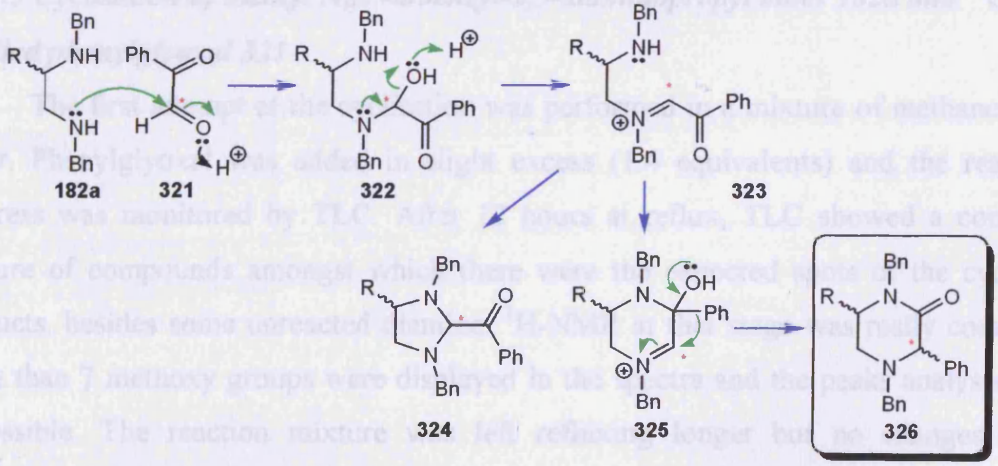

Scheme 74. Postulated mechanism for ^{13}C-labelled phenylglyoxal

6.4.1.2 Preparation of ^{13}C-phenylglyoxal

^{13}C-labelled phenylglyoxal was prepared by oxidation of a ^{13}C-acetophenone and selenium dioxide[155] in a mixture of dioxane:water, 1:1. The label was present on the methyl group of the acetophenone that was converted in aldehyde function. The reaction of non-labelled phenylglyoxal was done simultaneously and it was successful. The oxidation occurred in 24 hours and the work up consisted in easy decantation of solvent followed by evaporation on the high vacuum rotary evaporator to yield the labelled-phenylglyoxal as white solid in high yield (79 %).

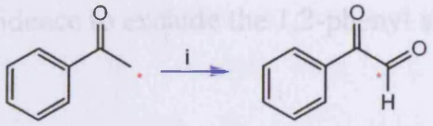

327 **321**

Scheme 75. *Reagents and conditions*: (i) SeO_2, H_2O, dioxane

The reaction progress was monitored by NMR. ^{1}H-NMR spectra of the acetophenone showed only two ^{13}C satellites for a singlet (δ 2.47 ppm, doublet, 127.5 Hz), besides the aromatics. ^{13}C-NMR showed only one signal, corresponding to the methyl group at 26.86 ppm.

^{1}H-NMR spectra of the oxidised product **321** showed disappearance of the two satellites and appearance of other two ^{13}C satellites for a singlet (δ 9.5 ppm, doublet, 186.2 Hz), attributed to the aldehyde peak. Similarly, ^{13}C-NMR showed complete disappearance of the methyl peak and appearance of a carbonyl peak at 191.36 ppm.

6.4.1.3 Cyclisation of methyl N,N'-dibenzyl-2,3-diaminopropyl ether 182a and ^{13}C labelled phenylglyoxal 321

The first attempt at the cyclisation was performed in a mixture of methanol and water. Phenylglyoxal was added in slight excess (1.4 equivalents) and the reaction progress was monitored by TLC. After 12 hours at reflux, TLC showed a complex mixture of compounds amongst which there were the expected spots of the cyclised products, besides some unreacted diamine. ^{1}H-NMR at that stage was really complex. More than 7 methoxy groups were displayed in the spectra and the peaks analysis was impossible. The reaction mixture was left refluxing longer but no changes were observed either on TLC or in the NMR.

Unfortunately, the outcome of the second attempt was the same as the first one. ^{13}C-NMR spectra of the crude mixture displayed a mixture of compounds and the label was present at carbonyl peaks.

The reactions were run in 100 mg scale due to the high cost of the labelled acetophenone therefore it was not possible to perform other attempts at the cyclisation. Further steps would have involved flash chromatography of the complex mixture and spectroscopic analysis of each single component. Due to the low amount of the crude mixtures and to the unsuccessful result for ^{13}C label in the NMR, chromatography was not carried out as we considered it time consuming without expecting any positive outcome.

^{13}C-NMR spectra of the crude mixture showed the label at carbonyl positions and this was a sufficient evidence to exclude the 1,2-phenyl shift during the cyclisation.

6.5 Conclusions

The cyclisation of the dibenzyl diamine **182a** with methylglyoxal was high regio- and diastereoselective (90:10 mixture of regioisomers, 100% formation of one diastereoisomer. The limit of this procedure was the methylglyoxal polymerisation that resulted in poor yield of products (15%).

The cyclisation of the same diamine **182a** with phenylglyoxal was not high regioselective (32:68 mixture of regioisomers). Unfortunately, ^{13}C labelled phenylglyoxal cyclisation reaction did not elucidate the reason of the unexpected loss of regioselectivity. Further investigations for the cyclisation mechanisms will be described in the next chapter.

CHAPTER 7 Benzil cyclisations

7.1 Introduction

The cyclisation between ^{13}C-phenylglyoxal and dibenzyl diamine, described in the final part of the preceding chapter, indicated that there was no 1,2-phenyl group shift occurring for the formation of 3,6-disubstituted piperazinones.

Parallel to that investigation, new cyclisations of our scaffold diamines with benzil were carried out. The idea behind these experiments was to "force" the 1,2-phenyl shift, which represented an essential step in the cyclisation mechanism. According to our postulated mechanism, preferential formation of piperazinone **332** should occur. The first step involved the attack from the more reactive N-4 to one keto group. At that point, there were two possible choices: the first (path **a**) was attack of N-1 to the second ketone to form the diaminol; the second (path **b**) was the departure of water molecule to form a tertiary carbocation **328**, highly stabilised by resonance from the adjacent amino lone pair and the phenyl group.

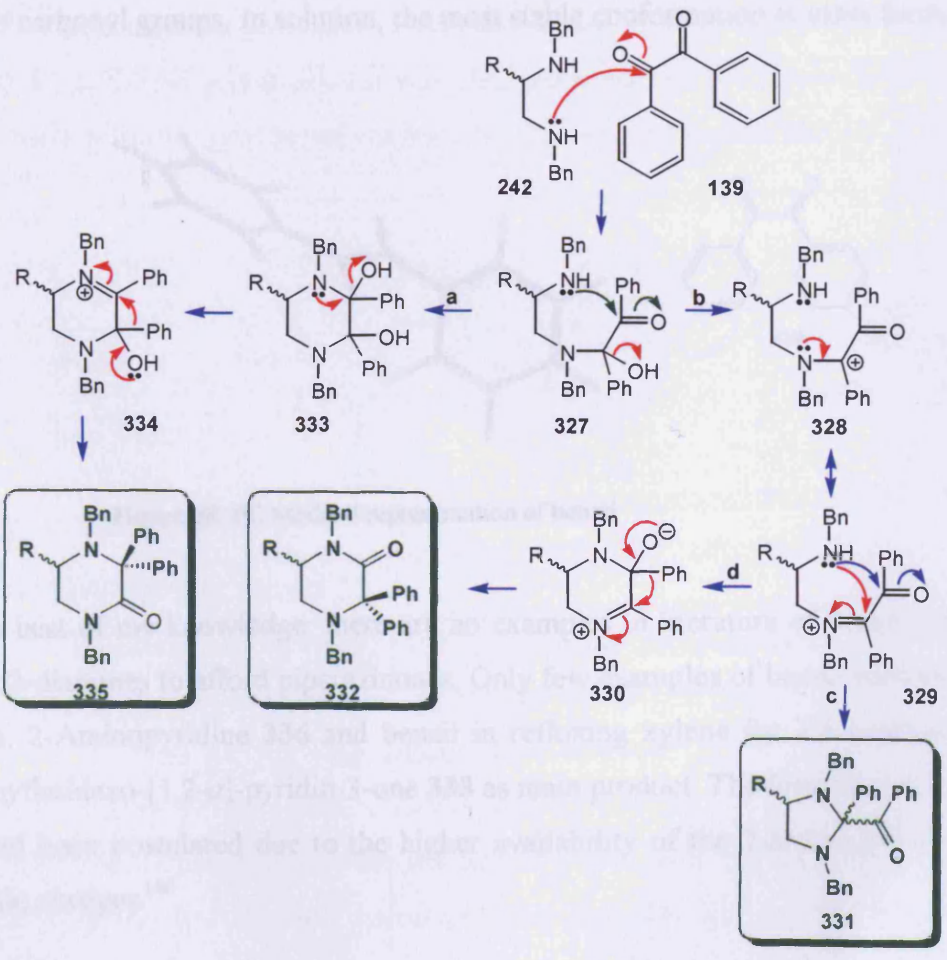

The latter path was considered to be the most favourable due to the presence of the reactive N-4 lone pair that would afford the iminium ion **329**.

After formation of the intermediate **329**, two possible pathways could take place. The path **c** (blue arrows) involved attack from N-1 to electrophilic iminium ion and led to the imidazolidine ring **331**. The path **d** (red arrows) involved formation of the new aminol **330** by attack of N-1 to the second keto function of benzil. In this pathway, a 1,2-phenyl group shift had to occur in order to complete the lactam formation and to restore the tertiary amine.

Our hypothesis also excluded the formation of the other regioisomer **335** as a direct consequence of the favourite loss of a water molecule in the aminol **327** and consequent iminium ion **329** formation (path **b**).

7.1.2 Benzil reactivity

Benzil is the simplest aromatic α-dicarbonyl compound. The structure of benzil is considered to be flexible with respect to the dihedral angle θ between the planes of the two carbonyl groups. In solution, the most stable conformation is *trans* form.

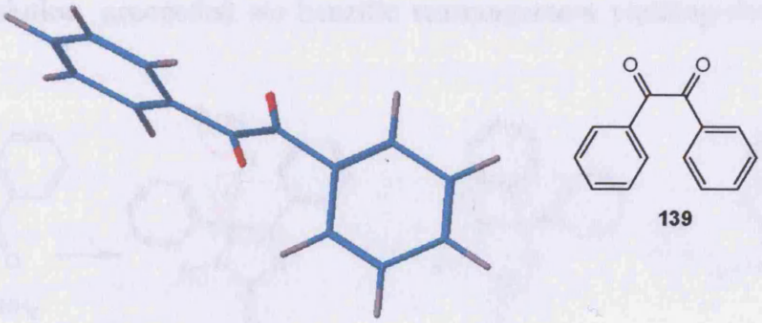

Figure 38. PC Model 8 representation of benzil

To the best of my knowledge, there are no examples in literature of benzil cyclisation with 1,2-diamines to afford piperazinones. Only few examples of benzil with amines are known. 2-Aminopyridine **336** and benzil in refluxing xylene for 7.5 hours gave 2,2-diphenylimidazo-[1,2-*a*]-pyridin-3-one **338** as main product. The formation of the imine **338** had been postulated due to the higher availability of the 2-amino group over the pyridine nitrogen[156].

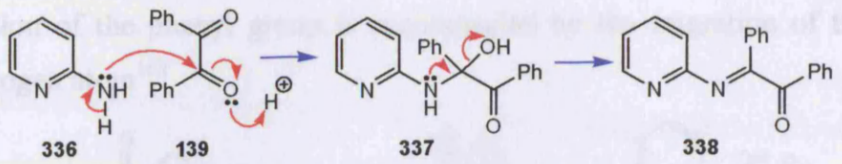

336 139 337 338

However, Sokov[157] postulated the formation of the diaminol **339**, which rearranged to the pyridinone **340** through pinacol rearrangement. The outcome of this experiment could be that the formation of the diaminol at high temperature was faster than imine formation.

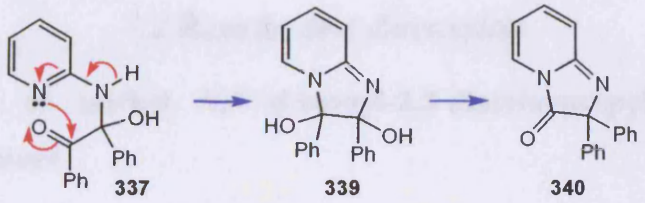

337 339 340

7.1.2.1 Biltz synthesis

A close example to our case was the condensation of benzil **139** or substituted benzil[158] with urea, known as Biltz synthesis, which gave phenytoin **344** in good yield (74%)[159]. The proposed mechanism for condensation of benzil with an alkylurea requires a 1,2-phenyl group shift. It was also proposed that the condensation reaction, run in basic solution, proceeded *via* benzilic rearrangement yielding the same adduct **344**[160,161].

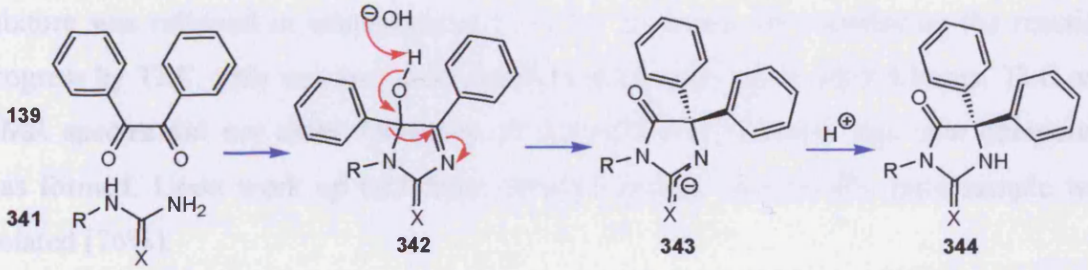

342 343 344

7.1.2.2 Benzilic rearrangement

The benzilic rearrangement is the base-induced transformation of an α-diketone into the salt of an α-hydroxyacid and, in case of substituted ones, is favoured when Rs are modest electron withdrawing groups. It is observed in aromatic, semiaromatic, acyclic and in aliphatic as well as heterocyclic α-diketones.

The first step is the reversible addition of a hydroxide ion to a C=O group of the α-diketone, giving the negatively charged intermediate. The first intermediate undergoes a rate determining intramolecular rearrangement, yielding a second intermediate, which is rapidly converted into the salt of he corresponding α-hydroxyacid by proton transfers.

The migration of the phenyl group is accompanied by the migration of the oxygen-bound hydrogen atom[162].

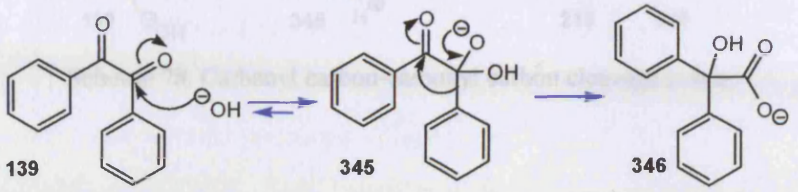

Scheme 76. Benzilic rearrangement mechanism

7.2 Results and discussion

7.2.1 Cyclisation of methyl *N,N'*-dibenzyl-2,3-diaminopropyl ether 182a in ethanol:water mixture

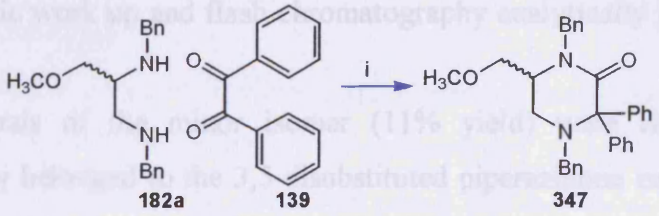

Scheme 77. *Reagents and conditions:* (i) EtOH:H_20, 1:1, reflux, N_2 atm.

The first attempt for the benzil cyclisation was performed using the same procedure as the other cyclisations with 1,2-dicarbonyl compounds. The reaction mixture was refluxed in ethanol:water (1:1) for 24 hours. By monitoring the reaction progress by TLC, only one spot was shown in the apolar region after 3 hours. TLC and NMR spectra did not show formation of piperazinones although one new compound was formed. Upon work up and flash chromatography, analytically pure sample was isolated (76%).

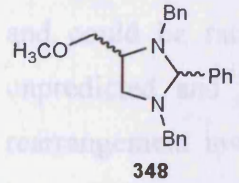
348

The NMR data was consistent with the 1,3- dibenzyl-4-methoxymethyl-2-phenyl imidazolidine **348** structure. Previous work by EGB showed the formation of the imidazolidine **348** by the condensation of the diamine **182a** with benzaldehyde **213**[130].

This result was unexpected and suggested that the scission of carbonyl carbon-carbonyl carbon bond of benzil might have occurred, affording benzaldehyde and benzoate.

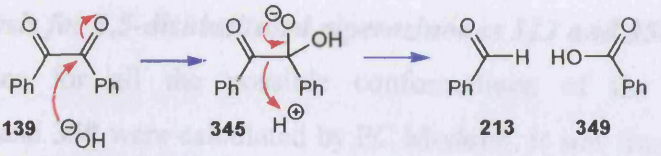

Scheme 78. Carbonyl carbon-carbonyl carbon cleavage in base

7.2.2 Cyclisation of methyl *N,N'*-dibenzyl-2,3-diaminopropyl ether 182a and benzil in DMSO

The following attempt at the cyclisation was performed at much higher temperature, in DMSO. After 20 hours at 165° C, two new products in the region of cyclised compounds were shown on TLC (R_f= 0.34, **312**; Rf= 0.25, **350**; petroleum ether: diethyl ether, 3:1) and a ratio of 43:57 was calculated in the crude ^{1}H-NMR spectra. Upon basic work up and flash chromatography analytically pure samples were isolated.

NMR signals of the minor isomer (11% yield) were familiar to us and unexpectedly, they belonged to the 3,5-disubstituted piperazinone isomer **312**, isolated in the phenylglyoxal cyclisation. The major isomer (30% yield) was unknown and NMR data analysis confirmed the structure as the epimer of piperazinone **350**.

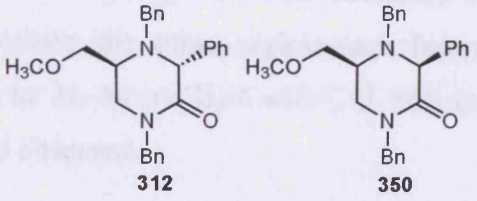

Reaction in DMSO at lower temperature such as 120° C gave mixture of imidazolidine adduct and piperazinones in a ratio of 62:31:6, **350**:**312**:**348**. Therefore the highest selectivity for the piperazinones was achieved at 165° C.

The isolation of these two piperazinone epimers **312** and **350** was totally unexpected and could be rationalised only by the loss of one phenyl group. This result was unpredicted and very exciting. We rationalised that the benzil had to undergo a rearrangement involving a scission of R carbon-carbonyl carbon bond to form an α-ketoacid or the reduced form, showing the same oxidation state of phenylglyoxal. Dephenylations of benzil had never been observed during the cyclisation reactions earlier in literature. However, it is known that this type of cleavage was achieved using 2,6-dihalobenzaldehydes with halogen substituents in ortho position.

7.2.2.1 NMR analysis for 3,5-disubstituted piperazinones 312 and 350

The energies for all the possible conformations of the 3,5-disubstituted piperazinones **312** and **350** were calculated by PC Model 8. It was found that the lowest energy belonged to the stereosiomer having both the methoxymethyl substituent and the phenyl substituent in equatorial positions (Figure **39**).

Unfortunately ^{1}H-NMR data were not complete due to the presence of overlapped signals hence the stereochemistry of these epimers could not be fully assigned. H-3 singlets for both epimers were at the same high chemical shift (δ 4.3), which suggested they could be in equatorial position. Small vicinal coupling constants (4.9, 2.7 Hz) were found for H_2-6 to H-5 for the isomer **350**, which suggested the H-5 in equatorial position. Unfortunately, for the other isomer **312**, only one small vicinal coupling constant was observed for H-6b (2.7 Hz) therefore stereochemistry at that centre could not be assigned.

According to our previous findings, methoxymethyl substituent should prefer to be in axial position. The only conformation we assigned was for piperazinone **350** and it was *trans-diaxial* conformer. If our prediction about H-3 is correct, the piperazinone **312** should then be *cis*-3_{ax},6_{eq} conformer.

As seen in chapter 3, HMBC spectra were necessary to confirm the structures unambiguously and to exclude the other regioisomer formation. Both compounds showed strong correlations for H_2-10 and H_2-6 with C-2. Moreover correlation of H-3 to C-5 and *vice versa* was also observed.

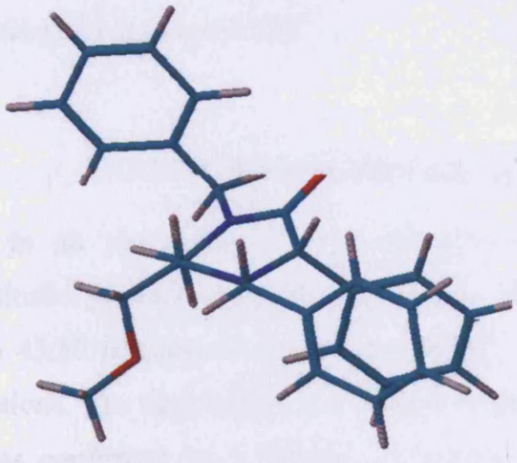

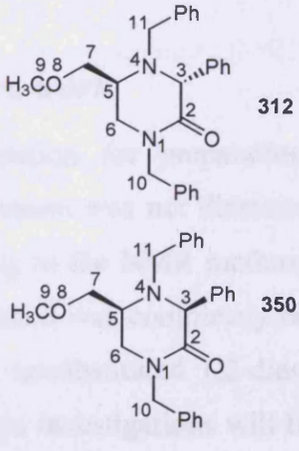

312

350

Figure 39. Lowest energy found (*cis*-diequatorial) by PC Model 8 for piperazinone **350**

H	5-Piperazinone 312	5-Piperazinone 350
H-3	4.34 (s)	4.35 (s)
H-5	3.0 (m)	3.1 (m)
H-6a	3.0 (m)	3.22 (dd, 7.9, 4.9)
H-6b	3.21 (dd, 11.7, 2.7)	3.41 (dd, 7.9, 2.7)
H-7a	3.16 (dd, 5.8, 3.2)	3.23 (m)
H-7b	3.26 (dd, 8.4, 3.2)	3.52 (m)
H_3-9	3.05 (s)	3.05 (s)
H-10a	4.51 (d, 14.6)	4.41 (d, 14.3)
H-10b	4.58 (d, 14.6)	4.6 (d, 14.3)
H-11a	3.82 (d, 14.0)	3.6 (d, 13.6)
H-11b	3.67 (d, 14.0)	3.54 (d, 13.6)

Table 32. ^{1}H-NMR chemical shifts and coupling constants for 3,5-disubstituted piperazinones **312** and **350**

7.2.3 Cyclisation of *N,N'*-dibenzyl ethylenediamine with benzil

Benzil was also reacted with *N,N'*-dibenzyl ethylenediamine **72d** in DMSO. The scope of the experiment was to confirm the loss of phenyl group in the cyclisation and to avoid formation of mixture of stereoisomers.

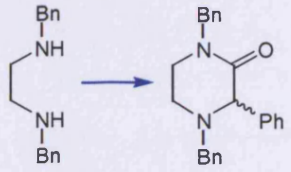

72d **351**

After 24 hours at 165° C, only one product was observed on TLC. After work up and flash chromatography, pure sample of 1,4-dibenzyl-3-phenyl-piperazin-2-one **351** was isolated (77%). The structure was confirmed by NMR analysis and the same adduct was also isolated by addition of phenylglyoxal and α-methyl bromophenylacetate to the unsubstituted 1,2-diamine **72d**[163].

7.3 Conclusions and future work

In an overview, a new regioselective cyclisation for preparation of 3,5-disubstituted piperazinones was discovered. The cyclisation was not diastereoselective since a 43:57 mixture of epimers was found, according to the NMR methoxy groups' integrations. The dephenylation of benzil in the cyclisation was completely unexpected and was confirmed by a further cyclisation with an unsubstituted 1,2-diamine. The reasons of this rearrangement are still unclear but future investigations will be focused on benzil behaviour with aliphatic 1,2-diamines, in order to monitor better aromatic protons changes in the NMR spectra. Possibly GC-MS experiments could elucidate

when the phenyl group is lost in the cyclisation mechanism and its nature as negative or positive fragment.

CHAPTER 8 Cyclisation of chiral 1,3-diamine

8.1 Introduction

Monocyclic medium ring nitrogen heterocycles are an important class of compounds that occur in a wide range of natural and unnatural compounds. The term medium ring is usually referred to alicyclic compounds having a ring size of 8 to 11. However, 7-membered and 12-membered rings are often included in this category[164]. Azepines and diazapeninones constitute important motifs in medicinal chemistry. Their synthesis using conventional ring closure methods is difficult. Amongst all strategies, the Staudinger ligation has been reported that provides access to 7- and 9-membered lactams[165].

On the basis of the successful investigations on regioselective cyclisations to afford piperazinones described in the preceding chapters, attempts to extend this procedure to the preparation of diazapenones were performed. The strategy used was the same as the previous cyclisations starting from 1,3-diamines and 1,2-dielectrophiles. Similarly to our previous work, a chiral centre was placed on the 1,3-diamine starting material in order to observe whether regioselectivity was present also for these cyclisations.

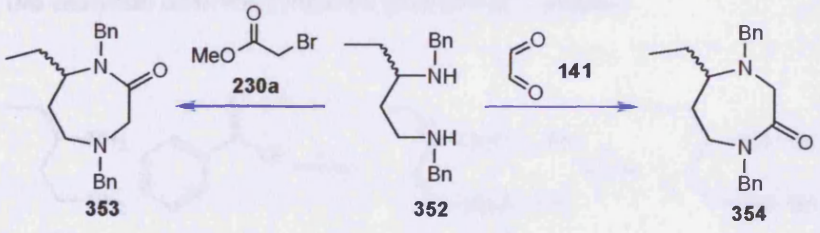

8.2 Preparation of N,N'-dibenzylpentane-1,3-diamine 352

Two different procedures were used for the preparation of *N,N'*-dibenzylpentane-1,3-diamine **352**.

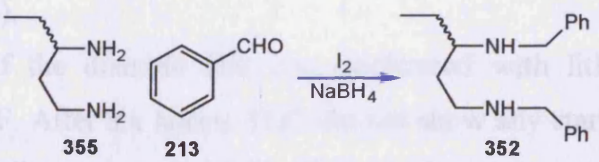

The one-step way was the reductive amination starting from the commercially available Dytec© 1,3-diamine **355** with benzaldehyde **213** in presence of sodium

borohydride. TLC and NMR of the crude were difficult to interpret due to the presence of mixture of products. The first attempt for this reductive amination was done on 1 g scale and the NMR of the crude after only 30 minutes showed the desired product **352** (68%) and benzyl alcohol (28%).

The second attempt was done on a larger scale (20 g) in more concentrated solution. TLC of the crude showed formation of mixture of at least 6 different compounds and NMR showed a lot of overlapped signals. Only 32% of the whole crude was assigned to be the expected diamine **352**. Extraction of the product **352** required first acidification with hydrochloric acid (pH 1.5) and extraction with dichloromethane to remove the benzyl alcohol byproduct. Subsequently, with basic washes (pH 14) and extraction with dichloromethane it was possible to isolate the basic products. Purification by flash chromatography with the use of longer column and slow gradient from apolar to polar solvents was required. There was an evident loss of crude mixture (20%) in the silica gel due to the high polarity of these molecules. The yield of the desired product was disappointing (30%). Byproducts such as mono-, tri- and tetrasubstituted adducts were probably formed during the reaction.

The second method used was the two-step sequence of dibenzoylation of the Dytec© 1,3-diamine **355** with benzoyl chloride in sodium hydroxide, followed by reduction of the diamide **356** with lithium aluminium hydride.

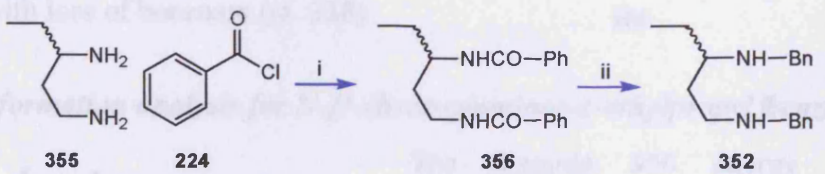

Scheme 79. *Reagents and conditions:* (i) NaOH, 89%; (ii) $LiAlH_4$, THF, 5 h, 55%

The first step was easily achieved in 2 hours. The product was a white precipitate in the reaction mixture and its extraction and purification was achieved by filtration and water washes, in order to remove the benzoate byproduct. The yield obtained was good (60%).

The reduction of the diamide **356** was performed with lithium aluminium hydride in refluxing THF. After six hours, TLC did not show any starting material left and one spot on the baseline appeared. NMR of the crude confirmed the formation of the desired diamine in high purify. Extraction of the diamine was done by quenching the unreacted hydride and then with basic washes with dichloromethane. The yield was

60%. Although this was a two-step sequence compared with the single reductive amination previously described, this method showed to be more reliable in terms of yield and ease of product purification.

8.2.1 Proof of the *N*-[3-(benzoylamino)-1-ethylpropyl]benzamide 356

Dibenzoylation of Dytec© 1,3-diamine **355** gave *N*-[3-(benzoylamino)-1-ethylpropyl]benzamide **356** in good yield (91%). It appeared as a white precipitate with melting point at 141° C, which was a low value compared with 310° C of phenylendiamine diamide derivative. Recrystallisation was attempted using a wide range of solvents but it resulted to be unsuccessful. NMR of **356** showed a triplet at 0.8 ppm indicating the terminal methyl group. H_2-4 were quite distinguishable showing two splitting at 1.93 and 2.92 ppm. The aromatic and aliphatic protons ratio was measured using the triplet of H_3-7 as standard. H-2 gave very complex signal due lo high level of splitting and at 6.0 ppm it was possible to see a sharp doublet for H-5. ^{13}C-NMR spectra showed all the expected signals and the two carbonyl groups at 167.1 (C-9) and 168.8 (C-8) ppm.

MS spectra showed a M+1 peak at 311 (100%) and M-PhCOO· **357** at 190 (30%), probably by the mechanism involved for the phenylendiamine derivative with loss of benzoate (cf. **228**).

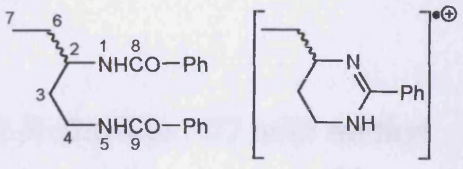

356 **357**

8.2.1.1 Conformation analysis for N-[3-(benzoylamino)-1-ethylpropyl]benzamide 356

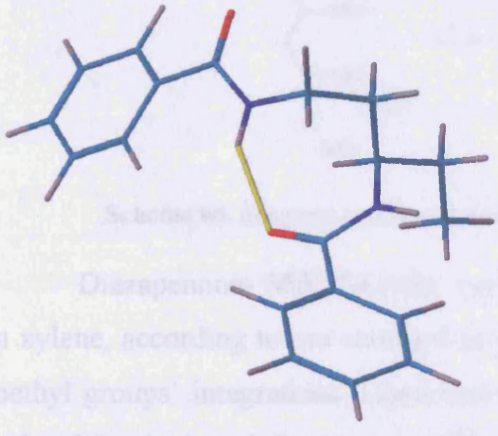

Figure 40. PC Model 8 representation of the diamide **356** (MMX Energy 17.876 kcal mol^{-1})

The diamide **356** energy calculation showed that the most stable conformation possessed a hydrogen bond (2.085 Å) between the amino group N-4 and the carbonyl group C-6 of the opposite side chain. This structure resulted to be much more flexible than the phenylendiamine diamide due to the presence of the propyl chain as bridge between the two amide groups in 1,3-relation.

Probably the high flexibility did not lock these structures to pack efficiently and hence yield crystals.

8.2.2 Proof of structure of *N,N'*-dibenzylpentane-1,3-diamine 352

^{1}H-NMR spectra of **352** showed the triplet for H_3-7 at 0.8 ppm, some overlapped signals at ~1.5 ppm that were assigned to be H_2-3 and H_2-6. H-3 and H_2-5 signals were adjacent and distinguishable at ~2.5 ppm. All benzylic protons gave a multiplet at 3.6 ppm. NMR spectra were similar to the Dytec diamine starting material **355** except for the presence of the benzylic protons. The NH groups gave a broad singlet at 1.8 ppm.

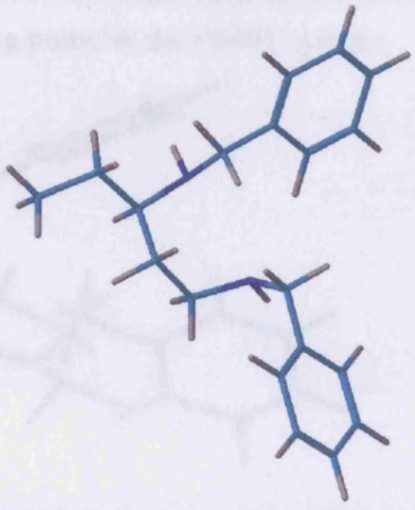

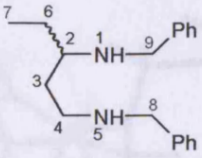

352

Figure 41. 1,3-Diamine **352** PC Model 8 representation (MMX Energy 27.100 kcal mol^{-1})

8.3 Cyclisation of N,N'-dibenzylpentane-1,3-diamine 352 with methyl bromoacetate 230a

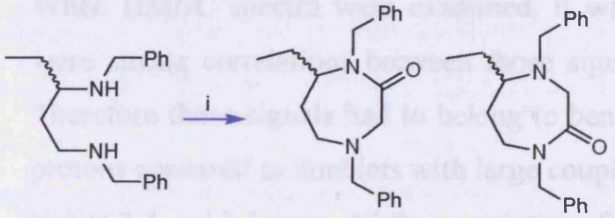

352 **353** **354**

Scheme 80. *Reagents and conditions:* (i) methyl bromoacetate, DIEA, xylene, 24 h

Diazapenones **353:354** ratio was established to be 90:10 after 20 hours of reflux in xylene, according to our standard procedure. Ratios were measured according to the methyl groups' integrations. Upon basic work up and flash chromatography, yields of isolated 7-substituted diazapenone **353** and for 5-substituted diazapenone **354** were low (40%, 2% respectively). The yields were slightly lower than expected when compared to the corresponding adducts from the cyclisation of 1,2-diamine and ethyl

bromoacetate[130]. Cyclisation of 1,3-diamines and methyl bromoacetate was expected to be more arduous due to the formation of 7-membered ring.

8.3.1 Proof of structure for 7-substituted diazapenones 353

^{1}H-NMR spectra analysis was very complex. H_3-9 appeared as a triplet at 0.8 ppm and it was used as our signal guide for measuring aliphatic-aromatic ratio and to use it as starting point for the HMBC spectra.

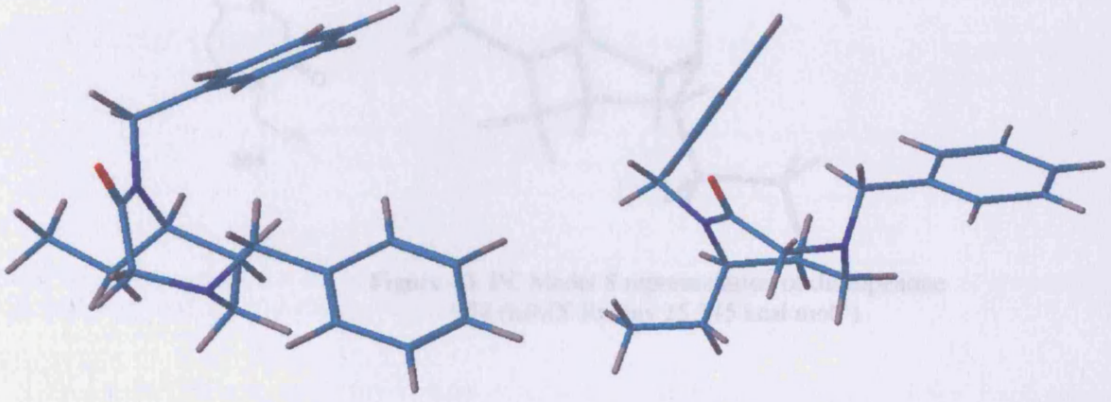

Figure 42. PC Model 8 representation of 7-substituted diazapenone **353** (MMX Energy 24.824 kcal mol^{-1})

Initially it was believed that the splittings found at 3.9 and 5.2 ppm (d, 14.7 Hz) belonged to H_2-3, on the basis of the similar pattern signals found for methylene group next to carbonyl group in the piperazinone rings.

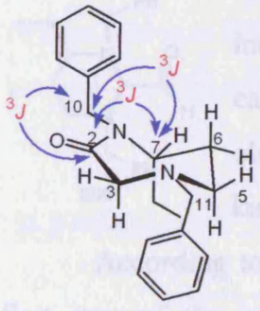

353

When HMBC spectra were examined, it was found that there were strong correlations between those signals and aromatics. Therefore those signals had to belong to benzylic protons. H_2-3 protons appeared as doublets with large coupling constants (15.7 Hz) at 3.4 and 3.5 ppm. All the correlations found confirmed our postulated structure.

8.3.2 Proof of structure for 5-substituted diazapenone 354

The structure of diazapenones **354** was unambiguously confirmed by HMBC spectra. The most important signals were: correlation between C-2 and H_2-7 and C-5 and H_2-3 and *vice versa*. Benzylic protons were assigned by correlation between H_2-10 and C=O correlation. H_2-3, H_2-10 and H_2-11 appeared as doublets with large coupling

constants (14.4, 15.7 and 13.7 Hz, respectively). No appearance of correlation between the methylene and the carbonyl group was seen. This was crucial for the distinction of the two regioisomers.

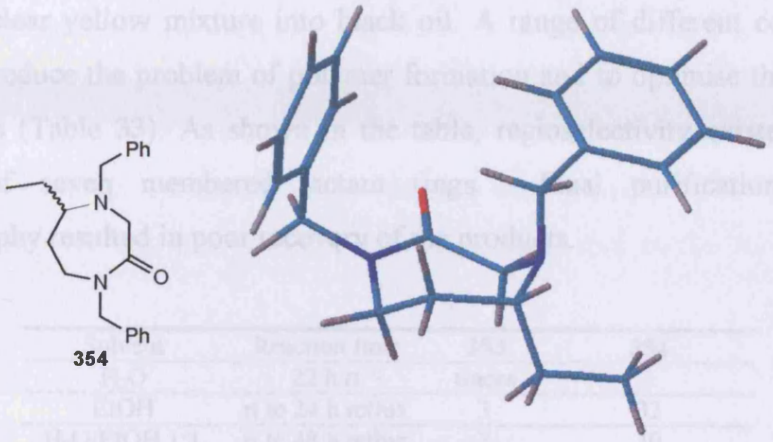

354

Figure 43. PC Model 8 representation of diazapenone 354 (MMX Energy 25.345 kcal mol^{-1})

8.4 Cyclisation of N,N'-dibenzylpentane-1,3-diamine 352 with glyoxal

The first attempt for the glyoxal cyclisation was done using water as solvent, instead of the mixture ethanol and water used in the standard procedure. When the reaction was left stirring at room temperature, a fast spot could be observed on TLC (R_f 0.85 in diethyl ether).

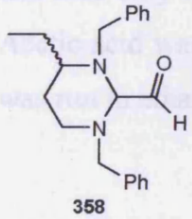

358

^{1}H-NMR at that stage showed a strong singlet around 9.5 ppm, which indicated the presence of the aldehyde derivative **358.** It was calculated to represent the 75% of the whole crude mixture. As also observed in the other glyoxal cyclisations, exclusive formation of kinetic products was observed at the beginning of the reaction.

According to a known procedure[166], the formation of six-membered ring is the first step of the reaction and it is very fast at very low temperature. When the temperature was increased until the solvent was refluxing, the crude mixture became gummy black oil that was very difficult to work up. The disappearance of the aldehyde derivative signal in the NMR and on TLC and the formation of the piperazinones were observed by ^{1}H-NMR spectra. The ratio measured for the isolated piperazinones was **354**:**353,** 25:2 relative to the aromatics. Purification by column chromatography was very difficult because the crude mixture was almost exclusively composed of polar

compounds, impossible to separate by chromatography. It was likely that polymeric species formed when the temperature was increased.

The cyclisation reactions were repeated several times in an attempt to monitor the change of the crude physical properties but little changes in temperature would suddenly change the clear yellow mixture into black oil. A range of different conditions were explored to reduce the problem of polymer formation and to optimise the yields of the diazapenones (Table **33**). As shown in the table, regioselectivity existed also for the formation of seven membered lactam rings. Final purification by column chromatography resulted in poor recovery of the products.

Solvent	Reaction time	**353**	**354**
H_2O	22 h rt	traces	3
EtOH	rt to 24 h reflux	3	32
H_2O/EtOH 1:1	rt to 48 h reflux	3	30

Table 33. Ratios calculated in the ^{1}H-NMR spectra of the crude mixture. * Integration of aromatic/10 represents one composite proton for the material present.

As mentioned previously, one of the most serious problems of the cyclisation reaction was the conversion of the crude mixture into black viscous oil when the temperature was increased. It was also observed that high temperatures were necessary for the formation of the diazapenones because at room temperature only formation of aldehyde **358** was observed. To avoid the problem of polymerisation the dilution was increased and each reagent was added dropwise with a syringe over 20 hours. Even in this case only 10% of piperazinone **354** formed.

Acetic acid was also used as catalyst to optimise the yields. In this case, the cyclisation was run in ethanol but the formation the diazapenone **3** was 6.6%.

8.5 "Crossed" experiment of N,N'-dibenzylpentane-1,3-diamine 352 and methyl N,N'-dibenzyl-2,3-diaminopropyl ether 182a

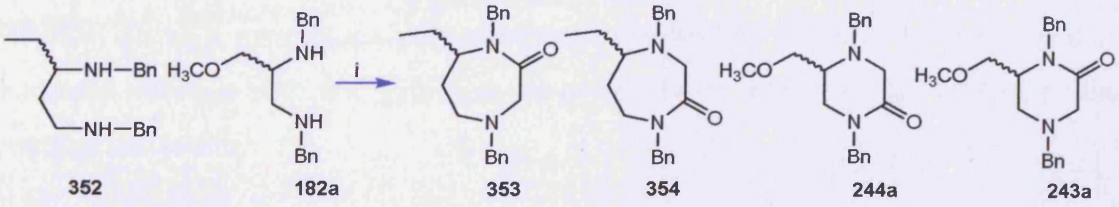

Scheme 81. *Reagents and conditions:* (i) glyoxal, EtOH/H_2O, 24 h reflux.

The reaction for the formation of seven-membered lactam rings showed to be poor in terms of yields obtained even when regioselectivity was present. A "double"

reaction was carried out in the same vessel to confirm this result. *N,N'*-Dibenzylpentane-1,3-diamine **352** and methyl *N,N'*-dibenzyl-2,3-diaminopropyl ether **182a** cyclised with glyoxal to give the four expected adducts. After purification pure samples of diazapenone **353** (6.9%), diazapenone **354** (12.7%), 5-piperazinone **244a** (69.8%) and 6-piperazinone **243a** (13.2%) were obtained. The major component of the crude was the six-membered ring 5-piperazinone **244a** as expected. In this case, regioselectivity was not observed for the seven-membered rings, this was probably due to the presence of the 1,2-diamine also reacting with glyoxal. The ^{1}H-NMR ratios observed were 93:7 for the piperazinones **244a**:**243a** and 63:36 for diazapenones **354**:**353**.

8.6 Conclusions

Methyl bromoacetate cyclisation showed to be regioselective giving a 90:10 mixture of regioisomers. The major component was the one similar to the piperazinone hence the same mechanistic pathways took place. Glyoxal cyclisation was not as regioselective as expected giving only 91:9 mixture of regioisomers. Also in this case, the major component was the expected adduct. Yields for both cyclisations were quite disappointing, probably due to polymerisation of the diamine starting material and for the difficulty of medium size ring formation.

CHAPTER 9 Towards the total synthesis of (S)-*N,N'*-dibenzyl-3-methoxy-propane-1,2-diamine

9.1 Introduction

In the introduction part of this thesis, it was described the biological relevance of peptidomimetics as therapeutic agents. Their application in the treatments of CNS's diseases is growing fast. A potential drug for treatment of Alzheimer's disease was designed by Dr. Robin Davies (Pharmacy Department, Cardiff University) and it was considered to be an efficient M_1 muscarinic agonist. The potential drug **359** is a pure enantiomer possessing two chiral centres and is a folded bicyclic system. The hydrogens on the two chiral centres are in *anti* position to each other, according to our PC Model 8 calculations (Figure **41**).

As stated in chapter 1, M_1 agonists are usually small molecules (MW 150) probably due the small active site of the receptor. Our proposed synthetic pathway for (*S*)-8-benzyl-4-methoxymethyl-2-methyl-hexahydro-pyrrolo[1,2-*a*]pyrazin-7-one **359** involved 10 steps and it was completed previously in my group using racemic starting materials.

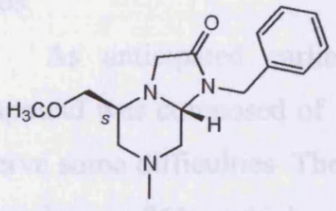

359 (*S*)-8-Benzyl-4-methoxymethyl-2-methyl-hexahydro-pyrrolo-1,2-a]pyrazin-7-one

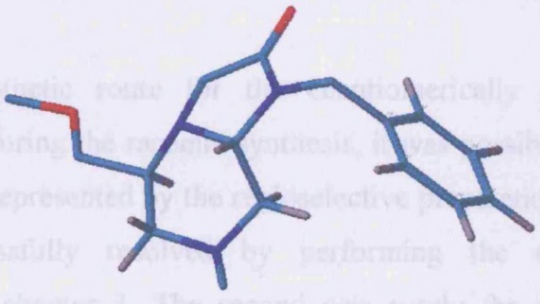

Figure 44. PC Model 8 representation of **359**

Regarding its possible interactions with the M_1 receptor, the phenyl ring will probably create π-interactions with other π-systems and the oxygens could take part in hydrogen bonding with any hydrogen donor present in amino acidic residues of the receptor active site.

9.2 Retrosynthetic approach for (S)-8-benzyl-4-methoxymethyl-2-methyl-hexahydro-pyrrolo[1,2-a]pyrazin-7-one 359

The most practical disconnections are shown below. The three intermediates **360**, **361**, and **362** represented the key compounds of the main sequence.

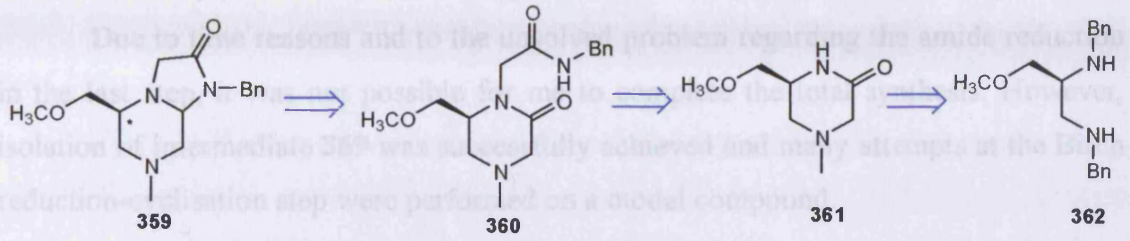

Scheme 82. Retrosynthesis of bicyclic system **359**

Previously in my group, Paul Lewis carried out the total synthesis of the racemic bicyclic compound **359**. *rac-N,N'*-Dibenzyl-3-methoxy-propane-1,2-diamine **362** was prepared starting from allyl bromide in three steps in appreciable yield, as previously described (section 2.1.1). In the pure enantiomer sequence, the preparation of the same diamine **362** required 4 steps starting from D-serine. All the other steps were the same for both racemic and enantiomeric routes. The racemic synthesis was carried out to have some indications regarding every step of the route and to optimise procedures and yields.

As anticipated earlier, the synthetic route for the enantiomerically pure compound was composed of 10 steps. During the racemic synthesis, it was possible to observe some difficulties. The first was represented by the regioselective preparation of piperazinone **361,** which was successfully resolved by performing the ethyl bromoacetate cyclisation, as shown in chapter 3. The second was surely the most complicated and still unclear reduction reaction of the lactam **360** followed by spontaneous cyclisation to yield the bicyclic system **359**. A model compound was then prepared in order to have cheap starting material and to investigate the reduction mechanism.

9.3 Synthesis of enantiomerically pure (S)-8-benzyl-4-methoxymethyl-2-methyl-hexahydro-pyrrolo[1,2-a]pyrazin-7-one 359

Preparation of the diamine **362** was achieved starting from D-serine in 4 steps. The overall yield was 49%. The second part of the total synthesis, starting from the enantiomerically pure diamine **362** was planned to be of further six steps.

Due to time reasons and to the unsolved problem regarding the amide reduction in the last step, it was not possible for me to complete the total synthesis. However, isolation of intermediate **369** was successfully achieved and many attempts at the Birch reduction-cyclisation step were performed on a model compound.

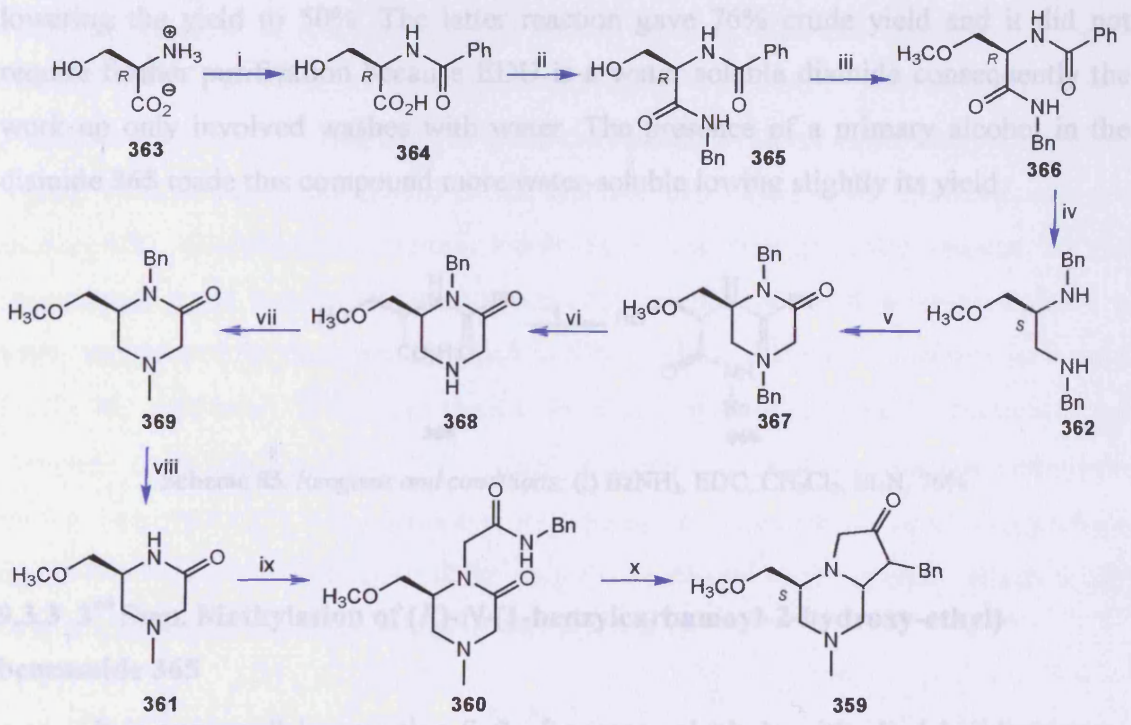

Scheme 83. *Reagents and conditions:* (i) BzCOCl, NaOH; (ii) $BzNH_2$, EDC, CH_2Cl_2, Et_3N; (iii) MeI, Ag_2O, CH_3CN; (iv) $LiAlH_4$, THF; (v) Ethyl bromoacetate, DIEA, xylene, 24 h reflux; (vi) H_2, Pt, MeOH; (vii) HCOOH, HCOH; (viii) Na, NH_3, THF, EtOH; (ix) *N*-benzyl-2-chloro-acetamide, NaH, THF; (x) Na, NH_3, THF, EtOH.

9.3.1 1st Step. Benzoylation of D-Serine

Benzoylation[167] of D-serine was a simple reaction and the amide **364** was prepared in high yield (89%, Scheme **84**). The mechanism of the reaction involved the attack of the carbonyl by the amine, as previously seen. Benzoic acid was the major by-product therefore purification of **364** required several water washes or recrystallisations of benzoic acid from hot ethanol and water mixtures.

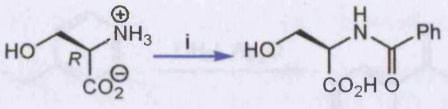

18 19

Scheme 84. *Reagents and conditions:* (i) BzCOCl, NaOH, 89%

9.3.2 2nd Step. EDC coupling reaction of (*R*)-2-benzoylamino-3-hydroxy-propionic acid 364

(*R*)-*N*-(1-Benzylcarbamoyl-2-hydroxy-ethyl)-benzamide **365** was prepared by two methods: DCC coupling[168] and EDC coupling[169] reactions. The former reaction gave crude yield of 90% but required extensive purification to remove DCU by-product, lowering the yield to 50%. The latter reaction gave 76% crude yield and it did not require further purification because EDU is a water soluble diamide consequently the work up only involved washes with water. The presence of a primary alcohol in the diamide **365** made this compound more water-soluble lowing slightly its yield.

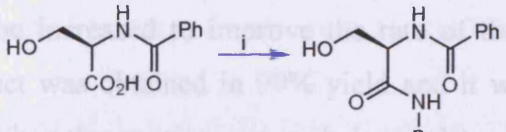

364 365

Scheme 85. *Reagents and conditions:* (i) $BzNH_2$, EDC, CH_2Cl_2, Et_3N, 76%

9.3.3 3rd Step. Methylation of (*R*)-*N*-(1-benzylcarbamoyl-2-hydroxy-ethyl)-benzamide 365

It is very well known that S_N2 of primary alcohols with alkyl halides occurs very slowly. Methylation of the intermediate **365** was attempted in several ways. One successful procedure was addition of a large excess methyl iodide (10 equivalents) and silver(I) oxide in acetonitrile for 5 days. According to a known procedure[170,171], an excess of silver (5 mole equivalents) was required to complete the conversion into the product. Unfortunately, this made this reaction too expensive when performed on a large scale. Alternative methods were carried out to avoid using large excess of silver oxide and to optimise the yield.

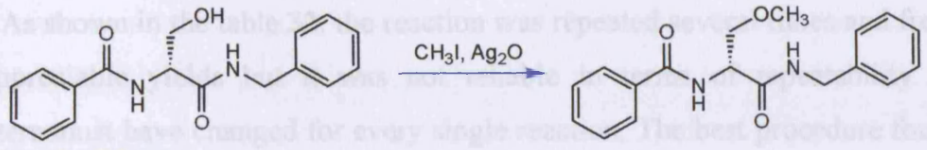

365 366

Other reagents were used like using dimethyl sulphate and sodium hydride in DMSO but mixtures of methoxy product **366** (3% after purification) and *N*-methyl (mono- and dimethylated, 30% yield) derivatives were formed.

This reaction never showed to be robust and reliable since every single attempt gave different starting material/product ratio. In particular, it presented two main problems: 1) rate of S_N2 displacement very slow; 2) in some attempts no reaction occurred. In order to increase the rate of the reaction, different solvents were used (toluene at 0° C, dichloromethane, Kuhn methylation with DMF[172]) but no improvement was seen. Sonication[173] was used to break the coating of silver oxide reagent by silver iodide, formed during the course of the reaction that might have interfered with the nucleophilic displacement. Methyl iodide is a low boiling point reagent so the temperature could not be increased to improve the rate of the displacement. On 1 g scale, the desired product was obtained in 99% yield and it was completed in 3 days (Table **34**, reaction **a**). When the reaction was scaled up (~10 g, Table **34**, reaction **c**) the complete methylated product (*R*)-*N*-[1-(benzyl-methyl-carbamoyl)-2-methoxy-ethyl]-*N*-methyl-benzamide **371** was obtained in 99% yield. This unexpected result was perhaps due to the higher concentration of the reagents compared to the solvent, which might have activated the amidic groups to act as nucleophiles.

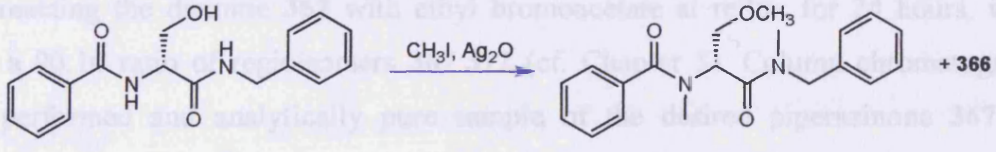

365 371

	365 (grams)	CH_3I (mol. eq.)	Ag_2O (mol. eq.)	Solvent (ml)	Time (days)	366 (yield)
a[171]	1	10	5	CH_3CN (20)	3	99%
b	3	25	15	CH_3CN (100)	7	75%
c	10[1]	25	6	CH_3CN (500)	4	99%
d	1.5	2.1	1.1	toluene+CH_2Cl_2(15)	5	60%
e	2.5	2	1	toluene+CH_2Cl_2(30)	4	80%
f	1.5	1.6	1	CH_3CN (15)	5	70%
g	3.5	2	1.5	CH_3CN (30)	3	25%
h	1	1.2	1	CH_3CN+pyridine	2	80%

Table 34. Reaction conditions for methylation of intermediate **365**.
[1]All product was trimethyl derivative **371**.

As shown in the table **32**, the reaction was repeated several times and frequently gave appreciable yields but it was not reliable in terms of repeatability. A few parameters must have changed for every single reaction. The best procedure found only required an equimolar concentration of silver oxide in presence of a catalytic amount of pyridine, to complete the reaction in two days (80% yield, Table **32**, reaction **h**).

9.3.4 4th Step. Preparation of (*S*)-*N*,*N*'-dibenzyl-3-methoxy-propane-1,2-diamine 362

The diamide **366** was reduced using an excess of lithium aluminium hydride (5 mole equivalents) in refluxing THF for 40 hours. The reaction was efficient and the product **362** was obtained in 67% yield.

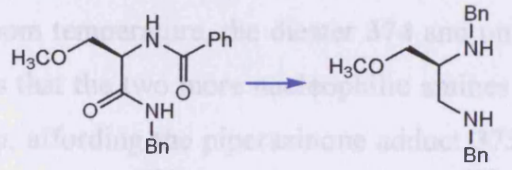

366 **362**

Scheme 87. *Reagents and conditions:* (i) $LiAlH_4$, THF, 67%

9.3.5 5th Step. Preparation of *N*,*N*'-1,4-dibenzyl-6-methoxymethyl-piperazin-2-one 367

The cyclisation step to prepare the intermediate **367** captured our attention and a lot of attempts were tried in the past in my group, in order to develop a reliable and highly regioselective cyclisation reaction. The best method for the preparation of **367** was reacting the diamine **362** with ethyl bromoacetate at reflux for 24 hours, which gave a 90:10 ratio of regioisomers **367**:**372** (cf. Chapter 3). Column chromatography was performed and analytically pure sample of the desired piperazinone **367** was obtained.

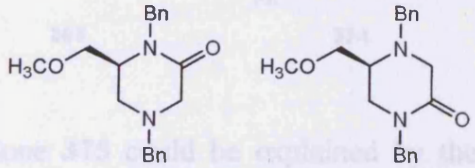

367 **372**

HPLC was run at this stage to check the purity of the enantiomer **367**. Analysis by HPLC was firstly performed on the racemic intermediate. Two resolved peaks were distinguished using a 97:3 mixture of hexane:isopropanol. Retention time for (*S*)-

enantiomer was 9.3 minutes, whereas it was 11.7 minutes for (*R*)-enantiomer (peak areas *R*:*S*, 63:37). When piperazinone **367** alone was injected, only one peak after 9.3 minutes was observed corresponding to (*S*)-enantiomer. No trace of (*R*)-enantiomer was observed. The *R*:*S* ratio found for the racemic adduct was surprising. Further tests would have been required to confirm the data.

9.3.5.1 Alternative route to preparation of piperazinone 367

Cyclisation was also attempted on the non-methylated adduct **365** in order to avoid the tedious and unclear methylation of diamide **365** previously described (section 9.3.3). Our hope was to prepare the hydroxy piperazinone **373** and then perform the methylation according to easier procedures, to give the adduct **367**.

Unfortunately, reaction of diamine **365** with ethyl bromoacetate (1.2 mole equivalents) gave mainly, even at room temperature, the diester **374** and unreacted starting material **365**. Our prediction was that the two more nucleophilic amines would react first, rather than the hydroxyl group, affording the piperazinone adduct **373**. The reason of the fast alkylation of the diamine **365** at both positions is still unclear, considering that the reaction condition and procedure were the same as our "standard" cyclisations. Reaction conditions were modified but no improvement was shown. The more reactive methyl bromoacetate was slowly added to the diamine but no changes for the products formation were shown.

The product **374** was then placed in refluxing xylene and the lactone **375** was prepared. The aim of the cyclisation was to observe the selectivity between formation of 6- or 7-membered rings.

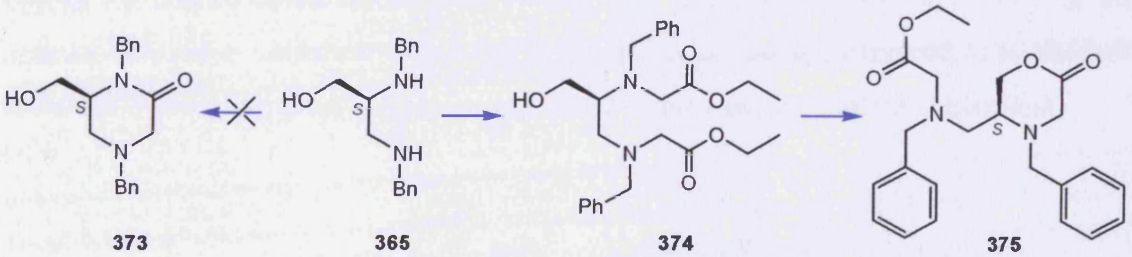

373 **365** **374** **375**

Formation of lactone **375** could be explained by the preferential mechanistic pathway (Scheme **88**, red arrows) where the cyclisation was a 6-*exo*-trig. The other possible lactone was the 7-membered ring **376** and its formation was explained by the mechanism below (Scheme **88**, green arrows). The cyclisation was a 7-*exo*-trig process but did not occur therefore no traces of the adduct **376** were observed.

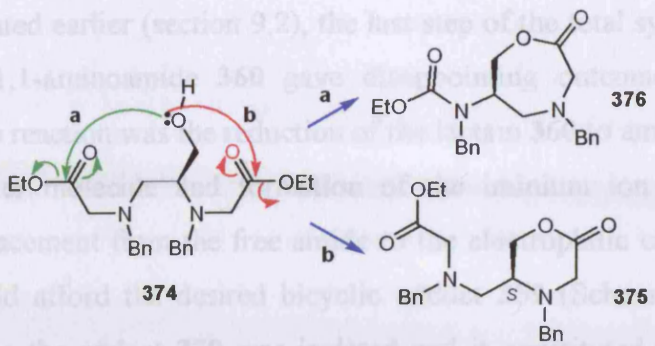

Scheme 88. Mechanism of cyclisation of the diester **374**

9.3.6 6th Step. *N*-Benzyl cleavage by hydrogenolysis

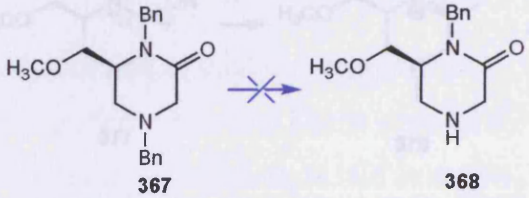

Scheme 89. *Reagents and conditions:* (i) H_2, 10% Pd/C

Paul Lewis performed this reaction for the racemic intermediate[111]. Several methods were attempted and the best catalyst for this hydrogenolysis was PtO_2. The same reaction for the enantiomer **367** was carried out in methanol and to our surprise, in one case, *N*-methylated product **369** was prepared in one step. In this case, the catalyst used was palladium on activated carbon (10%) and it was plausible to postulate a mechanism of reduction of the starting material **367** to free amine and toluene and at the same time oxidation of methanol to formaldehyde, both mediated by the palladium. An Eschweiler-Clarke reaction occurred *in situ* that gave the product **369**. This is an unusual behaviour: palladium is used as a reducing agent but it performed as an oxidant at the same time, in the same reaction pot. Yield of pure product **369** was excellent.

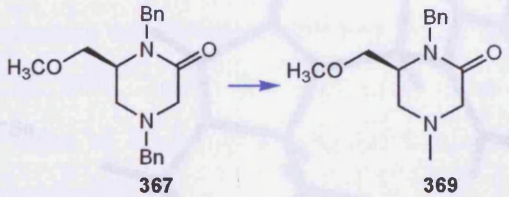

Scheme 90. *Reagents and conditions:* (i) H_2, 10% Pd/C, MeOH, 71%

9.4 Investigation on amide reduction reaction

As anticipated earlier (section 9.2), the last step of the total synthesis performed on the racemic 1,1-aminoamide **360** gave disappointing outcome. The postulated mechanism for the reaction was the reduction of the lactam **360** to aminol **377**, followed by loss of a water molecule and formation of the iminium ion **378**. Finally, the nucleophilic displacement from the free amide to the electrophilic carbon adjacent the iminium ion would afford the desired bicyclic adduct **359** (Scheme **91**, pathway **a**). Unfortunately, also the adduct **379** was isolated and it constituted the major product from the reduction reaction (Scheme **91**, pathway **b**).

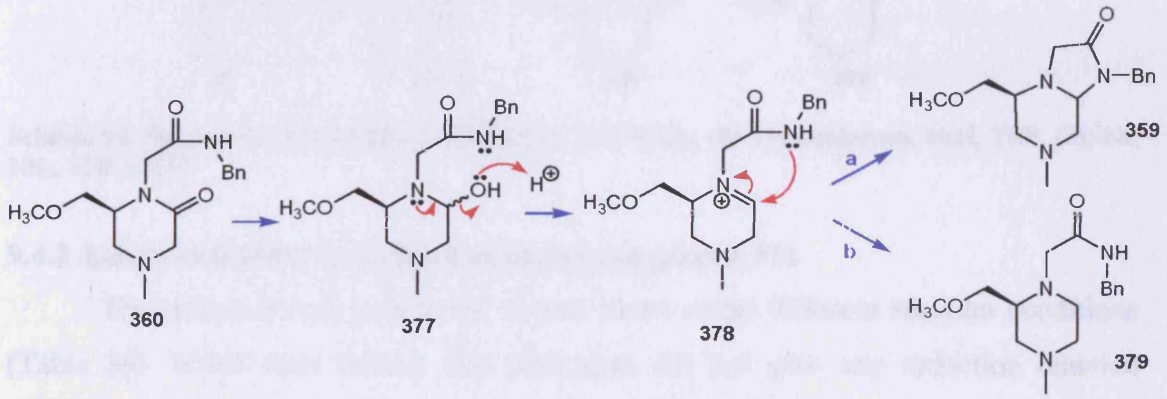

Scheme 91. Amide reduction-cyclisation sequence of 1,1-aminoamide **360**

Apparently although the reaction was performed using the minimum of two equivalents of metal in liquid ammonia, the intermediate **378** was even more susceptible to reduction than the starting lactam, resulting in "doubly-reduced" compound **379**. In order to investigate the reduction, a model compound was prepared and used as scaffold molecule.

9.4.1 Preparation of the model compound: 1-benzyl-hexahydro-imidazo[1,2-*a*]pyridin-2-one 370

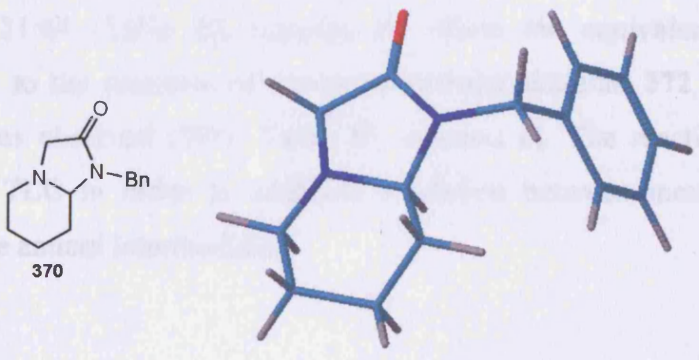

Figure 45. PC Model 8 representation of bicyclic compound **370** (MMX Energy 17.259 kcal mol^{-1})

1-Benzyl-hexahydro-imidazo[1,2-*a*]pyridin-2-one **370** was previously prepared by Paul Lewis in my group. The procedure consisted of a three step sequence (Scheme **92**). It started with a nucleophilic attack of acyl chloride **87** by benzylamine (step i) followed by S_N2 of the *N*-benzyl-2-chloro-acetamide **372** by the δ-valerolactam (step ii). Finally a Birch reduction of the adduct **370** to give a 1,1-aminoamide (step iii).

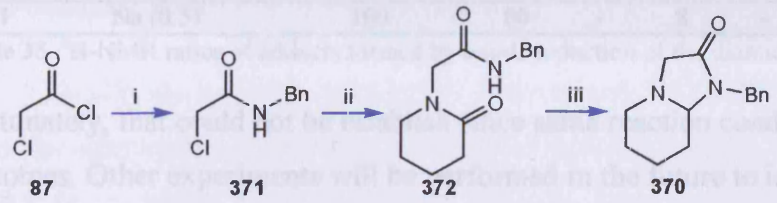

Scheme 92. *Reagents and conditions*: (i) $BnNH_2$, 0° C, CH_2Cl_2; (ii) δ-valerolactam, NaH, THF; (iii) Na, NH_3, THF, EtOH

9.4.2 Amide reduction-cyclisation of model compound 372

The reduction was performed several times under different reaction conditions (Table **35**). Metal such lithium and potassium did not give any reduction reaction resulting in fully recover of the starting material **372**. Sodium was the best metal and it was used for all successful attempts. The order of reagents addition was changed (NH_3, EtOH, Na) but no improvement was shown hence it did not affect the reduction pathway.

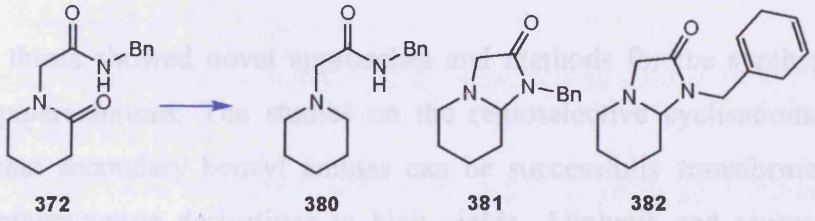

Scheme 93. *Reagents and conditions:* (i) Metal, NH_3, EtOH, dry THF

In most cases, starting material **372** was recovered and the best ratio of adducts **380**:**381** was 21:63 (Table **35**, reaction **a**). When the equivalents of metal were increased, due to the presence of unreacted starting material **372**, reduction of the phenyl ring was observed (99%, Table **35**, reaction **e**). The reaction was constantly monitored by TLC in order to establish a relation between metal equivalents and reduction of the aminol intermediate.

	Metal (mol. eq.)	EtOH (mol. eq.)	372	380	381	382
a	Na (10)	112	16	21	63	-
b	Li(5)	-	100	-	-	-
c	K (7)	-	99	1	-	-
d	Na (50)	40	33	-	16	50
e	Na 60)	1000	-	-	1	99
f	Na (20)	100	-	-	-	-
g	Na (2)	100	68	-	20	-
h	Na (2)	100	50	-	30	-
i	Na (0.5)	100	80	-	8	-

Table 35. ^{1}H-NMR ratios of adducts formed by amide reduction of the diamide **372**

Unfortunately, that could not be establish since same reaction conditions gave different outcomes. Other experiments will be performed in the future to investigate and optimise reaction conditions and yields.

9.5 Conclusions

Isolation of intermediate **360** of the total synthesis was successfully achieved in one-pot sequence of hydrogenolysis of *N*-benzyl and oxidation to *N*-methyl group. Attempts of Birch reduction for the model compound were carried out resulting in preparation of product mixtures. Therefore more experiments are needed to optimise the reaction conditions for the reduction.

This thesis showed novel approaches and methods for the synthesis of highly substituted piperazinones. The studies on the regioselective cyclisations lead to the conclusion that secondary benzyl amines can be successfully transformed in a large number of piperazinone derivatives in high yields. Aliphatic and aromatic diamines require more energetic conditions to be quantitatively converted into cyclised adducts.

Glyoxal and its derivatives showed to react regioselectively with 1,2-diamines and the yields were optimal with the dibenzyl diamine whereas they were poor with aliphatic and aromatic diamines.

As shown in Chapter 4, *N*-benzyl groups can be successfully cleaved using an extremely easy procedure and the reactivity of the free secondary amine could be used to introduce these rings into peptidomimetic peptidic sequences.

Chapter 10 Experimental data

Compounds were characterised by TLC mobility and ^{1}H-NMR spectra. Structures were assigned by a standard repertoire of NMR experiments, IR, MS and HRMS spectra.

^{1}H-NMR gave the main information about the number of protons, shifts and coupling constants (complicated splitting were analysed using the Multiplet software). ^{1}H, ^{1}H-COSY was mainly used to confirm adjacent protons through coupling constants connectivity. ^{13}C-NMR showed the number of carbons and ^{13}C-DEPT 135 showed different peaks for each carbon according to number of attached protons. HMQC ($^{1}J_{H,C}$) spectra allowed us to assign geminal protons through direct connectivity between protons and carbons, and to confirm the protons chemical shifts. HMBC ($^{3}J_{H,C}$) spectra represented the key experiments for final assignment of the structure, rooted on unambiguous chemical shifts, through the long-range proton-carbon coupling. Solution ^{1}H and ^{13}C NMR spectra were recorded on a bruker Spectrospin-Avance DPX 400 and DPX 500 MHz spectrometers. All measurements occurred at room temperature and are referenced to TMS (δ = 0 ppm). The chemical shifts are given in parts per million and the coupling constants in Hertz. Solvents used for NMR experiments were mainly $CDCl_3$ or C_6D_6.

IR spectra were recorded on a Perkin Elmer- FTIR 1600 Series spectrometer. The wavenumber aregiven in cm^{-1} and the following abbreviations are used: br-broad, s-strong, w-weak. Solid compounds were run in nujol or dissolved in volatile solvents. IR spectra of oils were run neat.

Compound masses were measured with AP+. Accurate mass peak measurements of molecular ion were set in Swansea at the EPSRC National Mass Spectrometry Service Centre, on the basis of molecular ion found in low resolution mass spectra.

High performance column chromatography was performed on Hewlett-Packard-Agilent 1100 Series instruments.

Flash column chromatography was carried out using Fischer Scientific silica gel 60A (37-70 μm). Analytical thin layer chromatography was carried out using Merck silica 60 F254 using a UV lamp and phosphomolibdic acid to visualise the components.

10.1 Preparation of *N,N′*-dicyclohexyl-3-methoxy-propane-1,2-diamine 182d

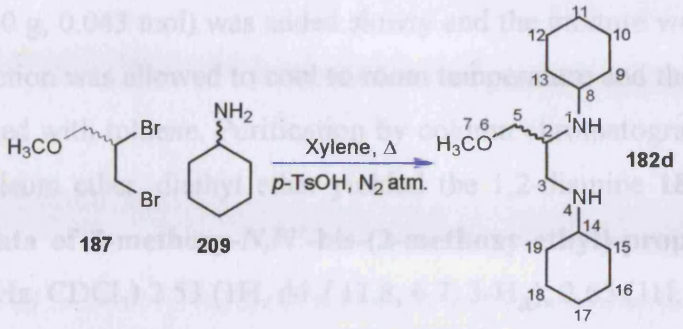

Cyclohexylamine **209** (31.74 g, 0.32 mol) in toluene (10 ml) with *p*-toluenesulphonic acid (0.76 g, 0.004 mol) was refluxed for 30 minutes, followed by slow addition of the dibromide **187** (10 g, 0.04 mol). The mixture was allowed to reflux for 24 hours before being dried to give a crude mixture as a brown oily substance (4.94 g). Purification by column chromatography using a slow gradient of petroleum ether to ethanol gave the diamine **182b** as brown viscous oil (2.74 g, 25%). **Spectroscopic data of *N,N′*-dicyclohexyl-3-methoxy-propane-1,2-diamine 182b:** δ_H (500 MHz, $CDCl_3$) 1.17 (10H, m, cyclohexyl-H); 1.59 (5H, m, cyclohexyl-H); 1.64 (2H, m, cyclohexyl-H); 1.79 (3H, m, cyclohexyl-H); 2.02 (3H, m, cyclohexyl-H); 2.65 (1H, m, 8-H); 2.82 (1H, m, 3-H_a); 2.92 (1H, tt *J* 11.2, 3.7, 14-H); 3.15 (1H, dd *J* 12.1, 4.0, 3-H_b); 3.3 (3H, s, 7-H_3); 3.39 (1H, m, 2-H); 3.45 (1H, dd *J* 7.7, 2.9, 5-H_a); 3.55 (1H, dd *J* 9.9, 3.9, 5-H_b); δ_C (DEPT, δ_H ^{1}H-^{13}C ^{1}*J*-COSY) 24.37-33.7 (CH_2, 1.17, 1.59, 1.64, 1.79, 10-cyclohexyl-C); 45 (CH_2, 2.82, 3.15, 3-C); 51 (CH, 3.39, 2-C); 55 (CH, 2.65, 8-C); 57.5 (CH, 2.92, 14-C); 59 (CH_3, 3.3, 7-C); 71 (CH_2, 3.45, 3.55, 5-C); *m/z* (APCI) 269 (M+1); HRMS ES+ calcd for [$C_{16}H_{32}N_2O$]: 269.2587, found: 269.2587, error 0.00 ppm; R_f = 0.59 (ethyl acetate: ethanol, 4:1).

10.2 Preparation of 3-methoxy-*N,N′*-bis-(2-methoxy-ethyl)-propane-1,2-diamine 182c

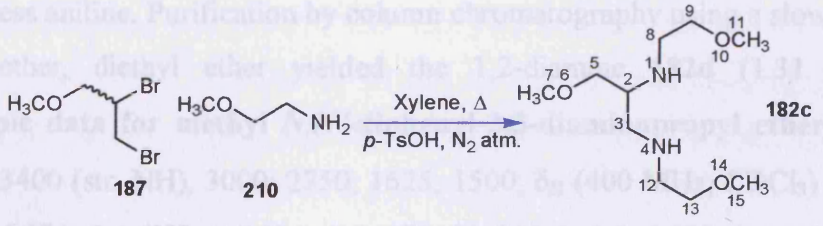

A mixture of 2-methoxyethylamine **210** (12.92 g, 0.172 mol), toluene (30 ml), *p*-toluenesulfonic acid (0.76 g, 0.0043 mol) was placed in a round bottom flask. The dibromide **187** (10 g, 0.043 mol) was added slowly and the mixture was refluxed for 20 minutes. The reaction was allowed to cool to room temperature and the salt formed was filtered and washed with toluene. Purification by column chromatography using a slow gradient of petroleum ether, diethyl ether yielded the 1,2-diamine **182c** (3.0 g, 32%). **Spectroscopic data of 3-methoxy-*N,N'*-bis-(2-methoxy-ethyl)-propane-1,2-diamine 182c:** δ_H (500 MHz, $CDCl_3$) 2.53 (1H, dd *J* 11.8, 6.7, 3-H_a); 2.65 (1H, dd *J* 11.7, 5.2, 3-H_b); 2.7 (3H, m, 12-H_2, 2-H); 2.78 (1H, t *J* 5.5, 8-H_a); 2.8 (1H, dd *J* 5.8, 5.4, 8-H_b); 3.28 (3H, s, 7-H_3); 3.29 (6H, s, 11-H_3, 15-H_3); 3.34 (2H, m, 5-H_2); 3.41 (4-H, m, 9-H_2, 13-H_2); δ_C (DEPT, δ_H, ^{1}H-^{13}C ^{1}*J*-COSY) 47 (CH_2, 2.78, 2.8, 8-C); 49.5 (CH_2, 2.7, 12-C); 51 (CH_2, 2.53, 2.65, 3-C); 57.3 (CH, 2.7, 2-C); 58.8 (CH_3, 3.29, 11-C, 15-C); 59 (CH_3, 3.28, 7-C); 72 (CH_2, 3.41, 9-C); 72.3 (CH_2, 3.41, 13-C); 74 (CH_2, 3.34, 5-C); *m/z* (APCI) 220 (M+1); R_f= 0.2 (ethanol).

10.3 Preparation of methyl *N,N'*-diphenyl-2,3-diaminopropyl ether 182d

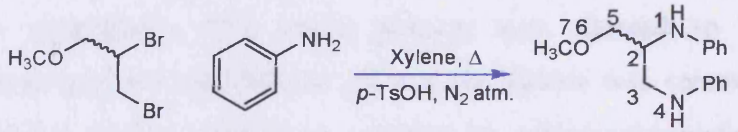

187 **211** **182d**

A mixture of aniline **211** (7.7 g, 0.08 mol) and *p*-toluenesulfonic acid (0.115 g, 0.06 mmol) in xylene (12 ml) was heated (145°C) in a round bottom flask, fitted with a condensor, under a nitrogen atmosphere. Methyl 3-(1,2-dibromopropyl) ether **187** (2.2 g, 9.5 mmol) was added dropwise from a pressure equalised dropping funnel over one hour. The mixture was refluxed under a nitrogen atmosphere for 20 hours. The reaction was allowed to cool to room temperature and the salt formed was filtered and washed with xylene (7 ml). The filtrate was concentrated under high vacuum to remove xylene and any excess aniline. Purification by column chromatography using a slow gradient of petroleum ether, diethyl ether yielded the 1,2-diamine **182d** (1.31 g, 85.3%). **Spectroscopic data for methyl *N,N'*-diphenyl-2,3-diaminopropyl ether 182d:** ν_{max} (neat)/cm^{-1} 3400 (str. NH), 3000; 2750; 1625; 1500; δ_H (400 MHz, $CDCl_3$) 3.3 (1H, dd *J* 12.6, 6.3, 5-H_a); 3.4 (3H, s, 7-H_3); 3.4 (1H, dd *J* 12.6, 5.5, 5-H_b); 3.5 (1H, dd *J* 9.4, 5.1, 3-H_a); 3.6 (1H, dd *J* 9.4, 3.2, 3-H_b); 3.8 (1H, m, 5-H); 4.0 (2H, bs, N-H); 7.2-6.7

(10H, m, ar-H); δ_C (DEPT, δ_H ^1H–^{13}C ^1J-COSY) 45.89 (CH_2, 3.5, 3.6, 3-C); 52.80 (CH_2, 3.8, 5-C); 59.65 (CH_3, 3.4, 7-C); 73.12 (CH, 3.3, 3.4, 5-C); 113.42-118.38 (CH, 7.2- 6.7, ar-C); 147.6-148.74 (C, ar-C); *m/z* (APCI) 257 (M+1); HRMS ES+ calcd for [$C_{16}H_{20}N_2O$]: 257.1648, found: 257.1651, error +1.1 ppm; R_f = 0.55 (petroleum ether: diethyl ether, 1 : 1).

10.4 Preparation of *N,N'*-di-(*p*-methoxy)phenyl-2,3-diaminopropyl ether 182e

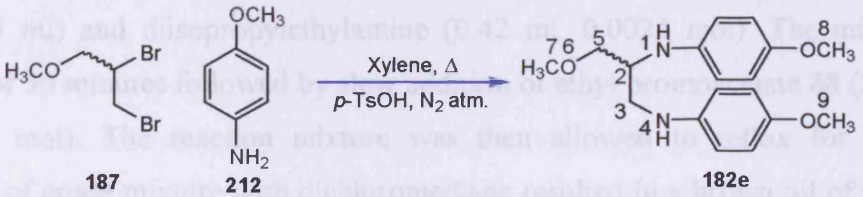

187 212 182e

p-Anisidine **212** (26.5 g, 0.21 mol) and *p*-toluenesulphonic acid (0.5 g, 2.6 mmol) were dissolved in xylene (100 ml) and the mixture was heated in an oil bath until reflux. Methyl 3-(1,2-dibromopropyl) ether **187** (10 g; 0.043 mol) was added slowly with an equalised pressure funnel over 2 hours. The reaction was refluxed for 24 hours under nitrogen atmosphere. The crude mixture was allowed to cool to room temperature, the precipitate was filtered off and the xylene was removed to give the crude product (7.92 g). The mixture was purified by column chromatography using a slow gradient of petroleum ether, diethyl ether, ethyl acetate to give the diamine **182e** (5.51 g, 85%). **Spectroscopic data for *N,N'*-di-(*p*-methoxy)-phenyl-2,3-diaminopropyl ether 182e:** ν_{max} (neat)/cm^{-1} 3372 (str., NH); 2931 (str., CH); 1617 (str., NH); 1240 (str., CN); 1037; 820; 760 (bend., NH); 965; δ_H (400 MHz, C_6D_6) 3.12 (3H, s, 7-H_3); 3.18 (1H, dd *J* 12.4, 6.8, 3-H_a); 3.25 (1H, dd *J* 9.3, 5.3, 5-H_a); 3.32 (1H, dd *J* 9.3, 3.3, 5-H_b); 3.4 (1H, dd *J* 12.3, 5.3, 3-H_b); 3.49 (3H, s, 9-H_3); 3.52 (3H, s, 8-H_3); 3.62 (1H, dq *J* 5.2, 3.3, 2-H); 6.5- 6.9 (8H, m, ar-H); δ_C (DEPT, δ_H ^1H–^{13}C ^1J-COSY) 46.6 (CH_2, 3.18, 3.4, 3-C); 53.82 (CH, 3.62, 2-C); 55.05 (CH_3, 3.52, 8-C); 55.07 (CH_3, 3.49, 9-C); 58.55 (CH_3, 3.12, 7-C); 72.58 (CH_2, 3.25, 3.32, 5-C); 113.05-153.16 (CH, 6.5-6.9, ar-C); *m/z* (APCI) 317 (M+1); HRMS ES+ calcd for [$C_{18}H_{24}N_2O_3$]: 317.1860, found: 317.1858, error +0.6 ppm; R_f= 0.3 (petroleum ether: ethyl acetate, 1:1).

10.5 Preparation of [(1-{[ethoxycarbonylmethyl-(2-methoxy-ethyl)-amino]-methyl}-2-methoxy-ethyl)-(2-methoxy-ethyl)-amino]-acetic acid ethyl ester 245c

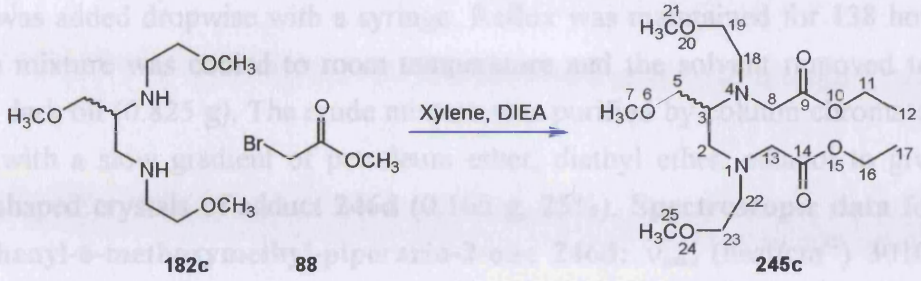

182c 88 245c

Diamine **182c** (0.5 g, 0.0024 mol) was placed in a round bottom flask with xylene (15 ml) and diisopropylethylamine (0.42 ml, 0.0024 mol). The mixture was refluxed for 30 minutes followed by slow addition of ethyl bromoacetate **88** (2.84 g, 1.4 ml, 0.017 mol). The reaction mixture was then allowed to reflux for 24 hours. Extraction of crude mixture with dichloromethane resulted in a brown oil of the diester **245c** (0.47 g, 54%). **Spectroscopic data of [(1-{[ethoxycarbonylmethyl-(2-methoxy-ethyl)-amino]-methyl}-2-methoxy-ethyl)-(2-methoxy-ethyl)-amino]-acetic acid ethyl ester 245c:** ν_{max} (neat)/cm^{-1} 1752.01, 1747.19, 1742.37, 1736.58, 1731.76, 1726.94 (str., br., C=O ester); δ_H ($CDCl_3$, 500 MHz) 1.2 (6H, m, 12-H_3, 17-H_3); 2.9 (2H,m); 3.25-3.26 (9H, s, 7-H_3, 21-H_3, 25-H_3); 3.45 (2H, m); 3.55 (2H, s); 3.61 (2H, m); 3.67 (2H, m); 4.1-4.16 (4H, m, 11-H_2, 16-H_2); 4.57 (2H, m); 4.7 (1H, m); δ_C (DEPT, δ_H, ^{1}H-^{13}C ^1J-COSY); 14 (CH, 1.2, 3-C); 53.5 (CH_2, 2.9); 57 (CH_2, 3.55); 56.8 (CH_2, 3.61); 56.9 (CH_2, 3.67); 59 (CH_3, 3.25-3.26, 7-C, 21-C, 25-C); 62-63 (CH_2, 4.1-4.16, 11-H_2, 16-H_2); 62.5 (CH_2, 4.57); 62.8 (CH_2, 4.57); 72 (CH_2, 3.45); 172.3-172.9 (C=O, 10-C, 15-C); R_f= 0.39 (diethyl ether: ethyl acetate, 1:1).

10.6 Preparation of *N,N'*-1,4-diphenyl-6-methoxymethyl-piperazin-2-one 246d

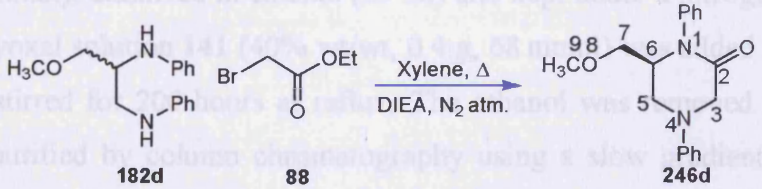

182d 88 246d

Into a 25 ml two necked round bottom flask methyl *N,N'*-diphenyl-2,3-diaminopropyl ether **182d** (0.5 g, 2.4 mmol), diisopropylethylamine (0.47 g, 3.7 mmol)

and xylene (2.5 ml) were placed. The flask was fitted with a condensor and kept under a nitrogen atmosphere. The mixture was warmed and ethyl bromoacetate **88** (0.38 g, 2.4 mmol) was added dropwise with a syringe. Reflux was maintained for 138 hours. The reaction mixture was cooled to room temperature and the solvent removed to give a viscous dark oil (0.825 g). The crude mixture was purified by column chromatography, eluting with a slow gradient of petroleum ether, diethyl ether, ethanol to give white needle shaped crystals of adduct **246d** (0.165 g, 25%). **Spectroscopic data for *N,N'*-1,4-diphenyl-6-methoxymethyl-piperazin-2-one 246d:** ν_{max} (neat/cm^{-1}) 3010; 2940; 1645 (str. br., C=O lactam); 1494; 1450 (str. sh., C-N-C); δ_H (400 MHz, $CDCl_3$) 3.21 (3H, s, 9-H_3); 3.3 (1H, dd *J* 8.9, 3.7, 7-H_a); 3.35 (1H, dd *J* 13.0, 3.3, 5-H_a); 3.55 (1H, t *J* 9.2, 7-H_a); 3.8 (1H, d *J* 17.2, 3-H_a); 3.9 (1H, dq *J* 9.5, 3.2, 6-H); 4.05 (1H, dd *J* 12.9, 2.6, 1.3, 5-H_b); 4.15 (1H, d *J* 17.1, 1.3, 3-H_b); 7.35-7.25 (10H, m, ar-H); δ_C (DEPT, δ_H ^{1}H–^{13}C ^{1}*J*-COSY) 47.6 (CH_2, 3.55, 4.05, 5-C); 52.8 (CH_2, 3.8, 4.15, 3-C); 58.6 (CH, 3.9, 6-C); 59.2 (CH_3, 3.21, 9-C); 70.9 (CH_2, 3.35, 3.3, 7-C); 112.6- 141.04 (CH, 7.35-7.25, ar-C); 141.7- 147.05 (C, ar-C); 168.3 (C=O, 2-C); *m/z* (APCI) 297 (M+1); HRMS ES+ calcd for [$C_{18}H_{20}N_2O_2$]: 297.1603, found: 297.1598, error +1.7 ppm; R_f= 0.25 (petroleum ether: diethyl ether, 1:1). **X-ray crystallography, Crystal data for piperazinone 246d:** $C_{17}H_{20}N_2O_2$, FW= 284.35, monoclinic, space group P21/n, *a* = 5.8967(5) Å, *b* = 16.7331(11) Å, *c* = 15.2858(16) Å, β = 91.948(3)°, *U* = 1507.4(2) Å^3, *T* = 150(2) K, λ = 0.71073 Å, *Z* = 4, *D*(cal) = 1.253 Mg/m^3, *F*(000) = 608, μ = 0.083 mm^{-1}. Crystal character: white needle. Crystal dimension 0.28 x 0.15 x 0.10 mm^3.

10.7 Preparation of *N,N'*-1,4-diphenyl-5-methoxymethyl-piperazin-2-one 247d

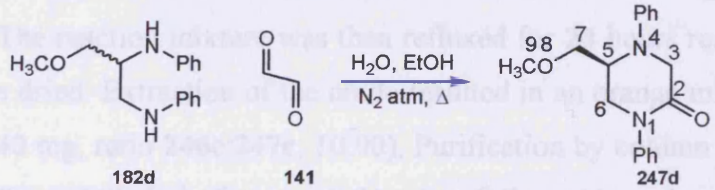

182d 141 247d

To a stirred solution of methyl *N,N'*-diphenyl-2,3-diaminopropyl ether **182d** (100 mg, 2.4 mmol), dissolved in ethanol (25 ml) and kept under a nitrogen atmosphere, an aqueous glyoxal solution **141** (40% wt/wt, 0.4 g, 68 mmol) was added dropwise. The reaction was stirred for 200 hours at reflux. The ethanol was removed and the crude product was purified by column chromatography using a slow gradient of petroleum ether, diethyl ether, ethanol to give white needle crystals of adduct **247d** (50 mg, 10 %) and **246d** (23 mg, 5%). **Spectroscopic data for *N,N'*-1,4-diphenyl-5-methoxymethyl-piperazin-2-one 247d:** ν_{max}(neat/cm^{-1}) 3056; 2985; 1669 (str. br., C=O lactam), 1498;

1418 (str. sh., C-N); δ_H (400 MHz, $CDCl_3$) 3.3 (3H, s, 9-H_3); 3.49 (1H, dd *J* 9.4, 4.5, 7-H_a); 3.53 (1H, t *J* 9.5, 7-H_b); 3.8 (1H, dd *J* 12.7, 2.4, 6-H_a); 3.93 (1H, d *J* 16.9, 3-H_a); 4.0 (1H, dd *J* 12.7, 3.6, 6-H_b); 4.08 (1H, d *J* 17.0, 3-H_b); 4.13 (1H, m, 5-H); 7.25-7.35 (10H, m, ar-H); δ_C (DEPT, δ_H ^1H–^{13}C ^1J-COSY) 49.9 (CH_2, 3.8, 4.0, 6-C); 50.3 (CH_2, 3.93, 4.08, 3-C); 52.2 (CH, 4.13, 5-C); 59.5 (CH_3, 3.3, 9-C); 68.0 (CH_2, 3.49, 3.53, 7-C); 112.6- 129.7 (CH, 7.25- 7.35, ar-C); 140.33- 149.01 (C, ar-C); 165.1 (C=O, 2-C); *m/z* (APCI) 297 (M+1); HRMS ES+ calcd for [$C_{18}H_{20}N_2O_2$]: 297.1598, found: 297.1598, error +0.00 ppm; R_f= 0.23 (petroleum ether: diethyl ether, 1:1).

10.8 Preparation of regioisomers 1,4-bis-(methoxy-ethyl)-6-methoxymethyl-piperazin-2-one 246c and 1,4-bis-(methoxy-ethyl)-5-methoxymethyl-piperazin-2-one 247c

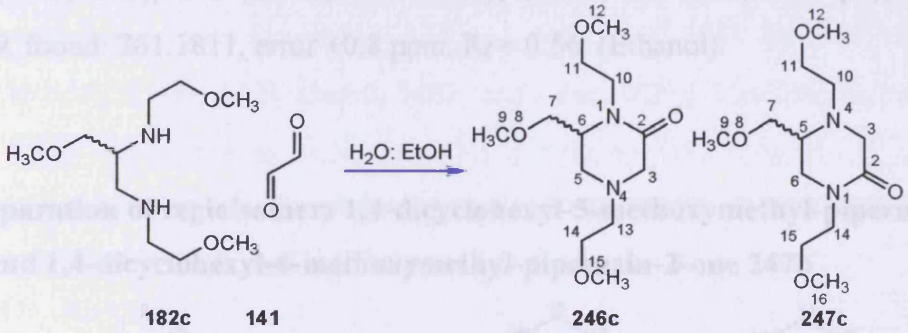

182c **141** **246c** **247c**

Diamine **182c** (0.5 g, 0.024 mol) was placed in a round bottom flask with a mixture of ethanol: water in 1:1 ratio (20 ml), followed by addition of glyoxal **141** (0.28 ml, 0.006mol). The reaction mixture was then refluxed for 24 hours resulting in orange oil that was then dried. Extraction of the crude resulted in an orange mixture of the two regioisomers (540 mg, ratio **246c**:**247c**, 10:90). Purification by column chromatography using a fast gradient of diethyl ether to ethyl acetate followed by a fast gradient of ethyl acetate to ethanol gave good separation of regioisomers **247c** (70 mg, 11%) and **246c** (240 mg, 39%). **Spectroscopic data of 1,4-bis-(methoxy-ethyl)-6-methoxymethyl-piperazin-2-one 247c:** ν_{max} ($CHCl_2$)/cm^{-1} 1637.4 (m., C=O lactam); 1119.3 (m.); δ_H ($CDCl_3$, 500 MHz) 2.44 (1H, dd *J* 11.8, 3.5, 5-H_a); 2.52 (2H, m, 13-H_2); 2.92 (1H, d *J* 16.6, 3-H_a); 2.95 (1H, m, 5-H_b); 3.18 (1H, ddd *J* 13.9, 7.7, 4.8, 10-H_a); 3.25 (3H, s, 9-H_3); 3.28 (3H, s, 12-H_3); 3.29 (3H, s, 15-H_3); 3.35 (1H, dd *J* 16.7, 1.4, 3-H_b); 3.44 (4H, m, 14-H_2, 6-H, 7-H_a); 3.48 (2H, m, 11-H_2); 3.58 (1H, dd *J* 16.6, 8.0, 7-H_b); 3.85 (1H, dt *J* 14.0, 4.7, 10-H_b); δ_C (DEPT, δ_H, ^1H-^{13}C ^1J-COSY) 45.3 (CH_2, 3.18, 3.85, 10-C);

51.63 (CH_2, 2.44, 2.95, 5-C); 56.34 (CH_2, 2.52, 13-C); 56.69 (CH, 3.44, 6-C); 57.72 (CH_2, 2.92, 3.35, 3-C); 58.81 (CH_3, 3.25, 9-C); 58.98 (CH_3, 3.28, 3.29, 12-C, 15-C); 70.21 (CH_2, 3.44, 14-C); 70.71 (CH_2, 3.48, 11-C); 72.19 (CH_2, 3.44, 3.58, 7-C); 167.97 (C=O, 2-C); m/z (APCI) 260 (M+1); HRMS ES+ calcd for [$C_{12}H_{25}N_2O_4$]: 261.1809, found: 261.1811, error +0.8 ppm; R_f = 0.63 (Ethanol). **Spectroscopic data of 1,4-bis-(methoxy-ethyl)-5-methoxymethyl-piperazin-2-one 246c:** ν_{max} (neat)/cm^{-1} 1683.55-1632.45 (str., br., C=O lactam); 1120.44 (str.); δ_H (C_6D_6, 500 MHz) 2.65 (1H, m, 10-H_a); 2.82 (1H, m, 10-H_b); 2.95 (1H, m, 5H), 3.23 (1H, d *J* 16.99, 3-H_a); 3.26 (3H, s, 9-H_3); 3.28 (6H, s, 13-H_3, 17-H_3); 3.35-3.5 (11H, m, 7-H_2, 6-H_2, 14-H_2, 15-H_2, 11-H_2, 3-H_b); δ_C (DEPT, δ_H, ^{1}H-^{13}C ^{1}*J*-COSY) 46.48 (CH_2); 49.7 (CH_2); 52.6 (CH_2, 2.65, 2.82, 10-C); 54.6 (CH_2, 3.23, 3.35-3.5, 3-C); 56.45 (CH, 2.95, 5-C); 58.6 (CH_3, 3.26, 9-C); 58.7 (CH_3, 3.28, 13-C); 59.1 (CH_3, 3.28, 17-C); 70.3 (CH_2); 70.4 (CH_2); 70.9 (CH_2); 167.37 (C=O, 2-C); m/z (APCI) 260 (M+1); HRMS ES+ calcd for [$C_{12}H_{25}N_2O_4$]: 261.1809, found: 261.1811, error +0.8 ppm; R_f = 0.56 (Ethanol).

10.9 Preparation of regioisomers 1,4-dicyclohexyl-5-methoxymethyl-piperazin-2-one 46 and 1,4-dicyclohexyl-6-methoxymethyl-piperazin-2-one 247b

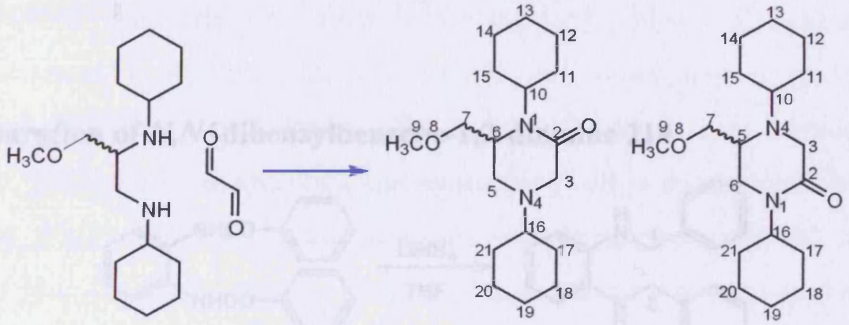

Diamine **182b** (0.8 g, 0.003 mol) was placed in a round bottom flask with a mixture of ethanol: water in 1:1 ratio (20 ml), followed by addition of glyoxal **141** (0.34 ml, 0.0075 mol). The reaction mixture was refluxed for 24 hours resulting in orange oil that was extracted with sodium hydroxide 2M and dichloromethane. The organic layer was then dried over anhydrous sodium sulphate and concentrated to give an orange mixture of the two regioisomers (600 mg, 65%). **Spectroscopic data of crude mixture of regioisomers 1,4-dicyclohexyl-5-methoxymethyl-piperazin-2-one 246b and 1,4-dicyclohexyl-6-methoxymethyl-piperazin-2-one 247b[174]:** δ_H ($CDCl_3$, 400 MHz) 1.16 (22H, m, cyclohexyl-H); 1.62 (22H, m, cyclohexyl-H); 2.4 (1H, m); 3.06(m); 3.2 (m);

3.27 (m); 3.75 (1H, t); 3.8 (1H, m); 4.32 (1H, m); *m/z* (APCI); R_f = 0.37 and 0.57 (petroleum ether: ethyl acetate, 3:1).

10.10 Preparation of *N*-[2-(benzoylamino)phenyl]benzamide 225

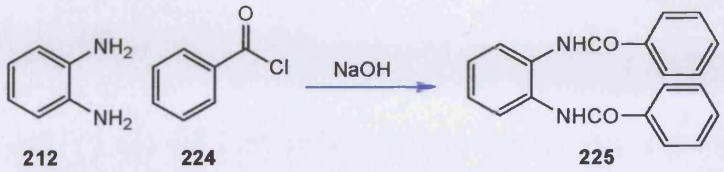

212 224 225

Benzoyl chloride **224** (25 g, 0.18 mol) was added dropwise to a solution of *o*-phenylendiamine **212** (10 g; 0.09 mol) in sodium hydroxide 10% w/w (200 ml). The dark precipitate was filtered off (4.1 g) and dissolved in refluxing dimethylformamide for recrystallisation. Needle white crystals of dibenzanilide **225** were obtained (3.60 g; 87%). **Spectroscopic data for adduct 225**: ν_{max} (neat)/cm^{-1} 3053 (str. NH); 2359 (str., CH); 1650 (str., C=O); 1421 (bend., NH); 1257 (str., CN); 758-749; δ_H (400 MHz, DMSO) 7.3- 7.7- 8.0 (14H, m, ar-H); 10.2 (2H, s, NH); δ_C (DEPT, δ_H ^{1}H–^{13}C ^{1}*J*-COSY) 126.04- 134.631 (CH, 7.3- 7.7- 8.0, ar-C); 165.9 (C, C=O); HRMS ES+ calcd for [$C_{20}H_{16}N_2O_2$]: 317.1285, found: 317.1284, error +3.15 ppm; m. p. 310°C.

10.11 Preparation of *N,N'*-dibenzylbenzene-1,2-diamine 214

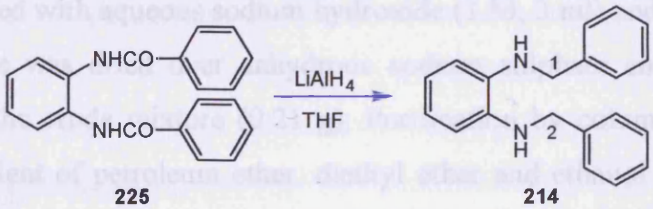

225 214

Lithium aluminium hydride (558 mg; 15.5 mmol) was added slowly to a solution of THF (20 ml) cooled in an ice bath. The crystals **225** (3.1 g; 3.1 mmol) were added slowly into the solution. The solution was refluxed for 5 hours under a nitrogen atmosphere. The reaction mixture was allowed to cool to room temperature and the lithium aluminium hydride was quenched adding ethanol (10 ml). The solvent was evaporated and sodium hydroxide (1 M) was added until the solution pH 12. The mixture was extracted with dichloromethane and dried over anhydrous sodium sulphate. The diamine **214** was a red oil (0.85 g; 98%). **Spectroscopic data for *N,N'*-**

dibenzylbenzene-1,2-diamine 214[125]: ν_{max} (neat)/cm^{-1} 3053 (str., NH); 2986; 1596 (bend., NH); 1265 (str. sh., CN), 737; 704; δ_H (400 MHz, $CDCl_3$) 3.58 (1H, t *J* 5.4, NH); 4.25 (4H, d *J* 5.8, 1-H_2, 2-H_2); 6.6-6.8 (10H, m, ar-H); 7.2-7.4 (4H, m, ar-H); δ_C (DEPT, δ_H ^{1}H–^{13}C ^{1}*J*-COSY) 30.5 (CH_2, 4.25, 1-C); 49.0 (CH_2, 4.25, 2-C); 111.9-139.4 (CH, 7.2- 7.4, ar-C); *m/z* (APCI) 289 (M+1); R_f= 0.52 (petroleum ether: diethyl ether, 3:1).

10.12 Cyclisation of *N,N'*-dibenzylbenzene-1,2-diamine 214 with methyl bromoacetate 88

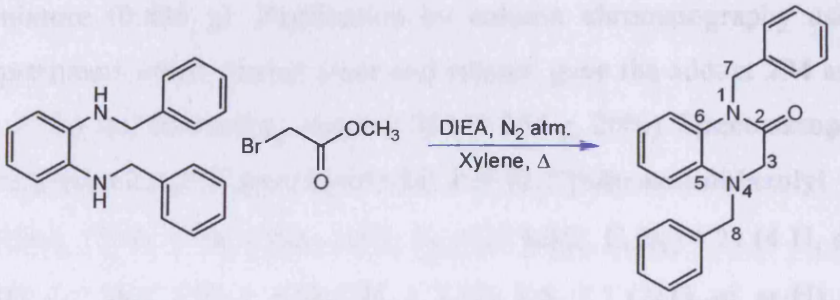

214 **88** **250**

Into a 25 ml two necked round bottom flask *N,N'*-dibenzylbenzene-1,2-diamine **214** (1 g; 3.47 mmol), diisopropylethylamine (686 mg; 5.31 mmol) and xylene (5 ml) were placed. The flask was fitted with a condensor and kept under a nitrogen atmosphere. Methyl bromoacetate **88** (531 mg; 3.47 mmol) was added with a syringe and the reaction was refluxed for 2 hours. The reaction mixture was cooled to room temperature, washed with aqueous sodium hydroxide (1 M, 3 ml) and with brine (3 ml). The organic phase was dried over anhydrous sodium sulphate and the solvent was removed to give the crude mixture (0.21 g). Purification by column chromatography using a slow gradient of petroleum ether, diethyl ether and ethanol gave piperazinone **250** (120 mg, 70 %) as clear oil. **Spectroscopic data for 1,4-dibenzyl-3,4-dihydro-1*H*-quinoxalin-2-one 250**: δ_H (400 MHz, $CDCl_3$) 3.82 (2H, s, 3-H_2); 4.33 (2H, s, 8-H_2); 5.12 (2H, s, 7-H_2); 6.9-7.3 (14H, m, ar-H); δ_C (DEPT, δ_H ^{1}H–^{13}C ^{1}*J*-COSY) 45.6 (CH_2, 5.12, 7-C); 49.0 (CH_2, 4.33, 8-C); 54.6 (CH_2, 3.82, 3-C); 112.3- 137.4 (CH, 6.9- 7.3, ar-C); 164.9 (C=O, 2-C); *m/z* (APCI) 329 (M+1); R_f= 0.37 (petroleum ether: diethyl ether, 3:1).

10.13 Cyclisation of *N,N'*-dibenzylbenzene-1,2-diamine 214 with glyoxal in EtOH

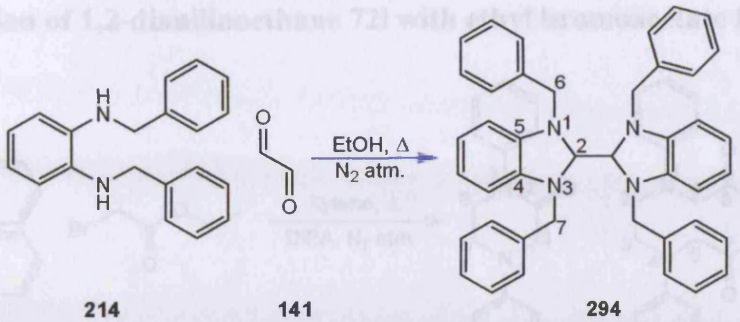

214 141 294

To a stirred solution of *N,N′*-dibenzylbenzene-1,2-diamine **214** (1g; 3.47 mmol), dissolved in ethanol (15 ml) and kept under nitrogen atmosphere, aqueous glyoxal (40% wt/wt, 503 mg; 8.67 mmol) was added. The reaction refluxed for 24 hours. The reaction mixture was allowed to cool to room temperature and the solvent was removed to give the crude mixture (0.895 g). Purification by column chromatography using a slow gradient of petroleum ether, diethyl ether and ethanol gave the adduct **294** as an orange oil (0.441 g, 42%) and the starting material **214** (0.254 g, 20%). **Spectroscopic data for 1,3,1′,3′-tetrabenzyl-2,3,2′,3′,tetrahydro-1*H*,1′*H*-[2,2′]bibenzoimidazolyl 294:** ν_{max} (neat)/cm^{-1} 2363; 1593; 1506; 1353- 1297; δ_H (400 MHz, C_6D_6) 4.21 (4 H, d *J* 16.3, 7-H_2); 4.58 (4H, d *J* 16.3, 6-H_2,); 4.65 (2H, s, 2-H); 6.6- 7.1 (28H, m, ar-H); δ_C (DEPT, δ_H ^{1}H–^{13}C ^{1}*J*-COSY) 55.53 (CH_2, 4.21, 4.58, 6-C, 7-C); 68.12 (CH, 4.65, 2-H); 112.023- 139.45 (CH, 6.6- 7.1, ar-C); HRMS ES+ calcd for [$C_{42}H_{38}N_4$]: 599.3169, found: 599.3153, error +2.6 ppm; HRMS ES+ calcd for [$C_{21}H_{19}N_2$]: 299.1543, found: 299.1546, error – 10.0 ppm; R_f = 0.54 (petroleum ether: diethyl ether, 1:1).

10.13.1 2° Attempt: Cyclisation of *N,N′*-dibenzylbenzene-1,2-diamine 214 with glyoxal in H_2O

To a stirred solution of *N,N′*-dibenzylbenzene-1,2-diamine **214** (800 mg; 2.77 mmol), dissolved in H_2O (12 ml) and kept under nitrogen atmosphere, aqueous glyoxal (40 % wt/wt, 401 mg; 6.9 mmol) was added. The reaction refluxed for 24 hours. The reaction mixture was allowed to cool to room temperature and sodium hydroxide pellets (0.5 g) were added. The mixture was extracted with dichloromethane (5× 10 ml), dried over anhydrous sodium sulphate, the solvent removed to give a yellow crude mixture (0.709 g). Purification by column chromatography using a slow gradient of petroleum ether, diethyl ether, ethanol gave the orange adduct **294** (0.467 g, 65 %) and the starting material diamine (50 mg, 10 %).

10.14 Cyclisation of 1,2-dianilinoethane 72l with ethyl bromoacetate 88

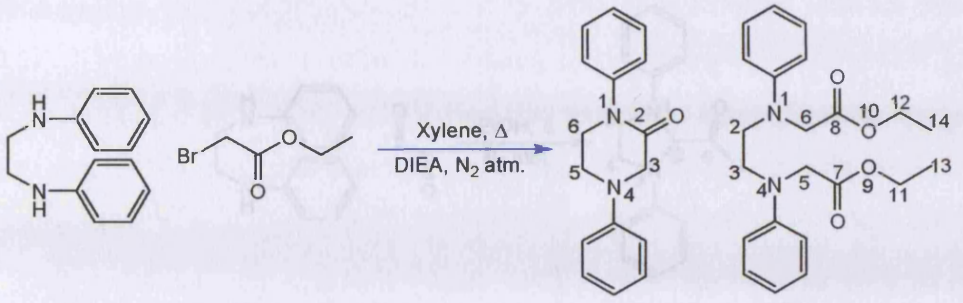

72l 88 76l 248

Into a 25 ml two necked round bottom flask were placed 1,2-dianilinoethane **72l** (1 g, 4.7 mmol), diisopropylethylamine (929 mg, 7.18 mmol) and xylene (5 ml). The flask was fitted with a condensor and placed under a nitrogen atmosphere. Ethyl bromoacetate **88** (785 mg, 4.7 mmol) was added dropwise with a syringe and the reaction mixture was refluxed for 24 hours. The reaction mixture was washed with aqueous sodium hydroxide (1 M, 3 ml) and with brine (3 ml). The organic phase was dried over anhydrous sodium sulphate and the solvent removed to give crude product (0.486 g). Purification by column chromatography of the mixture using a slow gradient petroleum ether, diethyl ether and ethanol gave two main products: adduct **76l** (47 mg, 10 %) and adduct **248** (163 mg, 33 %). **Spectroscopic data for *N,N'*-diphenylpiperazin-2-one 76l[102]:** ν_{max} (neat)/cm^{-1} 3054 (str., NH); 2987 (str., arCH); 1690 (str., C=O); 1494 (bend., NH); 1265 (bend., arCH); 895 (bend., NH); 734-704; δ_H (400 MHz, $CDCl_3$) 3.52 (2H, dd *J* 5.5, 5.0, 6-H_2); 3.8 (2H, dd *J* 5.3, 5.3, 5-H_2); 4.0 (2H, s, 3-H_2); 6.85-7.2 (10H, m, ar-H); δ_C (DEPT, δ_H ^{1}H–^{13}C ^{1}*J*-COSY) 46.5 (CH_2, 3.52, 6-C); 50 (CH_2, 3.8, 5-C); 53.4 (CH_2, 3-C); 125.75- 129.51 (CH, 6.85- 7.2, ar-C); 167.5 (C=O, 2-C); *m/z* (APCI) 254 (M+ 1), ES+ calcd for [$C_{16}H_{16}N_2O$]: 253.1335, found: 253.1336, error –3.95 ppm; R_f= 0.16 (petroleum ether: diethyl ether, 1:1); **Spectroscopic data for {[2-(ethoxycarbonylmethyl-phenyl-amino)-ethyl]-phenyl-amino}-acetic acid ethyl ester 248:** ν_{max} (neat)/cm^{-1} 3046-2975; 1744 (str. sh., C=O); 1599-1505; δ_H (400 MHz, $CDCl_3$) 1.2 (6H, t *J* 7.1, 14-H_3); 3.62 (4H, s, 6-H_2); 3.97 (4H, s, 2-H_2); 4.1 (4H, dd *J* 19.8, 7.1, 12-H_2); 6.6- 7.15 (10H, m, ar-H); δ_C (DEPT, δ_H ^{1}H–^{13}C ^{1}*J*-COSY) 14.2 (CH_3, 1.2, 14-C); 50.3 (CH_2, 3.62, 6-C); 53.5 (CH_2, 3.97, 2-C); 61.1 (CH_2, 4.1, 12-C); 126.4-128.3 (CH, 6.6- 7.15, ar-C); 171.2 (C=O, 3-C); *m/z* (APCI) 386 (M+ 1); HRMS ES+ calcd for [$C_{22}H_{28}N_2O_4$]: 385.2122, found: 385.2127, error +1.2 ppm; R_f= 0.25 (petroleum ether: diethyl ether, 1:1).

10.15 Cyclisation of 1,2-dianilinoethane 72l with glyoxal in EtOH

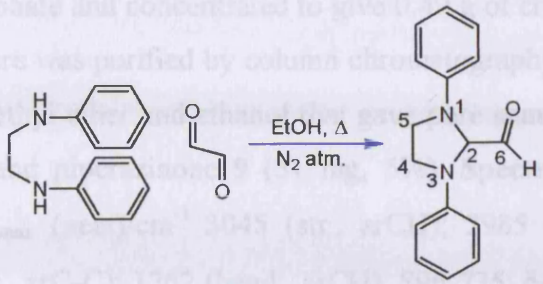

284

To a stirred solution of 1,2-dianilinoethane **72l** (500 mg, 2.35 mmol), dissolved in ethanol (15 ml) and kept under a nitrogen atmosphere, was added an aqueous 40% (wt/wt) glyoxal solution (145 mg, 2.35 mmol) dropwise over 5 minutes. The reaction was stirred for 48 hours at reflux. The reaction mixture was allowed to cool to room temperature and the ethanol was removed to give the crude product (0.665 g). No piperazinone was shown by TLC and in the ^{1}H-NMR spectrum. Purification by column chromatography using a slow gradient of petroleum ether, diethyl ether and ethanol gave a mixture of products containing the adduct **284** (0.35 g, 52% calculated yield). **Spectroscopic data for 1,3-diphenyl-imidazolidine-2-carbaldehyde 284[94]:** δ_H (400 MHz, $CDCl_3$) 3.68 (2H, dd *J* 8.5, 5.6, 4-H_a, 5-H_a), 3.82 (2H, dd *J* 8.5, 5.6, 4-H_b, 5-H_b), 4.99 (1H, d *J* 6.8, 2-H), 7.5 (10H, m, ar-H), 9.81 (1H, dd *J* 7.0, 6-H); R_f = 0.49 (petroleum ether: diethyl ether, 1:1).

10.16 Cyclisation of 1,2-dianilinoethane 72l with glyoxal in H_2O

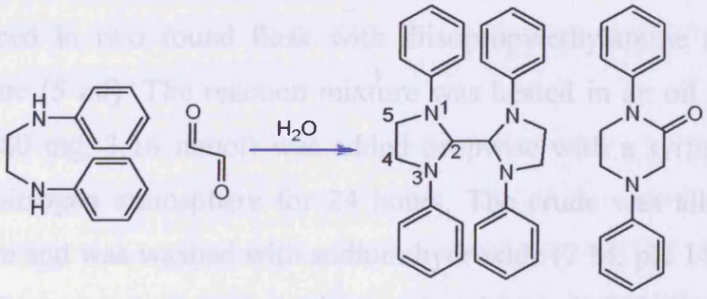

285 **76l**

A solution of 1,2-dianilinoethane **72l** (500 mg; 2.35 mmol) and H_2O (10 ml) was placed in a two neck round bottom flask. Acetic acid (21.15 mg; 0.35 mmol) was added to the mixture and the solution stirred for 30 minutes. Aqueous glyoxal (40% wt/wt, 197.4 mg, 4.525 mmol) was added dropwise over 15 minutes. The reaction mixture was refluxed for 24 hours under nitrogen atmosphere. Sodium hydroxide pellets (0.5 g) were

added and the mixture was extracted with ethyl acetate (3× 15 ml), dried over anhydrous sodium sulphate and concentrated to give 0.49 g of crude product (ratio **285**: **76l**, 69:31). The mixture was purified by column chromatography using a slow gradient of petroleum ether, diethyl ether and ethanol that gave pure samples of bis-imidazoline **285** (130 mg, 24%) and piperazinone **9** (51 mg, 5%). **Spectroscopic data for bis-imidazoline 285[94]:** ν_{max} (neat)/cm^{-1} 3045 (str., arCH); 2985 (str., NH); 1674-1594 (bend., NH); 1498 (str., arC-C); 1262 (bend., arCH); 896-735; δ_H ($CDCl_3$) 3.28 (2H, dd *J* 8.3, 5.5, 5-H_2); 3.42 (2H, dd *J* 8.1, 5.5, 4-H_2); 5.87 (1H, s, 2-H); 6.57-7.15 (20H, m, ar-H); δ_C (DEPT, δ_H ^{1}H–^{13}C ^{1}*J*-COSY) 46.45 (CH_2, 3.28, 3.42, 4-C, 5-C); 72.41 (CH, 5.87, 2-C); 112.31-145.65 (CH, 6.57- 7.15, ar-C); *m/z* (APCI) 447 (M+1); 223 (M/2); R_f= 0.48 (petroleum ether: diethyl ether, 1:1).

10.17 Preparation of methoxymethyl-1,4-bis-(4-methoxy-phenyl)-piperazin-2-one 246e

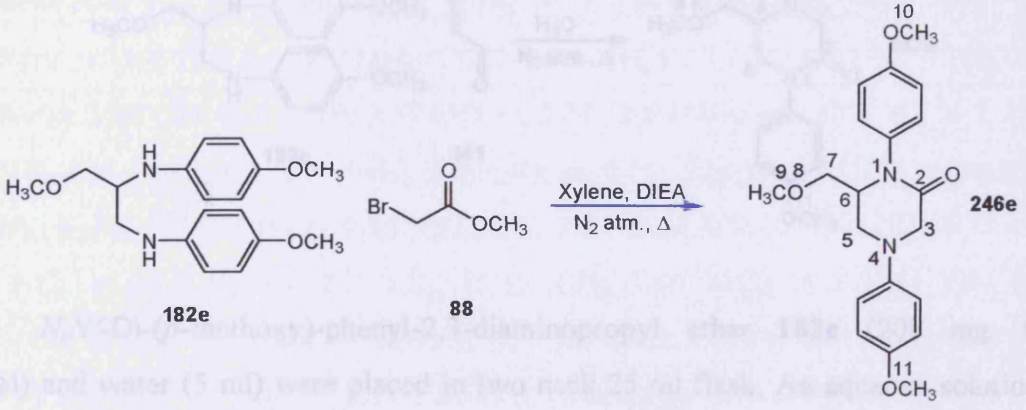

N,N'-Di-(*p*-methoxy)-phenyl-2,3-diaminopropyl ether **182e** (500 mg, 1.57 mmol) was placed in two round flask with diisopropylethylamine (304.4 mg, 3.14 mmol) and xylene (5 ml). The reaction mixture was heated in an oil bath and methyl bromoacetate (480 mg, 3.14 mmol) was added dropwise with a syringe. The mixture refluxed under nitrogen atmosphere for 24 hours. The crude was allowed to cool to room temperature and was washed with sodium hydroxide (2 M, pH 14) and with brine (10 ml). The solvent was removed to give crude mixture (0.809 g). Purification by column chromatography using a slow gradient of petroleum ether, diethyl ether, ethyl acetate gave the piperazinone **246e** (0.110 g; 20 %). **Spectroscopic data for 6-methoxymethyl-1,4-bis-(4-methoxy-phenyl)-piperazin-2-one 246e[129]:** ν_{max} (neat)/cm^{-1} 3052 (str., arC-H); 1656 (str., C=O); 1510 (str., arC-H); 1210 (str., CH-O); 1307; 895; 831; 737 (bend., arC-H); δ_H (500 MHz, $CDCl_3$) 3.0 (3H, s, 9-H_3); 3.02 (1H,

dd *J* 12.5, 3.4, 5-H_a); 3.24 (1H, dd *J* 8.8, 3.4, 7-H_a); 3.39 (3H, s, 10-H_3); 3.43 (3H, s, 11-H_3); 3.6 (1H, t *J* 9.0, 7-H_b); 3.78 (1H, d *J* 16.7, 3-H_a); 3.82 (1H, m, 6-H); 3.85 (1H, ddd *J* 12.5, 3.1, 1.5, 5-H_b); 4.18 (1H, dd *J* 16.7, 1.5, 3-H_b); 6.8-7.2 (8H, m, ar-H); δ_C (DEPT, δ_H ^1H–^{13}C ^1J-COSY) 49.4 (CH_2, 3.02, 3.85, 5-C); 54.46 (CH_3, 3.39, 10-C); 54.71 (CH_2, 3.78, 3-C); 54.88 (CH_3, 3.43, 11-C); 58.34 (CH, 3.82, 6-C); 58.69 (CH_3, 3.0, 9-C); 70.18 (CH_2, 3.24, 3.6, 7-C); 166.06 (C=O, 2-C); *m/z* (APCI) 357 (M+1); HRMS ES+ calcd for [$C_{20}H_{20}N_2O_4$]: 357.1809, found: 357.1807, error +4.5 ppm; R_f=0.22 (diethyl ether).

10.18 Preparation of 5-methoxymethyl-1,4-bis-(4-methoxy-phenyl)-piperazin-2-one 247e

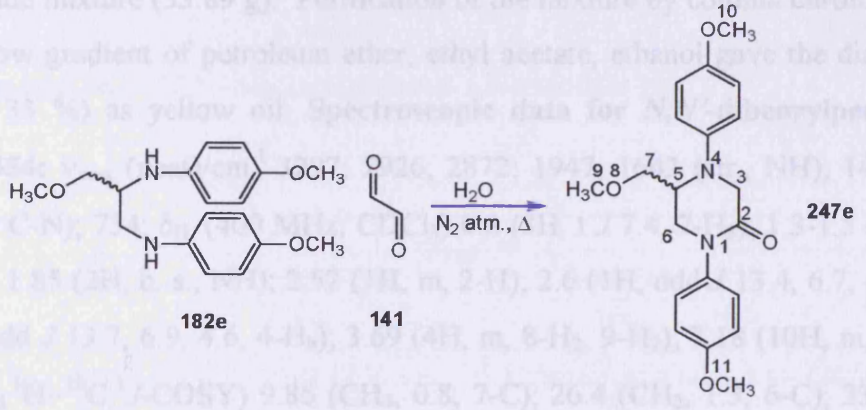

182e 141

N,N'-Di-(*p*-methoxy)-phenyl-2,3-diaminopropyl ether **182e** (208 mg, 0.65 mmol) and water (5 ml) were placed in two neck 25 ml flask. An aqueous solution of glyoxal **141** (40 % wt/wt, 1.5 g, 26.2 mmol) was added dropwise with a syringe. The reaction mixture was refluxed for 24 hours under a nitrogen atmosphere. The mixture was allowed to cool to room temperature, sodium hydroxide pellets (3 mg) were added and it was extracted with ethyl acetate. It was dried over anhydrous sodium sulphate and the solvent was evaporated to give 0.15 g of crude mixture. The products were purified by column chromatography using a slow gradient of petroleum ether, diethyl ether, and ethanol. The purification gave only one fraction in which both of regioisomers **247e**, **246e** (61 mg, 35%) were present in the ratio 60:40.

10.19 Preparation of *N,N'*-dibenzylpentane-1,3-diamine 352

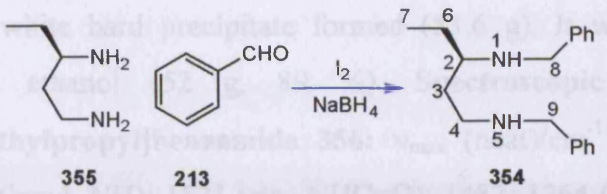

355 213 354

Benzaldehyde **213** (62.3 g, 0.6 mol) and iodine (7.69 g, 0.24 mol) were added to a solution of Dytec© diamine **355** (20 g, 0.19 mol) in methanol (350 ml). The reaction mixture stirred at room temperature for 15 minutes. Sodium borohydride (8.98 g, 0.24 mol) was added slowly and stirring continued for 30 minutes. The reaction mixture was diluted with water and HCl (2 M) was added until pH 1. The mixture was extracted with dichloromethane and the aqueous phase was basified until pH 14. It was extracted with dichloromethane, dried over anhydrous sodium sulphate and concentrated to give a yellow crude mixture (33.89 g). Purification of the mixture by column chromatography using a slow gradient of petroleum ether, ethyl acetate, ethanol gave the diamine **354** (17.08 g, 33 %) as yellow oil. **Spectroscopic data for *N,N'*-dibenzylpentane-1,3-diamine 354:** ν_{max} (neat)/cm^{-1} 3297; 2926; 2872; 1947; 1643 (str., NH); 1494; 1453; 1198 (str., C-N); 734; δ_H (400 MHz, $CDCl_3$) 0.8 (3H, t *J* 7.4, 7-H_3); 1.3-1.5 (4H, m, 3-H_2, 6-H_2); 1.85 (2H, b. s., NH); 2.52 (1H, m, 2-H); 2.6 (1H, ddd *J* 13.4, 6.7, 4.7, 4-H_a); 2.7 (1H, ddd *J* 13.7, 6.9, 4.6, 4-H_b); 3.69 (4H, m, 8-H_2, 9-H_2); 7.18 (10H, m, ar-H); δ_C (DEPT, δ_H ^{1}H–^{13}C ^{1}*J*-COSY) 9.86 (CH_3, 0.8, 7-C); 26.4 (CH_2, 1.3, 6-C); 33.23 (CH_2, 1.5, 3-C); 47.06 (CH_2, 2.6, 2.7, 4-C); 51.03 (CH_2, 3.69, 9-C); 54.2 (CH_2, 3.69, 8-C); 57.5 (CH, 2.52, 2-C); 126.87- 128.41 (CH, 7.18, ar-C); 140.18- 140.74 (C, ar-C); ***m/z*** (APCI) 284 (M+ 1); HRMS ES+ calcd for [$C_{19}H_{26}N_2$]: 283.2169, found: 283.2166, error +1.6 ppm; R_f= 0.1 (diethyl ether).

10.20 Preparation of *N*-[3-(benzoylamino)-1-ethylpropyl]benzamide 356

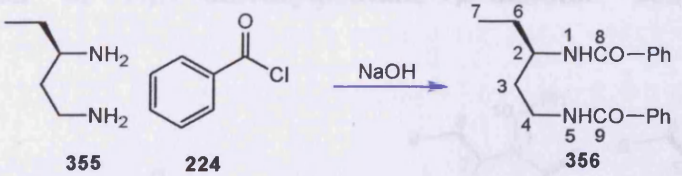

355 224 356

Dytec© diamine **355** (20 g, 0.19 mol) was placed in 2 neck round bottom flask in presence of sodium hydroxide (1 M, 300 ml) and benzoyl chloride **224** (80 g, 0.57 mol) was added dropwise with an equalized pressure funnel. The solution was stirred

for 2 hours and a white hard precipitate formed (53.6 g). It was filtered off and recrystallised from ethanol (52 g, 89 %). **Spectroscopic data for *N*-[3-(benzoylamino)-1-ethylpropyl]benzamide 356:** ν_{max} (neat)/cm^{-1} 3327; 3053; 1711 (bend., C=O); 1651 (bend. NH); 1521 (str., NHC=O); 1487; 1264 (str., CN); 895; 734; δ_H (400 MHz, $CDCl_3$) 0.8 (3H, t *J* 7.4, 7-H_3); 1.3-1.6 (4H, m, 6-H_2, 3-H_a, 5-H); 1.93 (1H, ddd *J* 10.8, 9.8, 3.5, 3-H_b); 2.92 (1H, ddt *J* 13.9, 10.9, 3.7, 4-H_a); 3.97 (1H, tt *J* 8.8, 4.3, 4-H_b); 4.1 (1H, ddd *J* 10.9, 5.4, 3.3, 2-H); 6.0 (1H, d *J* 8.9, 1-H); 7.4-7.8 (10H, m, ar-H); δ_C (DEPT, δ_H ^{1}H–^{13}C ^{1}*J*-COSY) 10.85 (CH_3, 0.8, 7-C); 28.7 (CH_2, 1.3, 6-C); 35.5 (CH_2, 1.3, 3-C); 36.07 (CH_2, 2.92, 3.97, 4-C); 49.16 (CH, 4.1, 2-C); 126.90- 134.21 (CH, 7.4- 7.8, ar-C); 167.1 (C=O, 9-C); 168.8 (C=O, 8-C); HRMS ES+ calcd for [$C_{19}H_{22}N_2O_2$]: 311.1754, found: 311.1753, error +3.2 ppm.

10.21 Preparation of *N,N'*-dibenzylpentane-1,3-diamine 352

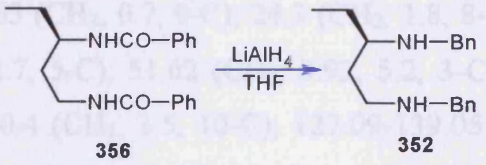

356 **352**

Lithium aluminium hydride (740 mg, 19.5 mmol) was added to THF (30 ml) in an ice bath. The precipitate **356** (1.233 g, 3.9 mmol) was added slowly and the reaction mixture was refluxing under nitrogen atmosphere for 6 hours. The reaction mixture was allowed to cool to room temperature and ethanol (20 ml) was added to destroy the excess of lithium aluminium hydride. The solvent was evaporated and the solution was diluted with water and NaOH (1 M) until pH 14. The crude mixture was extracted with dichloromethane, dried over anhydrous sodium sulphate and concentrated to give the diamine **352** (0.61 g; 55%).

10.22 Cyclisation of *N,N'*-dibenzylpentane-1,3-diamine 352 with methyl bromoacetate

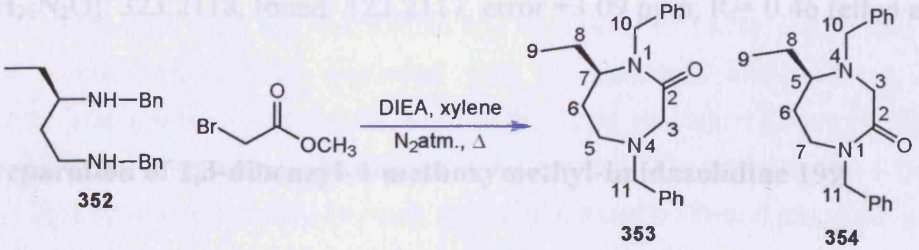

352 **353** **354**

Diisopropylethylamine (917 mg; 7.1 mmol) and *N,N'*-dibenzylpentane-1,3-diamine **352** (1 g; 3.59 mmol) were dissolved in xylene (10 ml). The reaction mixture was heated to reflux and methyl bromoacetate (1.08 g; 7.1 mmol) was added dropwise with an equalised pressure-dropping funnel. The mixture was refluxed for 20 hours. After cooling to room temperature, sodium hydroxide (2 M) was added until pH 14 and the reaction mixture was extracted. Brine was added and the mixture extracted again. The organic phase was dried over anhydrous sodium sulphate and the solvent was removed to give the crude mixture (0.896 g). Purification by column chromatography using a slow gradient of petroleum ether, ethyl acetate and ethanol gave the diazapenone **353** (25 mg; 2%) and diazapenone **354** (275 mg; 24%) as amber oils. **Spectroscopic data for 1,4-dibenzyl-7-ethyl-[1,4]diazepan-2-one 353:** ν_{max} (neat)/cm^{-1} 2967; 1625 (str. sh., C=O)); 1494 (bend., lactam NH); 1359 (str., lactam C-N); δ_H ($CDCl_3$) 0.7 (3H, t *J* 7.4, 9-H_3); 1.52 (1H, d *J* 12.6, 6-H_a); 1.8 (3H, m, 8-H_2, 6-H_b); 2.52 (1H, d *J* 12.6, 5-H_a); 2.7 (1H, ddd *J* 12.6, 12.6, 3.6, 5-H_b); 3.1 (1H, m, 7-H); 3.5 (4H, m, 10-H_2, 11-H_2); 3.93 (1H, d *J* 14.7, 3-H_a); 5.2 (1H, d *J* 14.7, 3-H_b); 7.2 (10H, m, ar-H); δ_C (DEPT, δ_H ^1H–^{13}C ^1J-COSY) 11.63 (CH_3, 0.7, 9-C); 24.3 (CH_2, 1.8, 8-C); 28.1 (CH_2, 1.52, 1.8, 6-C); 49.34 (CH_2,2.52, 2.7, 5-C); 51.62 (CH_2, 3.93, 5.2, 3-C); 58.71 (CH, 3.1, 7-C); 59.7 (CH_2, 3.5, 11-C); 60.4 (CH_2, 3.5, 10-C); 127.09-139.05 (CH, 7.2, ar-C); 172.99 (C=O, 2-C); *m/z* (APCI) 323 (M+1); HRMS ES+ calcd for [$C_{21}H_{26}N_2O$]: 323.2118, found: 323.2116, error +6.18 ppm; R_f= 0.37 (ethyl acetate). **Spectroscopic data for 1,4-dibenzyl-5-ethyl-[1,4]diazepan-2-one 354:** ν_{max} (neat)/cm^{-1} 2967; 1625 (str., C=O); 1494 (str., lactam NH); 1359 (str., lactam C-N); δ_H ($CDCl_3$) 0.82 (3H, t *J* 7.4, 9-H_3); 1.3 (4H, m, 6-H_2, 8-H_2); 2.62 (1H, m, 5-H); 3.2 (1H, m, 7-H_a); 3.35 (1H, m, 7-H_b); 3.4 (1H, d *J* 15.6, 11-H_a); 3.5 (1H, d *J* 13.7, 10-H_a); 3.8 (1H, d *J* 15.7, 11-H_b); 3.7 (1H, d *J* 13.7, 10-H_b); 4.51 (1H, d *J* 14.4, 3-H_a); 4.6 (1H, d *J* 14.4, 3-H_b); 7.3 (10H, m, ar-H); δ_C (DEPT, δ_H ^1H–^{13}C ^1J-COSY) 11.3 (CH_3, 0.82, 9-C); 18.8 (CH, 2.62, 5-C); 25.3 (CH_2, 1.3, 8-C); 29.3 (CH_2, 1.3, 6-C); 45.7 (CH_2, 3.2, 3.35, 7-C); 51.5 (CH_2, 4.51, 4.6, 3-C); 55.1 (CH_2, 3.5, 3.7, 10-C); 57.8 (CH_2, 3.4, 3.8, 11-C); 127.00-139.07 (CH, 7.3, ar-C); 174 (C=O, 2-C); *m/z* (APCI) 323 (M+1, 100%); 162 (M/2, 12%); HRMS ES+ calcd for [$C_{21}H_{26}N_2O$]: 323.2118, found: 323.2117, error +3.09 ppm; R_f= 0.46 (ethyl acetate).

10.23 Preparation of 1,3-dibenzyl-4-methoxymethyl-imidazolidine 199

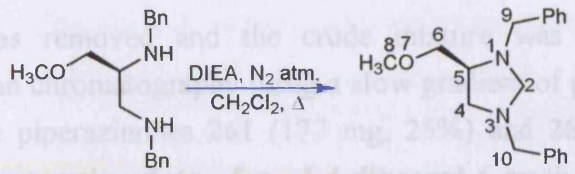

182a **199**

Methyl *N,N'*-dibenzyl-2,3-diaminopropyl ether **182a** (300 mg, 1.05 mmol) was placed in a round bottom flask with diisopropylethylamine (547.3 mg, 4.23 mmol) and dichloromethane (7 ml). The mixture was refluxed for 300 hours. The reaction mixture was allowed to cool to room temperature and sodium hydroxide (2 M) was added until pH 14. The mixture was extracted with chloroform, dried over anhydrous sodium sulphate and the solvent evaporated to give a pure imidazolidine **199** as a yellow oil (255 mg, 85%). **Spectroscopic data for 1,3-dibenzyl-4-methoxymethyl-imidazolidine 21:** ν_{max} (neat)/cm^{-1} 2952; 1512; 897; δ_H (400 MHz, $CDCl_3$) 2.5 (1H, dd *J* 9.4, 5.9, 6-H_a); 2.9 (1H, t *J* 7.7, 6-H_b); 3.02 (1H, m, 5-H); 3.2 (1H, d *J* 9.3, 2-H_a); 3.25 (3H, s, 8-H_3); 3.3 (1H, d *J* 9.3, 2-H_b); 3.5 (2H, m, 4-H_2); 3.62 (1H, d *J* 13.0, 9-H_a); 3.95 (1H, d *J* 13.1, 9-H_b); 7.5 (10H, m, ar-H); δ_C (DEPT, δ_H ^{1}H–^{13}C ^{1}*J*-COSY) 57.57 (CH_2, 3.62, 3.95, 9-C); 58.00 (CH_3, 3.25, 8-C); 58.58 (CH_3, 2.5, 2.9, 6-C); 61.53 (CH, 3.02, 5-C); 74.78 (CH_2, 3.5, 4-C); 75.74 (CH_2, 3.2, 3.3, 2-C); 125.98- 128.08 (CH, 7.5, ar-C); HRMS ES+ calcd for [$C_{19}H_{24}N_2O$]: 297.1961, found: 297.1963, error –4.72 ppm; R_f= 0.23 (petroleum ether: diethyl ether, 1:1).

10.24 Cyclisation of methyl *N,N'*-dibenzyl-2,3-diaminopropyl ether 182a with methyl α-bromo phenylacetate 253

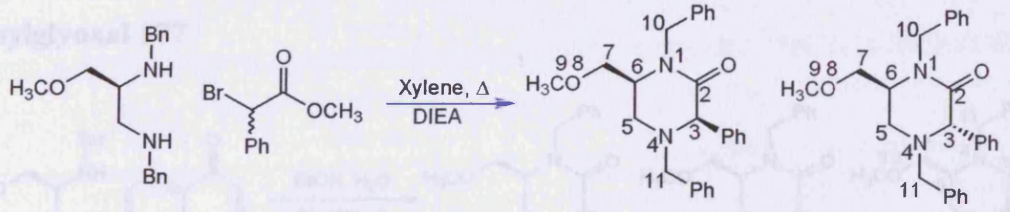

182a **253** **261** **262**

Methyl *N,N'*-dibenzyl-2,3-diaminopropyl ether **182a** (500 mg, 1.76 mmol), diisopropylethylamine (232 mg, 1.8 mmol) and xylene (5 ml) were placed into a 50 ml two neck round bottom flask provided with a condensor and under a nitrogen atmosphere. The mixture was heated until reflux and methyl α-bromophenylacetate (688 mg, 2.3 mmol) was added dropwise over 30 minutes. The reaction was refluxed for 3 hours. The reaction was cooled to room temperature and sodium hydroxide (2 M) was added until pH 14, was washed with brine (10 ml) and dried over anhydrous sodium

sulphate. Xylene was removed and the crude mixture was obtained (730 mg). Purification by column chromatography using a slow gradient of petroleum ether, ethyl acetate, ethanol gave piperazinones **261** (177 mg, 25%) and **262** (210 mg, 35%) as yellow oils. **Spectroscopic data for 1,4-dibenzyl-6-methoxymethyl-3-phenyl-piperazin-2-one 261:** ν_{max} (neat)/cm^{-1} 3000; 1645 (str. sh., C=O); 1494; 1266 (str. sh., lactam C-N); δ_H ($CDCl_3$) 2.03 (1H, dd *J* 12.1, 3.1, 5-H_a); 3.0 (1H, d, *J* 13.4, 11-H_a), 3.02 (1H, dd *J* 11.8, 3.5, 5-H_b); 3.18 (3H, s, 9-H_3); 3.3 (1H, m, 6-H); 3.61 (1H, dd *J* 8.8, 4.5, 7-H_a); 3.71 (1H, t *J* 8.0, 7-H_b); 3.71 (1H, d *J* 13.4, 11-H_b), 3.95 (1H, d *J* 14.8, 10-H_a); 4.0 (1H, s, 3-H); 5.0 (1H, d *J* 14.8, 10-H_b); 7.0-7.5 (15H, m, ar-H); δ_C (DEPT, δ_H ^{1}H–^{13}C ^{1}*J*-COSY) 47.96 (CH_2, 2.03, 3.0, 3.95, 5.0, 5-C, 10-C); 53.35 (CH, 3.3, 6-C); 57.65 (CH_2, 3.0, 3.71, 11-C); 57.91 (CH, 4.0, 3-C); 70.73 (CH_3, 3.18, 9-C); 72.00 (CH_2, 3.61, 3.71, 7-C); 125.54-137.14 (CH, 7.0-7.5, ar-C); 167.65 (C=O, 2-C); HRMS ES+ calcd for [$C_{26}H_{28}N_2O_2$]: 401.2224, found: 401.2224, error +0.00 ppm; R_f= 0.35 (petroleum ether: ethyl acetate, 2:1). **Spectroscopic data for 1,4-dibenzyl-6-methoxymethyl-3-phenyl-piperazin-2-one 262:** ν_{max} (neat)/cm^{-1} 2926; 1645 (str. sh., C=O); 1451 (bend. sh., NH); δ_H ($CDCl_3$) 2.44 (1H, dd *J* 12.2, 7.2, 5-H_b); 2.85 (1H, dd *J* 12.2, 4.1, 5-H_a); 3.09 (3H, s, 9-H_3); 3.18 (1H,d *J* 13.5, 11-H_a); 3.25 (1H, dd *J* 9.7, 3.6, 7-H_a); 3.4 (2H, m, 7-H_b, 11-H_b); 3.5 (1H, m, 6-H); 4.05 (1H, d *J* 14.9, 10-H_a); 4.2 (1H, s, 3-H); 5.25 (1H, d *J* 14.9, 10-H_b); 7.0-7.5 (15H, m, ar-H); δ_C (DEPT, δ_H ^{1}H–^{13}C ^{1}*J*-COSY) 47.01 (CH_2, 4.05, 5.25, 10-C); 47.97 (CH_2, 2.44, 2.85, 5-C); 54.81 (CH, 3.5, 6-C); 58.36 (CH_2, 3.18, 3.4, 11-C); 59.03 (CH_3, 3.09, 9-C); 71.74 (CH, 4.2, 3-C); 73.54 (CH_2, 3.25, 3.4, 7-C); 126.76-137.94 (CH, 7.0-7.5, ar-C); 169.66 (C=O, 2-C); HRMS ES+ calcd for [$C_{26}H_{28}N_2O_2$]: 401.2224, found: 401.2225, error –2.49 ppm; R_f= 0.24 (petroleum ether: ethyl acetate, 2:1).

10.25 Cyclisation of methyl *N,N'*-dibenzyl-2,3-diaminopropyl ether 182a with phenylglyoxal 177

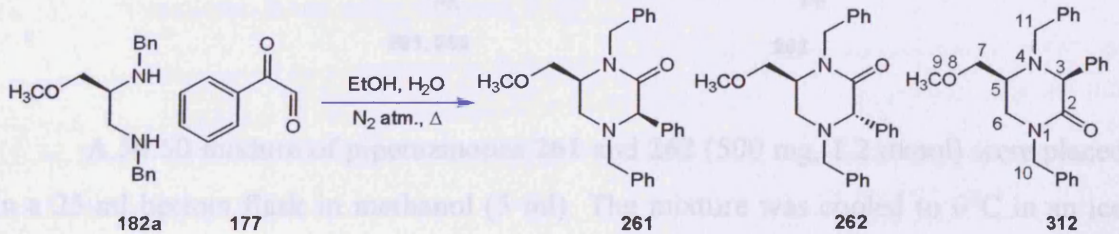

Methyl *N,N'*-dibenzyl-2,3-diaminopropyl ether **182a** (500 mg, 1.76 mmol) was placed in a 25 ml round bottom flask with a mixture of ethanol, water 9:1 (10ml). Phenylglyoxal **177** (1.18 g, 8.8 mmol) was added dropwise and the mixture was

refluxed for 20 hours. The reaction mixture was cooled to room temperature and the ethanol was removed. NaOH pellets (0.5 g) were added and the mixture was extracted with ethyl acetate (3×15 ml), dried over anhydrous sodium sulphate and concentrated. The crude mixture was a dark oil (680 mg). Purification by column chromatography using a slow gradient of petroleum ether, ethyl acetate, ethanol gave 6-piperazinone **261** (121 mg, 17%), 6-piperazinone **262** (167 mg, 24%) and 5-piperazinone **312** (178 mg, 25%) as yellow oils. **Spectroscopic data for 1,4-dibenzyl-5-methoxymethyl-3-phenyl-piperazin-2-one 312:** ν_{max} (neat)/cm^{-1} 3052; 1646 (str. sh., C=O); 1246 (str. sh., lactam C-N); δ_H ($CDCl_3$) 3.0 (2H, m, 5-H, 6-H_a); 3.05 (3H, s, 9-H_3); 3.16 (1H, dd, *J* 5.8, 3.2, 7-H_a); 3.21 (1H, dd, *J* 11.7, 2.7, 6-H_b); 3.26 (1H, dd, *J* 8.4, 3.2, 7-H_b); 3.7 (1H, d *J* 14.0, 11-H_a); 3.83 (1H, d *J* 14.0, 11-H_b); 4.35 (1H, s, 3-H); 4.52 (1H, d *J* 14.6, 10-H_a); 4.58 (1H, d *J* 14.6, 10-H_b); 7.2-7.5 (15H, m, ar-H); δ_C (DEPT, δ_H ^{1}H–^{13}C ^{1}*J*-COSY) 45.97 (CH_2, 3.0, 3.21, 6-C); 48.89 (CH_2, 4.52, 4.58, 10-C); 57.66 (CH, 3.0, 5-C); 57.72 (CH_3, 3.05, 9-C); 58.65 (CH_2, 3.7, 3.83, 11-C); 66.9 (CH, 4.35, 3-C); 72.43 (CH_2, 3.16, 3.26, 7-C); 125.7-135.0 (CH, 7.2-7.5, ar-C); 191.42 (C=O, 2-C); HRMS ES+ calcd for [$C_{26}H_{28}N_2O_2$]: 401.2224, found: 401.2223, error +2.49 ppm; R_f= 0.21 (petroleum ether: ethyl acetate, 2:1).

10.26 Equilibration of 1,4-dibenzyl-6-methoxymethyl-3-phenyl-piperazin-2-one 261 and 1,4-dibenzyl-6-methoxymethyl-3-phenyl-piperazin-2-one 262

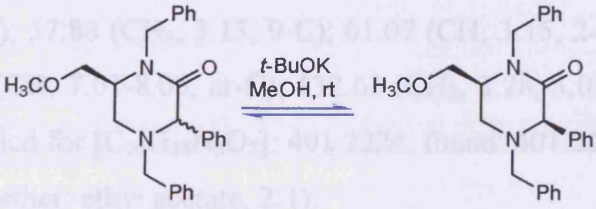

A 50:50 mixture of piperazinones **261** and **262** (500 mg, 1.2 mmol) were placed in a 25 ml bottom flask in methanol (5 ml). The mixture was cooled to 0°C in an ice bath and potassium t-butoxide (24 mg, 0.2 mmol) was added slowly. After 48 h stirring at room temperature the mixture was neutralised with hydrochloric acid (1 M, 6 ml), extracted with diethyl ether (3×10 ml) and washed with brine (15 ml). The organic layer was dried over anhydrous sodium sulphate and concentrated (432 mg). The ^{1}H-NMR spectrum showed a mixture of piperazinones **262**, **261** with ratio 84: 16.

10.27 Preparation of (1,3-dibenzyl-4-methoxymethyl-imidazolidin-2-yl)-phenyl-methanone 315a

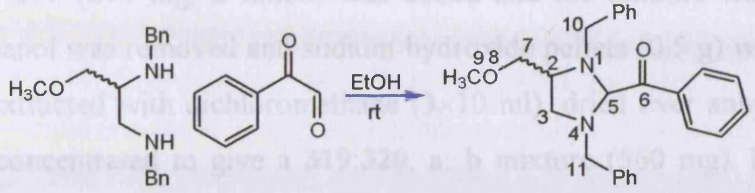

182a **177** **315a**

Methyl *N,N'*-dibenzyl-2,3-diaminopropyl ether **182a** (250 mg, 0.88 mmol) was placed in a 25 ml round bottom flask with ethanol (5 ml). Phenylglyoxal (295 g, 2.2 mmol) was added dropwise and the mixture was stirred for 5 days. The ethanol was removed and sodium hydroxide pellets (0.5 g) were added. The mixture was extracted with ethyl acetate (3×10 ml), dried over anhydrous sodium sulphate and concentrated. The crude mixture was a red oil (250 mg). Purification by column chromatography using a slow gradient of petroleum ether, ethyl acetate, ethanol gave piperazinones **262** and **312** (36 mg, 10%) and the (1,3-dibenzyl-4-methoxymethyl-imidazolidin-2-yl)-phenyl-methanone **315a** (20 mg, 8%) as yellow oils. **Spectroscopic data for (1,3-dibenzyl-4-methoxymethyl-imidazolidin-2-yl)-phenyl-methanone 315a:** ν_{max} (neat)/cm^{-1} 3053 (str., arC-H); 1645 (str. sh., C=O); 1451; 1265; δ_H ($CDCl_3$) 2.65 (1H, t *J* 8.8, 3-H_a); 3.05 (2H, ddd *J* 14.6, 10.9, 9.2, 3-H_b, 7-H_a); 3.13 (3H, s, 9-H_3); 3.15 (1H, m, 2-H); 3.28 (2H, m, 7-H_b, 11-H_a); 3.7 (1H, d *J* 13.3, 10-H_a); 3.75 (1H, d *J* 12.9, 11-H_b); 3.8 (1H, d *J* 13.3, 10-H_b); 3.97 (1H, s, 5-H); 7.01-8.05 (15H, m, ar-H); δ_C (DEPT, δ_H ^1H–^{13}C ^1J-COSY) 54.12 (CH_2, 2.65, 3.05, 3-C); 55.99 (CH_2, 3.28, 3.75, 11-C); 57.37 (CH_2, 3.7, 3.8, 10-C); 57.88 (CH_3, 3.13, 9-C); 61.07 (CH, 3.15, 2-C); 90.99 (CH, 3.97, 5-C); 127.01-129.9 (CH, 7.01-8.05, ar-C); 132.63 (CH_2, 3.28, 3.05, 7-C); 199.6 (C=O, 6-C); HRMS ES+ calcd for [$C_{26}H_{28}N_2O_2$]: 401.2224, found: 401.2224, error +0.00 ppm; R_f= 0.35 (petroleum ether: ethyl acetate, 2:1).

10.28 Preparation of (4-methoxymethyl-1,3-diphenyl-imidazolidin-2-yl)-phenyl-methanone 319, 320

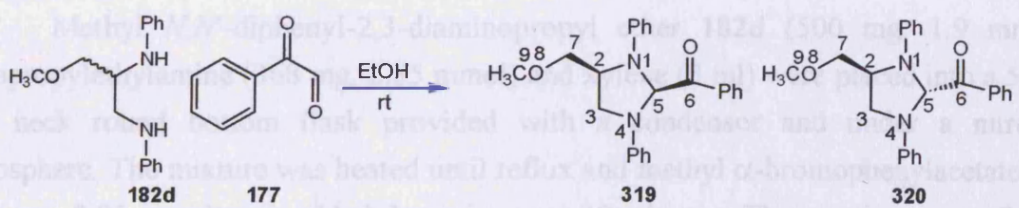

182d **177** **319** **320**

Methyl *N,N'*-diphenyl-2,3-diaminopropyl ether **182d** (500 mg, 1.95 mmol) was placed in a 25 ml round bottom flask with 9:1 ethanol, water mixture (10 ml). Phenylglyoxal **177** (274 mg, 2 mmol) was added and the mixture was stirred for 5 hours. The ethanol was removed and sodium hydroxide pellets (0.5 g) were added. The mixture was extracted with dichloromethane (3×10 ml), dried over anhydrous sodium sulphate and concentrated to give a **319**:**320**, a: b mixture (560 mg). Purification by column chromatography using a slow gradient of petroleum ether, diethyl ether, ethyl acetate gave one fraction containing a and b (65:35, 470 mg, 65%) as bright yellow gum. **Spectroscopic data for (4-methoxymethyl-1,3-diphenyl-imidazolidin-2-yl)-phenyl-methanone 319 and 320 (A is 319, B is 320):** ν_{max} (neat)/cm^{-1} 3053 (str., arC-H); 1597 (str. sh., C=O); 1501; 1265; δ_H ($CDCl_3$, 500 MHz) 2.92 (1H, t *J* 7.1, 7-$H_{a(A)}$); 3.08 (1H, t *J* 7.1, 7-$H_{a(B)}$); 3.2 (3H, s, 9-$H_{3(B)}$); 3.23 (3H, s, 9-$H_{3(A)}$); 3.41 (1H, dd *J* 9.3, 4.6, 7-$H_{b(B)}$); 3.6 (3H, m, 3-$H_{a(A)}$, 3-$H_{a(B)}$, 7-$H_{a(A)}$); 3.7 (1H, dd *J* 9.6, 1.5, 3-$H_{b(A)}$); 3.76 (1H, dd *J* 9.0, 7.8, 3-$H_{b(B)}$); 4.13 (1H, ddd *J* 12.3, 8.7, 4.3, 2-$H_{(B)}$); 4.42 (1H, pd *J* 4.6, 1.7, 2-$H_{(A)}$); 5.72 (1H, s, 5-$H_{(B)}$); 5.9 (1H, s, 5-$H_{(A)}$); 6.7-7.2 (10H, ar-$H_{(A)}$, ar-$H_{(B)}$); δ_C (DEPT, δ_H ^1H–^{13}C ^1J-COSY) 50.28 (CH_2, 3-$C_{(A)}$); 52.01 (CH_2,3-$C_{(B)}$); 56.31 (CH, 2-$C_{(A)}$); 59.18 (CH_3, 9-$C_{(A)}$, 9-$C_{(B)}$); 59.42 (CH, 2-$C_{(B)}$); 71.06 (CH_2, 7-$C_{(A)}$); 73.73 (CH_2, 7-$C_{(B)}$); 78.62 (CH, 5-$C_{(A)}$); 80.55 (CH, 5-$C_{(A)}$); 113.66-146.31 (CH, ar-$C_{(A)}$, ar-$C_{(B)}$); 199.65 (C=O, 6-$C_{(A)}$); 200.80 (C=O, 6-$C_{(B)}$); m/z (APCI) 373 (M+1, 100%), 265 (M-Bz, 18%); HRMS ES+ calcd for [$C_{24}H_{24}N_2O_2$]: 373.1911, found: 373.1911, error +0.00 ppm; ES+ calcd for [$C_{17}H_{21}N_2O$]: 265.1333, found: 265.1333, error +0.00 ppm; R_f= 0.32 (petroleum ether: diethyl ether, 3:1).

10.29 Preparation of 6-methoxymethyl-1,3,4-triphenylpiperazin-2-one 263, 264

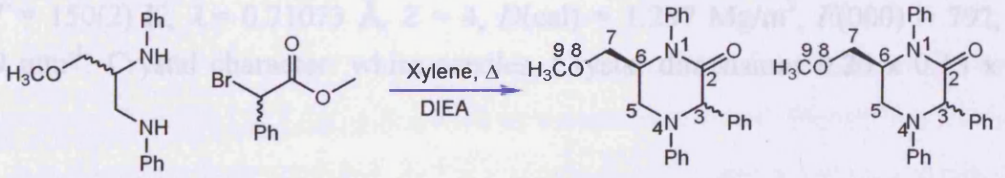

182d **253** **263** **264**

Methyl *N,N'*-diphenyl-2,3-diaminopropyl ether **182d** (500 mg, 1.9 mmol), diisopropylethylamine (368 mg, 2.85 mmol) and xylene (5 ml) were placed into a 50 ml two neck round bottom flask provided with a condensor and under a nitrogen atmosphere. The mixture was heated until reflux and methyl α-bromophenylacetate **253** (652 mg, 2.85 mmol) was added dropwise over 30 minutes. The reaction was refluxed

for 48 hours. The reaction was cooled to room temperature and sodium hydroxide (2 M) was added until pH 14, was washed with brine (10 ml) and dried over anhydrous sodium sulphate. Xylene was removed and the crude mixture was obtained (1.324 g). Purification by column chromatography using a slow gradient of petroleum ether, ethyl acetate, ethanol gave piperazinones **263** (231 mg, 34%) and **264** (199 mg, 29%) as needle crystals. **Spectroscopic data for 6-methoxymethyl-1,3,4-triphenylpiperazin-2-one 263:** ν_{max} (neat)/cm^{-1} 2929 (str., arC-H); 1652 (str. sh., C=O); 1505; δ_H ($CDCl_3$, 500 MHz) 3.28 (3H, s, 9-H_3); 3.4 (1H, dd *J* 8.8, 3.7, 7-H_a); 3.48 (1H, t *J* 9.3, 7-H_b); 3.9 (1H, dd *J* 13.7, 3.1, 5-H_a); 4.05 (1H, ddd *J* 9.5, 6.5, 3.2, 6-H); 4.32 (1H, dd *J* 13.7, 1.2, 5-H_b); 5.6 (1H, s, 3-H); 6.7-7.2-7.5 (15H, m, ar-H); δ_C (DEPT, δ_H ^{1}H–^{13}C ^{1}*J*-COSY) 46.35 (CH_2, 3.9, 4.32, 5-C); 58.79 (CH_3, 3.28, 9-C); 58.91 (CH, 4.05, 6-C); 67.81 (CH, 5.6, 3-C); 69.83 (CH_2, 3.4, 3.48, 7-C); 127.48-129.53(CH, 6.7-7.2-7.5, ar-C); 169.56 (C=O, 2-C); R_f= 0.28 (petroleum ether: diethyl ether, 3:1). **X-ray crystallography, crystal data for piperazinone 263:** $C_{24}H_{24}N_2O_2$, FW= 372.45, monoclinic, space group P 21/*n*, *a* = 8.8870(3) Å, *b* = 15.9610(6) Å, *c* = 13.6330(6) Å, β = 97.269(2)°, *U*= 1918.24(13) Å^3, *T* = 150(2) K, λ= 0.71073 Å, *Z* = 4, *D*(cal) = 1.290 Mg/m^3, *F*(000) = 792, μ = 0.082 mm^{-1}. Crystal character: white needle. Crystal dimensions 0.40 x 0.38 x 0.13 mm^3.

Spectroscopic data for 6-methoxymethyl-1,3,4-triphenylpiperazin-2-one 264: ν_{max} (neat)/cm^{-1} 2932 (str., arC-H); 1651 (str. sh., C=O); δ_H ($CDCl_3$, 500 MHz) 3.22 (3H, s, 9-H_3); 3.26 (1H, dd *J* 9.2, 3.5, 7-H_a); 3.54 (1H, dd *J* 9.2, 8.2, 7-H_b); 3.65 (1H, dd *J* 13.2, 4.1, 5-H_a); 3.93 (1H, dd *J* 13.2, 5.9, 5-H_b); 4.09 (1H, ddd *J* 9.5, 8.1, 4.0, 6-H); 5.25 (1H, s, 3-H); 6.7-7.2-7.5 (15H, m, ar-H); δ_C (DEPT, δ_H ^{1}H–^{13}C ^{1}*J*-COSY) 47.49 (CH_2, 3.65, 3.93, 5-C); 57.72 (CH, 4.09, 6-C); 59.08 (CH_3, 3.22, 9-C); 66.34 (CH, 5.25, 3-C); 70.85 (CH_2, 3.26, 3.54, 7-C); 127.43-140.25 (CH, 6.7-7.2-7.5, ar-C); 169.45 (C=O, 2-C); HRMS ES+ calcd for [$C_{24}H_{24}N_2O_2$]: 373.1911, found: 373.1911, error 0.00 ppm; R_f= 0.19 (petroleum ether: diethyl ether, 3:1). **X-ray crystallography, crystal data for piperazinone 264:** $C_{24}H_{24}N_2O_2$, FW= 372.45, monoclinic, space group P21/c, *a* = 10.3570(3) Å, *b* = 9.4610(3) Å, *c* = 20.4340(8) Å, β = 92.3750(10)°, *U* = 2000.56(12) Å^3, *T* = 150(2) K, λ = 0.71073 Å, *Z* = 4, *D*(cal) = 1.237 Mg/m^3, *F*(000) = 792, m = 0.079 mm^{-1}. Crystal character: white needles. Crystal dimensions 0.20 x 0.15 x 0.10 mm^3.

10.30 Equilibration of trans-6-methoxymethyl-1,3,4-triphenylpiperazin-2-one 263

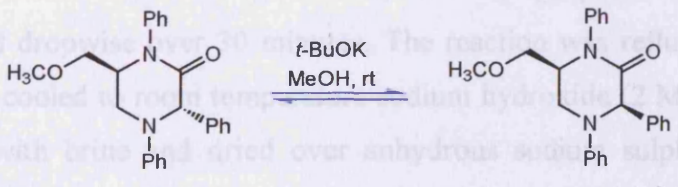

263 **264**

Pure crystals of piperazinone **263** (50 mg, 0.14 mmol) were placed in a 10 ml bottom flask in methanol (3 ml). The mixture was cooled to 0°C in an ice bath and potassium t-butoxide (27 mg, 0.28 mmol) was added slowly. After 48 h stirring at room temperature the mixture was neutralised with hydrochloric acid (1 M, 6 ml), extracted with diethyl ether (3×10 ml) and washed with brine (15 ml). The organic layer was dried over anhydrous sodium sulphate and concentrated (45 mg). The ^{1}H-NMR spectrum showed a mixture of piperazinones **263**:**264** in the ratio of 40:60.

10.30.1 Equilibration of cis-6-methoxymethyl-1,3,4-triphenylpiperazin-2-one 264

Pure crystals of piperazinone **264** (50 mg, 0.14 mmol) were placed in a 10 ml bottom flask in methanol (3 ml). The mixture was cooled to 0°C in an ice bath and potassium t-butoxide (27 mg, 0.28 mmol) was added slowly. After 48 h stirring at room temperature the mixture was neutralised with hydrochloric acid (1 M, 6 ml), extracted with diethyl ether (3×10 ml) and washed with brine (15 ml). The organic layer was dried over anhydrous sodium sulphate and concentrated (45 mg). The ^{1}H-NMR spectrum showed a mixture of piperazinones **264**:**263** in the ratio of 80:20.

10.31 Cyclisation of methyl *N,N'*-dibenzyl-2,3-diaminopropyl ether 182a with methyl 2-bromopropionate 252

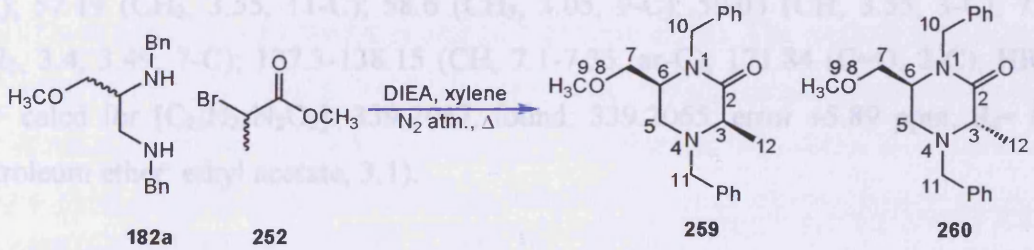

Methyl *N,N'*-dibenzyl-2,3-diaminopropyl ether **182a** (500 mg, 1.76 mmol), diisopropylethylamine (232 mg, 1.8 mmol) in xylene (5 ml) were placed in a 25 ml two neck round bottom flask provided with a condensor and under a nitrogen atmosphere. The mixture was heated until reflux and methyl 2–bromopropionate **252** (380 mg, 2.3 mmol) was added dropwise over 30 minutes. The reaction was refluxed for 24 hours. The reaction was cooled to room temperature sodium hydroxide (2 M) was added until pH 14, washed with brine and dried over anhydrous sodium sulphate. Xylene was removed and the crude mixture was obtained (545 mg). Purification by column

chromatography using a slow gradient of petroleum ether, ethyl acetate, ethanol gave piperazinone **259** (135-2, 163 mg, 30%) and piperazinone **260** (158-3, 140 mg, 25%) as red oils. **Spectroscopic data for 1,4-dibenzyl-6-methoxymethyl-3-methyl-piperazin-2-one 259:** ν_{max} (neat)/cm^{-1} 3053 (str., arC-H); 2984; 2929; 2813; 1652 (str. sh., C=O); 1265 (str. sh., lactam C-N); δ_H ($CDCl_3$) 1.5 (3H, d *J* 6.7, 12-H_3); 2.15 (1H, dd *J* 11.9, 3.3, 5-H_a); 2.7 (1H dd *J* 11.9, 2.3, 5-H_b); 3.05 (1H, d *J* 13.5, 11-H_b); 3.055 (1H, d *J* 6.6, 3-H); 3.09 (3H, s, 9-H_3); 3.15 (1H, m, 6-H); 3.43 (1H, dd *J* 4.8, 9.0, 7-H_a); 3.5 (1H, dd *J* 7.6, 8.9, 7-H_b); 3.9 (1H, d *J* 13.6, 11-H_b); 4.01 (1H, d *J* 14.9, 10-H_a); 5.12 (1H, d *J* 14.9, 10-H_b); 7.35 (10H, m, ar-H); δ_C (DEPT, δ_H ^1H–^{13}C ^1J-COSY) 16.06 (CH_3, 1.5, 12-C); 47.86 (CH_2, 2.15, 2.7, 5-C); 53.13 (CH, 3.15, 6-C); 57.54 (CH_2, 3.43, 3.5, 7-C); 57.78 (CH, 3.05, 3-C); 60.47 (CH_3, 3.05, 9-C); 71.74 (CH_2, 3.05, 3.9, 11-C); 125.89-142.51 (CH, 7.35, ar-C); 173.25 (C=O, 2-C); HRMS ES+ calcd for [$C_{21}H_{26}N_2O_2$]: 339.2067, found: 339.2064, error +8.84 ppm; R_f= 0.51 (petroleum ether: ethyl acetate, 3:1). **Spectroscopic data for 1,4-dibenzyl-6-methoxymethyl-3-methyl-piperazin-2-one 260:** ν_{max} (neat)/cm^{-1}3051 (str., arC-H); 1651 (str. sh., C=O); 1263 (str. sh., lactam C-N); δ_H ($CDCl_3$) 1.35 (3H, d *J* 6.9, 12-H_3); 2.55 (1H, dd *J* 12.2, 2.5, 5-H_a); 2.65 (1H, dd *J* 12.0, 2.1, 5-H_b); 3.05 (3H, s, 9-H_3); 3.15 (1H, m, 6-H); 3.4 (1H, dd *J* 9.0, 3.8, 7-H_a); 3.49 (1H, dd *J* 8.9, 7.9, 7-H_b); 3.55 (3H, m, 11-H_2, 3-H); 4.0 (1H, d *J* 15.0, 10-H_a); 5.2 (1H, d *J* 10-H_b); 7.1-7.35 (10H, m, ar-H); δ_C (DEPT, δ_H ^1H–^{13}C ^1J-COSY) 17.04 (CH_3, 1.35, 12-C); 44.49 (CH_2, 2.55, 2.65, 5-C); 47.72 (CH_2, 4.0, 5.2, 10-C); 54.94 (CH, 3.15, 6-C); 57.19 (CH_2, 3.55, 11-C); 58.6 (CH_3, 3.05, 9-C); 59.03 (CH, 3.55, 3-C); 71.93 (CH_2, 3.4, 3.49, 7-C); 127.3-138.15 (CH, 7.1-7.35, ar-C); 171.84 (C=O, 2-C); HRMS ES+ calcd for [$C_{21}H_{26}N_2O_2$]: 339.2067, found: 339.2065, error +5.89 ppm; R_f= 0.39 (petroleum ether: ethyl acetate, 3:1).

10.32 Equilibration of 1,4-dibenzyl-6-methoxymethyl-3-methyl-piperazin-2-one 259 and 1,4-dibenzyl-6-methoxymethyl-3-methyl-piperazin-2-one 260

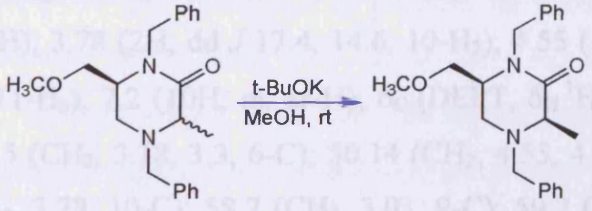

259, 260 **259**

A 50:50 mixture of piperazinones **259** and **260** (500 mg, 1.2 mmol) were placed in a 25 ml bottom flask in methanol-d_1 (5 ml). The mixture was cooled to 0°C in an ice bath and potassium *t*-butoxide (24 mg, 0.2 mmol) was added slowly. After 7 days stirring at room temperature the mixture was neutralised with hydrochloric acid (1 M, 6 ml) and extracted with dichloromethane (3× 10 ml). The organic layer was dried over anhydrous sodium sulphate and concentrated (472 mg). The ^{1}H-NMR spectrum showed a mixture of piperazinones **259**, **260** with ratio 69: 31.

10.33 Cyclisation of methyl *N,N'*-dibenzyl-2,3-diaminopropyl ether 182a with methylglyoxal 306

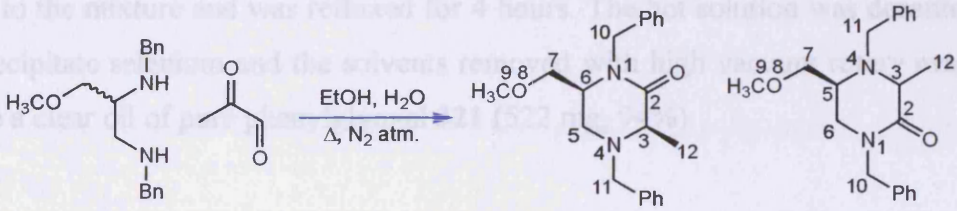

Methyl *N,N'*-dibenzyl-2,3-diaminopropyl ether **182a** (500 mg, 1.76 mmol) was placed in a 50 ml round bottom flask with a mixture of ethanol, water 9:1 (10 ml). Methylglyoxal **306** (139 mg, 1.93 mmol) was added dropwise with a pressure-equalised dropping funnel over 30 minutes. The reaction mixture refluxed for 110 hours. The ethanol was removed and NaOH pellets (0.5 g) were added. The mixture was extracted with ethyl acetate (3×20 ml), dried over anhydrous sodium sulphate and concentrated. The crude material was a black oil (589 mg). Purification by column chromatography using a slow gradient of petroleum ether, ethyl acetate and ethanol gave piperazinone **307** (138 mg, 25%) and piperazinone **259** (20 mg, 3%) as yellow oils. **Spectroscopic data for 1,4-dibenzyl-5-methoxymethyl-3-methyl-piperazin-2-one 307:** δ_H ($CDCl_3$) 1.3 (3H, d *J* 9.6, 12-H_3); 2.95 (1H, m, 5-H); 3.03 (3H, s, 9-H_3); 3.05 (1H, m, 7-H_a); 3.18 (1H, dd *J* 12.6, 6.8, 6-H_a); 3.25 (1H, dd *J* 9.3, 4.2, 7-H_b); 3.3 (1H, dd *J* 12.6, 4.2, 6-H_b); 3.35 (1H, d *J* 6.9, 3-H); 3.78 (2H, dd *J* 17.4, 14.6, 10-H_2); 4.55 (1H, d *J* 14.5, 11-H_a); 4.58 (1H, d *J* 14.5, 11-H_b); 7.2 (10H, m, ar-H); δ_C (DEPT, δ_H ^{1}H–^{13}C ^{1}*J*-COSY) 19.2 (CH_3, 1.3, 12-C); 46.5 (CH_2, 3.18, 3.3, 6-C); 50.14 (CH_2, 4.55, 4.58, 11-C); 56.7 (CH, 2.95, 5-C); 57.9 (CH_2, 3.78, 10-C); 58.7 (CH_3, 3.03, 9-C); 59.2 (CH, 3.35, 3-C); 72.7 (CH_2, 3.05, 3.25, 7-C); 125.64-139.24 (CH, 7.2, ar-C); 171.3 (C=O, 2-C); HRMS ES+

calcd for $[C_{21}H_{26}N_2O_2]$: 339.2067, found: 339.2067, error +0.00 ppm; R_f= 0.23 (petroleum ether:ethyl acetate, 3:1).

10.34 Preparation of ^{13}C-labelled phenylglyoxal 321

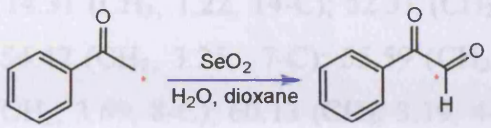

327 321

Selenium dioxide (0.4 g, 3.9 mmol) was placed in a 1:1 mixture of dioxane:water (3 ml). The solution was warmed to 50°C until the selenium dioxide was completely dissolved. ^{13}C-Labelled acetophenone **327** (0.5 g, 3.9 mmol) was slowly added to the mixture and was refluxed for 4 hours. The hot solution was decanted from the precipitate selenium and the solvents removed with high vacuum rotary evaporator to give a clear oil of pure phenylglyoxal **321** (522 mg, 94%).

10.35 Preparation of {Benzyl-[2-(ethoxycarbonylmethyl-amino)-1-methoxymethyl-ethyl]-amino}-acetic acid ethyl ester 245a

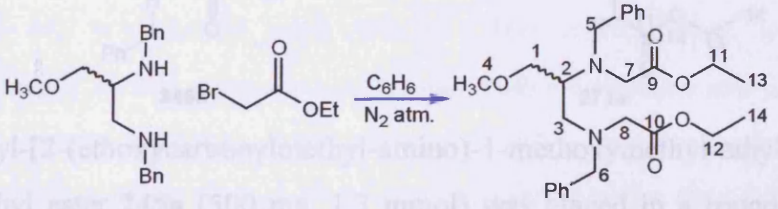

182a 88 245a

Ethyl bromoacetate **88** (3.25 g; 19.5 mmol) in benzene (7 ml) was placed in 25 ml bottom flask and kept at 0°C in an ice bath. Methyl *N,N'*-dibenzyl-2,3-diaminopropyl ether **182a** (1 g; 3.9 mmol) and diisopropylethylamine (1.512 g; 11.7 mmol) were added with a syringe. The mixture was stirred for 2 hours and sodium hydroxide (2 M) was added until pH 14. The mixture was extracted with dichloromethane (3×20 ml), dried over anhydrous sodium sulphate and concentrated to give the crude mixture (1.78 g). Purification by column chromatography using a slow gradient of petroleum ether, diethyl ether, ethyl acetate gave the diester **245a** as yellow oil (1.246 g, 85%). **Spectroscopic data for {Benzyl-[2-(ethoxycarbonylmethyl-amino)-1-methoxymethyl-ethyl]-amino}-acetic acid ethyl ester 245a**: ν_{max} (neat)/cm^{-1} 2925 (str., arC-H); 1744 (str. sh., C=O); 1639; 1453; 1167; δ_H ($CDCl_3$) 1.2 (3H, t *J* 7.1, 13-H_3); 1.22 (3H, t *J* 7.1, 14-H_3); 2.67 (1H, dd *J* 13.3, 7.7, 3-H_a); 2.83 (1H, dd *J* 13.3,

6.0, 3-H_b); 2.97 (1H, ddd *J* 10.7, 7.4, 4.9, 2-H); 3.19 (3H, s, 4-H_3); 3.25 (2H, s, 7-H_2); 3.33 (1H, d *J* 17.3, 5-H_a); 3.42 (1H, d *J* 17.3, 5-H_b); 3.47 (2H, d *J* 4.7, 1-H_2); 3.69 (2H, s, 8-H_2); 3.75 (1H, d *J* 13.9, 6-H_a); 3.82 (1H, d *J* 13.9, 6-H_b); 4.02 (2H, q *J* 7.2, 12-H_2); 4.05 (2H, q *J* 7.2, 11-H_2); 7.02-7.05 (10H, m, ar-H); δ_C (DEPT, δ_H ^{1}H–^{13}C ^{1}*J*-COSY) 14.25 (CH_3, 1.2, 13-C); 14.31 (CH_3, 1.22, 14-C); 52.31 (CH_2, 3.33, 3.42, 5-C); 53.50 (CH_2, 2.67, 2.83, 3-C); 54.42 (CH_2, 3.25, 7-C); 55.59 (CH_2, 3.75, 3.82, 6-C); 57.97 (CH, 2.97, 2-C); 58.77 (CH_2, 3.69, 8-C); 60.13 (CH_3, 3.19, 4-C); 72.54 (CH_2, 3.47, 1-C); 126.88-129.03 (CH, 7.02-7.05, ar-C); 139.15 (C, ar-C); 139.91 (C, ar-C); 171.67 (C=O, 9-C); 172.61 (C=O, 10-C); ***m/z*** (APCI) 457 (100%, M+1); HRMS ES+ calcd for [$C_{26}H_{36}N_2O_5$]: 457.2697, found: 457.2706, error –1.96 ppm; R_f= 0.23 (petroleum ether: ethyl acetate, 3:1).

10.36 Preparation of 5-methoxymethyl-(2-oxo-piperazin-1-yl)-acetic acid ethyl ester 271a

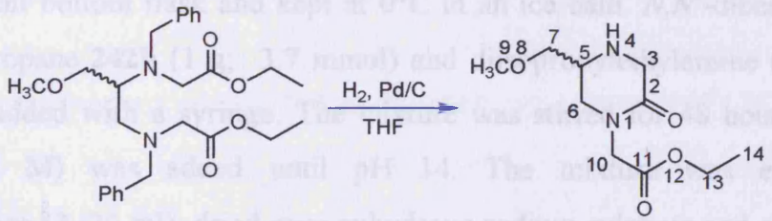

245a **271a**

{Benzyl-[2-(ethoxycarbonylmethyl-amino)-1-methoxymethyl-ethyl]-amino}-acetic acid ethyl ester **245a** (500 mg, 1.3 mmol) was placed in a round bottom flask with THF (20 ml) and 5% Pd/C (50 mg). The mixture was connected to an hydrogen line and it was stirred until the consumption of hydrogen ceased. The palladium was filtrated off and the sodium hydroxide (2 M) was added until pH 14. The mixture was extracted with dichloromethane (3× 15 ml), dried over anhydrous sodium sulphate and concentrated to give a clear oil (308 mg). Purification by column chromatography using a slow gradient of petroleum ether, diethyl ether, ethyl acetate gave the piperazinone **271a** as an amber oil (213 mg, 72%). **Spectroscopic data for 5-methoxymethyl-(2-oxo-piperazin-1-yl)-acetic acid ethyl ester 271a:** ν_{max} (neat)/cm^{-1} 3434 (str., NH); 2964 (str., arC-H); 1742 (str. sh., C=O ester); 1638 (str. sh., C=O lactam); 1204; 1098; δ_H ($CDCl_3$) 1.22 (3H, t *J* 7.1, 14-H_3); 2.26 (1H, bs, 4-H); 3.19 (1H, dd *J* 10.7, 3.3, 6-H_a); 3.25 (1H, dddd, 9.8, 5.2, 4.4, 3.3, 5-H); 3.29 (1H, m, 6-H_b); 3.3 (3H, s, 9-H_3); 3.37 (2H, t *J* 4.9, 7-H_2); 3.5 (1H, d *J* 17.5, 3-H_a); 3.59 (1H, d *J* 17.5, 3-H_b); 4.05 (2H, d *J* 10.6, 10-H_2); 4.2 (2H, q *J* 7.1, 13-H_2); δ_C (DEPT, δ_H ^{1}H–^{13}C ^{1}*J*-COSY) 14.17 (CH_3, 1.22, 14-C);

48.15 (CH_2, 4.05, 10-C); 49.05 (CH_2, 3.5, 3.59, 3-C); 50.82 (CH_2, 3.19, 3.29, 6-C); 52.13 (CH, 3.25, 5-C); 59.30 (CH_3, 3.3, 9-C); 61.40 (CH_2, 4.2, 13-C); 73.08 (CH_2, 3.37, 7-C); *m/z* (APCI) 457 (M+1); HRMS ES+ calcd for [$C_{10}H_{18}N_2O_4$]: 231.1339, found: 231.1340, error +4.3 ppm; R_f= 0.15 (petroleum ether: ethyl acetate, 3:1).

10.37 Preparation of {Benzyl-[2-(benzyl-ethoxycarbonylmethyl-amino)-1,1-dimethyl-ethyl]-amino}-acetic acid ethyl ester 245b

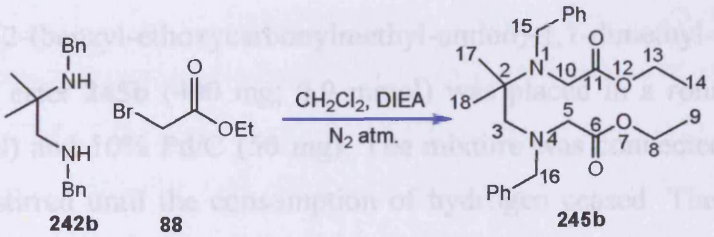

242b **88** **245b**

Ethyl bromoacetate **88** (1.87 g; 11.2 mmol) in dichloromethane (10 ml) was placed in 25 ml bottom flask and kept at 0°C in an ice bath. *N,N'*-dibenzyl-2-methyl-1,2-diaminopropane **242b** (1 g; 3.7 mmol) and diisopropylethylamine (1.488 g; 11.2 mmol) were added with a syringe. The mixture was stirred for 48 hours and sodium hydroxide (2 M) was added until pH 14. The mixture was extracted with dichloromethane (3×20 ml), dried over anhydrous sodium sulphate and concentrated to give the crude mixture (2.476 g). Purification by column chromatography using a slow gradient of petroleum ether, diethyl ether, ethyl acetate gave the diester **245b** as major product (1.15 g, 43%). **Spectroscopic data for {Benzyl-[2-(benzyl-ethoxycarbonylmethyl-amino)-1,1-dimethyl-ethyl]-amino}-acetic acid ethyl ester 245b**: ν_{max} (neat)/cm^{-1} 2249; 1729 (str. sh., C=O ester); 1453; 1378; δ_H ($CDCl_3$, 400 MHz) 1.1 (12H, m, 9-H_3, 14-H_3, 17-H_3, 18-H_3); 2.72 (2H, s, 3-H_2); 3.25 (2H, s, 10-H_2); 3.43 (2H, s, 5-H_2); 3.81 (2H, s, 15-H_2); 3.91 (2H, s, 16-H_2), 9.93 (2H, q *J* 7.1, 8-H_2); 4.05 (2H, q *J* 7.1, 13-H_2); 7.2 (10H, m, ar-H); δ_C (DEPT, δ_H ^1H-^{13}C ^1J-COSY) 14.52 (CH_3, 9-C); 14.7 (CH_3, 14-C); 24.00 (CH_3, 17-C, 18-C); 51.39 (CH_2, 10-C); 53.75 (CH_2, 15-C); 55.23 (CH_2, 5-C); 60.00 (CH_2, 16-C); 60.36 (C, 2-C); 60.40 (CH_2, 13-C); 60.60 (CH_2, 8-C); 62.17 (CH_2, 3-C); 127.04-141.17 (CH, ar-C); 172.58 (C=O, 6-C); 173.76 (C=O, 11-C); *m/z* (APCI) 441 (41%, M+1); 355 (26%, M- $CH_3CH_2OCOCH_2$-); 248 (100%); 130 (30%); HRMS ES+ calcd for [$C_{26}H_{36}N_2O_4$]: 441.2748, found: 441.2749, error –2.26 ppm; R_f= 0.45 (ethyl acetate: ethanol, 3: 1).

10.38 Preparation of (5,5-dimethyl-2-oxo-piperazin-1-yl)-acetic acid ethyl ester 271b

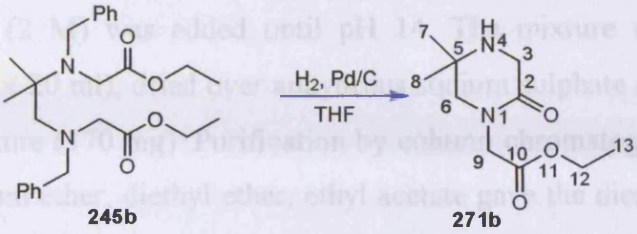

{Benzyl-[2-(benzyl-ethoxycarbonylmethyl-amino)-1,1-dimethyl-ethyl]-amino}-acetic acid ethyl ester **245b** (400 mg; 0.9 mmol) was placed in a round bottom flask with THF (20 ml) and 10% Pd/C (50 mg). The mixture was connected to a hydrogen line and it was stirred until the consumption of hydrogen ceased. The palladium was filtrated off and the sodium hydroxide (2 M) was added until pH 14. The mixture was extracted with dichloromethane (3× 15 ml), dried over anhydrous sodium sulphate and concentrated to give a clear oil of (5,5-dimethyl-2-oxo-piperazin-1-yl)-acetic acid ethyl ester **271b** as pure product (165 mg, 85 %). **Spectroscopic data for (5,5-dimethyl-2-oxo-piperazin-1-yl)-acetic acid ethyl ester 271b**: ν_{max} (neat)/cm^{-1} 3435 (str., NH); 2978 (str., arC-H); 1743 (str. sh., C=O ester); 1644 (str. sh., C=O lactam); 1204; δ_H ($CDCl_3$, 500 MHz) 1.1 (9H, m, 7-H_3, 8-H_3, 13-H_3); 3.15 (2H, s, 6-H_2); 3.52 (2H, s, 3-H_2); 4.08 (2H, s, 9-H_2); 4.15 (2H, q *J* 7.1, 12-H_2); δ_C (DEPT, δ_H ^{1}H-^{13}C ^{1}*J*-COSY) 14.18 (CH_3, 1.1, 13-C); 25.43 (CH_3, 1.1, 7-C, 8-C); 45.58 (CH_2, 3.52, 3-C); 48.31 (CH_2, 4.08, 9-C); 48.94 (C, 5-C); 59.59 (CH_2, 3.15, 6-C); 61.36 (CH_2, 4.15, 12-C); 167.90 (C=O, 2-C); 168.85 (C=O, 10-C); *m/z* (APCI) 215 (100%, M+1); 169 (16%, M- CH_3CH_2O-); 151 (33%); 139 (19%, M-CH_3CH_2OCO-); HRMS ES+ calcd for [$C_{10}H_{18}N_2O_3$]: 215.1390, found: 215.1388, error –9.29 ppm; R_f=0.25 (petroleum ether: diethyl ether, 3: 1).

10.39 Preparation of {Benzyl-[2-(benzyl-ethoxycarbonylmethyl-amino)-1-phenyl-ethyl]-amino}-acetic acid ethyl ester 245d

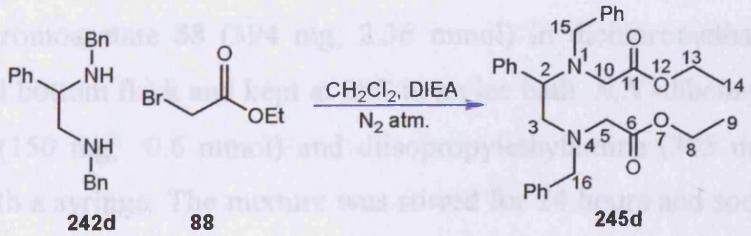

Ethyl bromoacetate **88** (295 mg; 1.77 mmol) in dichloromethane (2 ml) was placed in 10 ml bottom flask and kept at 0°C in an ice bath. N,N′-dibenzyl-1,2-diaminoethylenebenzene **242d** (140 mg; 0.44 mmol) and diisopropylethylamine (342 mg; 2.64 mmol) were added with a syringe. The mixture was stirred for 48 hours and sodium hydroxide (2 M) was added until pH 14. The mixture was extracted with dichloromethane (3× 20 ml), dried over anhydrous sodium sulphate and concentrated to give the crude mixture (170 mg). Purification by column chromatography using a slow gradient of petroleum ether, diethyl ether, ethyl acetate gave the diester **245d** as a clear oil (75 mg, 35 %). **Spectroscopic data for {Benzyl-[2-(benzyl-ethoxycarbonylmethyl-amino)-1-phenyl-ethyl]-amino}-acetic acid ethyl ester 245d**: ν_{max} (neat)/cm^{-1} 2253; 1731 (str. sh., C=O ester); 1455; 1387; δ_H ($CDCl_3$, 400 MHz) 1.15 (6H, m, 9-H_3, 14-H_3); 2.6 (1H, dd *J* 13.3, 6.9, 3-H_a); 3.05 (1H, d *J* 18.3, 15-H_a); 3.22 (1H, t *J* 6.8, 3-H_b); 3.25 (2H, d *J* 3.3, 16-H_2); 3.4 (1H, d *J* 18.2, 15-H_b); 3.52 (1H, d *J* 13.7, 10-H_a); 3.63 (1H, d *J* 13.3, 5-H_a); 3.72 (1H, d *J* 13.5, 5-H_b); 3.75 (1H, d *J* 13.3, 10-H_b); 4.02 (4H, m, 8-H_2, 13-H_2); 4.1 (1H, t *J* 6.7, 2-H); 7.1 (15H, m, ar-H); δ_C (DEPT, δ_H ^{1}H-^{13}C ^{1}*J*-COSY) 14.24 (CH_3, 1.15, 14-C); 14.31 (CH_3, 1.15, 9-C); 51.08 (CH_2, 3.05, 3.4, 15-C); 53.58 (CH_2, 3.25, 16-C); 54.95 (CH_2, 3.52, 3.75, 10-C); 56.49 (CH_2, 2.6, 3.22, 3-C); 58.59 (CH_2, 3.63, 3.72, 5-C); 60.06 (CH_2, 4.02, 13-C); 60.15 (CH_2, 4.02, 8-C); 62.49 (CH, 4.1, 2-C); 126.93-140.45 (CH, 7.1, ar-C); 171.58 (C=O, 6-C); 172.00 (C=O, 11-C); *m/z* (APCI) 489 (M+1); HRMS ES+ calcd for [$C_{30}H_{36}N_2O_4$]: 489.2748, found: 489.2747, error –2.04 ppm; R_f=0.22 (petroleum ether: diethyl ether, 3: 1).

10.40 Preparation of {Benzyl-[2-(benzyl-ethoxycarbonylmethyl-amino)-1-methyl-ethyl]-amino}-acetic acid ethyl ester 245c

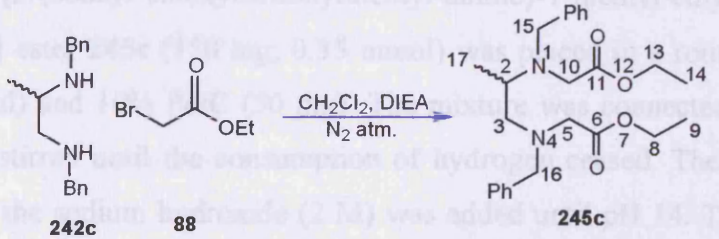

242c **88** **245c**

Ethyl bromoacetate **88** (394 mg; 2.36 mmol) in dichloromethane (2 ml) was placed in 10 ml bottom flask and kept at 0°C in an ice bath. *N,N′*-dibenzyl-propane-1,2-diamine **242c** (150 mg; 0.6 mmol) and diisopropylethylamine (305 mg; 2.36 mmol) were added with a syringe. The mixture was stirred for 24 hours and sodium hydroxide

(2 M) was added until pH 14. The mixture was extracted with dichloromethane (3×20 ml), dried over anhydrous sodium sulphate and concentrated to give the crude mixture (170 mg) containing the diester at 95%. Purification by column chromatography using a slow gradient of petroleum ether, diethyl ether, ethyl acetate gave the diester **245c** as a clear oil (167 mg, 65%). **Spectroscopic data of {Benzyl-[2-(benzyl-ethoxycarbonylmethyl-amino)-1-methyl-ethyl]-amino}-acetic acid ethyl ester 245c:** ν_{max} (neat)/cm^{-1} 3053 (str., arC-H); 1737 (str., C=O); δ_H ($CDCl_3$, 500 MHz) 0.9 (3H, d *J* 17-H_3); 1.2 (6H, m, 14-H_3, 9-H_3); 2.4 (1H, dd *J* 13.1, 7.2, 3-H_a); 2.8 (1H, dd *J* 13.1, 6.5, 3-H_b); 2.9 (1H, dt *J* 19.8, 6.6, 2-H); 3.2 (1H, d *J* 16.9, 15-H_a); 3.25 (1H, d *J* 16.9, 15-H_b); 3.3 (2H, d *J* 3.5, 10-H_2); 3.57 (2H, d *J* 3.5, 16-H_a); 3.6 (2H, s, 5-H_2); 3.75 (1H, d *J* 13.8, 16-H_b); 4.0 (4H, m, 13-H_2, 8-H_2); 7.1 (10H, m, ar-H); δ_C (DEPT, δ_H ^{1}H–^{13}C ^{1}*J*-COSY) 13.8 (CH_3, 0.9, 17-C); 14.22 (CH_3, 1.2, 14-C); 14.32 (CH_3, 1.2, 9-C); 51.49 (CH_2, 3.2, 3.25, 15-C); 53.52 (CH, 2.9, 2-C); 54.30 (CH_2, 3.3, 10-C); 54.47 (CH_2, 3.57, 3.75, 16-C); 57.38 (CH_2, 2.4, 2.8, 3-C); 58.66 (CH_2, 3.64, 5-C); 60.07 (CH_2, 4.0, 8-C); 60.31 (CH_2, 4.0, 13-C); 128.16-128.98 (CH, 7.1, ar-C); 167.35 (C=O, 6-C); 167.95 (C=O, 11-C); *m/z* (APCI) 427 (M+1); HRMS ES+ calcd for [$C_{25}H_{34}N_2O_4$]: 427.2591, found: 427.2591, error 0.00 ppm; R_f= 0.22 (petroleum ether: diethyl ether, 3:1).

10.41 Preparation of (5-methyl-2-oxo-piperazin-1-yl)-acetic acid ethyl ester 271c

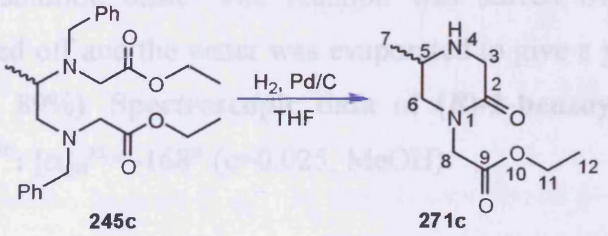

245c **271c**

{Benzyl-[2-(benzyl-ethoxycarbonylmethyl-amino)-1-methyl-ethyl]-amino}-acetic acid ethyl ester **245c** (150 mg; 0.35 mmol) was placed in a round bottom flask with THF (20 ml) and 10% Pd/C (50 mg). The mixture was connected to a hydrogen line and it was stirred until the consumption of hydrogen ceased. The palladium was filtrated off and the sodium hydroxide (2 M) was added until pH 14. The mixture was extracted with dichloromethane (3× 15 ml), dried over anhydrous sodium sulphate and concentrated to give a clear oil of (5-methyl-2-oxo-piperazin-1-yl)-acetic acid ethyl ester **271c** (42 mg, 60%). **Spectroscopic data for (5,5-dimethyl-2-oxo-piperazin-1-yl)-acetic acid ethyl ester 271c**: ν_{max} (neat)/cm^{-1} 3443 (str., NH); 2920 (str., arC-H);

1739 (str. sh., C=O ester); 1642 (str. sh., C=O lactam); δ_H ($CDCl_3$, 500 MHz) 0.8 (3H, d *J* 1.0, 7-H_3); 1.02 (3H, td *J* 7.1, 2.0, 12-H_3); 1.5 (1H, br. s, 4-H); 2.65 (1H, dd *J* 9.4, 3.2, 6-H_a); 2.72 (1H, ddd *J* 9.5, 6.1, 3.4, 5-H); 2.78 (1H, m, 6-H_b); 3.4 (1H, d *J* 17.1, 3-H_a); 3.55 (1H, d *J* 17.1, 3-H_b); 4.0 (2H, m, 8-H_2, 11-H_2); δ_C (DEPT, δ_H ^{1}H-^{13}C ^{1}*J*-COSY) 13.90 (CH_3, 0.8, 7-C); 18.53 (CH_3, 1.02, 12-C); 47.90 (CH_2, 4.0, 11-C); 48.14 (CH_2, 2.72, 5-C); 49.93 (CH_2, 3.4, 3.55, 3-C); 55.23 (CH_2, 2.65, 2.78, 6-C); 60.70 (CH_2, 4.0, 8-C); 167.57 (C=O, 2-C); 168.88 (C=O, 9-C); *m/z* (APCI) 201.1 (85%, M+1); 155.1 (100%, M-CH_3CH_2O-); 127.1 (M-CH_3CH_2OCO-); HRMS ES+ calcd for [$C_9H_{16}N_2O_3$]: 201.1234, found: 201.1235, error –4.59 ppm; R_f= 0.14 (petroleum ether: diethyl ether, 3: 1).

10.42 Preparation of (*R*)-2-benzoylamino-3-hydroxy-propionic acid 364[175]

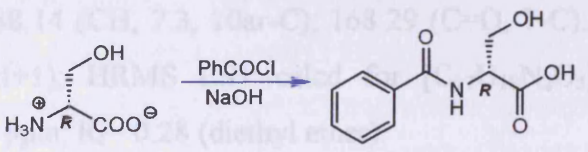

D-Serine **363** (30 g, 0.28 mol) was dissolved in sodium hydroxide (2M, 140 ml). The mixture was cooled to 0° C in an ice bath and benzoyl chloride (43.96 g, 0.31 mol) was added dropwise over 20 minutes with simultaneous addition of sodium hydroxide drops to keep the solution basic. The reaction was stirred overnight. The white precipitate was filtered off and the water was evaporated to give a yellow precipitate of pure product (52 g, 89%). **Spectroscopic data of (*R*)-2-benzoylamino-3-hydroxy-propionic acid 364[176]:** $[\alpha]_D^{25}$= -168° (c=0.025, MeOH).

10.43 Preparation of (*R*)-*N*-(1-benzylcarbamoyl-2-hydroxy-ethyl)-benzamide 365

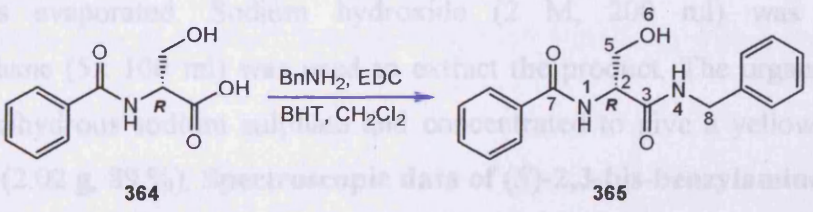

(*R*)-2-Benzoylamino-3-hydroxy-propionic acid **364** (30 g, 0.14 mol), benzylamine (17.97 g, 0.17 mol), triethylamine (16 g, 0.16 mol) and 1-

hydroxybenzotriazole (21.2 g, 0.16 mol) were placed in two neck round bottom flask with dichloromethane (1 L). The mixture was cooled to 0° C and EDC (30.15 g, 0.16 mol) was added over 30 minutes. The reaction mixture was stirred for 24 hours and the white precipitate was filtered off. The filtrate was washed with sodium hydroxide (3× 500 ml), water (3× 500 ml), hydrochloric acid (3× 500 ml) and water (3× 500 ml). The organic layer was dried over anhydrous sodium sulphate and concentrated. The product was obtained pure as yellow solid (32.54 g, 76 %). **Spectroscopic data of (*R*)-*N*-(1-benzylcarbamoyl-2-hydroxy-ethyl)-benzamide 365**[177,170]**:** m. p. 146° C; $[\alpha]_D^{25}$= -73° (c=0.12, MeOH); ν_{max} (neat)/cm^{-1} 3417 (str., br., OH, NH); 1645 (str., C=O amide); δ_H ($CDCl_3$, 500 MHz) 3.68 (1H, dd *J* 11.5, 5.0, 5-H_a); 4.18 (1H, dd *J* 11.5, 3.0, 5-H_b); 4.36 (2H, dd *J* 5.5, 4.1, 8-H_2); 4.62 (1H, m, 2-H); 7.3 (10H, m, ar-H); δ_C (DEPT, δ_H ^{1}H–^{13}C ^{1}*J*-COSY) 43.90 (CH_2, 4.36, 8-C); 54.08 (CH, 4.62, 2-C); 62.79 (CH_2, 3.68, 4.18, 5-C); 126.96-138.14 (CH, 7.3, 10ar-C); 168.29 (C=O, 7-C); 171.06 (C=O, 3-C); *m/z* (APCI) 299 (M+1); HRMS ES+ calcd for [$C_{17}H_{18}N_2O_3$]: 299.1390, found: 299.1393, error -1.00 ppm; R_f= 0.28 (diethyl ether).

10.44 Preparation of (*S*)-2,3-bis-benzylamino-propan-1-ol 382

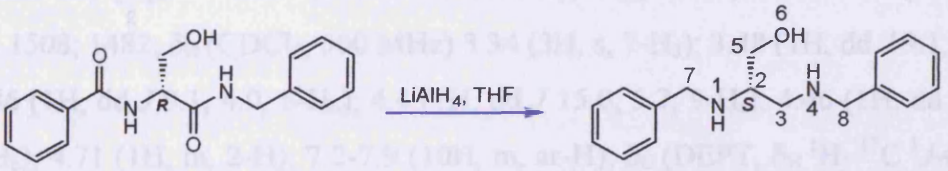

365 **382**

Lithium aluminium hydride (5 g, 134 mmol) was placed in THF (120 ml) at 0° C. The mixture refluxed and (*R*)-2-benzoylamino-3-hydroxy-propionic acid **365** (5 g, 16.7 mmol) in THF (60 ml) was added slowly over 2 hours. The reaction mixture was refluxed for 48 hours. Ethanol (60 ml) was added to quence the lithium in excess and the solvents evaporated. Sodium hydroxide (2 M, 200 ml) was added and dichloromethane (5× 100 ml) was used to extract the product. The organic layer was dried over anhydrous sodium sulphate and concentrated to give a yellow oil of pure product **382** (2.02 g, 89 %). **Spectroscopic data of (*S*)-2,3-bis-benzylamino-propan-1-ol 382**: ν_{max} (neat)/cm^{-1} 3301 (str., br., OH, NH); 3027 (str., arC-H); δ_H ($CDCl_3$, 500 MHz) 2.68 (1H, m, 2-H); 2.71 (2H, m, 3-H_2); 3.52 (1H, dd *J* 10.8, 3.2, 5-H_a); 3.62 (1H, m, 5-H_b); 3.65 (3H, m, 7-H_a, 8-H_2); 3.73 (1H, d *J* 1.6, 7-H_b); 7.2 (10H, m, ar-H); δ_C

(DEPT, δ_H ^{1}H–^{13}C ^1J-COSY) 51.47 (CH_2, 3.65, 3.73, 7-C); 51.78 (CH_2, 2.71, 3-C); 54.02 (CH_2, 3.65, 8-C); 56.70 (CH, 2.68, 2-H); 64.16 (CH_2, 3.52, 5-C); 126.99-140.38 (CH, 7.2, 10ar-C); *m/z* (APCI) 271 (M+1); 132; HRMS ES+ calcd for [$C_{17}H_{22}N_2O$]: 271.1805, found: 271.1805, error 0.00 ppm; R_f= 0.25 (diethyl ether: ethyl acetate, 2:1).

10.45 Preparation of (*R*)-*N*-(1-benzylcarbamoyl-2-methoxy-ethyl)-benzamide 366

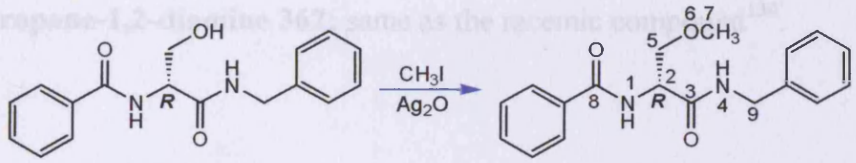

365 **366**

(*R*)-*N*-(1-Benzylcarbamoyl-2-hydroxy-ethyl)-benzamide **365** (1.0 g, 3.35 mmol) with acetonitrile (10 ml) and silver (I) oxide (3.88 g, 16.8 mmol) was placed in a round bottom flask. Methyl iodide (8.3 g, 66 mmol) was added dropwise over 2 hours. The reaction mixture was stirred for 3 days. The silver iodide was filtrated and the mixture was concentrated to give the pure product as yellow powder (1.00 g, 99%). **Spectroscopic data of (*R*)-*N*-(1-benzylcarbamoyl-2-methoxy-ethyl)-benzamide 366:** m. p. 124° C; $[\alpha]_D^{25}$= -116° (c=0.0075, MeOH); ν_{max} (neat)/cm^{-1} 1654 (str., C=O amide); 1508; 1482; δ_H ($CDCl_3$, 500 MHz) 3.34 (3H, s, 7-H_3); 3.48 (1H, dd *J* 9.1, 7.5, 5-H_a); 3.86 (1H, dd *J* 9.1, 4.0, 5-H_b); 4.4 (1H, dd *J* 15.0, 5.7, 9-H_a); 4.46 (1H, dd *J* 15.0, 6.0, 9-H_b), 4.71 (1H, m, 2-H); 7.2-7.9 (10H, m, ar-H); δ_C (DEPT, δ_H ^{1}H–^{13}C ^1J-COSY) 43.61 (CH_2, 4.4, 4.46, 9-C); 52.69 (CH, 4.71, 2-C); 59.19 (CH_3, 3.34, 7-C); 71.77 (CH_2, 3.48, 3.86, 5-C); 127.16 (CH, 7.2-7.9, 10ar-C); 167.32 (C=O, 8-C); 170.08 (C=O, 3-C); HRMS ES+ calcd for [$C_{18}H_{20}N_2O_3$]: 313.1547, found: 313.1544, error -1.26 ppm; R_f= 0.5 (diethyl ether).

10.46 LAH reduction of (*R*)-*N*-(1-benzylcarbamoyl-2-methoxy-ethyl)-benzamide 362

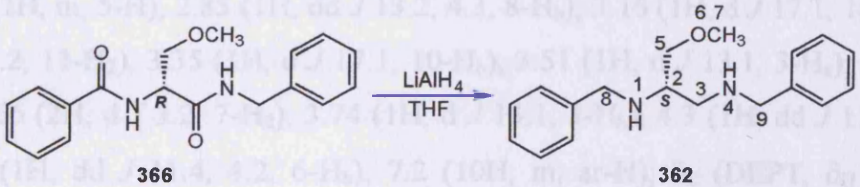

366 **362**

Lithium aluminium hydride (970 mg, 25 mmol) was placed in THF (50 ml) at 0° C. The mixture refluxed and (*R*)-*N*-(1-benzylcarbamoyl-2-methoxy-ethyl)-benzamide **366** (1 g, 3.2 mmol) in THF (10 ml) was added slowly over 2 hours. The reaction mixture was refluxed for 48 hours. Ethanol (20 ml) was added to quence the lithium in excess and the solvents evaporated. Sodium hydroxide (2 M, 200 ml) was added and dichloromethane (5× 100 ml) was used to extract the product. The organic layer was dried over anhydrous sodium sulphate and concentrated to give a yellow oil of pure product **362** (610 mg, 67 %). **Spectroscopic data for *N,N'*-dibenzyl-3-methoxypropane-1,2-diamine 362:** same as the racemic compound[130].

10.47 Cyclisation of (*S*)-2,3-bis-benzylamino-propan-1-ol 382 with methyl bromoacetate

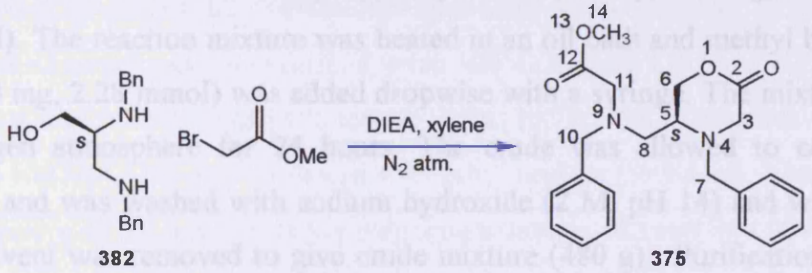

382 375

(*S*)-2,3-Bis-benzylamino-propan-1-ol **382** (500 mg, 1.76 mmol) was placed in two round flask with diisopropylethylamine (1.5 eq., 425 mg, 2.7 mmol) and xylene (5 ml). The reaction mixture was heated in an oil bath and methyl bromoacetate (1.5 eq., 425 mg, 2.7 mmol) was added dropwise with a syringe. The mixture refluxed under nitrogen atmosphere for 24 hours. The crude was allowed to cool to room temperature and was washed with sodium hydroxide (2 M, pH 14) and with brine (10 ml). The solvent was removed to give crude mixture (530 mg). Purification by column chromatography using a slow gradient of petroleum ether, diethyl ether, ethyl acetate gave the piperazinone **375** (56 mg; 10 %). **Spectroscopic data of [Benzyl-(4-benzyl-6-oxo-morpholin-3ylmethyl)-amino]-acetic acid methyl ester 375:** ν_{max} (neat)/cm^{-1} 1741 (str., C=O ester); 1365; 1187; δ_H ($CDCl_3$, 500 MHz) 2.64 (1H, dd *J* 13.2, 9.2, 8-H_a), 2.77 (1H, m, 5-H), 2.85 (1H, dd *J* 13.2, 4.3, 8-H_b), 3.16 (1H, d *J* 17.1, 10-H_a), 3.24 (2H, d *J* 1.2, 11-H_2), 3.35 (1H, d *J* 17.1, 10-H_b), 3.51 (1H, d *J* 13.1, 3-H_a), 3.6 (3H, s, 14-H_3), 3.66 (2H, d *J* 3.2, 7-H_2), 3.74 (1H, d *J* 13.1, 3-H_b), 4.3 (1H, dd *J* 11.4, 5.6, 6-H_a), 4.36 (1H, dd *J* 11.4, 4.2, 6-H_b), 7.2 (10H, m, ar-H); δ_C (DEPT, δ_H ^{1}H–^{13}C ^{1}*J*-

COSY) 50.98 (CH_2, 3.16, 3.35, 10-C), 51.02 (CH_3, 3.6, 14-C), 51.43 (CH_2, 2.64, 2.85, 8-C), 54.40 (CH_2, 2.77, 5-C), 54.43 (CH_2, 3.24, 11-C), 58.96 (CH_2, 3.66, 7-C), 59.02 (CH_2, 3.51, 3.74, 3-C), 69.38 (CH_2, 4.3, 4.36, 6-C), 127.40- 138.37 (CH, 7.2, ar-C), 169.59 (C=O, 2-C), 171.56 (C=O, 12-C); R_f= 0.56 (diethyl ether).

10.48 Preparation of (*S*)-1,4-dibenzyl-6-methoxymethyl-piperazin-2-one 367

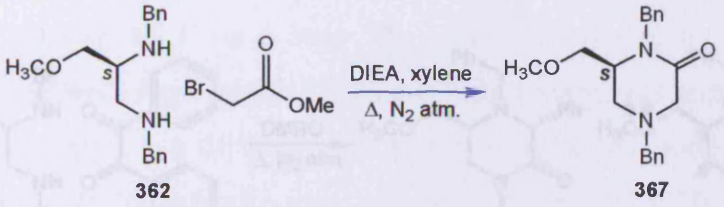

362 **367**

Methyl *N,N'*-dibenzyl-2,3-diaminopropyl ether **362** (500 mg, 1.76 mmol) was placed in two round flask with diisopropylethylamine (1.3 eq., 279 mg, 2.3 mmol) and xylene (5 ml). The reaction mixture was heated in an oil bath and methyl bromoacetate (1.3 eq., 350 mg, 2.28 mmol) was added dropwise with a syringe. The mixture refluxed under nitrogen atmosphere for 24 hours. The crude was allowed to cool to room temperature and was washed with sodium hydroxide (2 M, pH 14) and with brine (10 ml). The solvent was removed to give crude mixture (480 g). Purification by column chromatography using a slow gradient of petroleum ether, diethyl ether, ethyl acetate gave the piperazinone **367** (440 mg; 80 %). **Spectroscopic data for 6-methoxymethyl-1,4-bis-(4-methoxy-phenyl)-piperazin-2-one 367:** same NMR data as racemic product[130].

10.49 Preparation of (*S*)-1-benzyl-6-methoxymethyl-4-methyl-piperazin-2-one 369

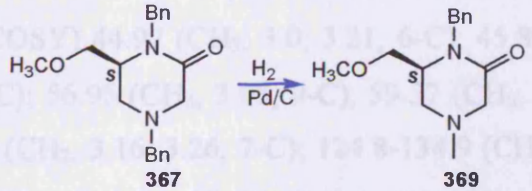

367 **369**

6-Methoxymethyl-1,4-bis-(4-methoxy-phenyl)-piperazin-2-one **367** (130 mg; 0.39 mmol) was placed in a round bottom flask with MeOH (5 ml) and 10% Pd/C (150 mg). The mixture was connected to a hydrogen line and it was stirred until the consumption of hydrogen ceased. The palladium was filtrated off and the sodium hydroxide (2 M) was added until pH 14. The mixture was extracted with

dichloromethane (3×15 ml), dried over anhydrous sodium sulphate and concentrated to give a clear oil of (*S*)-1-benzyl-6-methoxymethyl-4-methyl-piperazin-2-one **369** (70 mg, 71%). **Spectroscopic data for (*S*)-1-benzyl-6-methoxymethyl-4-methyl-piperazin-2-one 369:** same NMR data as racemic product[130].

10.50 Cyclisation of methyl *N,N'*-dibenzyl-2,3-diaminopropyl ether 182a with benzil 139

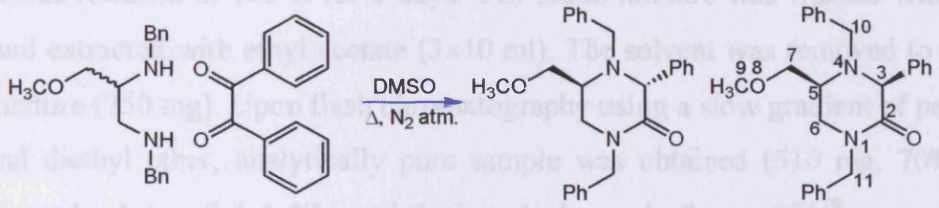

182a **139** **312** **350**

Methyl *N,N'*-dibenzyl-2,3-diaminopropyl ether **182a** (150 mg, 0.53 mmol) was placed in DMSO (4 ml) and was warmed up to 100°C. Benzil **139** (333 mg, 1.58 mmol) was added and the mixture was refluxed at 165°C for 3 days. The crude mixture was washed with NaOH (2 M) and extracted with ethyl acetate (3×10 ml). The solvent was removed to give a 50:50 mixture of the two piperazinones **312** and **350** (450 mg). Upon flash chromatography using a slow gradient of petroleum ether and diethyl ether, analytical pure sample were obtained (25 mg, 11%, **312**; 63 mg, 30%, **350**). The spectroscopic data of piperazinone **312** are described in section 10.25. **Spectroscopic data of 1,4-dibenzyl-5-methoxymethyl-3-phenyl-piperazin-2-one 350**: ν_{max} (neat)/cm^{-1} 3048; 1655 (str. sh., C=O); 1245 (str. sh., lactam C-N); δ_H ($CDCl_3$) 3.05 (3H, s, 9-H_3); 3.1 (1H, m, 5-H); 3.22 (1H, dd, *J* 7.9, 4.9, 6-H_a); 3.23 (1H, m, 7-H_a); 3.41 (1H, dd, *J* 7.9, 2.7, 6-H_b); 3.54 (1H, d *J* 13.6, 11-H_a); 3.6 (1H, d *J* 13.6, 11-H_b); 4.35 (1H, s, 3-H); 4.41 (1H, d *J* 14.3, 10-H_a); 4.6 (1H, d *J* 14.6, 10-H_b); 7.2-7.5 (15H, m, ar-H); δ_C (DEPT, δ_H ^1H–^{13}C ^1J-COSY) 44.97 (CH_2, 3.0, 3.21, 6-C); 45.89 (CH_2, 4.52, 4.58, 10-C); 55.66 (CH, 3.0, 5-C); 56.95 (CH_3, 3.05, 9-C); 59.57 (CH_2, 3.7, 3.83, 11-C); 65.95 (CH, 4.35, 3-C); 71.79 (CH_2, 3.16, 3.26, 7-C); 124.8-134.9 (CH, 7.2-7.5, ar-C); 190.92 (C=O, 2-C); HRMS ES+ calcd for [$C_{26}H_{28}N_2O_2$]: 401.2224, found: 401.2224, error +0.00 ppm; R_f= 0.21 (petroleum ether: ethyl acetate, 2:1).

10.51 Cyclisation of *N,N'*-dibenzyl ethylenediamine 72d with benzil 139

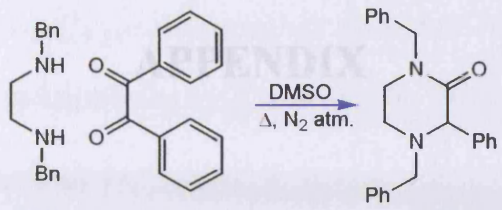

72d 351

N,N'-dibenzyl ethylenediamine **72d** (500 mg, 2.05 mmol) was placed in DMSO (8 ml) and was warmed up to 100°C. Benzil (517 mg, 2.5 mmol) was added and the mixture was refluxed at 165°C for 3 days. The crude mixture was washed with NaOH (2 M) and extracted with ethyl acetate (3×10 ml). The solvent was removed to give the crude mixture (750 mg). Upon flash chromatography using a slow gradient of petroleum ether and diethyl ether, analytically pure sample was obtained (510 mg, 70%, **351**). **Spectroscopic data of 1,4-dibenzyl-3-phenyl-piperazin-2-one 351[70]:** same data as literature.

APPENDIX

X-Ray Crystallographic data for *N*-[2-(benzoylamino)phenyl]benzamide diamide 225

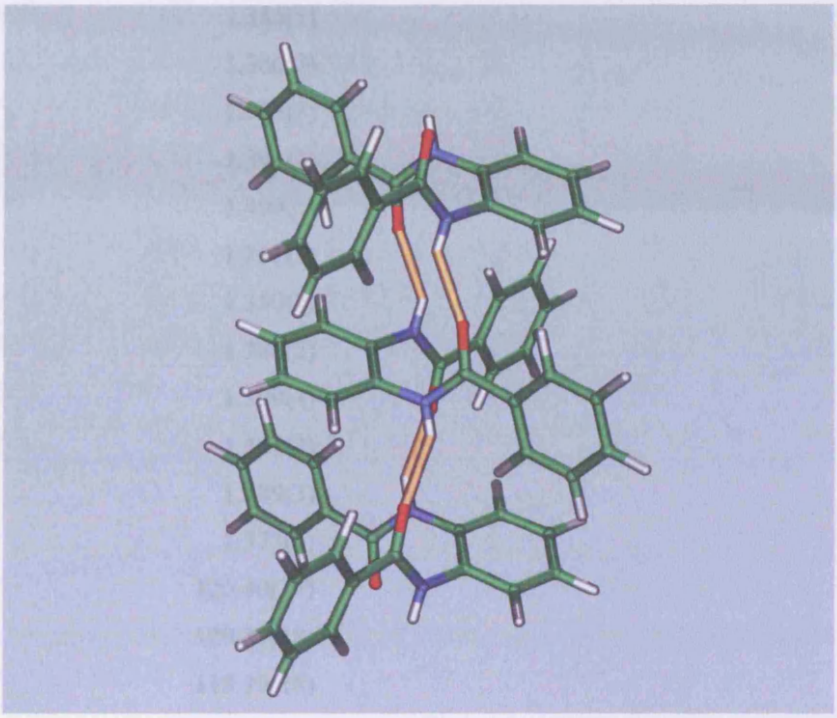

Table 1. Atomic coordinates (x 10^4) and equivalent isotropic displacement parameters ($Å^2$x 10^3) for **225**. U(eq) is defined as one third of the trace of the orthogonalized U^{ij} tensor.

	x	y	z	U(eq)
c(1)	3093(1)	7219(2)	7668(2)	23(1)
c(2)	2683(1)	6076(2)	7134(2)	27(1)
c(3)	2808(1)	5597(2)	5785(2)	29(1)
c(4)	3345(1)	6271(2)	4971(2)	27(1)
c(5)	3751(1)	7430(2)	5497(2)	22(1)
c(6)	3626(1)	7914(2)	6851(2)	18(1)
c(7)	4026(1)	9181(2)	7491(2)	18(1)
c(8)	4693(1)	11445(2)	7051(2)	19(1)
c(9)	4407(1)	12758(2)	6582(2)	24(1)
c(10)	4710(1)	14066(2)	7032(2)	30(1)
n(1)	4351(1)	10127(2)	6603(1)	19(1)
o(1)	4031(1)	9352(1)	8764(1)	27(1)

Table 2. Bond lengths [Å] and angles [°] for **225**.

c(1)-c(2)	1.381(3)
c(1)-c(6)	1.391(3)
c(2)-c(3)	1.385(3)
c(3)-c(4)	1.386(3)
c(4)-c(5)	1.385(3)
c(5)-c(6)	1.391(3)
c(6)-c(7)	1.499(2)
c(7)-o(1)	1.231(2)
c(7)-n(1)	1.350(2)
c(8)-c(9)	1.386(2)
c(8)-c(8)#1	1.399(4)
c(8)-n(1)	1.424(2)
c(9)-c(10)	1.389(3)
c(10)-c(10)#1	1.373(4)
c(2)-c(1)-c(6)	120.40(17)
c(1)-c(2)-c(3)	120.13(18)
c(2)-c(3)-c(4)	119.79(18)
c(5)-c(4)-c(3)	120.20(17)
c(4)-c(5)-c(6)	120.14(17)
c(5)-c(6)-c(1)	119.32(16)
c(5)-c(6)-c(7)	123.65(16)
c(1)-c(6)-c(7)	117.01(15)
o(1)-c(7)-n(1)	122.69(16)
o(1)-c(7)-c(6)	120.62(15)
n(1)-c(7)-c(6)	116.66(15)
c(9)-c(8)-c(8)#1	119.44(11)
c(9)-c(8)-n(1)	118.91(16)
c(8)#1-c(8)-n(1)	121.65(9)

Symmetry transformations used to generate equivalent atoms:

#1 -x+1,y,-z+3/2

Table 3. Anisotropic displacement parameters ($Å^2 x\ 10^3$)for **225**. The anisotropic displacement factor exponent takes the form: $-2\pi^2[\ h^2 a^{*2} U^{11} + ... + 2\ h\ k\ a^*\ b^*\ U^{12}\ ]$

U^{11}	U^{22}	U^{33}	U^{23}	U^{13}	U^{12}

c(1)	27(1)	25(1)	17(1)	-1(1)	2(1)	1(1)
c(2)	26(1)	29(1)	26(1)	6(1)	0(1)	-8(1)
c(3)	31(1)	26(1)	29(1)	-2(1)	-7(1)	-7(1)
c(4)	33(1)	28(1)	20(1)	-3(1)	0(1)	-2(1)
c(5)	24(1)	24(1)	19(1)	1(1)	1(1)	-2(1)
c(6)	18(1)	17(1)	18(1)	2(1)	-1(1)	3(1)
c(7)	19(1)	20(1)	16(1)	0(1)	-1(1)	4(1)
c(8)	22(1)	20(1)	15(1)	0(1)	2(1)	-2(1)
c(9)	25(1)	24(1)	24(1)	3(1)	-3(1)	2(1)
c(10)	35(1)	20(1)	36(1)	3(1)	-2(1)	5(1)
n(1)	25(1)	20(1)	13(1)	-1(1)	0(1)	-2(1)
o(1)	39(1)	28(1)	15(1)	0(1)	1(1)	-7(1)

Table 4. Hydrogen coordinates (x 10^4) and isotropic displacement parameters ($Å^2$x 10^3) for **225**.

	x	y	z	U(eq)
h(1)	3010	7534	8598	28
h(2)	2314	5617	7693	33
h(3)	2527	4809	5419	34
h(4)	3435	5937	4049	32
h(5)	4115	7895	4933	27
h(9)	4000	12763	5948	29
h(10)	4518	14961	6691	36
h(1a)	4352	9919	5707	23

X-Ray Crystallographic data for *N,N'*-1,4-diphenyl-6-methoxymethyl-piperazin-2-one 246d

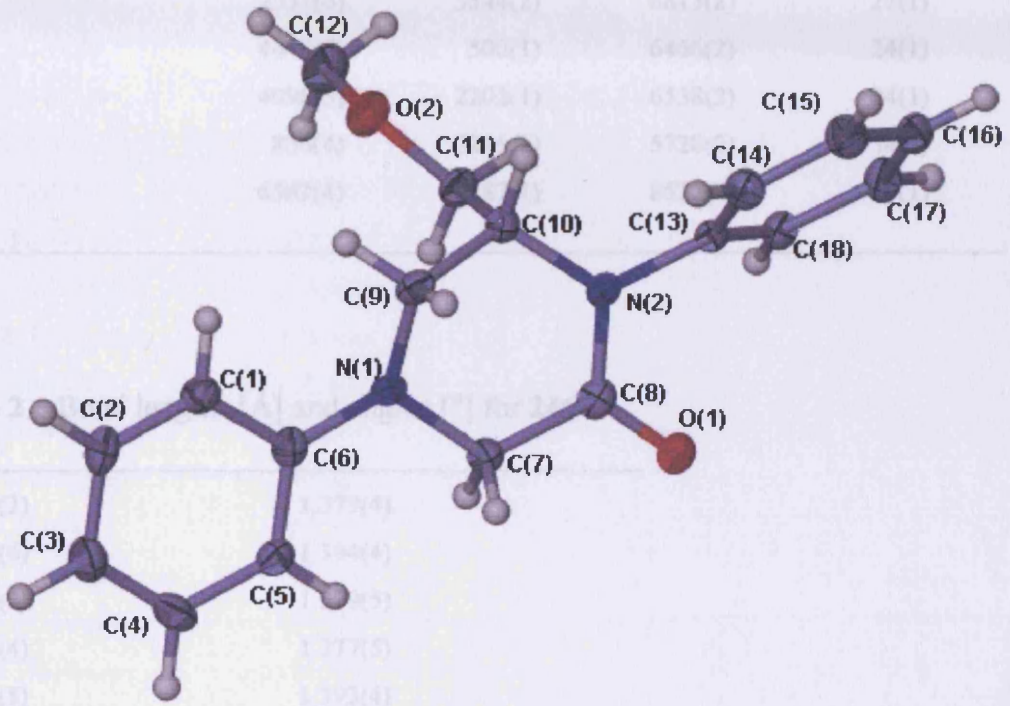

Table 1. Atomic coordinates (x 10^4) and equivalent isotropic displacement parameters ($Å^2$x 10^3) for **246d**. U(eq) is defined as one third of the trace of the orthogonalized U^{ij} tensor.

	x	y	z	U(eq)
C(1)	6724(6)	-724(2)	6523(2)	27(1)
C(2)	6949(7)	-1532(2)	6374(2)	34(1)
C(3)	5227(7)	-1969(2)	5971(2)	34(1)
C(4)	3261(7)	-1577(2)	5714(2)	32(1)
C(5)	3020(6)	-760(2)	5857(2)	28(1)
C(6)	4742(6)	-318(2)	6272(2)	25(1)
C(7)	2601(6)	909(2)	5997(2)	27(1)
C(8)	2420(6)	1808(2)	6087(2)	26(1)
C(9)	6451(5)	991(2)	6650(2)	25(1)
C(10)	5787(6)	1763(2)	7078(2)	27(1)
C(11)	4818(6)	1626(2)	7980(2)	29(1)

C(12)	5876(7)	1187(2)	9406(2)	45(1)
C(13)	4234(6)	3065(2)	6505(2)	24(1)
C(14)	6130(6)	3407(2)	6153(2)	29(1)
C(15)	6339(6)	4231(2)	6110(2)	34(1)
C(16)	4601(6)	4704(2)	6406(2)	31(1)
C(17)	2706(6)	4370(2)	6753(2)	32(1)
C(18)	2531(6)	3544(2)	6813(2)	27(1)
N(1)	4449(5)	500(1)	6466(2)	24(1)
N(2)	4098(5)	2202(1)	6538(2)	24(1)
O(1)	800(4)	2146(1)	5728(2)	34(1)
O(2)	6582(4)	1287(1)	8525(2)	35(1)

Table 2. Bond lengths [Å] and angles [°] for **246d**.

C(1)-C(2)	1.379(4)
C(1)-C(6)	1.394(4)
C(2)-C(3)	1.379(5)
C(3)-C(4)	1.377(5)
C(4)-C(5)	1.393(4)
C(5)-C(6)	1.391(4)
C(6)-N(1)	1.413(3)
C(7)-N(1)	1.455(4)
C(7)-C(8)	1.514(4)
C(8)-O(1)	1.223(4)
C(8)-N(2)	1.358(4)
C(9)-N(1)	1.457(4)
C(9)-C(10)	1.507(4)
C(10)-N(2)	1.468(4)
C(10)-C(11)	1.529(4)
C(11)-O(2)	1.427(4)
C(12)-O(2)	1.434(4)
C(13)-C(18)	1.380(4)
C(13)-C(14)	1.381(4)
C(13)-N(2)	1.447(4)
C(14)-C(15)	1.386(4)
C(15)-C(16)	1.384(4)
C(16)-C(17)	1.372(4)

C(17)-C(18)	1.390(4)

C(2)-C(1)-C(6)	121.1(4)
C(1)-C(2)-C(3)	121.3(4)
C(4)-C(3)-C(2)	118.3(3)
C(3)-C(4)-C(5)	120.8(4)
C(6)-C(5)-C(4)	121.1(3)
C(5)-C(6)-C(1)	117.3(3)
C(5)-C(6)-N(1)	121.2(3)
C(1)-C(6)-N(1)	121.4(3)
N(1)-C(7)-C(8)	118.5(3)
O(1)-C(8)-N(2)	123.2(3)
O(1)-C(8)-C(7)	118.4(3)
N(2)-C(8)-C(7)	118.4(3)
N(1)-C(9)-C(10)	110.3(3)
N(2)-C(10)-C(9)	111.5(3)
N(2)-C(10)-C(11)	108.4(3)
C(9)-C(10)-C(11)	111.9(2)
O(2)-C(11)-C(10)	107.4(3)
C(18)-C(13)-C(14)	120.1(3)
C(18)-C(13)-N(2)	121.7(3)
C(14)-C(13)-N(2)	118.3(3)
C(13)-C(14)-C(15)	120.3(3)
C(16)-C(15)-C(14)	119.1(3)
C(17)-C(16)-C(15)	121.0(3)
C(16)-C(17)-C(18)	119.7(3)
C(13)-C(18)-C(17)	119.9(3)
C(6)-N(1)-C(7)	116.6(3)
C(6)-N(1)-C(9)	118.8(3)
C(7)-N(1)-C(9)	114.8(2)
C(8)-N(2)-C(13)	120.5(3)
C(8)-N(2)-C(10)	120.7(3)
C(13)-N(2)-C(10)	118.8(3)
C(11)-O(2)-C(12)	111.4(3)

Symmetry transformations used to generate equivalent atoms:

Table 3. Anisotropic displacement parameters ($Å^2 x\ 10^3$) for **246d**. The anisotropic displacement factor exponent takes the form: $-2p^2[\ h^2a^{*2}U^{11} + ... + 2\ h\ k\ a^*\ b^*\ U^{12}\ ]$

	U^{11}	U^{22}	U^{33}	U^{23}	U^{13}	U^{12}
C(1)	27(3)	30(2)	24(2)	-1(2)	1(2)	3(2)
C(2)	34(3)	30(2)	36(3)	7(2)	1(2)	10(2)
C(3)	42(3)	26(2)	32(3)	0(2)	3(2)	3(2)
C(4)	47(3)	26(2)	24(2)	-4(2)	3(2)	-9(2)
C(5)	32(3)	29(2)	23(2)	2(2)	-4(2)	2(2)
C(6)	32(3)	25(2)	18(2)	2(2)	5(2)	4(2)
C(7)	25(2)	24(2)	31(2)	-1(2)	-5(2)	1(2)
C(8)	23(2)	31(2)	25(2)	3(2)	4(2)	2(2)
C(9)	25(2)	30(2)	21(2)	-1(2)	-2(2)	2(2)
C(10)	27(2)	22(2)	31(2)	3(2)	-5(2)	0(2)
C(11)	37(3)	29(2)	21(2)	1(2)	-2(2)	4(2)
C(12)	70(3)	45(2)	21(3)	5(2)	-2(2)	5(2)
C(13)	31(2)	21(2)	20(2)	0(2)	-5(2)	0(2)
C(14)	32(3)	29(2)	27(2)	-1(2)	2(2)	3(2)
C(15)	36(3)	32(2)	33(3)	0(2)	3(2)	-1(2)
C(16)	48(3)	26(2)	20(2)	3(2)	-3(2)	1(2)
C(17)	43(3)	28(2)	24(2)	-1(2)	3(2)	10(2)
C(18)	29(2)	26(2)	26(2)	3(2)	-2(2)	1(2)
N(1)	26(2)	24(2)	21(2)	-1(1)	-6(2)	1(1)
N(2)	23(2)	23(2)	25(2)	2(1)	-5(2)	1(1)
O(1)	34(2)	29(1)	38(2)	1(1)	-9(1)	5(1)
O(2)	48(2)	38(1)	20(2)	1(1)	-1(1)	9(1)

Table 4. Hydrogen coordinates ($x\ 10^4$) and isotropic displacement parameters ($Å^2 x\ 10^3$) for **246d**.

	x	y	z	U(eq)
H(1)	7939	-438	6802	32
H(2)	8319	-1793	6552	40
H(3)	5392	-2526	5873	40

H(4)	2055	-1868	5435	38
H(5)	1657	-500	5669	34
H(7A)	1159	675	6190	32
H(7B)	2717	785	5367	32
H(9A)	7217	1106	6097	30
H(9B)	7528	696	7041	30
H(10)	7174	2104	7151	32
H(11A)	4304	2138	8230	35
H(11B)	3506	1257	7935	35
H(12A)	5563	1711	9662	68
H(12B)	7084	921	9754	68
H(12C)	4498	859	9407	68
H(14)	7297	3075	5940	35
H(15)	7657	4467	5881	41
H(16)	4722	5269	6369	38
H(17)	1521	4702	6950	38
H(18)	1241	3309	7066	33

X-Ray Crystallographic data for 6-methoxymethyl-1,3,4-triphenylpiperazin-2-one 263

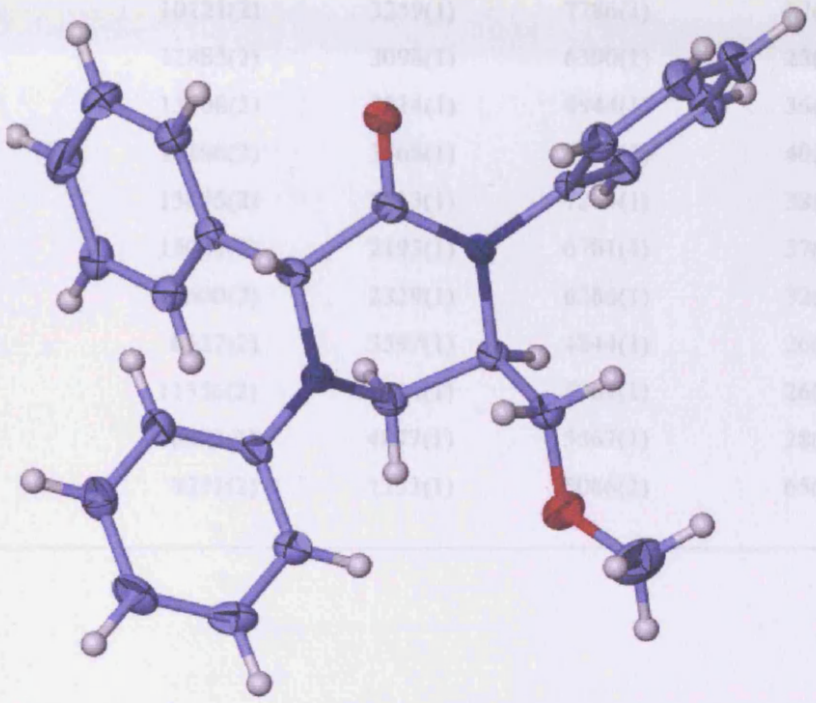

Table 1. Atomic coordinates (x 10^4) and equivalent isotropic displacement parameters ($Å^2$x 10^3) for **263**. U(eq) is defined as one third of the trace of the orthogonalized U^{ij} tensor.

	x	y	z	U(eq)
C(1)	9307(2)	2805(1)	4684(1)	30(1)
C(2)	9142(2)	4186(1)	5494(1)	24(1)
C(3)	10611(2)	3986(1)	6187(1)	24(1)
C(4)	11000(2)	2935(1)	4927(1)	31(1)
C(5)	8690(2)	2105(1)	5281(2)	39(1)
C(6)	8482(3)	761(2)	4559(2)	62(1)
C(7)	7131(2)	3787(1)	4229(1)	27(1)
C(8)	7103(2)	3801(1)	3209(1)	33(1)
C(9)	5755(3)	3979(1)	2611(2)	44(1)
C(10)	4462(2)	4154(1)	3030(2)	50(1)
C(11)	4495(2)	4147(1)	4049(2)	45(1)

C(12)	5824(2)	3956(1)	4651(2)	34(1)
C(13)	10193(2)	3992(1)	7242(1)	24(1)
C(14)	9809(2)	4747(1)	7662(1)	32(1)
C(15)	9307(2)	4758(1)	8586(1)	39(1)
C(16)	9211(2)	4023(1)	9108(1)	38(1)
C(17)	9628(2)	3275(1)	8715(1)	33(1)
C(18)	10121(2)	3259(1)	7786(1)	27(1)
C(19)	12885(2)	3098(1)	6390(1)	25(1)
C(20)	13708(2)	3714(1)	6944(1)	36(1)
C(21)	15196(2)	3568(1)	7366(2)	40(1)
C(22)	15895(2)	2813(1)	7244(1)	38(1)
C(23)	15085(2)	2193(1)	6701(1)	37(1)
C(24)	13600(2)	2329(1)	6286(1)	32(1)
N(1)	8527(2)	3597(1)	4844(1)	26(1)
N(2)	11356(2)	3204(1)	5961(1)	26(1)
O(1)	8574(1)	4877(1)	5567(1)	28(1)
O(2)	9391(2)	1333(1)	5086(2)	65(1)

Table 2. Bond lengths [Å] and angles [°] for **263**.

C(1)-N(1)	1.470(2)
C(1)-C(4)	1.513(2)
C(1)-C(5)	1.526(3)
C(1)-H(1)	1.0000
C(2)-O(1)	1.2210(19)
C(2)-N(1)	1.359(2)
C(2)-C(3)	1.544(2)
C(3)-N(2)	1.463(2)
C(3)-C(13)	1.531(2)
C(3)-H(3)	1.0000
C(4)-N(2)	1.469(2)
C(4)-H(4A)	0.9900
C(4)-H(4B)	0.9900
C(5)-O(2)	1.422(2)
C(5)-H(5A)	0.9900
C(5)-H(5B)	0.9900
C(6)-O(2)	1.361(3)

C(6)-H(6A)	0.9800
C(6)-H(6B)	0.9800
C(6)-H(6C)	0.9800
C(7)-C(12)	1.386(3)
C(7)-C(8)	1.388(2)
C(7)-N(1)	1.439(2)
C(8)-C(9)	1.390(3)
C(8)-H(8)	0.9500
C(9)-C(10)	1.375(3)
C(9)-H(9)	0.9500
C(10)-C(11)	1.386(3)
C(10)-H(10)	0.9500
C(11)-C(12)	1.384(3)
C(11)-H(11)	0.9500
C(12)-H(12)	0.9500
C(13)-C(18)	1.390(2)
C(13)-C(14)	1.395(2)
C(14)-C(15)	1.388(3)
C(14)-H(14)	0.9500
C(15)-C(16)	1.380(3)
C(15)-H(15)	0.9500
C(16)-C(17)	1.379(3)
C(16)-H(16)	0.9500
C(17)-C(18)	1.392(3)
C(17)-H(17)	0.9500
C(18)-H(18)	0.9500
C(19)-C(20)	1.391(2)
C(19)-C(24)	1.397(2)
C(19)-N(2)	1.419(2)
C(20)-C(21)	1.392(3)
C(20)-H(20)	0.9500
C(21)-C(22)	1.376(3)
C(21)-H(21)	0.9500
C(22)-C(23)	1.383(3)
C(22)-H(22)	0.9500
C(23)-C(24)	1.385(3)
C(23)-H(23)	0.9500
C(24)-H(24)	0.9500
N(1)-C(1)-C(4)	108.93(14)
N(1)-C(1)-C(5)	110.03(14)

C(4)-C(1)-C(5)	113.44(15)
N(1)-C(1)-H(1)	108.1
C(4)-C(1)-H(1)	108.1
C(5)-C(1)-H(1)	108.1
O(1)-C(2)-N(1)	122.80(15)
O(1)-C(2)-C(3)	117.62(14)
N(1)-C(2)-C(3)	119.58(14)
N(2)-C(3)-C(13)	111.91(13)
N(2)-C(3)-C(2)	114.76(13)
C(13)-C(3)-C(2)	106.61(13)
N(2)-C(3)-H(3)	107.8
C(13)-C(3)-H(3)	107.8
C(2)-C(3)-H(3)	107.8
N(2)-C(4)-C(1)	109.74(14)
N(2)-C(4)-H(4A)	109.7
C(1)-C(4)-H(4A)	109.7
N(2)-C(4)-H(4B)	109.7
C(1)-C(4)-H(4B)	109.7
H(4A)-C(4)-H(4B)	108.2
O(2)-C(5)-C(1)	109.87(17)
O(2)-C(5)-H(5A)	109.7
C(1)-C(5)-H(5A)	109.7
O(2)-C(5)-H(5B)	109.7
C(1)-C(5)-H(5B)	109.7
H(5A)-C(5)-H(5B)	108.2
O(2)-C(6)-H(6A)	109.5
O(2)-C(6)-H(6B)	109.5
H(6A)-C(6)-H(6B)	109.5
O(2)-C(6)-H(6C)	109.5
H(6A)-C(6)-H(6C)	109.5
H(6B)-C(6)-H(6C)	109.5
C(12)-C(7)-C(8)	120.28(16)
C(12)-C(7)-N(1)	120.28(16)
C(8)-C(7)-N(1)	119.44(15)
C(7)-C(8)-C(9)	119.64(19)
C(7)-C(8)-H(8)	120.2
C(9)-C(8)-H(8)	120.2
C(10)-C(9)-C(8)	120.1(2)
C(10)-C(9)-H(9)	119.9
C(8)-C(9)-H(9)	119.9

C(9)-C(10)-C(11)	120.11(18)
C(9)-C(10)-H(10)	119.9
C(11)-C(10)-H(10)	119.9
C(12)-C(11)-C(10)	120.3(2)
C(12)-C(11)-H(11)	119.9
C(10)-C(11)-H(11)	119.9
C(11)-C(12)-C(7)	119.55(19)
C(11)-C(12)-H(12)	120.2
C(7)-C(12)-H(12)	120.2
C(18)-C(13)-C(14)	118.54(15)
C(18)-C(13)-C(3)	121.89(14)
C(14)-C(13)-C(3)	119.51(14)
C(15)-C(14)-C(13)	120.41(16)
C(15)-C(14)-H(14)	119.8
C(13)-C(14)-H(14)	119.8
C(16)-C(15)-C(14)	120.33(17)
C(16)-C(15)-H(15)	119.8
C(14)-C(15)-H(15)	119.8
C(17)-C(16)-C(15)	119.94(17)
C(17)-C(16)-H(16)	120.0
C(15)-C(16)-H(16)	120.0
C(16)-C(17)-C(18)	119.96(16)
C(16)-C(17)-H(17)	120.0
C(18)-C(17)-H(17)	120.0
C(13)-C(18)-C(17)	120.76(15)
C(13)-C(18)-H(18)	119.6
C(17)-C(18)-H(18)	119.6
C(20)-C(19)-C(24)	117.52(16)
C(20)-C(19)-N(2)	123.30(15)
C(24)-C(19)-N(2)	119.14(15)
C(19)-C(20)-C(21)	120.80(17)
C(19)-C(20)-H(20)	119.6
C(21)-C(20)-H(20)	119.6
C(22)-C(21)-C(20)	121.08(18)
C(22)-C(21)-H(21)	119.5
C(20)-C(21)-H(21)	119.5
C(21)-C(22)-C(23)	118.69(17)
C(21)-C(22)-H(22)	120.7
C(23)-C(22)-H(22)	120.7
C(22)-C(23)-C(24)	120.65(18)

C(22)-C(23)-H(23)	119.7
C(24)-C(23)-H(23)	119.7
C(23)-C(24)-C(19)	121.24(17)
C(23)-C(24)-H(24)	119.4
C(19)-C(24)-H(24)	119.4
C(2)-N(1)-C(7)	118.65(13)
C(2)-N(1)-C(1)	122.25(13)
C(7)-N(1)-C(1)	118.86(13)
C(19)-N(2)-C(3)	116.79(13)
C(19)-N(2)-C(4)	115.99(13)
C(3)-N(2)-C(4)	113.74(13)
C(6)-O(2)-C(5)	115.74(17)

Symmetry transformations used to generate equivalent atoms:

Table 3. Anisotropic displacement parameters ($Å^2 x\ 10^3$)for **263**. The anisotropic displacement factor exponent takes the form: $-2p^2[\ h^2a^{*2}U^{11} + ... + 2\ h\ k\ a^*\ b^*\ U^{12}\ ]$

	U^{11}	U^{22}	U^{33}	U^{23}	U^{13}	U^{12}
C(1)	28(1)	33(1)	28(1)	-11(1)	-3(1)	7(1)
C(2)	24(1)	28(1)	20(1)	0(1)	4(1)	1(1)
C(3)	22(1)	27(1)	23(1)	-3(1)	2(1)	1(1)
C(4)	27(1)	37(1)	27(1)	-9(1)	0(1)	5(1)
C(5)	31(1)	32(1)	52(1)	-5(1)	-7(1)	2(1)
C(6)	60(2)	50(1)	73(2)	-25(1)	-6(1)	0(1)
C(7)	24(1)	25(1)	31(1)	-2(1)	-3(1)	0(1)
C(8)	37(1)	30(1)	32(1)	-2(1)	-2(1)	-4(1)
C(9)	56(1)	31(1)	40(1)	1(1)	-20(1)	-5(1)
C(10)	39(1)	29(1)	72(2)	-2(1)	-26(1)	3(1)
C(11)	26(1)	32(1)	77(2)	-9(1)	-3(1)	2(1)
C(12)	28(1)	32(1)	43(1)	-5(1)	4(1)	0(1)
C(13)	22(1)	27(1)	22(1)	-2(1)	-2(1)	-1(1)
C(14)	45(1)	25(1)	26(1)	-1(1)	4(1)	1(1)
C(15)	59(1)	34(1)	26(1)	-7(1)	6(1)	7(1)
C(16)	48(1)	44(1)	22(1)	1(1)	6(1)	1(1)
C(17)	36(1)	34(1)	28(1)	6(1)	-1(1)	-4(1)

C(18)	28(1)	25(1)	29(1)	-2(1)	-2(1)	1(1)
C(19)	21(1)	30(1)	24(1)	2(1)	4(1)	1(1)
C(20)	32(1)	31(1)	41(1)	-3(1)	-4(1)	2(1)
C(21)	30(1)	43(1)	45(1)	0(1)	-8(1)	-5(1)
C(22)	22(1)	53(1)	37(1)	9(1)	0(1)	3(1)
C(23)	31(1)	41(1)	40(1)	3(1)	6(1)	12(1)
C(24)	30(1)	33(1)	32(1)	-2(1)	4(1)	2(1)
N(1)	24(1)	29(1)	25(1)	-4(1)	-2(1)	4(1)
N(2)	23(1)	28(1)	26(1)	-7(1)	0(1)	4(1)
O(1)	28(1)	28(1)	26(1)	-2(1)	2(1)	5(1)
O(2)	49(1)	33(1)	102(1)	-20(1)	-27(1)	10(1)

Table 4. Hydrogen coordinates (x 10^4) and isotropic displacement parameters ($Å^2$x 10^3) for **263**.

	x	y	z	U(eq)
H(1)	9088	2658	3967	36
H(3)	11343	4454	6130	29
H(4A)	11538	2406	4824	37
H(4B)	11345	3366	4483	37
H(5A)	8894	2235	5996	47
H(5B)	7578	2059	5101	47
H(6A)	7756	534	4974	93
H(6B)	9105	306	4347	93
H(6C)	7930	1034	3976	93
H(8)	8001	3688	2921	40
H(9)	5728	3981	1912	53
H(10)	3544	4280	2620	59
H(11)	3602	4274	4336	55
H(12)	5841	3940	5349	41
H(14)	9891	5257	7314	38
H(15)	9029	5274	8860	47
H(16)	8859	4033	9737	45
H(17)	9578	2770	9078	40
H(18)	10411	2742	7520	33

H(20)	13250	4241	7037	43
H(21)	15737	3997	7744	48
H(22)	16913	2719	7528	46
H(23)	15552	1668	6610	44
H(24)	13057	1892	5924	38

X-Ray Crystallographic data for 6-methoxymethyl-1,3,4-triphenylpiperazin-2-one 264

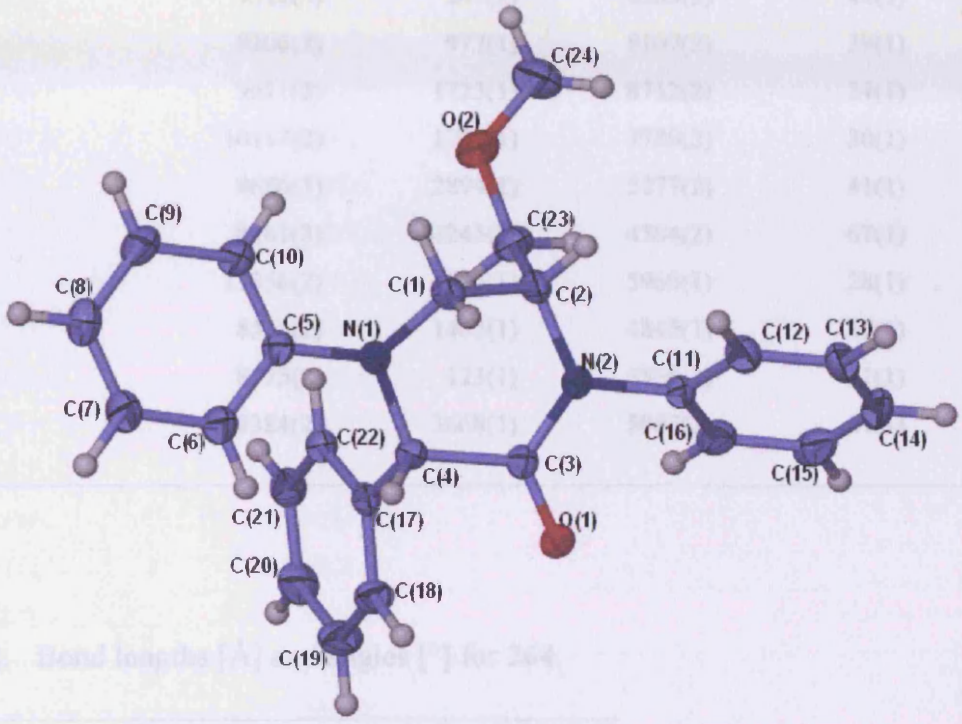

Table 1. Atomic coordinates (x 10^4) and equivalent isotropic displacement parameters ($Å^2$x 10^3) for **264**. U(eq) is defined as one third of the trace of the orthogonalized U^{ij} tensor.

	x	y	z	U(eq)
C(1)	10993(2)	2064(1)	4927(2)	33(1)
C(2)	9308(2)	2194(1)	4686(2)	32(1)
C(3)	9145(2)	815(1)	5496(2)	25(1)
C(4)	10602(2)	1013(1)	6186(2)	26(1)
C(5)	12887(2)	1902(1)	6390(2)	27(1)
C(6)	13710(2)	1285(1)	6947(2)	37(1)
C(7)	15193(3)	1433(2)	7364(2)	41(1)
C(8)	15891(3)	2185(2)	7243(2)	39(1)
C(9)	15085(3)	2803(2)	6703(2)	39(1)
C(10)	13604(2)	2669(1)	6288(2)	34(1)
C(11)	7127(2)	1213(1)	4228(2)	28(1)
C(12)	7102(3)	1200(1)	3212(2)	35(1)
C(13)	5757(3)	1018(1)	2613(2)	45(1)

C(14)	4462(3)	847(2)	3032(2)	51(1)
C(15)	4494(3)	853(1)	4049(2)	48(1)
C(16)	5820(2)	1045(1)	4649(2)	36(1)
C(17)	10192(2)	1008(1)	7245(2)	25(1)
C(18)	9803(3)	254(1)	7662(2)	34(1)
C(19)	9312(3)	247(2)	8583(2)	42(1)
C(20)	9206(3)	977(1)	9107(2)	39(1)
C(21)	9621(2)	1723(1)	8712(2)	34(1)
C(22)	10117(2)	1737(1)	7789(2)	30(1)
C(23)	8686(3)	2894(1)	5277(2)	41(1)
C(24)	8481(3)	4245(2)	4564(2)	67(1)
N(1)	11356(2)	1795(1)	5960(1)	28(1)
N(2)	8528(2)	1402(1)	4845(1)	29(1)
O(1)	8575(2)	123(1)	5568(1)	31(1)
O(2)	9384(2)	3668(1)	5087(2)	67(1)

Table 2. Bond lengths [Å] and angles [°] for **264**.

C(1)-N(1)	1.468(3)
C(1)-C(2)	1.506(3)
C(1)-H(1A)	0.9900
C(1)-H(1B)	0.9900
C(2)-N(2)	1.472(3)
C(2)-C(23)	1.522(3)
C(2)-H(2)	1.0000
C(3)-O(1)	1.224(2)
C(3)-N(2)	1.356(3)
C(3)-C(4)	1.535(3)
C(4)-N(1)	1.468(2)
C(4)-C(17)	1.532(3)
C(4)-H(4)	1.0000
C(5)-C(6)	1.393(3)
C(5)-C(10)	1.395(3)
C(5)-N(1)	1.423(3)
C(6)-C(7)	1.388(3)
C(6)-H(6)	0.9500
C(7)-C(8)	1.369(3)

C(7)-H(7)	0.9500
C(8)-C(9)	1.376(3)
C(8)-H(8)	0.9500
C(9)-C(10)	1.383(3)
C(9)-H(9)	0.9500
C(10)-H(10)	0.9500
C(11)-C(12)	1.383(3)
C(11)-C(16)	1.385(3)
C(11)-N(2)	1.443(3)
C(12)-C(13)	1.390(3)
C(12)-H(12)	0.9500
C(13)-C(14)	1.375(4)
C(13)-H(13)	0.9500
C(14)-C(15)	1.383(4)
C(14)-H(14)	0.9500
C(15)-C(16)	1.381(3)
C(15)-H(15)	0.9500
C(16)-H(16)	0.9500
C(17)-C(22)	1.386(3)
C(17)-C(18)	1.393(3)
C(18)-C(19)	1.381(3)
C(18)-H(18)	0.9500
C(19)-C(20)	1.377(3)
C(19)-H(19)	0.9500
C(20)-C(21)	1.375(3)
C(20)-H(20)	0.9500
C(21)-C(22)	1.386(3)
C(21)-H(21)	0.9500
C(22)-H(22)	0.9500
C(23)-O(2)	1.420(3)
C(23)-H(23A)	0.9900
C(23)-H(23B)	0.9900
C(24)-O(2)	1.362(3)
C(24)-H(24A)	0.9800
C(24)-H(24B)	0.9800
C(24)-H(24C)	0.9800
N(1)-C(1)-C(2)	109.93(17)
N(1)-C(1)-H(1A)	109.7
C(2)-C(1)-H(1A)	109.7
N(1)-C(1)-H(1B)	109.7

C(2)-C(1)-H(1B)	109.7
H(1A)-C(1)-H(1B)	108.2
N(2)-C(2)-C(1)	108.88(17)
N(2)-C(2)-C(23)	110.03(17)
C(1)-C(2)-C(23)	113.78(19)
N(2)-C(2)-H(2)	108.0
C(1)-C(2)-H(2)	108.0
C(23)-C(2)-H(2)	108.0
O(1)-C(3)-N(2)	122.5(2)
O(1)-C(3)-C(4)	117.54(19)
N(2)-C(3)-C(4)	119.92(18)
N(1)-C(4)-C(17)	111.87(17)
N(1)-C(4)-C(3)	114.71(17)
C(17)-C(4)-C(3)	107.07(16)
N(1)-C(4)-H(4)	107.6
C(17)-C(4)-H(4)	107.6
C(3)-C(4)-H(4)	107.6
C(6)-C(5)-C(10)	117.4(2)
C(6)-C(5)-N(1)	123.31(19)
C(10)-C(5)-N(1)	119.25(19)
C(7)-C(6)-C(5)	120.6(2)
C(7)-C(6)-H(6)	119.7
C(5)-C(6)-H(6)	119.7
C(8)-C(7)-C(6)	121.4(2)
C(8)-C(7)-H(7)	119.3
C(6)-C(7)-H(7)	119.3
C(7)-C(8)-C(9)	118.6(2)
C(7)-C(8)-H(8)	120.7
C(9)-C(8)-H(8)	120.7
C(8)-C(9)-C(10)	120.8(2)
C(8)-C(9)-H(9)	119.6
C(10)-C(9)-H(9)	119.6
C(9)-C(10)-C(5)	121.2(2)
C(9)-C(10)-H(10)	119.4
C(5)-C(10)-H(10)	119.4
C(12)-C(11)-C(16)	120.2(2)
C(12)-C(11)-N(2)	119.39(19)
C(16)-C(11)-N(2)	120.4(2)
C(11)-C(12)-C(13)	119.7(2)
C(11)-C(12)-H(12)	120.2

C(13)-C(12)-H(12)	120.2
C(14)-C(13)-C(12)	120.0(3)
C(14)-C(13)-H(13)	120.0
C(12)-C(13)-H(13)	120.0
C(13)-C(14)-C(15)	120.1(2)
C(13)-C(14)-H(14)	119.9
C(15)-C(14)-H(14)	119.9
C(16)-C(15)-C(14)	120.2(2)
C(16)-C(15)-H(15)	119.9
C(14)-C(15)-H(15)	119.9
C(15)-C(16)-C(11)	119.7(2)
C(15)-C(16)-H(16)	120.2
C(11)-C(16)-H(16)	120.2
C(22)-C(17)-C(18)	118.4(2)
C(22)-C(17)-C(4)	122.14(18)
C(18)-C(17)-C(4)	119.37(18)
C(19)-C(18)-C(17)	120.1(2)
C(19)-C(18)-H(18)	120.0
C(17)-C(18)-H(18)	120.0
C(20)-C(19)-C(18)	121.0(2)
C(20)-C(19)-H(19)	119.5
C(18)-C(19)-H(19)	119.5
C(21)-C(20)-C(19)	119.3(2)
C(21)-C(20)-H(20)	120.3
C(19)-C(20)-H(20)	120.3
C(20)-C(21)-C(22)	120.1(2)
C(20)-C(21)-H(21)	119.9
C(22)-C(21)-H(21)	119.9
C(21)-C(22)-C(17)	120.95(19)
C(21)-C(22)-H(22)	119.5
C(17)-C(22)-H(22)	119.5
O(2)-C(23)-C(2)	110.19(19)
O(2)-C(23)-H(23A)	109.6
C(2)-C(23)-H(23A)	109.6
O(2)-C(23)-H(23B)	109.6
C(2)-C(23)-H(23B)	109.6
H(23A)-C(23)-H(23B)	108.1
O(2)-C(24)-H(24A)	109.5
O(2)-C(24)-H(24B)	109.5
H(24A)-C(24)-H(24B)	109.5

O(2)-C(24)-H(24C)	109.5
H(24A)-C(24)-H(24C)	109.5
H(24B)-C(24)-H(24C)	109.5
C(5)-N(1)-C(4)	116.94(17)
C(5)-N(1)-C(1)	116.26(16)
C(4)-N(1)-C(1)	113.58(17)
C(3)-N(2)-C(11)	118.97(17)
C(3)-N(2)-C(2)	122.04(18)
C(11)-N(2)-C(2)	118.76(17)
C(24)-O(2)-C(23)	116.2(2)

Symmetry transformations used to generate equivalent atoms:

Table 3. Anisotropic displacement parameters ($Å^2 x\ 10^3$)for **264**. The anisotropic displacement factor exponent takes the form: $-2p^2[\ h^2a^{*2}U^{11} + ... + 2\ h\ k\ a^*\ b^*\ U^{12}\ ]$

	U^{11}	U^{22}	U^{33}	U^{23}	U^{13}	U^{12}
C(1)	27(1)	40(1)	31(1)	12(1)	1(1)	-7(1)
C(2)	26(1)	38(1)	31(1)	10(1)	-4(1)	-6(1)
C(3)	24(1)	31(1)	22(1)	-1(1)	4(1)	-2(1)
C(4)	22(1)	27(1)	30(1)	4(1)	1(1)	-2(1)
C(5)	22(1)	31(1)	27(1)	-1(1)	4(1)	-1(1)
C(6)	30(1)	35(1)	46(2)	2(1)	-4(1)	-1(1)
C(7)	31(1)	42(2)	48(2)	2(1)	-6(1)	4(1)
C(8)	25(1)	52(2)	39(2)	-8(1)	2(1)	-2(1)
C(9)	33(1)	42(1)	44(2)	-2(1)	7(1)	-12(1)
C(10)	32(1)	34(1)	35(1)	0(1)	3(1)	-2(1)
C(11)	24(1)	26(1)	32(1)	1(1)	-4(1)	0(1)
C(12)	36(1)	34(1)	35(2)	1(1)	-2(1)	3(1)
C(13)	57(2)	33(1)	40(2)	-2(1)	-19(1)	4(1)
C(14)	39(2)	33(1)	72(2)	2(1)	-26(2)	-3(1)
C(15)	26(1)	34(1)	81(2)	8(1)	0(1)	-1(1)
C(16)	30(1)	33(1)	46(2)	5(1)	5(1)	-3(1)
C(17)	21(1)	30(1)	24(1)	2(1)	-1(1)	0(1)
C(18)	44(1)	27(1)	30(1)	-1(1)	4(1)	-2(1)
C(19)	60(2)	37(1)	29(2)	5(1)	8(1)	-8(1)
C(20)	49(2)	45(2)	24(1)	-2(1)	6(1)	0(1)

C(21)	36(1)	33(1)	31(1)	-6(1)	0(1)	4(1)
C(22)	25(1)	29(1)	34(1)	3(1)	-3(1)	-1(1)
C(23)	33(1)	30(1)	58(2)	5(1)	-3(1)	-3(1)
C(24)	62(2)	52(2)	82(2)	25(2)	-10(2)	-1(2)
N(1)	22(1)	33(1)	30(1)	6(1)	-1(1)	-5(1)
N(2)	23(1)	31(1)	31(1)	4(1)	-2(1)	-5(1)
O(1)	30(1)	30(1)	32(1)	2(1)	2(1)	-6(1)
O(2)	49(1)	35(1)	106(2)	20(1)	-28(1)	-10(1)

Table 4. Hydrogen coordinates (x 10^4) and isotropic displacement parameters ($Å^2$x 10^3) for **264**.

	x	y	z	U(eq)
H(1A)	11337	1633	4482	39
H(1B)	11532	2593	4822	39
H(2)	9091	2340	3968	39
H(4)	11332	544	6129	32
H(6)	13253	758	7042	45
H(7)	15736	1004	7740	49
H(8)	16909	2278	7527	46
H(9)	15554	3328	6614	47
H(10)	13064	3107	5926	40
H(12)	8000	1314	2925	42
H(13)	5732	1012	1915	54
H(14)	3543	724	2622	61
H(15)	3602	725	4335	57
H(16)	5835	1063	5346	44
H(18)	9876	-257	7312	40
H(19)	9044	-270	8860	51
H(20)	8849	966	9735	47
H(21)	9567	2228	9073	40
H(22)	10410	2254	7524	36
H(23A)	7575	2938	5093	50
H(23B)	8883	2763	5992	50
H(24A)	7973	3986	3959	101

H(24B)	9102	4716	4391	101
H(24C)	7717	4447	4967	101

Bibliography

1. How structural features influence the biomembrane permeability of peptide, P. S. Burton, R. A. Conradi, N. F. H. Ho, A. R. Hilgers, R. T. Borchardt, *J. Pharmaceutical Sciences*, 1996, **85**, 1336-1340
2. Optimising oral systems for the delivery of therapeutic proteins and peptides, I. M. Arhewoh, E. I. Ahonkhai, A. O. Okhamafe, *African J. of Biotechnology*, 2005, **4**, 1591-1597
3. Concepts and progress in the development of peptide mimetics, G. L. Olson et al., *J. Med. Chem.*, 1993, **36**, 3039-3053
4. Bioactive conformation of luteinizing hormone-releasing hormone: evidence from a conformationally constrained analogue, R. M. Freidinger, D. F. Veber, D. Schwenk Perlow, J. R. Brooks, R. Saperstein, *Science*, 1980, **210**, 656
5. Conformationally restriced arginine analogues, T. R. Webb, C. Eigenbrot, *J. Org. Chem.*, 1991, **56**, 3009-3016
6. Constrained peptides: models of bioactive peptides and protein substructures, J. Rizo, L. M. Gierasch, *Annu. Rev. Biochem.*, 1992, **61**, 387-418
7. Designing peptide receptor agonists and antagonists, V. J. Hruby, *Nature Rev. Drug Disc.*, 2002, **1**, 847-858
8. Efficient synthesis of conformationally constrained peptidomimetics containing 2-oxopiperazinones, A. Pohlman, V. Schanen, D. Guillaume, J.-C. Quirion, H.-P. Husson, *J. Org. Chem.*, 1997, **62**, 1016-1022
9. New routes to conformationally restricted peptide building blocks: a convenient preparation of bicyclic pipierazinone derivatives, Y. M. Fobian, D. A. d'Avignon, K. D. Moeller, *Bioorg. & Med. Chem. Letts.*, 1996, **6**, 315-318
10. The discovery of the α-helix and β-sheet, the principal structural features of proteins, D. Eisenberg, *Perspective*, 2003, **100**, 11207-11210
11. Stereochemistry of polipeptide chain configurations, G. N. Ramachandran, C. Ramakrishnan, V. Sasisekharan, *J. Mol. Biol.*, 1963, **7**, 95-99
12. Potent dibasic GPIIb/IIIa antagonists with reduced prolongation of bleeding time: synthesis and pharmacological evaluation of 2-oxopiperazine derivatives, S. Kitamura, H. Fukushi, T. Miyawaki, M. Kawamura, N. Konishi, Z. Terashita, T. Naka, *J. Med. Chem.*, 2001, **44**, 2438-2450
13. Synthesis and evaluation of derivatives of leucine enkephalin as potential affinity labels for δ opioid receptors, H. Choi, T. F. Murray, J. V. Aldrich, *Biopolymers*, 2003, **71**, 552-557
14. Biosynthesis of the enkephalins and enkephalin-containing polypeptides, R. V. Lewis, A. S. Stern, *Ann. Rev. Pharmacol. Toxicol.*, 1983, **23**, 353-372

15. Design and synthesis of a bicyclic non-peptide β-bend mimetic of enkephalin, B. L. Currie, J. L. Krstenansky, Z.-L. Lin, J. Ungwitayatorn, Y.-H. Lee, M. del Rosario-Chow, W.-S. Sheu, M. E. Johnson, *Tet.*, 1991, **49**, 3489-3500

16. Synthesis of a constrained enkephalin analogue to illustrate a novel route to the piperazinone ring structure, K. Shreder, L. Zhang, M. Goodman, *Tet. Letts.*, 1998, **39**, 221-224

17. Solid phase organic synthesis of piperazinone containing enkephalin mimetics: a readily derivatized, traceless scaffold, K. Shreder, L. Zhang, J. P. Gleeson, J. A. Ericsson, V. V. Yalamoori, M. Goodman, *J. Comb. Chem.*, 1999, **1**, 383-387

18. Synthesis of chiral piperazin-2-ones as model peptidomimetics, J. Di Maio, B. Belleau, *J. Chem. Soc. Perkin Trans. 1*, 1989, **1**, 1687-1689

19. Ipamorelin, the first selective growth hormone secretagogue, K. Raun, B. S. Hansen, N. L. Johansen, H. Thøgersen, K. Madsen, M. Ankersen, P. H. Andersen, *Eur. J. of Endocrinology*, 1998, **139**, 552-561

20. Novel orally active growth hormone secretagogues, T. K. Hansen, M. Ankersen, B. S. Hansen, K. Raun, K. K. Nielsen, J. Lau, B. Peschke, B. F. Lundt, H. Thøgersen, N. L. Johansen, K. Madsen, P. H. Andersen, *J. Med. Chem.*, 1998, **41**, 3705-3714

21. Synthesis of piperazinones and their application in constrained mimetics of the growth hormone secretagogue NN703, T. K. Hansen, N. Schlienger, B. S. Hansen, P. H. Andersen, M. R. Bryce, *Tet. Letts.*, 1999, **40**, 3651-3654

22. Synthesis of chiral piperazinones as versatile scaffolds for peptidomimetics, F. Rübsam, R. Mazitschek, A. Giannis, *Tet.*, 2000, **56**, 8481-8487

23. Conformationally constrained substance P analogues: the total synthesis of a constrained peptidomimetic for the Phe^7-Phe^8 region, Y. Tong, Y. M. Fobian, M. Wu, N. D. Boyd, K. D. Moeller, *J. Org. Chem.*, 2000, **65**, 2484-2493

24. Solid-support synthesis of a peptide β-turn mimetic, A. Golebiowski, S. R. Klopfenstein, X. Shao, J. J. Hen, A. O. Colson, A. L. Grieb, A. F. Russell, *Org. Letts.*, 2000, **2**, 2615-2617

25. β-Turn topography, J. B. Ball, R. A. Hughes, P. F. Alewood, P. R. Andrews, *Tet.*, 1993, **49**, 3467-3478

26. Protein folding, I. D. Kuntz, *J. Am. Chem. Soc.*, 1972, **94**, 4009-4012

27. Synthesis of pipecolic acid-based spiro bicyclic lactam scaffolds as β-turn mimics, R. V. Somu, R. L. Johnson, *J. Org. Chem.*, 2005, **70**, 5954-5963

28. Design, synthesis, and conformational analysis of eight-membered cyclic peptidomimetics prepared using ring closing metathesis, C. J. Creighton, G. C. Leo, Y. Du, A. B. Reitz, *Bioorg. & Med. Chem.*, 2004, **12**, 4375-4385

29. Effect of sequence on peptide geometry in 5-*tert*-butylprolyl Type VI β-turn mimics L. Halab, W. D. Lubell, *J. Am. Chem. Soc.*, 2002, **124**, 2474-2484

30. Topological side-chain classification of β-turns: Ideal motifs for peptidomimetic development, T. T. Tran, J. McKie, W. D. F. Meutermans, G. T. Bourne, P. R. Andrews, M. L. Smythe, *J. Computer-Aided Mol. Design*, 2005, **19**, 551-66

31. Synthesis and conformational studies of dipeptides constrained by disubstituted 3-(aminoethoxy)propionic acid linkers, D. S. Reddy, D. V. Velde, J. Aubé, *J. Org. Chem.*, 2004, **69**, 1716-1719
32. Systematic study of the synthesis of macrocyclic dipeptide β-turn mimics possessing 8-, 9-, and 10-membered rings by ring-closing methathesis, R. Kaul, S. Surprenant, W. D. Lubell, *J. Org. Chem.*, 2005, **70**, 3838-3844
33. Design and synthesis of novel conformationally restricted peptide secondary structure mimetics, H. O. Kim, H. Nakanishi, M. S. Lee, M. Kahn, *Org. Letts.*, 2000, **2**, 301-302
34. Novel bicyclic lactams as XaaPro type VI β-turn mimcs: design, synthesis, and evaluation, K. Kim, J. Dumas, J. P. Germanas, *J. Org. Chem.*, 1996, **61**, 3138-3144
35. Synthesis and evaluation of δ-lactams (piperazones) as elastase inhibitors, J. Seibel, D. Brown, A. Amour, S. J. Macdonald, N. J. Oldham, C. J. Schofield, *Bioorg. Med. Chem. Letts.*, 2003, **13**, 387-389
36. http://fig.cox.miami.edu/~cmallery/150/protein/sf26x11b.jpg
37. Molecular recognition of protein-ligand complexes: applications to drug design, R. E. Babine, S. L. Bender, *Chem. Rev.*, 1997, **97**, 1420-1437
38. Design, synthesis, and structure–activity relationships of unsubstituted piperazinone-based transition state factor Xa inhibitors, W. Huang, M. A. Naughton, H. Yang, T. Su, S. Dam, P. W. Wong, A. Arfsten, S. Edwards, U. Sinha, S. Hollenbach, R. M. Scarborough, B. Y. Zhu, *Bioorg. & Med. Chem. Lett.*, 2003, **13**, 723-728
39. Synthesis and evaluation of 1-arylsulfonyl-3-piperazinone derivatives as Factor Xa inhibitors III. Effect of ring opening of piperazinone moiety on inhibition, H. Nishida, Y. Miyazaki, T. Mukaihira, H. Shimada, K. Suzuki, F. Saitoh, M. Mizuno, T. Matsusue, A. Okamoto, Y. Hosaka, M. Matsumoto, S. Ohnishi, H. Mochizuki, *Chem. Pharm. Bull.*, 2004, **52**, 459-462
40. The design of competitive, small-molecule inhibitors of coagulation Factor Xa, H. W. Pauls, W. R. Ewing, *Curr. Top. Med. Chem.*, 2001, **1**, 83-100
41. *N*-Arylpiperazinone inhibitors of farnesyltransferase: discovery and biological activity, T. M. Williams et al., *J. Med. Chem.*, 1999, **42**, 3779-3784
42. http://www.bmb.psu.edu/faculty/tan/lab/gallery/ras_ribbon1a.jpg
43. Macrocyclic piperazinones as potent dual inhibitors of farnesyltransferase and geranylgeranyltransferase-I, C. L. Dinsmore et al., *Bioorg. & Med. Chem. Lett.*, 2004, **14**, 639-643
44. Insight into the selective inhibition of *Candida Albicans* secreted aspartyl protease:a docking analysis study, S. K. Kumar, V. M. Kulkarni, *Bioorg. & Med. Chem. Lett.*, 2002, **10**, 1153-1170
45. http://www.clunet.edu/BioDev/omm/hiv_protease/images/pr-dimer.gif
46. Pseudotheonamides, serine protease inhibitors from the marine sponge *Theonella swinhoei,* Y. Nakao, A. Masuda, S. Matsunaga, N. Fusetani, *J. Am. Chem. Soc.*, 1999, **121**, 2425-2429
47. http://www.ice.mpg.de/main/news/theonella%20swinhoei%20.jpg
48. Synthesis of marine sponge bisindole alkaloids dihydrohamacanthins, F. Y. Miyake, K. Yakushijin, D. A. Horne, *Org. Letts.*, 2002, **4**, 941-943

49. New bisindole alkaloids of the topsentin and hamacanthin classes from the mediterranean marine sponge *Rhaphisia lacazei,* A. Casapullo, G. Bifulco, I. Bruno, R. Riccio, *J. Nat. Prod.*, 2000, **63**, 447-451

50. Synthesis and antiretroviral evaluation of 3-alkyl 2-piperazinone nucleoside analogs, A. Benjahad *et al.*, *Tet. Letts.*, 1994, **35**, 9545-9548

51. Alzheimer's disease: molecular understanding predicts amyloid-based therapeutics, D. J. Selkoe, D. Schenk, *Annu. Rev. Pharmacol. Toxicol.*, 2003, **43**, 545-584

52. http://www.ahaf.org/alzdis/about/AD_2003.jpg

53. http://www.crystalinks.com/alzheimersbrain.jpg

54. A novel application of a [3+2] cycloaddition reaction for the synthesis of the piperazinone rings of pseudotheonamides A_1 and A_2, M. K. Gurjar, S. Karmakar, D. K. Mohapatra, U. D. Phalgune, *Tet. Letts.*, 2002, **43**, 1897-1900

55. Peptide interactions with G-coupled protein receptors, G. R. Marshall, *Biopolymers*, 2001, **60**, 246-257

56. Muscarinic receptor agonists and antagonists, K. J. Broadley, D. R. Kelly, *Molecules*, 2001, **6**, 142-193

57. Modelling of the binding site of the human m_1 muscarinic receptor: experimental validation and refinement, H. Bourdon, S. Trumpp-Kallmeyer, H. Schreuder, J. Hoflack, M. Hibert, C.-G. Wermuth, *J. Computer-Aided Mol. Design*, 1997, **11**, 317-332

58. Cholinesterase inhibitors for Alzheimer's disease, J. Birks, *The Cochrane Database of Systematic Reviews,* 2006, **3**, 1-106

59. Electrochemical characterisation of tacrin, an antiAlzheimer's disease drug, and its determination in pharmaceuticals, S. Bollo, L. Muñoz, L. J. Nuñez-Vergara, J. A. Squella, *Electroanalysis*, 2000, **12**, 376-382

60. 3-Year study of donepezil therapy in Alzheimer's Disease: effects of early and continuous therapy, B. Winblad, A. Wimo, K. Engedal, H. Soininen, F. Verhey, G. Waldemar, A. L. Wetterholm, A. Haglund, R. Zhang, R. Schindler, *Dement. Geriatr. Cogn. Disord.*, 2006, **21**, 353-363

61. Cholinergic agonists and the treatment of Alzheimer's disease, W. S. Messer Jr., *Curr. Top. In Med. Chem.*, 2002, **2**, 353-358

62. http://www.mycovaud.ch/albums/smv2003/amanita_muscaria_moiry_DSCN0815.sized.jpg

63. Pharmacological characterisation of human m_1 Muscarinic acetylcholine receptors with double mutations at the junction of TM VI and the third extracellular domain, X.-P. Huang, F. E. Williams, S. M. Peseckis, W. S. Messer Jr., *J.Pharm. and Exp. Therapeutics*, 1998, **286**, 1129-1139

64. Efficient synthesis of substituted piperazinones via tandem reductive amination–cyclization, C. J. Dinsmore, C. B. Zartman, *Tet. Letts.*, 2000, **41**, 6309-6312

65. Conversion of β-chloroacetyl-L-diaminoprpionic acid to L-2-ketopiperazine-5-carboxylic acid, R. J. Koegel, S. M. Birnbaum, C. G. Baker, H. A. Sober, J. P. Greenstein, *J. Biol. Chem.*, 1952, **201**, 547-551

66. Novel cholecystokinin receptor ligands: Oxopiperazines derived from Boc-CCK-4, A. R. Batt, D. A. Kendrick, E. Matthews, D. P. Rooker, H. Ryder, G. Semple, M. Szelke, *Bioorg. Med. Chem. Letts.*, 1994, **4**, 867-872

67. The synthesis of bicyclic piperazine-2-carboxylic acids from L-proline, S. Hanessian, R. Sharma, *Heterocycles*, 2000, **52**, 1231-1238

68. Syntheses and proton NMR conformational analyses of diastereomeric 4,4'-(4,5-dihydroxy-1,2-cyclohexanediyl)bis(2,6-piperazinedione)s and a synthetically related tricyclic octahydro-2,2-dimethyl-6-oxo-1,3-dioxolo[4,5-g]quinoxaline-5,8-diacetic acid ester, D. T. Witiak, Y. Wei, *J. Org. Chem.*, 1991, **56**, 5408-5417

69. Synthesis of two stereoisomeric polydentate ligands, *trans* and *cis* cyclopentane-1,2-diaminotetraacetic acids, and complexation by ^{111}In and ^{153}Sm, S. G. Gouin, J. F. Gestin, K. Joly, A. Loussouarn, A. Reliquet, J. C. Meslin, D. Deniaud, *Tet.*, 2002, **58**, 1131-1136

70. Synthesis of piperazinones and benzopiperazinones from 1,2-diamines and organoboronic acids, N. A. Petasis, Z. D. Patel, *Tet. Letts.*, 2000, **41**, 9607-9611.

71. Ueber α-γ-diacipiperazine, C. A. Bischoff, O. Nastvogel, *Berichte*, 1889, **22**, 1783-1792

72. *N,N'*-Dialkylmonoketopiperazines, W. B. Martin, A. E. Martell, *J. Am. Chem. Soc.*, 1950, **72**, 4301-4302

73. 3-(Piperazinylpropyl)indoles: Selective, Orally Bioavailable h5-HT_{1D} ReceptorAgonists as Potential Antimigraine Agents, M. S. Chambers, L. J. Street, S. Goodacre, S. C. Hobbs, P. Hunt, R. A. Jelley, G. Matassa, A. J. Reeve, F. Sternfeld, M. S. Beer, J. A. Stanton, D. Rathbone, A. P. Watt, A. M. MacLeod, *J. Med. Chem.*, 1999, **42**, 691-705

74. Structure and spectral properties of β-carbolines. Part 3. Synthesis and stereochemistry of 1,2,3,4,6,7,9,10,15b,15c-decahydropyrido[1'',2'':1',2']pyrazino[4',3':1,2]pyrido[3,4-b]indoles, S. Misztal, M. Dukat, J. L. Mokrosz, J. Chem. Soc. Perkin Trans. 1, 1990, **8**, 2311-2315

75. Novel bifunctional macrocyclic chelating agents appended with a pendant-type carboxymethylamino ligand and nitrobenzyl group and stability of the 88YIII complexes, K. Takenouchi, K. Watanabe, Y. Kato, T. Koike, E. Kimura, *J. Org. Chem.*, 1993, **58**, 1955-1958

76. Preparation of substituted piperazinones via tandem reductive amination-(*N,N'*-acyl transfer)-cyclisation, D. C. Beshore, C. J. Dinsmore, *Org. Letts.*, 2002, **4**, 1201-1204

77. A simple entry to chiral non-racemic 2-piperazinone derivatives, G. P. Pollini, N. Baricordi, S. Benetti, C. De Risi, V. Zanirato, *Tet. Letts.*, 2005, **46**, 3699-3701

78. Tryptophan-derived NK_1 antagonists: conformationally constrained heterocyclic bioisosteres of the ester linkage, R. T. Lewis, A. M. Macleod, K. J. Merchant, F. Kelleher, I. Sanderson, R. H. Herbert, M. A. Cascieri, S. Sadowski, R. G. Ball, K. Hoogsten, *J. Med. Chem.*, 1995, **38**, 923-933

79. Synthesis and NMDA antagonistic properties of the enantiomers of 4-(3-phosphonopropyl)piperazine-2-carboxylic acid (CPP) and of the nsaturated analog (E)-4-(3-phosphonoprop-2-enyl)piperazine-2-carboxylic acid (CPP-ENE), B. Aebischer, P. Frey, H. Haerter, P. L. Herrling, W. Mueller, H. J. Olverman, J. C. Watkins, *Helvetica chim. Acta*, 1989, **72**, 1043-1051

80. Potent, orally active GPIIb/IIIa antagonists containing a nipecotic acid subunit. Structure-activity studies leading to the discovery of RWJ-53308, W. J. Hoekstra, B. E. Maryanoff, B. P. Damiano, P. Andrare-Gordon, J. H. Cohen, M. J. Costanzo, at al., *J. Med. Chem.*, 1999, **42**, 5254-5265

81. Practical synthesis of 1-aryl-6-(hydroxymethyl)-2-ketopiperazines via a 6-*exo* amide-epoxide cyclization, N. A. Powell, F. L. Ciske, E. C. Clay, W. L. Cody, D. M. Downing, P. G. Blazecka, D. D. Holsworth, J. J. Edmunds, *Org. Letts.*, 2004, **6**, 4069-4072

82. Discovery of novel non-peptidic ketopiperazine-based renin inhibitors, D. D. Holsworth, N. A. Powell, D. M. Downing, C. Cai, W. L. Cody, J. M. Ryan, R. Ostroski, M. Jalaie, J. W. Bryant, J. J. Edmunds, *Bioorg. Med. Chem.*, 2005, **13**, 2657-2664

83. Equipotent activity in both enantiomers of a series of ketopiperazine-based renin inhibitors, N. A. Powell, E. H. Clay, D. D. Holsworth, J. W. Bryant, M. J. Ryan, M. Jalaie, E. Zhang, J. J. Edmunds, *Bioorg. Med. Chem.*, 2005, **15**, 2371-2374

84. Solid phase syntheses of β-turn analogues to mimic or disrupt protein-protein interactions, K. Burgess, *Acc. Chem. Res.*, 2001, **34**, 826-835

85. Solid supported high-throughput orgainc synthesis of peptide β-turn mimetics via Petasis reaction/ diketopiperazinone formation, A. Golebiowski, S. R. Klopfenstein, J. J. Chen, X. Shao, *Tet. Letts.*, 2000, **41**, 4841-4844

86. A peptoid synthesis of di- and tri-substituted 2-oxopiperazines on solid support, D. A. Goff, *Tet. Letts.*, 1998, **39**, 1473-1476

87. Solid phase synthesis of 3,4-disubstituted-7-carbamoyl-1,2,3,4-tetrahydroquinoxalin-2-ones, J. Lee, W. V. Murray, R. A. Rivero, *J. Org. Chem.*, 1997, **62**, 3874-3879

88. Solid phase chemical technologies for combinatorial chemistry, S. Balasubramanian, *J. Cell. Biochem. Suppl.*, 2001, **37**, 28-33

89. Stereoselective reductive amination of β-keto esters derived from dipeptides. Stereochemical and mechanistic studies on the formation of 5-carboxymethyl-2-oxopiperazine derivatives, R. Patiño-Molina, R. Herranz, M. T. García-López, R. González-Muñiz, *Tet.*, 1999, **55**, 15001-15010

90. A new efficient synthesis of (*R,R*)-2,2′-bipyrrolidine: an interesting chiral 1,2-diamine with C_2 symmetry, A. Alexakis, A. Tomassini, C. Chouillet, S. Roland, P. Mangeney, G. Bernardinelli, *Angew. Chem. Int. Ed.*, 2000, **39**, 4093-4095

91. N-(3-Methyl-4-oxo-3,4-dihydro-pteridin-2-yl)glycine: hydrogen-bonded sheets of $R_4(22)$ and $R_4(30)$ rings, P. Arranz Mascarós, M. D. Gutiérrez Valero, J. N. Low, C. Glidewell, *Acta Crystall.*, 2004, **60**, 795-797

92. Action of ethylenediamine on succinic acid, A. T. Mason, *J. Chem. Soc.*, 1889, **55**, 97-102

93. The conformational analysis of saturated heterocycles. Part 76. Ring and nitrogen inversion in *cis*- and *trans*-1, 4, 5, 8-tetramethyldecahydropyrazino[2,3-*b*]pyrazine, I. J. Ferguson, A. R. Katritzky, R. J. Patel, *J. Chem. Soc., Perkin Trans. 2*, 1976, **13**, 1564-1568

94. Products of the reaction of *N,N'*-dibenzylethylenediamine and glyoxal, R. L. Willer, D. W. Moore, D. J. Vanderah, *J. Org. Chem.*, 1985, **50**, 2365-2368

95. Chiral aminals: Powerful auxiliaries in asymmetric synthesis, A. Alexakis, P. Mangeney, N. Lensen, J.-P. Tranchier, R. Gasmini, S. Raussou, *Pure Appl. Chem.*, 1996, **68**, 531-542

96. T. Hayashi, *Sci. Pap. Inst. Phys. Chem. Res.*, 1941, **38**, 455

97. Lactam formation from the condensation of stilbenediamine with glyoxal, L. L. Darko, J. Karliner, *J. Org. Chem.*, 1971, **36**, 3810-3812

98. Condensation of glyoxal with triethylenetetraamine. Stereochemistry, cyclization and deprotection, G. Hervé, H. Bernard, N. Le Bris, M. Le Baccon, J. J. Yaouanc, H. Handel, *Tet. Letts.*, 1999, **40**, 2517-2520.

99. Synthesis and X-ray crystal structure determination of the first transition metal complexes of the tetracycles fomed by tetraazamacrocycle-glyoxal condensation: PdL^*Cl_2 (L= cyclam-glyoxal condensate (1), cyclen-glyoxal condensate (2)), T. J. Hubin, J. M. McCormick, N. W. Alcock, D. H. Busch, *Inorg. Chem.*, 1998, **37**, 6549-6551

100. Tricyclic tetraamines by glyoxal - linear tetraamine condensation, J. Jazwinski, R. A. Kolinski, *Tet. Letts.*, 1981, **22**, 1711-1714

101. A powerful route to *C*-functionalised tetraazamacrocycles, F. Boschetti, F. Denat, E. Espinosa, J.-M. Lagrange, R. Guilard, *Chem. Comm.*, 2004, **5**, 588-589

102. Réactions de dismutation à partir du glyoxal et de molécules basiques difonctionnelles, D. Chassonery, F. Chastrette, M. Chastrette, A. Blanc, G. Mattioda, *Bull. Soc. Chim. Fr.*, 1994, **131**, 188-199

103. Asymmetric synthesis of α-amino acids from a chiral masked form of glyoxal, C. Agami, F. Couty, C. Puchot-Kadouri, *Synlett*, 1998, 449-456

104. An organic template approach for the synthesis of selectively functionalised tetraazacycloalkanes, F. Boschetti, F. Denat, E. Espinosa, R. Guilard, *Chem. Comm.*, 2002, **4**, 312-313

105. Bis-aminals of linear tetraamines: kinetic and thermodynamic aspects of the condensation reaction, F. Chuburu, R. Tripier, M. Le Baccon, H. Handel, *Eur. J. Org. Chem.*, 2003, **5**, 1050-1055

106. The reaction of phenylglyoxal with primary aliphatic and aromatic amines. Synthesis of phenylglyoxal monoimines and some derivatives, B. Alcaide, G. Escobar, R. Pérez-Ossorio, J. Plumet, D. Sanz, *J. Chem. Research*, 1984, **5**, 144-145

107. Phenylglyoxal for polyamines modification and cyclam synthesis, R. Tripier, F. Churubu, M. Le Baccon, H. Handel, *Tet. Letters* 2003, **59**, 4573-4579

108. Enantioselective addition of diethylzinc to aldehydes catalyzed by chiral hydroxy aminal, M. Asami, S. Inoue, *Chem. Lett.*, 1991, **4**, 685-688

109. Regio- and stereoselectivity of the formation of 1,3-oxazolidines in the reaction of *l*-ephedrine with phenylglyoxal. Unexpected rearrangement of 2-benzoyl-3,4-dimethyl-5-phenyl-l,3-oxazolidine to 4,5-Dimethyl-3,6-diphenylmorpholin-2-one, F. Polyak, T. Dorofeeva, G. Zelchans and G. Shustov, *Tet. Letts.*, 1996, **37**, 8223-8226

110. Compared reactivity of a β-aminothiol and a β–aminoalcohol towards phenylglyoxal, C. Agami, F. Couty, B. Prince, O. Venier, *Tet. Letts.*, 1993, **34**, 7061-7062

111. Pual Lewis, Cardiff University, unpublished work

112. Pyrolysis of esters. VIII. Effect of methoxy and dimethylamino groups on the direction of elimination, W. J. Bailey, L. Nicholas, *J. Org. Chem.*, 1956, **21**, 648-650

113. The use of alkyl vinyl ethers in olefin synthesis, D. C. Rowlands, K. W. Greenlee, J. M. Derfer, C. E. Boord, *J. Org. Chem.*, 1952, **6**, 807-811

114. Lewis acid induce rearrengement of 1-hetero-2,3-epoxides. Synthesis, reactivity and synthetic applications of homochiral thiiranium and aziridinium ion intermediates, C. M. Rayner, *Synlett*, 1997, 11

115. Nucleophilic ring opening of aziridines, X. E. Hu, *Tet.*, 2004, **60**, 2701-2734

116. The preparation of β-substituted amines from mixtures of epoxide opening products via a common aziridinium ion intermediate, S. R. Anderson, J. T. Ayers, K. M. DeVries, F. Ito, D. Mendenhall, B. C. Vanderplas, *Tet. Asymmetry*, 1999, **10**, 2655-2663

117. Two expedient method for the preparation of chiral diamines, S. E. de Sousa, P. O'Brien, P. Poumellec, *J. Chem. Soc., Perkin Trans. 1*, 1998, **9**, 1483-1492

118. The reaction of amines with methylene chloride. Evidence of rapid aminal formation from *N*-methylene pyrrolidinium chloride and pyrrolidine, J. E. Mills, C. A. Maryanoff, D. F. McComsey, R. C. Stanzione, L. Scott, *J. Org. Chem.*, 1987, **52**, 1857-1859

119. Dichloromethane as reactant in synthesis: an expedient transformation of prolinamide to a novel pyrrolo[1,2-*c*]imidazolone, H.-J. Federsel, E. Könberg, L. Lilljequist, B.-M. Swahn, *J. Org. Chem.*, 1990, **55**, 2254-2256

120. Rules for ring closure, J. E. Baldwin, *J. Chem. Soc., Chem. Commun.*, 1976, 734-736

121. New *N*-acyl, *N*-alkyl, and *N*-bridged derivatives of *rac*-6,6′,7,7′-tetramethoxy-1,1′,2,2′,3,3′,4,4′-octahydro-1,1′-bisisoquinoline, S. Busato, D. C. Craig, Z. M. A. Judeh, R. W. Read, *Tet.*, 2003, **59**, 461-472

122. Synthesis of chiral 1,2-diamines by asymmetric lithiation-substitution, I. Coldman, R. C. B. Copley, T. F. N. Haxell, S. Howard, *Org. Letts.*, 2001, **3**, 3799-3801

123. Sodium borohydride-iodine, an efficient reagent for reductive amination of aromatic aldehydes, I. Saxena, R. Borah, J. C. Sarma, *Indian Journal of Chemistry*, 2002, **41B**, 1970-71

124. Reductive amination of aldehydes and ketones with sodium triacetoxyborohydride. Studies on direct and indirect reductive amination procedure, A. F. Abdel-Magid, K. G. Carson, B. D. Harris, C. A. Maryanoff, R. D. Shah, *J. Org. Chem.*, 1996, **61**, 3849-3862

125. Catalytic alkyl group exchange reaction of primary snd secondary amines, S.-I. Murahashi, N. Yoshimura, T. Tsumiyama, T. Kojima, *J. Am. Chem. Soc.*, 1983, **105**, 5002-5011

126. Synthesis and structures of 1,3,1′,3′-tetrabenzyl-2,2′-biimidazolidinylidenes (electron-rich alkenes), their aminal intermediates and their degradation products, B. Cetinkaya, E. Cetinkaya, J .A. Chamizo, P. B. Hitchcock, H. A. Jasim, H. Kucukbay, M. F. Lappert, *J. Chem. Soc. Perkin Trans. 1*, 1998, **13**, 2047-2054.

127. Mass spectrometer as a probe in the synthesis of 2-substituted benzimidazoles, D. V. Ramana, E. Kantharaj, *Tet.*, 1994, **50**, 2485-2496

128. The reduction of acid amides with lithium aluminium hydride, V. M. Mićović, M. L. J. Mihailović, *J. Org. Chem.*, 1953, **18**, 1190

129. A selective reductive amination of aldehydes by hte use of Hantzsch dihydropyridine as reductant, T. Itoh, K. Nagata, M. Miyazaki, H. Ishikawa, A. Kurihara, A. Ohsawa, *Tet.*, 2004, **60**, 6649-6655

130. Elsa Garcia Borrell, Cardiff University, unpublished work

131. Phenyl tetraacetic acid ligands for gadolinium: potential magnetic resonance image enhancing agents, A. B. McLaren, R. J. Baker, J. G. Wilson, *Austr. J. Chem.*, 1987, **40**, 449-54

132. Biohydroxylations of Cbz-protected alkyl substituted piperidines by *Beauveria bassiana* ATCC 7159, S. J. Aitken, G. Grogan, C. S.-Y. Chow, N. J. Turner, S. L. Flitsch, *J. Chem. Soc., Perkin Trans. 1*, 1998, **20**, 3365-3370

133. Stereochemistry of microbiological hydroxylation. II. Oxygenation of 1-benzoylalkylpiperidines, R. A. Johnson, H. C. Murray, L. M. Reineke, G. S. Fonken, *J. Org. Chem.*, 1969, **34**, 2279

134. A tuneable method for *N*-debenzylation of benzylamino alcohols, E. J. Grayson, B. G. Davies, *Org. Letts.*, 2005, **7**, 2361-2364

135. Conformationally homogeneous secondary amines at room temperature, J. T. Ippoliti, S. Leta, S. Gorun, *Corporate Research Laboratory Exxon Research and Engineering Company, unpublished article*

136. Synthesis of met- and leu-enkephalin analogues containing chiral *N,N'*-ethylene-bridged phenylalanyl-methionine and –leucine, H. Takenaka, H. Miyake, Y. Kojima, M. Yasuda, M. Gemba, T. Yamashita, *J. Chem. Soc. Perkin Trans. 1*, 1993, **8**, 933-937

137. Synthesis and biological activity of 1,2,4-oxadiazole derivatives: highly potent and efficacious agonists for cortical muscarinic receptors, L. J. Street, R. Baker, T. Book, C. O. Kneen, A. M. MacLeod, K. J. Merchant, G. A. Showell,, J. Saunders, R. H. Herbert, S. B. Freedman, E. A. Harley, *J. Med. Chem.*, 1990, **33**, 2690-2697

138. Reaction of 1,2-dibromoethane with primary amines: formation of *N,N'*-disubstituted ethylenediamines RNH-CH_2CH_2-NHR and homologous polyamines RNH-$[CH_2CH_2NR]_n$-H, M. K. Denk, M. J. Krause, D. F. Niyogi, N. K. Gill, *Tet.*, 2003, **59**, 7565-7570

139. A practical and simple synthesis of (2S,5R)- and (2S,5S)-5-hydroxylysine and of related α-amino acid required for the synthesis of the collagen cross-link pyridinoline, P. Allevi, M. Anastasia, *Tet. Asym.*, 2004, **15**, 2091-2096

140. Synthesis and metal chelate stability of *N,N'*-ethylene-bis(aminomalonis) acid, M. Mashihara, T. Ando, I. Murase, *Bull. Chem. Soc. Japan*, 1973, **46**, 844-847

141. Nuclear magnetic resonance determination of the absolute configuration of complexes of cobalt (III) with asymmetric tatradentate ligands, L. N. Schoenberg, D. W. Cooke, C. F. Liu, *Inorganic Chemistry*, 1968, **7**, 2386-2393

142. Chelating polymers. I. The synthesis and acid dissociation behavior of several *N*-(*p*-vinylbenzenesulfonyl)-substituted diaminopolyacetic acid monomers, monomeric analogues, and related intermediates, R. M. Genik-Sas-Berezowsky, I. H. Spinner, *Can. J. Chem.*, 1970, **48**, 163

143. Diglycylethylenediamine, T. L. Cottrell, J. E. Gill, *J. Chem. Soc.*, 1947, 129-130

144. Stereoselective synthesis of 1,2-difunctional compounds through the addition of organometallic reagents to chiral masked forma of glyoxal, G. Martelli, D. Savoia, *Curr. Org. Chem.*, 2003, 7, 1049-1070

145. Glyoxal derivatives. IV. 2-DImethoxymethyl-4,5-dimethoxy-1,3-dioxolane and 2,2′-bis(4,5-dimethoxy-1,3-dioxolane), J. M. Kliegman, E. B. Whipple, M. Ruta, R. K. Barnes, *J. Org. Chem.*, 1972, **37**, 1276-1279

146. Monoaminals of glyoxal: versatile chirons, A. Alexakis, J.-P. Tranchier, N. Lensen, P. Mangeney, *J. Am. Chem. Soc.*, 1995, **117**, 10767-10768

147. Facile synthesis of 1,3,6-oxadiazepines from 2,2′-(1,2-ethanediyldiimino)bisphenols, M. E. Ochoa, S. Rojas-Lima, H. Höpfl, P. Rodríguez, N. Farfán, R. Santillan, *Tet.*, 2001, **57**, 55-64

148. D. R. Kelly, unpublished work.

149. Products of the reaction of *N,N′*-dibenzylethylenediamine and glyoxal, R. L. Willer, D. W. Moore, *J. Org. Chem.* 1985, **50**, 2365-2368; Trans-1,4,5,8-tetracarboethoxy- and 1,4,5,8-tetramethyl-1,4,5,8-tetraazadecalin (tad)', B. Fuchs, S. Weinman, U. Shmueli, A.R. Katritzky, R.C. Patel, *Tet. Lett.*, 1981, **22**, 3541-3544.

150. Lactam formation from the condensation of stilbenediamine with glyoxal, L. L. Darko, J. Kerliner, *J. Org. Chem.*, 1971, **36**, 3810-3812

151. Monoaminals of glyoxal: versatile chirons, A. Alexakis, J. P. Tranchier, N. Lensen, P. Mangeney, *J. Am. Chem. Soc.* 1995, **117**, 10767- 1076

152. Compared reactivity of a β-aminothiol and aminoalcohol towards phenylglyoxal, C. Agami, F. Couty, B. Prince, O. Venier, Tet. Letts., 1993, **34**, 7061-7062

153. Tandem oxidation processes for the preparation of nitrogen containing heteroaromatic and heterocyclic compounds, S. A. Raw, C. D. Wilfred and R. J. K. Taylor, *Org. Biomol. Chem.*, 2004, **2**, 788-796

154. 2-Substituierte 1,3-Dinaphthylimidazolidine aus *N,N′*-Dinaphthylethylendiaminen, A. Schönberg, E. Singer, P. Eckert, *Chem. Ber.*, 1980, **113**, 2823-2826

155. Phenylglyoxal, H. A. Riley, A. R. Gray, *Org. Synth.*, 1943, **2**, 509

156. The reaction of benzil and 2-aminopyridine: a correction, B. Alcaide, R. Pérez-Ossorio, J. Plumet, M. A. Sierra, *Tet. Letts.*, 1985, **26**, 247-248

157. P. G. Sokov, *J. Gen. Chem.*, 1940, **10**, 1457

158. Versatile access to benzhydryl-phenylureas through an unexpected rearrangement during microwave-enhanced synthesis of hydantoins, G. C. Muccioli, J. Wouters, J. H. Poupaert, B. Norberg, W. Poppitz, G. K. E. Scriba, D. M. Lambert, *Org. Letts.*, 2003, **5**, 3599-3602

159. A rapid and efficient microwave-assisted synthesis of hydantoins and thiohydantoins, G. G. Muccioli, J. H. Poupaert, J. Wouters, B. Norberg, W. Poppitz, G. K. E. Scriba, D. M. Lambert, *Tet.*, 2003, **59**, 1301-1307

160. Molecular rearrangements. I. The base-catalyzed condensation of benzil with urea, W. R. Dunnavant, F. L. James, *J. Am. Chem. Soc.*, 1956, **78**, 2740-2743

161. Reactions of carbonyl compounds in basic solutions. Part 36: The base-catalysed reactions of 1,2-dicarbonyl compounds, K. Bowden, W. M. F. Fabian, *J. Phys. Org. Chem.*, 2001, **14**, 794-796

162. Benzilic acid and related rearrangements, S. Selman, J. F. Eastham, *Chem. Soc. Rev.*, 1960, **14**, 221-235

163. Valentin Day report, Cardiff Univeristy

164. Medium ring nitrogen heterocycles, P. A. Evans, A. B. Holmes, *Tet.*, 1991, **47**, 9131-9166

165. Intramolecular Staudinger ligation: a powerful ring-closure method to form medium-sized lactams, *Angew. Chemie*, 2003, **42**, 4373-4375

166. Bis-aminals of linear tetraamines: Kinetic and thermodynamic aspects of the condensation reaction, F. Chuburu, R. Tripier, M. Le Baccon, H. Handel, *Eur. J. Org. Chem.*, 2003, **6**, 1050-1055.

167. Structure of mildiomycin, a new antifungal nucleoside antibiotic, S. Harada, E. Mizuta, T. Kishi, *Tet.*, 1981, **37**, 1317-1327

168. Ozonolysis of (cyclohexa-l,4-dienyl)-alanine.An approach to the synthesis of new unnatural amino acids. X-Ray molecular structure of 2-hydroxy-7-methyl-3-phenylpyrazolo[*1,5-a]* pyrimidine, G. Zvilichovsky, V. Gurvich, *J. Chem. Soc. Perkin Trans. 1*, 1995, **19**, 2509-2516

169. A novel approach to the synthesis of chiral terminal 1,2-diamines, T. Markidis, G. Kokotos, *J. Org. Chem.*, 2001, **66**, 1919-1923

170. Synthesis and anticonvulsant activities of (*R*)-(*O*)-methylserine derivative, S. V. Andurkar, J. P. Stables, H. Kohn, *Tet. Asym.*, 1998, **9**, 3841-3854

171. Solid-phase synthesis of *O*-phosphorothioylserine- and threonine- containing peptides as well as of *O*-phosphoserine and threonine containing peptides, D. B. A. de Bont, W. J. Moree, J. H. van Boom, R. M. J. Liskamp, *J. Org. Chem.*, 1993, **58**, 1309-1317

172. Pyranose-furanose equilibria. studies on the methylation of 2,3-0-isopropylidene-L-rhamnose A. C. Ferguson, A. H. Haines, *J. Chem. Soc.*, 1969, 2372-2375

173. Studied on the synthesis of the aplysiatoxins: synthesis of a selectively-protected form of the C27-C3g (dihydroxybutanoate) moiety of oscillatoxin A, R. D. Walkup, R. T. Cunningham, *Tet. Letts.*, 1987, **28**, 4019-4022

174. Damian Dunford report, Cardiff University

175. Structure of mildiomycin, a new antifungal nucleoside antibiotic, S. Harada, E. Mizuta, T. Kishi, *Tet.*, 1981, **37**, 1317-1327

176. Phosphatidyl serine, E. Baer, J. Maurukas, *J. Biol. Chem.*, 1955, **212**, 25-38

177. Solid-phase synthesis of O-phosphorothioylserine- and -threonine-containing peptides as well as of O-phosphoserine- and -threonine-containing peptides, D. B. A. de Bont, W. J. Moree, J. H. van Boom, R. M. J. Liskamp, *J. Org. Chem.*, 1993, **58**, 1309-1317